Investigating the mechanisms of acquired resistance to ALK inhibitors in EML4-ALK-driven lung cancer

A thesis submitted to the University of Manchester for the degree of Doctor of Philosophy in the Faculty of Biology, Medicine and Health.

2019

Athanasios-Rafail Paliouras

Cancer Research UK Manchester Institute

List of Contents

List of figures

List of tables

Word count

49,925 excluding references

Abstract

Targeted therapies have had a great impact on the management of oncogene-driven non-small cell lung cancer, where a subset of lung adenocarcinomas is driven by the EML4-ALK translocation. While ALK inhibitors such as crizotinib or alectinib lead to excellent initial responses in the clinic, the majority of patients show disease progression due to the development of acquired resistance. Mutations in the ALK kinase domain occur in a significant percentage of patients and lead to poor ALK inhibition and therefore, drug resistance. Parallel pathway alterations also significantly contribute to the development of acquired resistance. In this thesis, the aim was to gather new insight into the mechanisms of development of resistance, as well as evaluate the role of non-coding RNAs in differential drug response.

EML4-ALK^{mut} cell lines treated long-term with ALK inhibitors were used as models of acquired resistance. Data from RNA sequencing & subsequent protein analysis evidenced an upregulation of CDK1, CDK6, cyclin B1, and cyclin E1. Treatment of cells with the pan-CDK inhibitors alvocidib and dinaciclib, as well as the CDK7/12 inhibitor THZ1 led to decreased cell proliferation as well as induction of apoptosis. Furthermore, there was specificity of these compounds for EML4-ALK cells compared with normal epithelial cells or compared with other lung cancer cell lines of different genetic background. Mechanistically, apoptosis was evidenced through the downregulation of the anti-apoptotic proteins Survivin and MCL-1, initiated by transcriptional inhibition. These data were translated *in vivo*, where treatment of a mouse xenograft model of crizotinib & alectinib resistance with alvocidib led to delayed tumour growth.

In addition, the role of the non-coding genome was examined. Through transcriptomic analysis, it was found that crizotinib-resistant cells exhibit upregulation of the oncogenic miR-25 and miR-30c and the tumour suppressing miR-149 and miR-103. It was further shown that CDK6 is an indirect target of miR-149 and a direct target of miR-103. The upregulation of miR-25 and miR-30c was clinically relevant since some patients who developed resistance to ALK inhibitors in the clinic had increased levels of circulating miR-25 and miR-30c in their plasma.

Taken together, these results suggest a multifactorial development of resistance to ALK inhibitors, which can be targeted by exploiting a vulnerability of EML4-ALK^{mut} cells to transcriptional inhibition. Through these findings, clinical testing of CDKi compounds could lead to the addition of new therapeutics to the armamentarium intended for a cohort of patients with very limited treatment options.

Declaration

No portion of the work referred to in the thesis has been submitted in support of an application for another degree or qualification of this or any other university or other institute of learning.

Copyright statement

Acknowledgements

Experimental contribution of others

Except for the experimental contribution of others noted below, the data presented in this thesis are my own work.

I am grateful to Assistant Professor Christine Lovly (Vanderbilt University) for the ongoing collaboration and provision of the drug-resistant cell lines.

I am grateful to Dr Sudhakar Sahoo and Dr Hui-Sun Leong for mapping the reads, normalising and performing statistics on the RNA-seq data. Also, Dr Sahoo analysed the patient RNA-seq data from [1]. I am grateful to Dr Ian Donaldson for mapping and statistically analysing the Chip-seq reads.

I am grateful to Dr Gianpiero Di Leva for the analysis of the miRNA nanostring data of H3122 cells treated with crizotinib.

I am grateful to Dr Matteo Fassan (University of Padua, Italy) for analysing and quantifying the *in situ* immunohistochemistry images.

I am grateful to Dr Lei Shi for assistance during the preparation of the Chip-seq samples and for assistance with *in vivo* experiments.

Members of the Histology Core Facility performed tumour sectioning and IHC.

Members of the Molecular Biology Core facility, for sanger sequencing services, mycoplasma testing services and most importantly, preparing the libraries and sequencing all the RNA samples.

Members of the Biological Resources Unit weighed the mice and measured tumour size and also administered the compounds when oral gavage was used.

Thanks to

To members of the Biological Resources Unit for tirelessly monitoring my mice and training me in the relevant regulated procedures.

Professor Fiona Blackhall provided us with ALK^{mut} patient samples. Dr Matthew Krebs was instrumental in supporting this collaboration. Matthew Carter helped with the characterisation of these samples and made sure that there was no haemolysis before further processing.

Denys Holovanchuk for providing feedback, moral support and reagents whenever needed. Joe Maltas for providing jokes, moral support, H1299, and Beas-2B cells.

Dr Srivatsava Naidu for being immensely helpful, usefully critical and a great colleague overall.

Dr Lei Shi for constant advice, helping with the *in vivo* experiments and sharing good times.

Dr Peter Magee for being ever-present and available to help. Without his support, no experiments described here would be possible.

Dr Tiziana Monteverde for being so easy to work with, for advice, reagents and putting up with me.

Manuela La Montagna for being a reliable source of coffee, being a great colleague and for putting up with me.

Marta Buzzetti for helping with experiments and being a nice person to work with.

Professor Angeliki Malliri for her guidance, constant support, and contribution of key cell lines and antibodies.

Dr Donald Ogilvie, Professor Tim Somervaille and Dr Crispin Miller for interesting and helpful discussions.

I would like to thank the faculty members of the Democritus University of Thrace, Alexandroupolis, Greece, who offered me all the tools to undertake molecular biology research. Especially Associate Professor Margy Koffa and Assistant Professor Sotiria Boukouvala, for without their guidance and help I would never have enrolled in this PhD programme.

Lastly, Dr Michela Garofalo, since without her mentoring and trust, none of this would have been possible.

Abbreviations

1. ALCL: Anaplastic Large Cell Lymphoma
2. ALK: Anaplastic Lymphoma Kinase
3. CCLE: Cancer Cell-Line Encyclopaedia
4. CDK: Cyclin-dependent Kinase
5. CDKi: Cyclin-dependent Kinase inhibitor
6. CLL: Chronic Lymphocytic Leukemia
7. CRISPR: Clustered regularly interspaced short palindromic repeats
8. E2F1: E2F Transcription Factor 1
9. EGFR: Epidermal Growth Factor Receptor
10. EML4: Echinoderm Microtubule Associated Protein Like 4
11. EMT: Epithelial to Mesenchymal Transition
12. ERK: Extracellular Signal-Regulated Kinase
13. GWAS: Genome-wide association study
14. FDA: Food and Drug Administration
15. FGFR: Fibroblast Growth Factor Receptor
16. HELP: Hydrophobic Echinoderm Microtubule-Associated Protein-Like Protein
17. MAPK: Mitogen-activated protein kinase
18. MEK: Mitogen-activated protein kinase kinase
19. MYB: MYB proto-oncogene
20. MYC: MYC proto-oncogene
21. NGS: Next Generation Sequencing
22. NKIRAS2: NF-kappa-B inhibitor-interacting Ras-like protein 2
23. NPM: Nucleophosmin
24. NSCLC: Non-Small Cell Lung Cancer
25. PARP: Poly (ADP-Ribose) Polymerase
26. PDX: Patient-Derived Xenograft
27. PBS: Phosphate-Buffered Saline
28. PCR: Polymerase chain reaction
29. PDAC: Pancreatic ductal adenocarcinoma
30. PI: Propidium Iodide
31. RAC1: Ras-related C3 botulinum toxin substrate 1
32. RPKM: Reads Per Kilobase of transcript per Million mapped reads
33. RT: Room temperature
34. RTK: Receptor Tyrosine Kinase
35. RT-qPCR: Reverse transcription-quantitative polymerase chain reaction
36. SDS-PAGE: Sodium dodecyl sulphate polyacrylamide gel electrophoresis
37. TGFβ: Transforming growth factor-beta
38. TKI: Tyrosine Kinase Inhibitor
39. TRAIL: TNF-related apoptosis-inducing ligand

40. TSS: Transcription Start Site

Glossary of small-molecule inhibitors

Drug name	Primary target(s)	Other targets
Crizotinib	ALK	MET, ROS1
Ceritinib	ALK	IGF1-R, InsR
Alectinib	ALK	RET
Lorlatinib	ALK	ROS1
Erlotinib	EGFR (reversible)	ERBB family
Osimertinib	EGFR (irreversible & mutant selective)	ERBB family
Bemcemtinib	AXL	MER
Galunisertib	TGFβ-R1	TGF-β-R2
Alvocidib	CDK1, CDK2, CDK4, CDK6, CDK9	CDK7, EGFR, SRC
Dinaciclib	CDK1, CDK2, CDK5, CDK9	-
Palbociclib	CDK4/6	-
THZ1	CDK7/12	-

1 Materials

WESTERN BLOTTING	CATALOG NUMBER	COMPANY
WesternBright ECL spray	K-12049-D50	Advansta
Full-Range Rainbow Molecular Weight Marker	RPN800E	Amersham
Nupage Novex 3-8% Tris-Acetate Gels	EA03752BOX	Invitrogen
Nupage Novex 4-12% Bis-tris Gels	NP0321BOX	Invitrogen
Nupage sample reducing agent	NP0004	Invitrogen
Nupage Transfer Buffer	NP00061	Invitrogen
Nupage MOPS buffer	NP0001	Invitrogen
Nupage Tris Acetate buffer	LA0041	Invitrogen
Complete cocktail protease inhibitors	4693116001	Roche
PhosStop	4906845001	Roche
Pierce BCA protein assay kit	23225	Thermo Fisher Scientific
Tween 20	P9416	Sigma-Aldrich
RIPA Lysis Buffer	R0278-50ML	Sigma-Aldrich
PVDF membrane	IPVH00010	Immobilon
RT-qPCR	**CATALOG NUMBER**	**COMPANY**
DNA Free Kit	AM1906	Ambion
Trizol	15596026	Invitrogen
Chloroform	288306	Sigma-Aldrich
Taqman microRNA Reverse Transcription kit	4366596	Applied Biosystems
FastStart Universal Probe Master (ROX)	04 913 949 001	Roche
FastStart Universal SYBR Green Master (Rox)	4913850001	Roche
Verso cDNA synthesis kit	AB1453A	Molecular Probes
β-Actin Taqman Probe	Hs01060665_g1	Applied Biosystems
GAPDH Taqman Probe	Hs02786624_g1	Applied Biosystems
ath-miR-159a spike-in Taqman Probe	000338	Applied Biosystems
RNU44 Taqman Probe	001094	Applied Biosystems
RNU48 Taqman Probe	001006	Applied Biosystems
U6 snRNA Taqman Probe	001973	Applied Biosystems
let-7c Taqman Probe	000379	Applied Biosystems
miR-10a Taqman Probe	000387	Applied Biosystems
miR-17 Taqman Probe	002308	Applied Biosystems
miR-18a Taqman Probe	002422	Applied Biosystems
miR-19a Taqman Probe	000395	Applied Biosystems
miR-19b Taqman Probe	000396	Applied Biosystems
miR-20a Taqman Probe	005800	Applied Biosystems
miR-23b Taqman Probe	000400	Applied Biosystems
miR-24 Taqman Probe	000402	Applied Biosystems
miR-25 Taqman Probe	000403	Applied Biosystems

miR-27b Taqman Probe	000409	Applied Biosystems
miR-30c Taqman Probe	000419	Applied Biosystems
miR-106b Taqman Probe	000442	Applied Biosystems
miR-103 Taqman Probe	000439	Applied Biosystems
miR-149-5p Taqman Probe	002255	Applied Biosystems
miR-182 Taqman Probe	002334	Applied Biosystems
miR-200c Taqman Probe	002300	Applied Biosystems
miR-205 Taqman Probe	000509	Applied Biosystems
miR-221 Taqman probe	000524	Applied Biosystems
miR-222 Taqman probe	002276	Applied Biosystems
miR-330-3p Taqman Probe	002230	Applied Biosystems
miR-345-5p Taqman Probe	002186	Applied Biosystems
miR-381 Taqman Probe	000571	Applied Biosystems
miR-3065-5p Taqman Probe	242265_mat	Applied Biosystems
TRANSFECTION OLIGOS & REAGENTS	**CATALOG NUMBER**	**COMPANY**
Dharmafect-1	T-2001-01	Dharmacon
Optimem	11058-021	Gibco
Lipofectamine 2000	11668-027	Invitrogen
Lipofectamine RNAiMax	13778-075	Invitrogen
Silencer siRNA negative control #1	4390843	Ambion
PLK1 positive control siRNA	4390824	Ambion
miRNA mimic negative control #1	4464058	Ambion
ath-miR-159a spike-in	MC10332	Ambion
miR-17-5p mimic	MC12412	Ambion
miR-18a-5p mimic	MC12973	Ambion
miR-19b-1-3p mimic	MC10629	Ambion
miR-20a-5p mimic	MC10057	Ambion
miR-23b mimic	MC10711	Ambion
miR-24 mimic	MC10737	Ambion
miR-25-3p mimic	MC10584	Dharmacon
miR-27b mimic	MC10750	Ambion
miR-30c precursor	PM11060	Ambion
miR-103a-3p mimic	MC10632	Ambion
miR-149-5p mimic	MC12788	Ambion
miR-205-5p mimic	MC11015	Ambion
miR-221-3p precursor	PM10337	Ambion
miR-222-3p precursor	PM11376	Ambion
miR-345-5p mimic	MC12733	Ambion
miR-3065-5p mimic	MC18328	Ambion
miRIDIAN microRNA Hairpin Inhibitor Negative Control #1	IN-001005-01-05	Dharmacon
miR-19b hairpin inhibitor	IH-300489-05-0005	Dharmacon
miR-25-3p hairpin inhibitor	IH-300498-07-0002	Dharmacon
miR-30c-5p hairpin inhibitor	IH-300541-05-0002	Dharmacon
miR-30a-5p hairpin inhibitor	IH-300505-05-0002	Dharmacon

miR-221-3p hairpin inhibitor	IH-300578-07-0002	Dharmacon
Non target #3 siRNA	D-001810-03-05	Dharmacon
BCL2L11 (Bim) smartpool siRNA	E-004383-00	Dharmacon
PIAS3 smartpool siRNA	L-004164-00	Dharmacon
STAT3 smartpool siRNA	L-003544-00-0005	Dharmacon
EGFR smartpool siRNA	L-003114-00-0005	Dharmacon
CDK1 smartpool siRNA	L-003224-00-0005	Dharmacon
CDK2 smartpool siRNA	L-003236-00-0005	Dharmacon
CDK6 siRNA	551	Ambion
CDK7 smartopool siRNA	L-003241-00-0005	Dharmacon
CDK9 smartpool siRNA	L-003243-00-0005	Dharmacon
CDK12 smarpool siRNA	L-004031-00-0005	Dharmacon
CCNB1 4x siRNA	GS891	Qiagen
All star negative control siRNA	1027280	Qiagen
c-FOS 4x siRNA	GS2353	Qiagen
MCL-1 4X siRNA	GS4170	Qiagen
c-IAP2 (BIRC3) smartpool siRNA	L-004099-00-0005	Dharmacon
STAT5A 4x siRNA	GS6776	Qiagen
GapMer Negative Control	339515 LG00000002-DDA	Qiagen
GapMers	custom design	Qiagen
COMPOUNDS	**CATALOG NUMBER**	**COMPANY**
Crizotinib	S1068	Selleck
Crizotinib *in vivo*	HY-50878	MedChemExpress
Ceritinib (LDK-378)	S7083	Selleck
Alectinib	S2762	Selleck
Volasertib	S2235	Selleck
Galunisertib	S2230	Selleck
Palbociclib	S1116	Selleck
Alvocidib	S1230	Selleck
Alvocidib *in vivo*	HY-10005	MedChemExpress
THZ1	S7549	Selleck
THZ1 *in vivo*	HY-80013	MedChemExpress
Erlotinib	S7786	Selleck
Osimertinib	S7297	Selleck
Dinaciclib	S2768	Selleck
Dinaciclib *in vivo*	HY-10492	MedChemExpress
Actinomycin D	A1410-2MG	Sigma
Lorlatinib	HY-12215	MedChemExpress
S63845	HY-100741	MedChemExpress

JQ1	A1910	APEXbio
VARIOUS CHEMICALS	**CATALOG NUMBER**	**COMPANY**
DMSO	D2650	Sigma-Aldrich
Crystal Violet 0.5% staining solution	32909	Sigma-Aldrich
Formaldehyde solution 37%	252549	Sigma-Aldrich
PEG300	202371-500G	Sigma-Aldrich
CELL CULTURE REAGENTS	**CATALOG NUMBER**	**COMPANY**
T25 flasks	3056	Corning
T75 flasks	430641	Corning
RPMI 1640	21875-034	Gibco
Fetal Bovine Serum	270106	Gibco
DMEM	11995-065	Gibco
Trypsin-EDTA 0.05%	25300054	Gibco
Opti-MEM™ I Reduced Serum Medium	11058021	Gibco
Matrigel reduced growth factor	354230	Corning
DNA PREPARATION & CLONING	**CATALOG NUMBER**	**COMPANY**
DH5a competent cells	18265-017	Invitrogen
One-shot TOP 10 competent cells	C4040-06	Invitrogen
UltraPure Agarose	16500500	Invitrogen
SYBR Safe DNA gel stain	S33102	Invitrogen
T4 DNA ligase	15224-017	Invitrogen
Quick-Load 2-Log DNA Ladder(0.1-10.0 kb)	N0469S	New England Biolabs
Gel loading dye (Purple)	B7024S	New England Biolabs
Quickchange II XL Site-Directed mutagenesis kit	200522	Agilent
Q5 High-Fidelity 2X Master Mix	M0492S	New England Biolabs
KaPa High Fidelity Hot Start Ready Mix	KK2601	Roche
Human genomic DNA	G3041	Promega
PureLink™ HiPure Plasmid DNA Purification Kit	K2100-02	Thermo Fisher Scientific
BglII FastDigest	FD0083	Thermo Fisher Scientific
BshTI FastDigest	FD1464	Thermo Fisher Scientific
FastAP Alkaline Phosphatase	EF0654	Thermo Fisher Scientific
HindIII FastDigest	FD0504	Thermo Fisher Scientific
KpnI FastDigest	FD0524	Thermo Fisher Scientific
MluI FastDigest	FD0564	Thermo Fisher Scientific
NotI FastDigest	FD0593	Thermo Fisher Scientific
PstI FastDigest	FD0614	Thermo Fisher Scientific
XbaI FastDigest	FD0684	Thermo Fisher Scientific
Dynabeads™ Protein G for Immunoprecipitation	10004D	Thermo Fisher Scientific
KITS & ASSAYS	**CATALOG NUMBER**	**COMPANY**
CellTiter 96®AQueous Non-Radioactive Cell Proliferation Assay	G5421	Promega
Dual-Luciferase® Reporter Assay System	E1960	Promega
FxCycle™ PI/RNase Staining Solution	F10797	Molecular Probes

TACS Annexin V-FITC Kit	4830-01-K	Trevigen
miRNeasy Serum/Plasma Kit	217184	Qiagen
Qiaprep spin mini-prep kit	27106	Qiagen
Qiaprep Plasmid Midi Kit	12143	Qiagen
PCR purification kit	28104	Qiagen
Gel extraction kit	28704	Qiagen
ANTIBODIES	**CATALOG NUMBER**	**COMPANY**
Phospho-ALK (Tyr1604) Antibody	3341	Cell Signaling
ALK (D5F3®) XP® Rabbit mAb	3633	Cell Signaling
Anti-BMF RabMab	ab181148	Abcam
Bim (C34C5) Rabbit mAb	2933	Cell Signaling
BID Antibody (Human Specific)	2002	Cell Signaling
Mcl-1 (22)	sc-12756	Santa Cruz Biotechnology
Ras (D2C1) Rabbit mAb	8955	Cell Signaling
Anti-STAT3 (phospho Y705) antibody [EP2147Y]	ab76315	Abcam
Stat3 (124H6) Mouse mAb	9139	Cell Signaling
PIAS3 (D5F9) XP® Rabbit mAb	9042	Cell Signaling
Met (C-12)	sc-10	Santa Cruz Biotechnology
PDGF Receptor a Antibody	3164	Cell Signaling
PDGF Receptor b (28E1) Rabbit mAb	3169	Cell Signaling
DUSP6 monoclonal antibody (M01) clone 3G2	H00001848-M01	Abnova
Akt (5G3) Mouse mAb	2966	Cell Signaling
Phospho-Akt (Ser473) (D9E) XP® Rabbit mAb	4060	Cell Signaling
NF-κB p65 (L8F6) Mouse mAb	6956	Cell Signaling
Phospho-NF-κB p65 (Ser536) (93H1) Rabbit mAb	3033	Cell Signaling
Anti-CDK1 antibody [A17]	ab18	Abcam
Cdk2 (78B2) Rabbit mAb	2546	Cell Signaling
Cdk4 antibody [EPR4513-54-3]	ab108355	Abcam
CDK6 (D4S8S) Rabbit mAb	13331	Cell Signaling
Cdk7	sc-7344	Santa Cruz Biotechnology
CDK9 [EPR3119Y]	ab76320	Abcam
Anti-p21 antibody [EPR362]	ab109520	Abcam
PARP (46D11) Rabbit mAb	9532	Cell Signaling
Anti-ERK1 + ERK2 antibody [EPR17526]	ab184699	Abcam
Phospho-p44/42 MAPK (Erk1/2) (Thr202/Tyr204) Antibody	9101	Cell Signaling
c-IAP2 (58C7)	3130	Cell Signaling
p-EGFR Antibody (Tyr 1173)	sc-12351	Santa Cruz Biotechnology
SOCS1 (A156) Antibody	3950	Cell Signaling
SOCS3 Antibody	2923	Cell Signaling
Cyclin B1 (D5C10) XP® Rabbit mAb	12231	Cell Signaling
Cyclin E1 (HE12) Mouse mAb	4129	Cell Signaling
c-Myc Antibody	9402	Cell Signaling
Anti-TGF beta Receptor I antibody	ab31013	Abcam

Anti-TGF beta Receptor II antibody [EPR14673]	ab184948	Abcam
Vimentin (D21H3) XP® Rabbit mAb	5741	Cell Signaling
Anti-rabbit IgG, HRP-linked Antibody	7074	Cell Signaling
Anti-rabbit IgG, peroxidase-linked species-specific whole antibody (from donkey)	NA 934	Amersham
Anti-mouse IgG, HRP-linked Antibody	7076	Cell Signaling
β-Actin (C4)	sc-47778	Santa Cruz Biotechnology
α-Tubulin (11H10) Rabbit mAb	2125	Cell Signaling
GAPDH (14C10) Rabbit mAb	2118	Cell Signaling
Human Apoptosis Antibody Array - Membrane (43 Targets)	ab134001	Abcam
Anti-STAT5a antibody [E289]	ab32043	Abcam
Anti-c-Fos antibody	ab190289	Abcam
Anti-Survivin antibody [EP2880Y]	ab76424	Abcam
Anti-Axl antibody [EPR21107]	ab215205	Abcam
Anti-RNA polymerase II CTD repeat YSPTSPS (phospho S2)	ab193468	Abcam
Anti-RNA polymerase II total	ab140509	Abcam
Cleaved Caspase-3 (Asp175)	9661	Cell Signaling
Anti-RNA polymerase II Total chip-grade	C15200004	Diagenode
PRIMERS		**SEQUENCE**
Sequencing		
ALK_TK_FW	5'-	TACAACCCCAACTACTGCTTTGCT
ALK_TK_REV	5'-	AGGCACTTTCTCTTCCTCTTCCAC
Cloning		
FW_mir-17-92	5'-	TTTCTTCCCCATTAGGGATTATGCTG
REV_mir-17-92	5'-	CCCCAAAAGTGAAATGTTTTTGAATG
Bim_19_FW	5'-	ACT TCTAGA TAA GTA ACT TGA CTA CTT TTA TTT GGG
Bim_19_REV	5'-	ACT TCTAGA GTT TAA AAA TCT GCA GTT ATT TAC AGC
PIAS3_18_FW	5'-	ACTTCTAGACTCATGGCCCTGTAGTTA
PIAS3_18_REV	5'-	ACTTCTAGACAACCTTTATTATGGGTGAGAG
PUMA_221_FW	5'-	TAAGCACCGGTCCTCCCACCTCCTGACACCCT
PUMA_221_REV	5'-	TGCTTCTGCAGCTGAGTCCATCAGCCGTCCCTCTC
CDK6 103 WT 1st FW	5'-	TAAGC ACCGGT TTAAGCTGATCCTGCGGAGAAC
CDK6 103 WT 1st REV	5'-	TGCTT CTGCAG TAACTCAGCTGTGCCTGGATTAC
CDK6 103 WT 2nd FW	5'-	TAAGC ACCGGT GTGCTCAGTTGGCTCTAGTAA
CDK6 103 WT 2nd REV	5'-	TGCTT CTGCAG TTGTATGGCCCATCTCCTTTAT
CDK6 103 1st MUT FW	5'-	ATTTGATTTTTCTAACCTTGACAGT

		GTGGAGTGGGTAATCC
CDK6 103 1st MUT REV	5'-	GGATTACCCACTCCACACTGTCAAG GTTAGAAAAATCAAAT
CDK6 103 2nd MUT FW	5'-	GATTTTCAAAGAATGGAGGTCTCA GAAAATAATTCAGATC
CDK6 103 2nd MUT REV	5'-	GATCTGAATTATTTTCTGAGACCTC CATTCTTTGAAAATC
CDK6_149_FW	5'-	TAAGCACCGGTGCAAACCTAACAG GGTCACATA
CDK6_149_REV	5'-	TGCTTCTGCAGCTAGAGCCAACTG AGCACTAAAC
CCNE1 103 WT FW	5'-	TAAGC ACCGGT CCCATCCTTCTCCACCAA AGA
CCNE1 103 WT REV	5'-	TGCTT CTGCAG GGCATTGTACACTGTCA ACTGATAA
lncRNA cloning		
AC144831.1 XbaI FW	5'-	TAAGCA TCTAGA CCCAGTCCAGCCTCCCTA CT
AC144831.1 NotI REV	5'-	TGCTTA GCGGCCGC TTGAATAGAAGATCCA GTGACTAGTGAG
RP11-1275H24.1 XbaI FW	5'-	TAAGCA TCTAGA ATTCCCGCTTTCCCCA
RP11-1275H24.1 NotI REV	5'-	TGCTTA GCGGCCGC TTATTTTTATAAATGT TTAATGTTTTCACC
RP11-367H1.1 XbaI FW	5'-	TAAGCA TCTAGA GCAAATCCCATGCCATTT TATACAAGAG
RP11-367H1.1 NotI REV	5'-	TGCTTA GCGGCCGC TTGGATTATCAAAGCT TTATTCACGTTTGT
RT-qPCR		
Housekeeping		
β-Actin FW	5'-	TGACATTAAGGAGAAGCTGTGCTA C
β-Actin REV	5'-	GAGTTGAAGGTAGTTTCGTGGATG
GAPDH FW	5'-	ATGTTCGTCATGGGTGTGAA
GAPDH REV	5'-	TGTGGTCATGAGTCCTTCCA
B2M FW	5'-	CCAGCGTACTCCAAAGATTCA
B2M REV	5'-	TGGATGAAACCCAGACACATAG
TUBB FW	5'-	GGAATGGGCACTCTCCTTATC
TUBB REV	5'-	GGCACCACACTGAAGGTATT
lncRNAs		
AC005355.2 2nd FW	5'-	TCTAGCTGACCTTGAGACCTAT
AC005355.2 2nd REV	5'-	GAAGCAAAGTGCTGCTCATAAA
MANCR_FW_Paper	5'-	TGTTGGAGGATACCTGTGCAT
MANCR_REV_Paper	5'-	TGCCATTCCCAGATTGTGGAG
AC144831.1_FW	5'-	CAGCATTTGACACGGAATCG
AC144831.1_REV	5'-	CCTCCCTGACAGTGTGATTT
CTD-2292M16.8_FW	5'-	CCTCTCTGCCACCATGAATAAA

CTD-2292M16.8_REV	5'-	CCTTTGGGCATTGCCTTTG
CTD-2587M2.1_FW	5'-	CTCCTGGTCTCCCTAAACATAATC
CTD-2587M2.1_REV	5'-	CAACGCTGGAAGCAAAGTAAA
LINC00482_FW	5'-	CATGGCCAGACGGGATTC
LINC00482_REV	5'-	AGGGAGATGGACTCGAAGG
LINC00607_FW	5'-	CTTCTTGGCATCTGACACTTGG
LINC00607_REV	5'-	TGCCTGCCCTCTGGAAA
RP11-7K24.3_FW	5'-	GGGTTGTTGGGAGGATAGTATG
RP11-7K24.3_REV	5'-	CCTGTCCTGCAACAGCTTAT
RP11-367H1.1_FW	5'-	CGTGTGGGTCCTGTAACG
RP11-367H1.1_REV	5'-	CCCTACTCATGTTACGAGCTTAAT
RP11-563J2.2_FW	5'-	CCAGCACGGTTGAGAACTATT
RP11-563J2.2_REV	5'-	TTCAGTCCCTACCAGCATCT
RP11-1038A11.1_FW	5'-	CAATTCCTCACTCCTTGCTACTC
RP11-1038A11.1_REV	5'-	GGTGTCTCCTCCCATTCAGATA
RP11-1275H24.1_FW	5'-	GGCTGCGGCCATAAATCT
RP11-1275H24.1_REV	5'-	GTTCCCTGCGCAGTCTC
Genes		
Bim qPCR FW	5'-	CAGGCCTTCAACCACTATCTC
Bim qPCR REV	5'-	AACTCTTGGGCGATCCATATC
Bid qPCR FW	5'-	CCTACCCTAGAGACATGGAGAA
Bid qPCR REV	5'-	GGTGCGTAGGTTCTGGTTAATA
Mcl-1 qPCR FW	5'-	GAAAGCTGCATCGAACCATTAG
Mcl-1 qPCR REV	5'-	AGAACTCCACAAACCCATCC
Survivin qPCR FW	5'-	ACTTGGCCCAGTGTTTCTT
Survivin qPCR REV	5'-	CCTCCCAAAGTGCTGGTATT
SMAC qPCR FW	5'-	CGCAGATCAGGCCTCTATAAC
SMAC qPCR REV	5'-	CCAGCTTGGTTTCTGCTTTC
AXL_v1_FW	5'-	GTCCTCATCTTGGCTCTCTTC
AXL_v1_REV	5'-	GACTACCAGTTCACCTCTTTCC
LOX_v1_FW	5'-	TACCCAGCCGACCAAGATA
LOX_v1_REV	5'-	TGGCATCAAGCAGGTCATAG
SNAI2_refseq_FW	5'-	AACTACAGCGAACTGGACAC
SNAI2_refseq_REV	5'-	GAGGATCTCTGGTTGTGGTATG
VIM_refseq_FW	5'-	GATTCACTCCCTCTGGTTGATAC
VIM_refseq_REV	5'-	GTCATCGTGATGCTGAGAAGT
APAF1_FW	5'-	GGACGACAGCCATTTCCTAATA
APAF1_REV	5'-	GCAGCTTAGCTTGCTGATAAAC
BAK_FW	5'-	ACCCAGAGATGGTCACCTTA
BAK_REV	5'-	GTCATAGCGTCGGTTGATGT
BAX_FW	5'-	GTCACTGAAGCGACTGATGT
BAX_REV	5'-	CTTCTTCCAGATGGTGAGTGAG
CASP3_FW	5'-	CTCTGGAATATCCCTGGACAAC
CASP3_REV	5'-	ACATCTGTACCAGACCGAGA
CASP8_FW	5'-	GTCTGTGCCCAAATCAACAAG
CASP8_REV	5'-	GAGTCCGAGATTGTCATTACCC
CASP9_FW	5'-	GTCGAAGCCAACCCTAGAAA

CASP9_REV	5'-	CACCAAATCCTCCAGAACCA
CYTOCHROME_C_FW	5'-	GGAGAGGATACACTGATGGAGTA
CYTOCHROME_C_REV	5'-	GTCTGCCCTTTCTTCCTTCTT
CDK1 FW	5'-	GAGAAGGTACCTATGGAGTTGTG
CDK1 REV	5'-	CCCTTCCTCTTCACTTTCTAGTC
CDK2 FW	5'-	AGATGGACGGAGCTTGTTATC
CDK2 REV	5'-	CTTGGTCACATCCTGGAAGAA
CDK6 FW	5'-	TCACGAACAGACAGAGAAACC
CDK6 REV	5'-	CTCCAGGCTCTGGAACTTTATC
CDK7 FW	5'-	AGCAGGAGACGACTTACTAGAT
CDK7 FW	5'-	CCTGGCCGATTACTGAAATACT
CDK9 FW	5'-	TGGGCTGTTGAGCAATGT
CDK9 REV	5'-	GATGTAGTAGAGGCCGTTAAGC
CDK12 FW	5'-	GCTGAATAACAGTGGGCAAATC
CDK12 REV	5'-	AGGTCGGTACCACAAAGTAATG
CCNB1 FW	5'-	GATGCAGAAGATGGAGCTGAT
CCNB1 REV	5'-	TCCCGACCCAGTAGGTATTT
CCNE1 FW	5'-	CGGTATATGGCGACACAAGAA
CCNE1 REV	5'-	GGTGCAACTTTGGAGGATAGA

2 Methods

2.1 Cell culture

HEK293T and A549 cells were a kind gift from Dr John Brognard. H1299 and Beas-2B cells were a kind gift from Prof. Angeliki Malliri. HBEC, H2228 and H460 cells were purchased from ATCC. The following cell sources have been described before; H3122 [2], STE-1 [3], PC-9 and isogenic clones [4] and H1975 and isogenic clones [4]. H3122 and STE-1 parental cells were STR-profiled upon receipt and found to be free of contamination with another line. All cell lines were routinely monitored for mycoplasma contamination using an in-house Core Facility service.

2.1.1 Maintenance

All cell lines were maintained at 37°C, 5% CO_2 in a humidified incubator. HEK293T cells were maintained in DMEM with 1g/l glucose (Gibco) + 10 % Fetal Bovine Serum (Gibco). HBEC cells were maintained in Airway Epithelial Cell Basal Medium (ATCC) combined with a Bronchial Epithelial Cell Growth kit (ATCC). H2228, H3122 parental, H3122 CrizR1, H3122 CrizR4, H3122 CrizR5, H3122 CeritR, STE-1 parental, STE-1 AlecR, PC-9 parental, PC-9 OsimR, PC-9 ErlotR, H1975 parental , H1975 OsimR, A549, H1299 and H460 cell lines were cultured in RPMI-1640 medium supplemented with 10% FBS. Cells were grown in standard T75 flasks to 80-90% confluence and passaged 2 times a week. For the passage procedure, cells were briefly rinsed with PBS to remove traces of serum. Then 0.05% Trypsin-EDTA solution was added until cell detachment was observed and was subsequently inactivated by the addition of complete growth medium and the appropriate volume of cells was transferred to a new T75 flask. Cells were expanded, frozen and the stocks were verified to be mycoplasma free by PCR-based detection (MBCF Core Facility) and by DNA staining followed by microscopic observation. Cells in culture were discarded after 15 passages and frozen cells from the same stock were thawed to ensure reproducibility of experiments.

2.1.2 Frozen stocks

Cells from multiple flasks were harvested during the exponential growth phase by the standard passaging procedure. The cells suspensions were pooled in a single tube and centrifuged at 200 x g for 5 minutes. The cell pellet was then re-suspended in complete growth medium supplemented with 10% FBS and 10% DMSO and transferred in cryogenic tubes. Cells were maintained for short term storage at -80°C and for long term storage at ~ -175°C in the vapour phase of liquid nitrogen.

2.1.3 Thawing

For recovering frozen stocks, cryogenic tubes were rapidly thawed in a 37°C water bath, then the contents of the tube were transferred in 9ml of pre-warmed complete growth medium and centrifuged at 125 x g for 5 minutes. The cell pellet was re-suspended in 1 ml of complete growth medium and transferred to a T25 flask.

2.2 Generation of drug-resistant cell lines

In collaboration with Dr Christine Lovly, NCI-H3122 cells were exposed to increasing concentrations of ALK inhibitors until cells could tolerate >500 nM. By that method, the clones that were generated were named CrizR1, CrizR4, CrizR5 (crizotinib resistant), and CeritR (ceritinib resistant). STE-1 cells were exposed to increasing concentrations of alectinib until cells could proliferate in the presence of at least 500nM alectinib. PC-9 ErlotR/OsimR and H1975 OsimR have been described before [4]. All the drug-resistant cell lines used can be found in (**Table 1**).

Specifically, EML4-ALK^{mut} or EGFR^{mut} parental cells were exposed in different flasks to a concentration of the primary inhibitor that was enough to inhibit the proliferation of 50% of the cells (IC_{50}). After cells had adapted to this concentration and became confluent again, the cells were exposed to a 20% higher concentration of the drug (without being passaged to a new flask). Again, on confluence, the concentration was similarly increased, until the cells could tolerate more than 500nM ceritinib or alectinib or more than 1uM of crizotinib, erlotinib or osimertinib. Then cells were expanded, and if multiple flasks were grown, indicated as different number clones and sequenced for the ALK kinase domain. On-kinase domain mutations were detected in some of the clones that were not used in this study, for example, the F1174L mutation in a ceritinib-resistant clone.

Table 1: All oncogene-driven, drug-resistant cell lines used in this thesis separated by driver oncogene, primary inhibitor & potential kinase domain mutations.

Cell line	Growth medium	Driver oncogene	Inhibitor used	Kinase domain mutations
H3122	RPMI	EML4-ALK (E13;A20)	-	-
H3122 CrizR1	RPMI	EML4-ALK (E13;A20)	1uM crizotinib	None detected
H3122 CrizR4	RPMI	EML4-ALK (E13;A20)	1uM crizotinib	None detected
H3122 CrizR5	RPMI	EML4-ALK (E13;A20)	1uM crizotinib	None detected
H3122 CeritR	RPMI	EML4-ALK (E13;A20)	500nM ceritinib	None detected
STE-1	RPMI	EML4-ALK (E13;A20)	-	-
STE-1 AlecR	RPMI	EML4-ALK (E13;A20)	500nM alectinib	None detected
PC-9	RPMI	EGFR (exon19del E746–A750)	-	-
PC-9 ErlotR	RPMI	EGFR (exon19del E746–A750)	1uM erlotinib	T790M
PC-9 OsimR	RPMI	EGFR (exon19del E746–A750)	1uM osimertinib	Not tested
H1975	RPMI	EGFR (L858R/T790M)	-	-
H1975 OsimR	RPMI	EGFR (L858R/T790M)	1uM osimertinib	T790M

2.3 Transfection

2.3.1 Transfection of miRNA mimics or anti-miRs

MiRNA mimics or miRNA inhibitors (Ambion) were transfected at 100 nM final concentration using Lipofectamine 2000 reagent. For a 60mm cell culture-treated dish, cells were plated at various

densities and transfected after 24 hours. 7.5 ul of Lipofectamine 2000 was mixed with 500 ul of Optimem serum-free medium and complexed with another mix containing 500 ul Optimem with 100 nM of mimic/inhibitor. The transfection reagent and the oligonucleotides were complexed for 20 minutes at room temperature (RT, 15-25 °C) and added with an additional 1 ml of Optimem to the dish. Reagent volumes were adjusted accordingly for different dish sizes. The effects after overexpression or inhibition of miRNAs were analysed at least 48 hours after transfection.

2.3.2 Transfection of siRNA

SiRNA oligonucleotides were obtained from either Qiagen, Ambion or Dharmacon and can be found in the 'Materials' section. SiRNA concentration was optimized according to the individual targets at a final concentration of 25-100nM. SiRNA was transfected using Lipofectamine 2000 reagent or Lipofectamine RNAiMAX. SiRNA effects were assessed at least 48 hours after transfection.

2.3.3 Transfection of Gapmers

Locked Nucleic Acid Gapmers were custom-made and purchased from Qiagen. Gapmers were transfected at 50nM using Lipofectamine RNAiMAX. Gapmer effects were assessed 48 hours after transfection.

2.4 Preparation of cell lysates

Cells were rinsed with ice-cold PBS and detached from the dish with a cell scraper. Cells were pelleted by centrifugation at 500 x g, 5 minutes at 4°C. The pellet was then re-suspended in RIPA lysis buffer (Sigma-Aldrich) supplemented with complete Protease Inhibitor and anti-phosphatase PhosSTOP Cocktail Tablets (Roche). The cell lysate was incubated on ice for 20 minutes with intermittent vortexing. The lysate was centrifuged at 13,000 x rpm for 10 minutes and 4°C. The supernatant was removed, stored at -80°C and protein concentration was quantified with the use of a Pierce BCA Protein Assay kit (Thermo Scientific) according to the manufacturer's instructions.

2.5 Western blot analysis

30-50 µg of protein extracts were subjected to SDS-PAGE, using either 4-12% Bis-Tris or 3-8% Tris-Acetate Novex NuPage gels (Invitrogen) according to the manufacturer's instructions. The separated proteins were transferred to a 0.45 µm PVDF membrane in a wet tank XCell II Blot Module, at 30V for 1.30 hour. The membrane was blocked in 5% non-fat dry milk in TBS-T (TBS 1X, 0.1% v/v Tween 20) for 1 hour at RT. After blocking, the membrane was incubated overnight at 4°C with a primary antibody-containing buffer. Primary antibodies were diluted in either 5% non-fat dry milk in TBS-T or 5% BSA in TBS-T and used as mentioned in the 'Materials – Antibodies' section. After removing the primary antibody buffer, membranes were washed 3 times, for 5 minutes with TBS-T. Then the membrane was incubated with either 1:5000 anti-rabbit HRP (Amersham) or 1:10,000 anti-mouse HRP (Cell Signaling) for 1 hour at RT. Then, membranes were washed 3 times, for 5 minutes with TBS-T and sprayed with ECL reagent (Amersham). After 3 minutes the chemiluminescence was captured with a Chemidoc Touch imager (Biorad).

2.5.1 Protein array blotting

To profile changes in multiple proteins at once, a protein array was used. This array is a membrane that has blotted validated, primary antibodies against a variety of human proteins at predetermined positions in the membrane as well as loading controls. The one used in this thesis is an Abcam apoptotic array, which has blotted antibodies for 43 different apoptotic proteins. The membrane was blocked in blocking agent provided with the array kit, then 200ug protein extracts were hybridised O/N at 4°C. Then, the membrane was washed, incubated with signal amplifiers according to the manufacturer's instructions and sprayed with ECL reagents. Luminescence was recorded in a Biorad Chemidoc instrument and quantified with the use of ImageJ.

2.6 RNA isolation

2.6.1 From cells

Cells were rinsed with ice-cold PBS and detached from the dish with a cell scraper. Cells were pelleted by centrifugation at 500 x g, 5 minutes at 4°C and re-suspended in 1 ml Trizol reagent (Ambion). Then, 200 ul of chloroform were added in the Trizol and samples were vortexed to a homogenous mixture. To separate the phases, samples were centrifuged at 12,000 x g for 15 minutes and 4°C, then the aqueous phase was transferred to a new tube. To precipitate the RNA, 500 ul of RT isopropanol were added to the tube and incubated for 10 minutes at RT. The RNA pellet was isolated by centrifugation at 12,000 x g, 10 minutes at 4°C, then the pellet was washed 3 x times with the addition of 75% ethanol followed by centrifugation at 7,500 x g, 5 minutes at 4°C. The supernatant was discarded and the pellet was re-suspended in 40 ul nuclease-free H_2O. The RNA concentration and quality were measured by absorbance at 260 nm using a NanoDrop One device (Thermo Scientific). Only RNA with $A_{260/280} > 1.8$ and $A_{260/230} > 2$ was considered of adequate quality and stored at -80°C.

2.6.2 From blood samples

All plasma samples were obtained with informed consent under the "Improving knowledge of treatment resistance in patients with lung cancer" clinical trial ethics.

Blood samples were centrifuged at 1900 x g for 10 mins and 4°C. The upper (yellow) plasma phase was transferred to a new tube without disturbing the intermediate layer (containing white blood cells and platelets).

Plasma was then centrifuged for 10 mins at 16,000 x g and 4°C. The supernatant was aliquoted in new tubes and stored frozen at –80°C. To extract RNA, a 200 ul plasma aliquot was thawed at room temperature (RT) and centrifuged at 16,000 x g for 5 mins and 4°C. The supernatant was incubated with 1ml of Qiazol RNA reagent. After incubating the samples for 5 mins with Qiazol, a synthetic RNA spike-in (ath-miR-159a) was added at 500pM. The sample was subsequently processed with the use of a miRNAEASY Serum/Plasma kit (Qiagen) according to the manufacturer's instructions.

2.6.3 From mouse tumour samples

Tumour pieces were snap-frozen in liquid nitrogen. Then, tumours were sliced in fine pieces with a scalpel and re-suspended in Trizol. The rest of the extraction was performed according to the Trizol protocol, as described above.

2.7 Quantitative Reverse Transcription PCR

2.7.1 MiRNA Taqman

CDNA was synthesized from 10 ng of sample total RNA with the use of a Taqman MicroRNA Reverse transcription Kit (Applied Biosystems) and of a specific reverse transcription stem-loop primer (Applied Biosystems). 1 ul of the cDNA reaction was mixed with 0.5 ul of a Taqman probe (Applied Biosystems) and FastStart Universal Probe Master Mix (Roche) in a final volume of 10ul according to the manufacturer's instructions. Each reaction was performed in triplicate, loaded into a 96 well plate and qPCR was performed in a Lightcycler 96 instrument (Roche). The PCR reaction consisted of 10 minutes pre-incubation at 95°C followed by 2 steps of 95°C for 15 sec and 60°C for 60 sec for a total of 40 cycles. Cq values were then exported to an Excel spreadsheet and relative expression was normalized to U6 or RNU48 with the use of the 2-ΔΔCT method [5].

2.7.2 Gene-specific SYBR green

Depending on the expression levels of the studied transcript, 50-400 ng of RNA were used as a template for cDNA synthesis using the Verso cDNA kit (Molecular Probes) using oligo-DT primers. From this cDNA, 1 ul was used per reaction using the FastStart Universal SYBR Green Master (Roche) in 20 ul final volume. Each reaction was performed in triplicate, loaded into a 96 well plate and qPCR was performed in a Lightcycler 96 instrument (Roche). The PCR reaction consisted of 10 minutes pre-incubation at 95°C followed by 2 steps of 95°C for 15 sec and 60°C for 60 sec for a total of 40 cycles. Cq values were then exported to an Excel spreadsheet and relative expression was normalized to β-Actin with the use of the 2-ΔΔCT method [5].

2.8 RNA sequencing

2.8.1 Small-RNA

Small RNA libraries were prepared with a NEBNext Kit (New England Biolabs) using 1 μg of total RNA as input. For each sample, 3 replicate libraries were prepared and sequenced in parallel. Each cDNA library was multiplexed, size-selected for small RNAs and sequenced for 75bp using a Nextseq500 (Illumina) instrument. The run resulted in a sequencing depth of between 20 and 30 million reads per sample. Sequencing reads were quality checked and low-quality bases were trimmed from the 3' end. Subsequently, reads were trimmed for adapter sequences by FASTX. Trimmed reads were aligned to miRBase (version 21) and hg19 genome and quantification of miRNAs was performed using miRDeep2. The DESeq2 [6] package was used to generate miRNA differential expression profiles based on statistical significance (p-value).

2.8.2 Poly-A sequencing

Poly-A libraries were prepared with a Sureselect PolyA kit (Agilent) using 1 µg of total RNA as input. For each sample, 3 replicate libraries were prepared and sequenced in parallel. The indexed primer sequences are described in the company's manual under reference number # G9691-90010. Each cDNA library was multiplexed and sequenced in 75bp runs using a Nextseq500 (Illumina) instrument. The run resulted in a sequencing depth of between 25 and 30 million reads per sample.

RNA-seq reads were quality checked and aligned to the human genome assembly (GRCh37) using the RSubread package aligner [7] with the default settings. Mapped reads were converted to gene level integer read counts using featureCounts [8] available within the RSubread package and the Ensemble GTF annotation (Homo_sapiens.GRCh37.74).

Differential expression (DE) was evaluated comparing the gene level integer read count data for the knockdown and control samples using the DESeq2 Bioconductor package [6]. DESeq2 DEG estimation involves multiple steps. In brief, it uses a normalization factor to model read counts to account for sequencing depth. Then it estimates gene-wide dispersions and performs shrinkage analysis to generate more accurate estimates of dispersion to model the counts. Finally, it fits the negative binomial model and performs hypothesis testing using the Wald test.

The resulting P-values were adjusted using the Benjamini and Hochberg approach to control the false discovery rate. Genes with an adjusted P-value determined to be <0.05 (FDR < 0.05) by DESeq2 and that had a fold change value ≥ 1.5 ($|\text{Log2 fold change}| \geq 0.55$) between two groups were considered to be differentially expressed.

2.9 CHIP-sequencing

CrizR1 cells (100×10^6 per condition) were treated with DMSO, 200nM alvocidib or 100nM THZ1 for 6 h. Then, chromatin was isolated according to the published protocol [9] using 10ug of total-RNA polymerase II antibody (Diagenode, # C15200004). Then, purified chromatin was used as input to generate PCR-amplified libraries using the Diagenode Microplex kit according to the manufacturer's instructions. The library was sequenced on a Nextseq500 instrument using paired-end sequencing at a sequencing depth of 60-80 million reads per sample.

Afterwards, the quality of the sequenced reads was assessed by the FASTQC/fastq screen output supplied by the CRUK computational biology facility. For each sample, reads from four sequencing lanes were merged into a single file. Reads were filtered using Trimmomatic v0.36, to remove any remaining adapter sequences, poor quality 5' ends of reads, or reads shorter than 35 nucleotides. Reads were then mapped to the human genome (UCSC hg38 analysis set) using Bowtie2 v2.3.0. The peaks were called by the use of MACS2 v2.1.2 with the default parameters. Only binding regions with a Qvalue of <0.05 were considered. The MACS2 output was converted into a spreadsheet where candidate regions are sorted by fold enrichment.

Differential binding analysis was performed using diffReps v1.55.6 using the midpoint coordinate (mean of the start of first read and the end of the last read) of the filtered mapped paired-reads. Only genes within 100K of peaks were considered with the distance being calculated between the closest edge of the summit region and the TSS of each gene. The heatmap and profiles were created using Deeptools v3.2.1. The input was the bigWig files created for the UCSC sessions. For the Heatmap, bigwigCompare was used to subtract the background model signals from the ChIP signals. A matrix of the three samples was made using computeMatrix.

2.10 Detection-based assays

2.10.1 MTS proliferation assay

Cells were plated in 96 well plates. The cell number was optimized for each cell line and varied from 3,000 to 5,000 cells per well. The next day cells were transfected or drug-treated, as specified in each experiment. Cells were incubated with drugs for 72 hours and then 20 µl of MTS reagent (Cell Titer 96 Aqueous Non-Radioactive Cell Proliferation Assay, Promega) were added per well (with the modification described in [10]) and the cells were incubated for 1 hour at 37°C. After the incubation, the absorbance at 490nm was measured and subsequent readings every 30 minutes were taken as long as the readings remained within the linear detection range of the assay. Values were subtracted for blank wells' absorption and normalized to the vehicle control. Values were exported to Prism 7 (GraphPad) and then the x-axis values log-transformed. Values were fitted with a non-linear regression curve and analysed with the equation log (inhibitor) vs normalized response – variable slope to generate the IC_{50} value.

2.11 Drug treatments

All chemicals for *in vitro* assays were purchased from Selleck or as specified in the 'Materials - Compounds' section, dissolved in DMSO, aliquoted and stored at -80°C for long term storage, or at -20°C for on-going experimentation. For all drug conditions, the dilution resulted in a maximum of 0.3% DMSO per well. For drug treatments, cell media were replaced with complete growth medium containing drugs at the appropriate concentrations.

2.12 Sanger sequencing of ALK clones

Total RNA was extracted from each ALK-rearranged clone and cDNA was synthesized using a Verso cDNA synthesis kit (Molecular Probes). Then, the kinase domain was PCR-amplified with a Q5 high fidelity polymerase (New England Biolabs), using the primers [11] 5' – TACAACCCCAACTACTGCTTTGCT -3' (forward) and 5 -AGGCACTTTCTCTTCCTCTTCCAC -3' (reverse). The 963 bp product was PCR-purified (Qiagen) and was subjected to standard Sanger sequencing from both ends.

2.13 Bioinformatics work

2.13.1 3′ UTR target prediction identification.

To identify targets of miRNAs of interest, publicly available algorithms such as DIANA [12], Targetscan Release 7.1 [13] and microRNA.org August 2010 release [14] were utilized. Potential miRNA targets were not ranked according to probability, instead, the presence of a potential 7mer or 8mer binding site in the 3′ UTR was deemed enough to pursue as a potential target.

2.13.2 GSEA

Gene-set enrichment analysis was performed with the use of the GSEA Software from the Broad Institute [15]. The software was fed differentially expressed RNA-seq data, which were analysed as described before. By default, to look at pathway-level collections, we used the available BROAD-included gene sets, namely Hallmark, Positional, Curated (KEGG, REACTOME), Motif, Computational, GO and Oncogenic gene sets.

2.13.3 Heatmap generation

Normalized reads across each sample were transformed to z-score. Then these values were plotted using the R Package pHeatmap (distributed under a GPL-2 license by Raivo Colde). Values were clustered based on Euclidean distance.

2.13.4 Analysis of CCLE RNA-seq expression data

Normalized RPKM values from the cancer cell line encyclopaedia (CCLE) were downloaded and isolated for lung adenocarcinoma cell lines only [16]. Then, these values were transformed to z-score using the formula [(gene value- average of all values per gene)/(standard deviation of all values)]. The z-scores were plotted in Heatmaps according to the gene sets described in the text. Upon identification of genes of interest, the individual RPKM values were plotted in an XY axis for the LUAD cell lines.

2.14 Flow cytometry

2.14.1 Cell cycle analysis

Cells were plated in 6-well plates, in a density optimized according to the cell line. Following the indicated treatment, cells were trypsinised and transferred to centrifugation tubes. Cells were then centrifuged at 500 x g for 5 mins and washed with PBS. Then cells were fixed with ice-cold, 70% ethanol for 1 hr on ice. Cells were then stained with a FxCycle™ PI/RNase Staining Solution (Life Technologies), in the dark for 15 mins at RT. Samples were then run through a Novocyte instrument (ACEA Biosciences). For Propidium Iodide imaging, the BL3 laser was used (615/20 nm). No-stain controls were run first, followed by positive controls that warranted cell cycle arrest (i.e. PLK1 inhibition). At least 20,000 cells were analysed per sample. Samples were gated first to exclude debris, then to exclude doublets, then gated on the PI+ positive population, and the remaining population was analysed for PI intensity. Cells were automatically fitted according to the Novocyte cell cycle algorithm and were separated in G0/G1, S and G2/M phase, with increasing PI intensity (DNA content).

2.14.2 Annexin/PI staining

Cells were plated in 6-well plates, at a density optimized according to the cell line. Following the appropriate treatment, the supernatant was collected and the remaining cells were trypsinised and transferred to centrifugation tubes. Cells were then centrifuged at 500 x g for 5 mins and washed with ice-cold PBS twice. Cells were then stained with an Annexin V/PI solution (Trevigen) for 20 mins in the dark at RT. For Annexin V-FITC imaging the BL1 laser was used (530/30 nM), while for Propidium iodide imaging, the BL3 laser was used (615/20 nm). Samples were then run through a Novocyte instrument (ACEA Biosciences). Compensation was performed by running no-stain controls, PI-only controls, and Annexin-only controls. Positive controls that induced apoptosis were also run. At least 20,000 cells were analysed per sample. Samples were gated first to exclude debris, then to exclude doublets. Quadrant gates were drawn according to the negative/positive control intensity on the remaining population and the percentage of Annexin V + cells was calculated.

2.15 In vivo work

2.15.1 Compound preparation

In all experiments crizotinib and alvocidib were dissolved in 5% DMSO, 40% PEG300 and 55% sterile PBS and the same mix was used as vehicle control. In the AlecR experiment, P.O. group, alectinib was dissolved in 30% PEG400, 0.5% Tween80, 5% Propylene Glycol and 64.5% sterile PBS and the same mix was used as vehicle control. In the AlecR experiment, I.P. group, alvocidib and dinaciclib were dissolved in 10% DMSO, 40% PEG300, 5% Tween80 and 45% PBS and the same mix was used as vehicle control. Solvents were added in the stated order, the solution warmed at 37%, re-suspended by vortexing and sterile filtered. Drug solutions were maintained at -20 °C for long-term storage and at 4 °C during dosing. Alectinib was purchased from Selleck, while crizotinib, alvocidib, dinaciclib, and THZ1 were purchased from MedChemExpress.

2.15.2 Treatments

To initiate the xenograft mouse model, cells were grown to 70% confluence and tested for mycoplasma/MHV contamination just before the final injection. Cells were then harvested and cells were re-suspended in PBS and injected subcutaneously in the right flank of nude mice. Mice were regularly monitored for tumour growth and treatment commenced when the tumour average reached 100-200 mm^3.

Female athymic nude mice or NOD-SCID mice from Charles River were used at 6-8 weeks old. Mice were injected with 2.5 million CrizR4 cells, or 5 million AlecR cells in 50% matrigel (Corning. When tumours reached between 100-200 mm^3, mice were randomized in different groups and were treated with:

CrizR4 experiment: 10 ml/kg vehicle control or 10 mg/kg alvocidib, by I.P. injection, daily for 3 weeks. In the crizotinib group, mice were treated with 10ml/kg vehicle control or 50mg/kg crizotinib daily, by oral gavage.

AlecR experiment: 10ml/kg vehicle control by oral gavage 3x/week (n=5), 10mg/kg alectinib 3x/week (n=5), 10ml/kg vehicle control by I.P. injection 3x/week (n=6), 10mg/kg alvocidib by I.P. injection 3x/week (n=6) or 20mg/kg dinaciclib by I.P. injection 3x/week (n=6). After 3 weeks of consecutive treatment, a one week on / one week off pattern was adopted for the alvocidib/dinaciclib/I.P. control group. The vehicle control group measurements were then superimposed in order to have all the measurements in the same graph.

Mice were observed daily for clinical signs of ill health. Mice were weighed 3x/week and if weight loss was observed, weighed daily and put on a mash diet. The humane endpoint for this was a limit of 20% weight loss. Tumour size was measured twice a week and calculated using the formula [volume = $(width)^2(length)/2$]. The tumour size measurements were taken by a member of the in-house animal facility who was blinded to the conditions of the experiment. The humane endpoint for tumour size was a limit of 1,500mm^3.

Due to the aggressive nature of the CrizR4 cell line, some of the mice developed tumour ulceration followed by bleeding and were sacrificed. The number of these mice is indicated in the figure legends according to each experiment. Furthermore, any mice that did not develop tumours larger than the 200mm^3 limit were excluded. When endpoints were reached, mice were sacrificed by a humane method and the tumours excised. Half of the tumour was preserved in formalin and half was snap-frozen and used later for RNA extraction.

All the animal procedures were approved by the CRUK Manchester Institute Animal Welfare and Ethical Review Body.

2.16 *In-situ* Immunohistochemistry (IHC)

Tumours in formalin were embedded in paraffin blocks and different slices were obtained. For the antibody staining, cleaved Caspase 3 antibody (Cell signaling) was used at 1/100 dilution, run on a Leica Bond Rx instrument with the use of the Refine kit. As added steps, a casein blocking step was used at 105 ºC followed by an antigen retrieval step with ER1 buffer (citrate-based) at pH 6 for 20 minutes.

2.17 Clonogenic assay/ crystal violet staining

For short-term crystal violet staining, cells were seeded at medium-density (50,000-100,000 cells) in 6-well plates. Cells were allowed to reach confluence (typically ~7 days).) and then fixed in 4% PFA for 20 mins at RT. Then colonies were stained with 0.05% crystal violet (Sigma) for 20 mins at RT. Excess of crystal violet was removed by washing with ddH_2O. Plates were allowed to dry and then images were taken.

For the long-term, persister assay, H3122 parental cells were treated with 1μM crizotinib and alectinib, which resulted in extensive cell death. The remaining, "persister" cells were kept in the same concentrations of drug medium until they started to proliferate again. At this point, persister cells were treated with the indicated concentrations of compound until the control

(crizotinib/alectinib only) well approached confluence, at which point the plate was fixed and stained as above.

2.18 3′ UTR cloning

First, 3′ UTR binding sites were identified through Targetscan (see method 2.12). Then, a 400 bp region containing the binding site was PCR-amplified with a Kapa Hi-Fi polymerase (Kapa Biosystems)(list of primers given in the 'Materials-Primers' section). The PCR product was run on an agarose gel to verify the specificity of the product and was then purified with a PCR purification kit (Qiagen). The PCR product and the vector were then digested with BshTI and PstI for 2 hours at 37 ºC. The vector was also de-phosphorylated in the same reaction, with the use of calf-intestine alkaline phosphatase (Thermo Fisher). The digested products were gel-extracted (Qiagen), and ligated with a T4 ligase (Thermo Fisher) at RT for an hour, using a 3:1 insert: vector ratio. From this ligation reaction, 4 ul were used to transform DH5a competent bacteria (Thermo Fisher) using the classic heat-shock method. The next day, colonies were screened for successful cloning. The correct insert was verified through confirming digestions followed by Sanger sequencing. The described, receiving vector is a pGL3 Control vector (Promega) expressing the Firefly luciferase gene, modified to contain sites for BshTI and PstI enzymes (Fermentas).

2.19 Site-directed mutagenesis

Site-directed mutagenesis was performed with a QuikChange II XL Site-Directed Mutagenesis Kit (Agilent) using the manufacturer's instructions. For 3′ UTR mutagenesis, the entire miRNA binding site was deleted and confirmed by Sanger sequencing.

2.20 Dual Luciferase Reporter Assay

Al luciferase reporter assays were performed either in the cell line under investigation or in HEK293T cells, as indicated in the figure legends. Cells were plated in 12-well plates and transfected with 1ug of pGL3 Control – 3′ UTR plasmid. To normalize transfection efficiency, cells were also transfected with a plasmid containing a Renilla luciferase gene (pGL3 SV40 Renilla) at a ratio of 1:50 Firefly:Renilla. 24h post-transfection, cells were lysed with the use of a kit (Dual Luciferase Assay System, Promega). 20ul of each sample were loaded in white-walled plates and analysed using an automated injector-luminometer (Glomax, Promega). After recording the raw Firefly and Renilla luminescence, the ratio Firefly:Renilla was used to calculate differences among conditions.

2.21 Statistical comparisons

All statistical tests were performed with the use of Prism 7 (GraphPad). Plotted graphs show means ± SD from n = 3 biological replicates unless otherwise stated. For all grouped, pairwise comparisons, a two-tailed Student's t-test was used where * = $p < 0.05$, ** = $p < 0.01$, *** = $p < 0.001$, N.S. = Not Significant. For linear regression curves, conditions were compared evaluating the probability of a shift in the IC_{50} with the use of an extra sum of squares F test.

All quantitative experiments were repeated 3 times unless indicated in the figure legend (i.e. apoptotic array experiment, repeated twice).

3 General introduction

3.1 Lung Cancer incidence and types

Despite laborious efforts, lung cancer remains undefeated to a great extent. The latest worldwide statistics suggest that it is the most frequent form of cancer, accounting for about 13% of cancers diagnosed in 2012. Following diagnosis, tumours are classified based on histological typing as either Small Cell Lung Cancer (SCLC) or Non-Small Cell Lung Cancer (NSCLC), and patients are treated accordingly. The major subtypes of NSCLC are large-cell lung carcinoma, squamous-cell lung carcinoma, and adenocarcinoma [17]. Persistent efforts to provide a molecular profile for these subtypes have started to be fruitful and as genomic technologies progress, we will gain a deeper understanding of the genetic changes that drive this remarkably heterogeneous disease (The current mutational overview for lung adenocarcinomas can be found in **Figure 1**). Both adenocarcinomas and squamous-cell carcinomas seem to harbour mutations in well-known oncogenic pathways, including point mutations and copy number alterations, as reviewed by [18,19]. Driver oncogenes may be very attractive prospective targets but attempts to drug them with small molecule inhibitors often fail. A typical example is the well-known RAS family of genes, which happens to be mutated in about 30% of lung adenocarcinomas [20], for which a selective inhibitor is yet to be discovered.

3.1.1 Treating metastatic NSCLC

Early-stage diagnosis usually permits the effective management of disease with surgery [21]. However, NSCLC is typically diagnosed at the late stages III or IV. Until very recently, the standard of care for the treatment of metastatic NSCLC lacking actionable genomic aberrations was some variation of platinum-based chemotherapy, such as cisplatin/gemcitabine or carboplatin/paclitaxel [22]. With the recent success of immunotherapy and the results of checkpoint inhibitor trials, some combination of immunotherapy is starting to become the standard of care in this context [23,24]. Specifically, a trial that compared the anti-PD-1 antibody pembrolizumab versus chemotherapy, showed superior efficacy and a more favourable safety profile for pembrolizumab in patients that scored at least 50% for PD-L1 expression [25]. This made single-agent immunotherapy a new option in the first-line setting as well. The Keynote-189 trial concluded that the addition of pembrolizumab to standard chemotherapy regimens can also be beneficial in the first-line setting, especially in patients with less than 50% PD-L1 score, who would normally not benefit from single-agent pembrolizumab [26]. This development was the first time in decades that an improvement in five-year survival was observed in advanced NSCLC.

3.1.2 Molecular signatures of NSCLC

Hyper-active kinases are present in many cancer types. It is often the case that tumours are addicted to the expression of certain genes, in other words, they rely on specific driver oncogenes to maintain their transformed properties, and NSCLC is no exception [27]. The theory of oncogene addiction was particularly strengthened after the effectiveness of treating Chronic Myeloid Leukaemia by targeting the mutant fusion BCR-ABL kinase. Human Receptor Tyrosine Kinases

(RTKs) are subdivided in 20 families [28] and among other important driver oncogenes, seem to have a governing role in NSCLC (**Figure 1**). In particular, Epidermal Growth Factor Receptors (EGFR) including the HER2 protein, Anaplastic Lymphoma Kinase (ALK) and Hepatocyte Growth Factor Receptor (HGFR, encoded by MET), are frequently altered in NSCLC [29]. Other RTKs, such as Rearranged During Transfection (RET), Neurotrophic Receptor Tyrosine Kinase 1 (NTRK1) and ROS proto-oncogene 1 (ROS1), are mutated at low frequencies but their inhibition with small molecule inhibitors can still lead to clinical benefit [30]. Also, it is worth noting that NSCLC patients exhibit frequent mutations of the tumour suppressor *TP53.* Specifically, p53 is mutated in about 50% of lung adenocarcinomas, and about 80% of Squamous cell carcinomas [31](and analysis from TCGA).

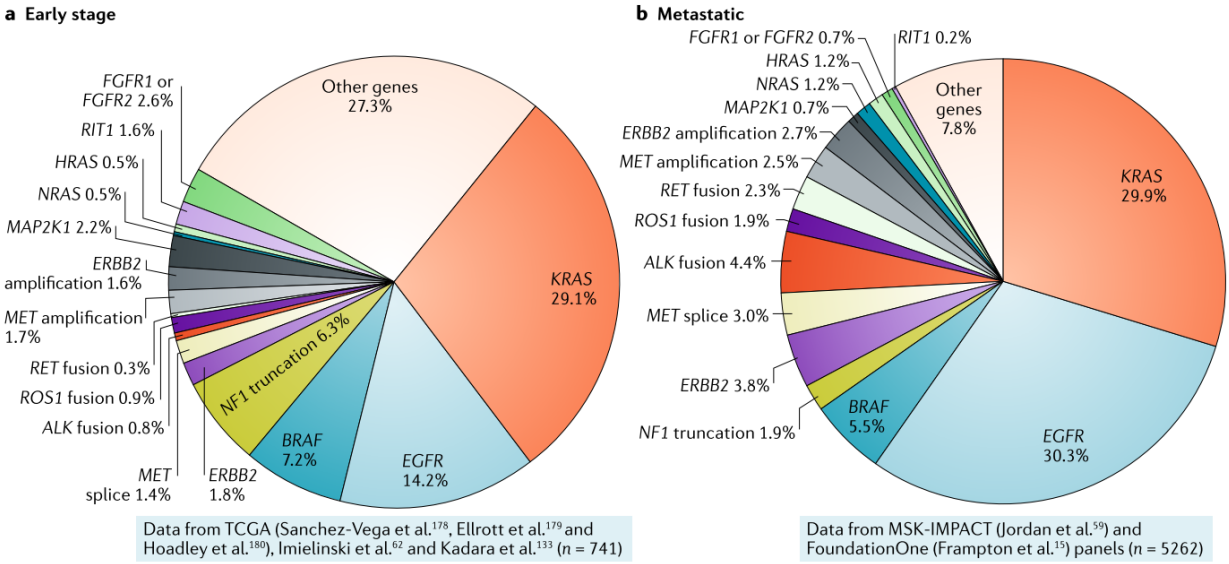

Figure 1: The mutational landscape of NSCLC

Intensive research has shaped the initial histological classification into a molecular categorization of tumours according to driver mutations. Curated with TCGA data, early-stage lung cancer shows fewer driver oncogenes on diagnosis, presumably due to inadequate material for accurate molecular testing. On the other hand, late-stage lung cancer shows a significant enrichment in driver oncogenes, the most frequent of which, KRAS and EGFR, account for as much as 60% of lung adenocarcinomas. Other oncogenes such as ALK and BRAF are mutated at 4-5% of patients translating still to a large number of patients that can benefit from targeted therapies. The last 7.8% remains with either low-confidence, or low-frequency driver mutations. Image adapted from [19].

3.2 ALK-rearranged lung cancer

ALK is a poorly-characterized kinase, which is speculated to play a role in the development of the nervous system. Specifically, mice with ALK deletion are born normally and exhibit only minor behavioural alterations later in life [32]. Its ligand was only recently confirmed to be heparin [33] and its partner effectors and downstream pathways are not completely understood (well-established interactions are depicted in **Figure 2**), largely due to the fact that most studies are being conducted in cancer-related mutant forms of ALK [34]. ALK is frequently mutated in human cancers, a typical example being the chromosomal rearrangement that results in the abnormal fusion of ALK with nucleophosmin (NPM1). NPM-ALK is responsible for a type of Anaplastic Large Cell Lymphoma and has been well studied and proved to be a driver oncogene [35]. In 2007, it

was discovered that the intracellular kinase domain of ALK, fused with the Echinoderm Microtubule-associated protein-Like protein 4 (EML-4), isolated from the DNA of a patient with uncharacterized lung adenocarcinoma, can cause the transformation of mouse fibroblasts. The elucidation of the mechanism, that the kinase is then constitutively dimerized and activated provided excellent ground for its establishment as an oncogenic drug target [36].

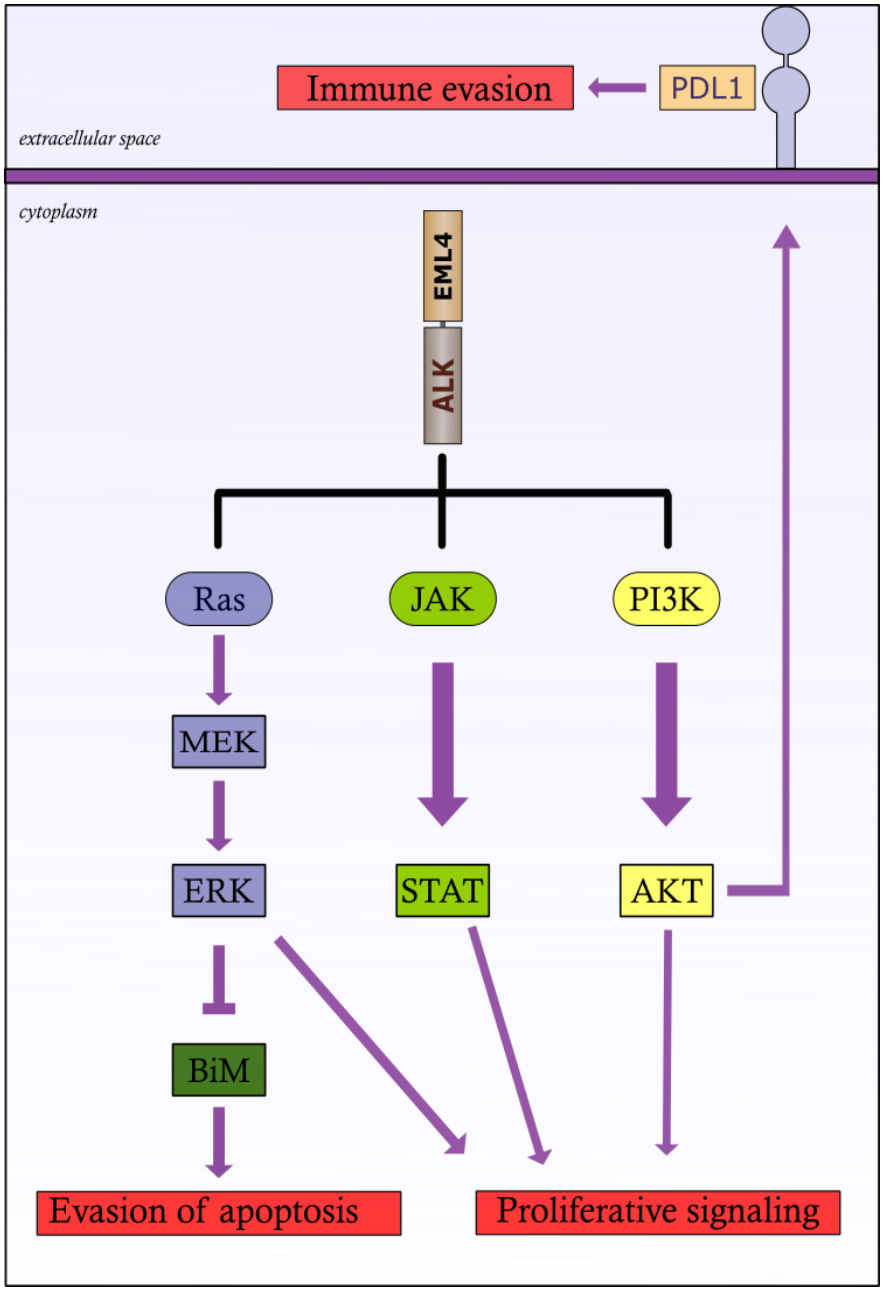

Figure 2: EML4-ALK activates 3 major downstream pathways

A well-researched finding of EML4-ALK signalling is that there is significant MEK/ERK pathway engagement in order to promote proliferation and evade apoptosis [37,38]. The contribution of the JAK-STAT and PI3K-AKT pathways in proliferative signalling is documented [37], but it is not clear whether they are essential for EML4-ALK induced carcinogenesis [39]. Recently, PD-L1 was shown to be downstream of the EML4-ALK-PI3K-AKT axis [40], despite this finding having not been translated to the clinic. Presented is a linearised version of the signalling pathways for reasons of simplicity, however, a more extensive review of ALK signalling can be found in [34,35].

This rearrangement is the result of a paracentric inversion in the short arm of chromosome 2. After that, the exons 20-29 of ALK are retained and are fused with a different number of exons of EML4, which always retains the N-terminal oligomerization domain [41]. The most prevalent variant is variant 1 (E13:A20) (**Figure 3**). The frequency of the 3 most prevalent variants in the rearranged ALK population can be found in (**Table 2**) and is manually curated through the COSMIC database [42] and the work of [43].

Table 2: Frequent EML4-ALK variants

EML4-ALK variant	Frequency	Established cell lines
1 (E13:A20)	24.9-33 %	H3122, STE-1, DFC1032
2 (E20:A20)	7-9 %	-
3a/b (E6a/b:A20)	18.4-29 %	H2228

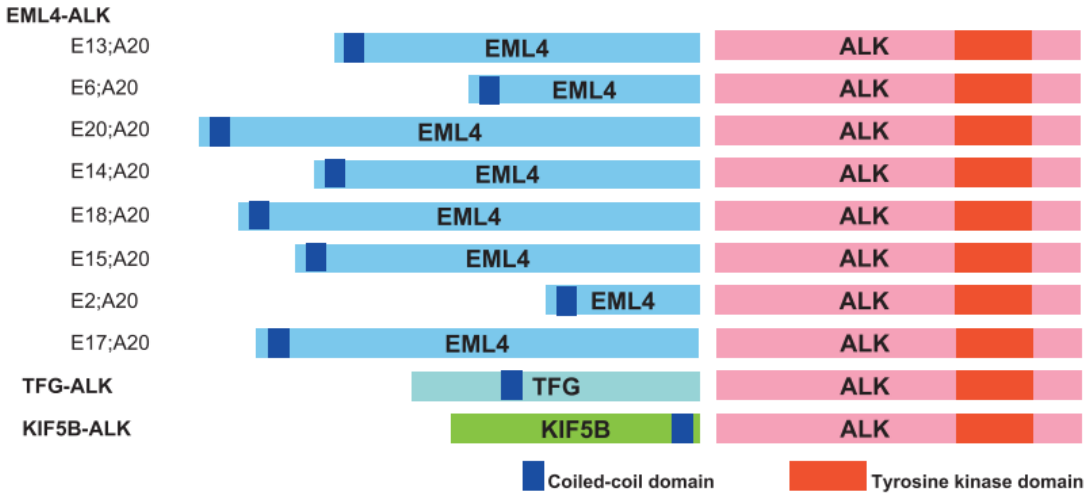

Figure 3: Different EML4-ALK fusion variants

Depicted are the most frequent variants of ALK fusions. E indicates the exon number breakpoint of EML4 and A indicates the exon number breakpoint for ALK. The E13;A20 fusion represents variant 1, which is the most frequently found in the clinic. Clearly, the ALK tyrosine kinase domain is always conserved in different fusions, as is the N-terminal oligomerisation domain of EML4. Adapted from [43]**.**

An initial study in 2009 verified the existence of the EML-4 – ALK fusion in 4-5% of a lung cancer patient cohort [44]. This number was confirmed in a large-scale study of 2013, which very interestingly showed that mutations in EGFR and ALK are mutually exclusive, at least in ALK inhibitor-responsive patients [45]. Similarly, ALK mutations are typically exclusive of other known oncogenic mutations, such as KRAS or BRAF, even though these have been known to arise after the development of resistance to ALK inhibitors [46,47]. In terms of p53 status, about 1/4 of the patients present with an inactivating mutation of the *TP53* gene [48].

There are many other fusion partners for ALK, such as Kinesin 5B (KIF5B), albeit not as frequent as EML4 [49], identified in a variety of human tumours and it has been shown that the partner regulates the fusion protein's subcellular localization and is responsible for the trans-autophosphorylation of the kinase domain. ALK activation results in the downstream activation of several pathways, the most important of which are the PI3K-Akt, JAK-STAT and Ras-MAPK pathway (Hallberg and Palmer, 2013). However, a lot of downstream effectors of ALK are studied in an NPM-ALK context and since the fusion partner can control almost all aspects of downstream activation we should be cautious to assume that the same protein interactions are taking place in EML4-ALK without experimental data to support this.

3.2.1 Variant 3a/b

Interestingly, the shorter variant 3a/b lacks a HELP domain and that is enough to uncouple EML4-ALK from RAS signalling [37], showing that a variant of the same fusion partner can engage different proteins. Substantial differences between variants 1 and 3a/b have been noted in another study, where variant 3a/b was shown to engage the kinases NEK7 and NEK9 to promote cell migration [41]. There are about 15 variants identified to date and the clinical significance of most of these is currently not defined. In [50] it seems that variant 1 correlates with longer survival-free disease compared to the other variants analysed as a group. However, this study took place in only 35 patients so more patients were needed to draw that conclusion. Very interestingly, patients who carry the variant 3 seem to disproportionately develop more on-target mechanisms of resistance, with the G1202R alectinib-resistant mutation being developed only in patients who carry the variant 3 [51]. Furthermore, from the same study, progression-free survival data favoured variant 1, but the number of patients was not large enough to establish this with confidence. However, this was more conclusively demonstrated in a later study [52].

3.3 EML4-ALK signalling

The fusion partner of ALK is crucial for downstream signalling. For example, in neuroblastoma, an activating mutation of ALK signals only through STAT3 and AKT, not through ERK [53]. This suggests that EML4 as a partner is crucial for RAS-MAPK signalling. This was further strengthened later when the EML4-ALK variant 1 was shown to be uniquely engaged with MAPK signalling [37]. Interestingly, there is ubiquitous RAS engagement, since KRAS knockdown itself is not enough to abrogate MAPK signalling but rather H- and N-RAS are concurrently required.

Not all downstream effectors of EML4-ALK are essential for cell proliferation and survival. While inhibition of STAT3 activity does not reduce cell proliferation [37,54], genetic activation of STAT3 can modestly rescue H3122 cells from crizotinib treatment [37]. Regarding the PI3K-Akt pathway, there is contradicting evidence regarding whether it is a downstream and actionable effector of EML4-ALK. An early study found that overexpression of EML4-ALK in 3T3 cells or knockdown in H3122 cells does not affect PI3K-Akt [38]. Hrustanovic et al., reported that reactivation of PI3K-Akt cannot rescue H3122 cells from crizotinib treatment. On the contrary, in neuroblastoma, PI3K-Akt activity is lost after ALK inhibition [55]. Surprisingly, a PI3K/mTOR inhibitor suppressed the proliferation of H3122 cells [54].

Ultimately, the most clinically-relevant evidence comes from *in vivo* engineered models of EML4-ALK. The first study in this regard reported that treatment of EML4-ALK^{MUT} mice with an ALK inhibitor led to reduced phosphorylation of ERK, STAT3 and Akt [54]. In a newer, CRISPR-genetically engineered mouse model of EML4-ALK, upon EML4-ALK activation the tumours stained positively for pERK, pSTAT3 and for pAKT but with less frequency (and intensity) [56]. Therefore, it is most likely that all these described signalling pathways are downstream of EML4-ALK, but with the MAPK-ERK pathway being the most important for proliferation. A newer report suggests that PD-L1, an important new target for immunotherapy is directly in control of EML4-ALK [40]. Despite this fact, PD-L1 antibodies have failed to produce any effect on EML4-ALK^{mut} patients [57].

3.3.1 MAPK pathway significance:

The significance of the MAPK pathway for cell proliferation, particularly in cancer has been known for a long time. The canonical model requires activation of an RTK, which triggers the loading of RAS with GTP, which can then recruit a MAPKKK to the plasma membrane. Then, this activation of a MAPKKK (such as RAF) results in the phosphorylation of a MAPKK (such as MEK). The MAPKK then phosphorylates the last component of the cascade, a MAPK (such as ERK, JNK or p38) [58]. From this, we can assume that an over-activation of this pathway can occur in several spots. The RTK can become over-activated due to gene amplification, activating mutations or ligand amplification. Downstream components can similarly become over-activated due to overexpression or activating mutations.

The importance of this pathway in EML4-ALK cancer has been corroborated recently, with evidence that a combination of upfront ALK and MEK inhibition can prevent or greatly delay the emergence of resistance to these inhibitors [37,59]. Surprisingly, MEK inhibition does not affect cell proliferation in ALK+ ALCL [60], suggesting that MAPK dependence is not a feature of ALCL. These data dictated the commencement of a clinical trial where EML4-ALK patients will be treated with crizotinib or alectinib in combination with low dose trametinib or another MEK inhibitor. This trial is enrolling patients for a Phase I study at the time of writing. Lastly, we should note that the engagement of the MAPK pathway is not a unique feature of EML4-ALK cancer, as a multitude of oncogene-driven cancers primarily activate the canonical MAPK pathway.

3.4 EGFR-driven NSCLC

In advanced NSCLC, a subset of tumours relies on mutant EGFR for proliferation. This is typically the effect of an exon 19 deletion or an L858R point mutation in exon 21 [61]. The frequency of activating EGFR mutations varies a lot among the population, with Asian patients having as much as 45% EGFR mutations among NSCLC patients, while European and American populations range in 15-22% [62]. Gefitinib is a kinase inhibitor that was approved for metastatic NSCLC [63]. Paradoxically, only after the trial and regulatory approval of gefitinib, it became apparent that the effectiveness of gefitinib comes from it inhibiting the EGFR kinase domain [64,65]. Subsequently, erlotinib, another first-generation EGFR inhibitor, was also FDA-approved, providing another clinical option for treatment of this cohort of patients. Erlotinib was trialled versus chemotherapy in patients with EGFR exon 19 deletions and showed an impressive increase in progression-free survival (13.1 months versus 4.6 for chemotherapy) with significantly less toxicity [66]. Later, the irreversible inhibitors afatinib and osimertinib entered clinical development and subsequently received approval. Afatinib is a first-line valid option however it offers similar effectiveness with erlotinib [67].

It is worth noting that osimertinib is breaking new ground by targeting only the mutant form of EGFR and not the wild-type, thus not interfering with the background EGFR activity required by certain somatic cells. The addition of osimertinib as second-line therapy in patients who present the T790M EGFR mutation can provide an average of 13 months of progression-free survival [68].

With all these inhibitors, after initial promising responses, patients often develop resistance [69]. This comes as no surprise given the basic mechanism behind this phenomenon. Development of resistance to RTK inhibitors is inevitable, due to the fact that receptor kinase cascades exist in parallel and utilize the same downstream signals and thus inactivation of one can presumably be replaced by another [70]. Lately, after resistance to EGFR inhibitors arises, it has been shown that patients can derive some benefit by adding the PD-L1 antibody atezolizumab and the VEGF inhibitor bevacizumab to the typical chemotherapy regimen [71].

3.4.1 Mechanisms of resistance

As with ALK inhibitors, on-target kinase domain mutations prevail. Strikingly, EGFR on-target resistance seems to be dominated by the T790M mutation [72], which is effectively inhibited by afatinib and osimertinib. Patients who do not develop kinase domain mutations will typically show a parallel pathway alteration or other oncogenic mutation.

As an example, the levels of the pro-apoptotic protein BIM were shown to be crucial for the response to EGFR inhibition [73]. BIM loss was later shown to contribute to erlotinib resistance, through a BIM polymorphism [74]. In another study, increased signalling mediated by SRC-family kinases (SFK/FAK) was an early event upon osimertinib treatment and subsequently reduced osimertinib efficacy. The authors showed that concurrent inhibition of EGFR with osimertinib and of SRC kinases with dasatinib led to the delayed emergence of resistance *in vitro* and reduced tumour growth *in vivo* in a xenograft model [75]. Lastly, treatment with 3rd generation EGFR inhibitors

such as osimertinib was shown to lead to increased AURKA activity, in cooperation with TPX2. This activity drives persistent resistance to EGFR inhibition. This is a targetable aberration since the combination of EGFR and AURKA inhibition led to the elimination of tumours in a mouse xenograft model of $EGFR^{mut}$ T790M+ lung cancer [76]. Adding to the complexity of the response to TKIs, increased PARylation of RAC1 upon treatment with EGFR inhibitors was observed in numerous cell models [77]. While this is an early event presumed to protect cells from excessive reactive oxygen species generation, it also causes cells to become addicted to PARP activity and therefore become uniquely sensitive to PARP inhibition. Indeed, treatment of mouse xenograft models of TKI resistance with olaparib or niraparib resulted in tumour regression in combination with osimertinib. These data have led to the initiation of a Phase I trial investigating a combination of PARPi + EGFRi in patients resistant to EGFRi (Trial no. NCT03891615).

In addition, interrogation of data obtained from patients who acquired resistance to EGFR inhibitors in the clinic showed once again the heterogeneity of resistance [78]. For example, it was shown that patients who developed resistance to osimertinib developed mutations in oncogenes such as *KRAS*, *MET* and *PIK3CA* [79]. To formally prove that such mutations are the actual driver of resistance, we should expect patient response upon their inhibition. However, for some oncogenes such as KRAS, effective treatments do not exist and it is only through *in vitro* experimentation that we can gather evidence for their action as mechanisms of resistance.

3.5 Diagnosis and treatment of ALK-driven NSCLC

Upon diagnosis of metastatic lung adenocarcinoma, patients are now routinely tested for mutations in known driver oncogenes [80]. The first test that was approved for the detection of the EML4-ALK fusion was a fluorescence in situ hybridization (FISH)-based kit [81]. Later, an IHC-based test was also approved with commercial ALK antibodies. Despite not being as reliable as the FISH-based test, IHC has the advantage of detecting ALK expression *per se*, thus theoretically being capable of detecting novel fusions or other ALK alterations [82]. However, none of the above assays can detect different EML4-ALK variants. Therefore, the use of targeted NGS panels is becoming increasingly common, which allows detection of different variants as well as other driver oncogenes in the same assay [82]. The challenges faced in detecting driver oncogenes in lung cancer has been extensively reviewed in [83].

Following the discovery of ALK-rearranged NSCLC, the small molecule crizotinib (Pfizer) - a potent ALK, ROS-1 and c-MET inhibitor was rapidly tested in clinical trials and gained accelerated approval in 2011 for the treatment of ALK-positive NSCLC [84]. After a primary response of ~60%, patients progress typically within a few months, when resistance to the drug emerges [85]. Specifically, the 2011 trial showed a progression-free survival of 9.7 months and that it was well tolerated. A later trial comparing chemotherapy with crizotinib showed a progression-free survival of 7.7 months for crizotinib and 3 months for chemotherapy, as well as increased quality of life with crizotinib [86].

Several other ALK inhibitors have been developed, whose better affinity for the ALK kinase domain aims to counteract mutations that induce resistance to crizotinib. Of those, ceritinib (or LDK378, by Novartis) was the 2nd to gain FDA approval. In the first-line setting, ceritinib showed a very similar objective response rate of 58% as compared with crizotinib and is effective in approximately half the patients who have become resistant to crizotinib [87]. In the second-line setting, ceritinib extends progression-free survival by at least 4 months compared with chemotherapy [88].

Brigatinib (Takeda) is a second-generation ALK inhibitor which has also received FDA approval. In the first-line setting, brigatinib extended progression-free survival for 2 months compared with crizotinib [89], however, these trial data have not matured and we are eagerly awaiting the results of the updated analysis. Analysis of the reported adverse effects suggests even better tolerability of brigatinib compared with alectinib, which means that if a progression-free survival endpoint is achieved, brigatinib may well become the standard of care replacing alectinib.

Alectinib (Roche), a second-generation inhibitor is the latest addition to the arsenal against ALK-rearranged lung cancer, with accelerated FDA approval for patients who have progressed on crizotinib. Recent data show that first-line alectinib doubles the progression-free survival in a trial compared directly against crizotinib, therefore making alectinib the current standard of care [90]. Interestingly, alectinib was also more well-tolerated and exhibited far superior CNS penetrance and activity against brain metastases. The activity against CNS lesions can very well be the primary reason why alectinib is so potent and has outperformed other ALK inhibitors. Hypothetically, crizotinib can have great activity at the primary lung site, but its failure to penetrate the CNS can lead to earlier disease progression.

Another molecule, ensartinib (Xcovery) is currently undergoing clinical trials, in an attempt to effectively inhibit ALK mutants which are resistant to crizotinib [2]. In preliminary data from a phase I/II trial, ensartinib showed an 80% response rate in ALK inhibitor-naïve patients and 69% response rate in patients pre-treated with crizotinib [91]. Furthermore, in crizotinib-refractory patients, there was still a median of 9-month progression-free survival and intracranial responses. From this cohort, it is evident that ensartinib has meaningful clinical activity where other inhibitors have failed and can be a useful addition in the physician's arsenal, but its use as first-line therapy will probably be rare as alectinib has shown the most impressive first-line response.

The third-generation inhibitor lorlatinib (Pfizer) has undergone a clinical trial as second-line therapy after first or second-generation inhibitors have failed [92] and has subsequently received FDA approval. It is also being tested as first-line therapy and the data will show whether it is going to replace alectinib as the standard of care. Results from the Phase 2 trial suggest that lorlatinib shows high objective response rates in the context of ALK inhibitor-naïve patients, crizotinib-treated patients, or patients treated with at least 2 ALK inhibitors. Given that lorlatinib is very potent in inhibiting the G1202 alectinib-resistant mutation, it is more likely that the clinical use of lorlatinib will be limited to addressing alectinib failure, rather than used in the first-line setting.

Additionally, the impressive outcomes of alectinib will make a head-to-head comparison in the first-line setting difficult as mature results will take several years to become available.

Analysis of aggregate data has shown that the median overall survival (OS) of ALK+ patients is now 6.8 years [93]. As mentioned before, resistance to these new inhibitors is nearly inevitable, due to the nature of the RTK pathways. If the resistance is due to secondary mutations that do not allow for efficient drug binding, then the development of an inhibitor with enhanced target binding properties can typically overcome this problem. However, in the case of patients harbouring parallel pathway alterations, for example, EGFR amplification, inhibition of ALK signalling can be substituted by the amplified parallel pathway. Hence, a new molecule whose only advantage is a more potent inhibition of ALK is not expected to be active in this instance. This highlights the need for new therapeutics.

In the clinical setting, choosing which ALK inhibitor to use is not always easy, as there are more than one approved inhibitors that have different potencies against ALK mutations. Using crizotinib in the first-line setting is likely going to be abandoned due to poor potency as well as poor CNS penetration. Ceritinib is also likely to be abandoned due to the high incidence of side effects. Real-world evidence has made it clear that patients derive the greatest benefit by switching ALK inhibitors upon on-target mutations [94]. We can, therefore, speculate that in the clinical setting we should like to "push" the tumours towards developing on-target alterations rather than switching to different driver oncogenes. While there is no rational basis on how to achieve this, empirical evidence shows that alectinib produces more on-target alterations compared to first-generation inhibitors [47]. The high prevalence of the alectinib-resistant G1202R kinase domain mutation suggests that patients may benefit from the great initial responses offered by alectinib, and then switched to brigatinib or lorlatinib to target the G1202R mutation.

3.6 Other ALK-driven cancers and different fusion partners

In NSCLC, while the EML4-ALK fusion represents the majority of ALK mutations, there have been numerous other fusion partners reported. Soon after EML4, Kinesin-1 heavy chain (KIF5B) was detected as a novel fusion partner of ALK in lung cancer samples [49]. After this discovery, a multitude of new fusion partners was discovered, typically at very low frequency. Specifically, other fusions discovered are TRK-fused gene (TFG-ALK), Dynactin subunit I (DCTN1-ALK), Sequestosome-1 (SQSTM1), Cysteine-rich motor neuron 1 protein (CRIM1-ALK), Striatin (STRN-ALK), Huntingtin-interacting protein 1 (HIP1-ALK), Tyrosine-protein phosphatase non-receptor type 3 (PTPN3-ALK), Kinesin light chain 1 (KLC1-ALK), Clathrin heavy chain 1 (CLTC-ALK), and F-box only protein 36 (FBXO36-ALK), as reviewed in [95]. While there is evidence that several of these fusions respond to ALK inhibition, it is not clear whether every ALK fusion is a *bona fide* driver of disease and is therefore amenable to the use of ALK inhibitors in the clinic. In a case report, a NSCLC patient with a novel myelin transcription factor-like 1 gene (MYT1L-ALK) fusion showed a partial response to crizotinib, ceritinib and alectinib, however without long-term efficient disease control [96]. Most recently, concomitant double ALK fusions of dysferlin gene (DYSF)-ALK and integrin subunit alpha V gene(ITGAV)-ALK were found in the same patient by sequencing material

from a pleural effusion [97]. The patient responded to crizotinib, highlighting again the complexity of lung disease and the opportunities for the application of personalized medicine.

NSCLC is not the only disease that is driven by ALK fusions. About 8-10 % of neuroblastoma patients exhibit amplification of ALK as well as activating mutations, some of which are sensitive to lorlatinib treatment [53,98]. In the clinic, ALK inhibition was not as rapidly tested in neuroblastoma as it was in NSCLC, with a Phase I/II trial of crizotinib only now being undertaken. Anaplastic Large Cell Lymphoma (ALCL) is so influenced by ALK mutation status that is primarily separated in ALK^- and ALK^+ subtypes. The most common fusion partner for ALCL is Nucleophosmin (NPM-ALK) [99]. In patients with relapsed ALCL, crizotinib treatment led to a 90% objective response rate and was deemed an effective therapy [100]. Except for ALCLC, a patient with a myofibroblastic tumour presented a fusion with Tropomyosin 3 (TPM3-ALK). Importantly, this patient responded to crizotinib and upon progression to crizotinib then responded to ceritinib with a prolonged response, confirming the hypothesis that this fusion had an oncogenic capacity in this context [101].

In renal cell carcinoma (RCC), a karyotypic examination of a cohort of pediatric patient samples led to the discovery of a novel fusion with Vinculin (VCL-ALK) [102]. Notably, in a phase II trial of the pan-TRK and ALK inhibitor entrectinib, a patient with ALK+ RCC had an objective response to entrectinib [103]. In the same trial, a novel ALK rearrangement (CAD-ALK, Carbamoyl-phosphate synthetase 2, aspartate transcarbamylase, and dihydroorotase-ALK) was detected in a patient with colorectal cancer, who also showed an objective response to entrectinib.

Other than fusions, in melanoma, alternative transcription initiation leads to novel ALK isoforms which code for mutant ALK proteins that can initiate tumourigenesis in mice. These tumours respond to crizotinib and were surprisingly detected in a large number of melanoma patients, suggesting that as many as 11% of patients with melanoma may carry this aberration and could potentially benefit from ALK inhibitors [104]. Most importantly, since there is no genomic alteration, this would be exceptionally hard to detect through conventional sequencing of a limited clinical sample. Lately, the actual oncogenicity of the ALK^{ATI} mutation is being questioned in the clinic [105].

All these data suggest that there is likely a significant number of tumours, the underlying driver of which is some sort of ALK mutation, which cannot be detected through conventional means. Subsequently, these tumours are going to remain unidentified unless ALK mutations are investigated specifically. Furthermore, the successful individual case reports suggest that if a genomic screening (which allows fusion detection) was routinely performed in cancer, a lot of patients would benefit from personalized, targeted therapies.

4 CDK inhibition as an approach to circumvent acquired drug resistance

4.1 Introduction

It is speculated that the variation in response to crizotinib treatment in the clinic can be accounted to intrinsic resistance but this has not been researched thoroughly yet. Given the lack of initial response in a percentage of patients [90], a case can be made for pre-existing mechanisms of resistance to ALK inhibitors. An overview of intrinsic or acquired mechanisms of resistance follows below:

4.1.1 Tools for studying mechanisms of resistance

After years of research, the accumulating evidence points to the fact that mechanisms of resistance can vary widely from patient to patient. As a result, the clinical action against these mechanisms is very challenging, since an aberration in just one patient can be clinically meaningful for this particular patient, but not for others. In a cohort of several patients or clinical samples, a mutation or aberration in only one of them will most likely be overlooked in the absence of previous functional data that would implicate this aberration. This makes the use of cell culture models invaluable, where proof of principle for certain aberrations can be obtained beforehand and subsequently inform clinical findings. As an example, by artificial overexpression of human cDNAs in EML4-ALK cell lines, the transcription factors ETV1 and c-FOS were shown to be able to confer resistance to crizotinib [1]. While to my knowledge, amplification of these has never been observed in EML4-ALK^{+} patients, the knowledge obtained from this cell culture model may help to direct a clinical decision should these genes appear dysregulated in the clinic.

In addition to cell culture models, there are also EML4-ALK mouse models available. Arguably, the genetically engineered mouse model that most closely recapitulates the human disease is an insertion of the EML4-ALK fusion by the CRISPR-Cas9 system in the lungs of mice by Adenoviral infection, which leads to EML4-ALK-driven lung tumours within a few months [56]. These tumours respond to ALK inhibitors, so to study mechanisms of resistance they would require serial passaging in several mice until these tumours became refractory to the drug. Lastly, the ideal model would be a patient-derived xenograft after this patient became non-responsive in the clinic. Some of these models are now starting to become commercially available.

4.1.2 Mechanisms of resistance to ALK inhibitors

4.1.2.1 On-target kinase mutations

Secondary ALK kinase domain mutations or gene amplifications have been reported in about one-third of patients treated with crizotinib and may be higher for patients treated with newer ALK inhibitors such as alectinib [45,47]. These mutations are detected after cancer tissue extraction with a follow-up biopsy or using liquid biopsy testing after it was shown that blood and tissue NGS-genotyping has high concordance [106]. Since this test is either NGS-based or PCR-based, it

requires highly specialized personnel and equipment, thus is typically outsource to companies or diagnostic centres outside of the primary hospital centre.

It is worth noting that the possibility that a kinase domain mutation has been missed in the post-resistance biopsy can't be excluded, either due to clonal heterogeneity or failure of the diagnostic assay. Therefore, the actual clinical frequency of on-target mutations may be higher.

A typical mutation in the ALK kinase domain is the L1196M gatekeeper mutation, reminiscent of the T790M gatekeeper mutation in the EGFR kinase domain. This results in hindered small molecule binding and resistance to pharmacological inhibition [11]. In [47], 20% of samples from crizotinib-resistant patients contained ALK mutations. Recent studies have reported results for newer ALK inhibitors. Interestingly, second-generation ALK inhibitors exhibited higher rates of on-target mutations. Ceritinib-resistant specimens harboured ALK mutations at a rate of 54%, while alectinib-resistant specimens at 52%. Even more interestingly, as we progress towards better ALK inhibitors, the range of potential ALK alterations decreases. With crizotinib, there were at least 9 on-target mutations identified, while with ceritinib and alectinib there were 5 and 4 respectively. Alectinib seems to be particularly hampered by the G1202R mutation which was the most prevalent in this cohort. Fortunately, this mutation is successfully targeted by the 3rd generation inhibitor, lorlatinib [107]. Lorlatinib-resistant mutations appear to be harder to appear and are usually compound mutations [108]. However, even in the case of the lorlatinib-resistant mutation L1198F, it actually re-sensitised the patient to crizotinib treatment [109]. It is therefore evident that on-target, kinase domain mutations can be treated and kept in remission by alternating drugs for an extended period of time which was previously unimaginable in NSCLC. However, this leaves a significant number of patients with acquired resistance with an unexplained underlying mechanism. Amplifications or alterations in converging oncogenic pathways can typically explain the aforementioned mechanism (**Figure 4**).

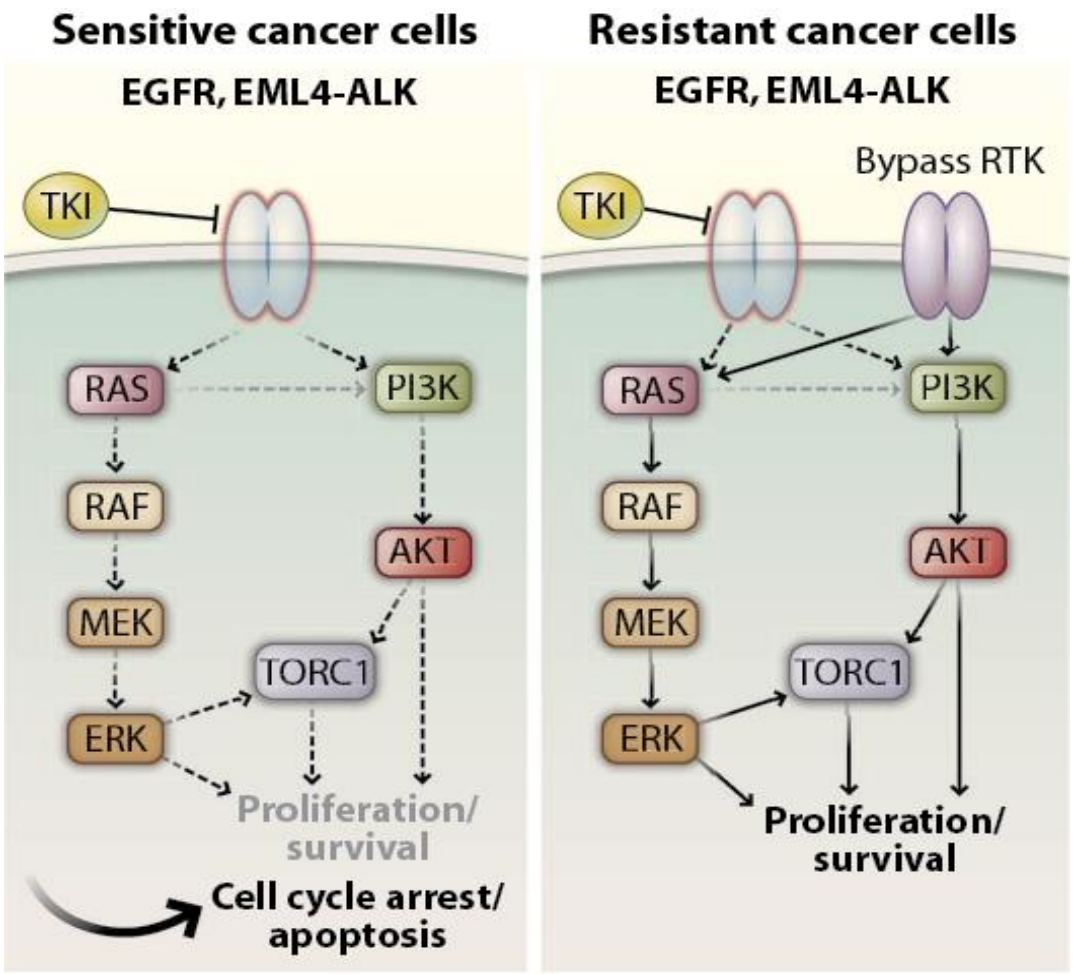

Figure 4: How a parallel RTK pathway can compensate for the loss of another.
In the left panel, disruption of oncogenic signalling by driver oncogenes such as EGFR or EML4-ALK, leads to cell cycle arrest and/or apoptosis. In the right panel, in cells with acquired resistance to TKIs, another bypass receptor tyrosine kinase is frequently over-activated and compensates for EGFR or EML4-ALK inhibition by engaging the same oncogenic pathways. Adapted from [110].

4.1.2.2 ALK loss

One of the most puzzling mechanisms of resistance is an oncogenic switch, which replaces the main driver oncogene with a different one. In this case, the two oncogenes were initially driving the disease albeit with unequal contribution. After the emergence of resistance, the balance is shifted towards one of the oncogenes which assumes the main role. An example of this can be found in rhabdoid tumours, where PDGFRα and FGFR1 over-activation co-existed initially, however after the tumours became resistant to the multi-kinase inhibitor pazopanib, PDGFRa was largely lost and FGFR1 overactivation substituted for this loss. Interestingly, this over-activation renders the cells sensitive to FGFR1 inhibition, highlighting an opportunity for rapid drug switching when the underlying molecular causes of resistance are well studied [111]. In EML4-ALK cancer, this has been observed *in vitro* and *in vivo* [46].

4.1.2.3 EGFR upregulation

Among the most important proteins implicated in crizotinib resistance is the family of Epidermal Growth Factor Receptors. It has been speculated that there are similarities between EGFR- and ALK-driven NSCLC, including similarities in resistance mechanisms. Accordingly, numerous genes that can confer resistance to ALK inhibition also increase resistance to EGFR inhibition when overexpressed in cell lines [1]. The use of EGFR inhibitors increased cell death in ALK-rearranged patient models suggesting that EGFR signalling was over-activated in these occasions [112]. Also, crizotinib-resistant cell lines had significant upregulation of the EGF receptor identified through increased mRNA as well as increased ligand levels (amphiregulin and NRG1), [113]. Notably, this upregulation cannot by itself account for the resistance, since the use of EGFR inhibitors was not potent enough to suppress cell growth, suggesting that there might be a co-existent, undiscovered mechanism. In another study in cell lines accompanied by a clinical observation, EGFR, HER2 and HER3, as well as the EGF ligand, were found to be upregulated in a crizotinib-resistant context [114].

4.1.2.4 KRAS activation

Analysis of patient material has revealed an interesting phenomenon, where a KRAS activating mutation was discovered in a patient after the emergence of crizotinib resistance. Strikingly, EML4-ALK was not found after treatment in the same patient [46]. A possible explanation for this is that a subset of tumour cells lack rearranged ALK, but have mutant KRAS which is a known potent oncogene. After crizotinib treatment, the EML4-ALK$^+$ population is diminished, resulting in cells with mutant KRAS becoming now more numerous and eventually overtaking the tumour population. In such a setting, the initial screening cannot identify whether these mutations are present in the same cells and also the post-treatment screening may come up paradoxically as EML4-ALK-negative.

4.1.2.5 HER2/HER3 and P2Y2 as mediators of resistance

In a high-throughput screening attempt to identify genomic areas whose overexpression can confer resistance to ALK inhibitors, the authors show that overexpression of the purinergic receptor (P2Y) family makes EML4-ALK^{mut} cells more resistant to crizotinib [1]. Through *in vivo* screening of patient samples, it became apparent that while this is a rare mechanism of resistance, it can still be detected in the clinic. Upfront inhibition of ALK with crizotinib/ceritinib and P2Y with sotrastaurin greatly delayed the emergence of resistance in H3122 cells. Unfortunately, good compounds against the purinergic receptors have not been developed, otherwise, the clinical effectiveness of a P2Y2 inhibitor would prove that this is the actual mediator of crizotinib resistance. Another hit in the screen that has been re-capitulated in the literature is NRG1 (neuregulin) [113], which activates HER2/HER3 signalling, however, this result was not expanded on in that study.

4.1.2.6 IGF1-R activation

The emergence of IGF1-R signalling as a substitute for ALK was discovered studying a patient who participated in a clinical trial and responded very well to therapy with an anti-IGFR1-R antibody. After experiments with EML4-ALK cell lines with acquired resistance to ALK inhibitors, it became apparent that IGF-1 ligand upregulation can over-activate IGF1-R signalling and over-compensate for the lack of EML4-ALK signalling [3]. Interestingly, ceritinib is a potent IGF1-R inhibitor, suggesting that patients with this particular mechanism of resistance would respond well to second-line ceritinib.

4.1.2.7 Similarities with other oncogene-driven cancers

Oncogene-driven lung adenocarcinomas seem to share a lot of similarities. Particularly EGFR- and ALK-mutant cancer share common alternative receptor tyrosine kinase activation, such as MET, c-KIT and others as reviewed in [115]. Furthermore, RET-rearranged lung cancer has been shown to become resistant to RET inhibition mainly through reactivation of the MAPK pathway [116]. Still, there are also unique differences. For example, in EGFR-mutant NSCLC, there was activation of NF-κB in response to EGFR inhibition shown *in vitro* [117]. However, this was not the case in EML4-ALK mutant cells which did not activate NF-κB.

4.1.2.8 SRC inhibition without an obvious molecular alteration

The call for personalised medicine has attracted the development of new methods for drug screening, such as testing large panels of compounds in patient-derived cell lines. In an approach by Crystal et al., [112], apart from effective drug combinations, new mechanisms of resistance to ALK were identified. By measuring the effect on cell proliferation of various small molecule inhibitors, the authors were able to identify the non-receptor protein kinase SRC as vital in mediating resistance to RTK inhibition. Specifically, SRC inhibitors were able to suppress cell proliferation in the majority of patient models. These data may suggest that ALK normally suppresses SRC, which is supported by the extensive upregulation of SRC observed upon ALK inhibition. Reinforcing these findings, synchronous SRC and ALK inhibition largely relieved xenograft tumours in mice from tumour growth over 60 days. The benefit of this approach is that it dictates a new therapeutic regimen in an agnostic fashion, even when the underlying biological

interactions are not known or studied yet. This is in contrast with genetic screening which requires the previous knowledge of the mutations to be screened. Additionally, since SRC activation is not associated with any one particular mechanism of resistance, this opens the possibility to exploit SRC inhibition as a ubiquitous measure of re-sensitising refractory patients to ALK inhibitors. Of course, this would be tested in the context of patients who do not harbour ALK kinase domain mutations.

It is easy to gather that the heterogeneous and constantly evolving mechanisms of resistance make it very challenging to achieve long-term control of the disease. Even if there was a method to rapidly screen for the mechanism of resistance and address it pharmacologically, this would only be effective for a short period of time before another mechanism of resistance arose. Therefore, we could conceive that rational, upfront drug combinations that can prevent the emergence of resistance have a higher likelihood of success.

4.1.2.9 Upfront MEK inhibition- DUSP6

From the above, we can deduce that the majority of the mechanisms of acquired resistance rely on re-activation of the MAPK pathway. This was further substantiated in [37], where EML4-ALK was shown to activate all 3 major Ras isoforms causing extensive MAPK signalling and driving cell proliferation, which was insufficiently suppressed by ALK inhibition. The potential outcomes of MAPK pathway activation can be quite diverse. Acting through a kinase cascade, this pathway results in the activation of a variety of transcription factors, which are mainly responsible for cell proliferation but have also been shown to initiate apoptosis [58]. Reactivation of the MAPK pathway has also been demonstrated in the resistance to targeted therapies in melanoma, which gives reason to further investigate this occurrence, perhaps as a general mechanism of drug resistance that appears in various solid tumours [118].

This observation likely gave rise to the hypothesis that treating patients with low concentrations of MEK inhibitors along with crizotinib might prevent MAPK pathway reactivation and form a good basis for a novel therapeutic approach [37]. In this study, two potential mechanisms were identified as able to enhance MAPK signalling and were also confirmed in patient samples. Firstly, while no activating mutations were observed, $KRAS^{WT}$ showed focal amplification or gene duplication in some cells and this was enough to stimulate pervasive cell proliferation. Secondly, the ERK-specific phosphatase and critical regulator, DUSP6, was found to be downregulated in crizotinib-resistant cells. DUSP6 knockdown could re-sensitise these cells to crizotinib. Moreover, low-dose trametinib in combination with ALK inhibitors was enough to prevent the emergence of acquired resistance, both *in vitro* and *in vivo.* It is surprising that in a previous dataset only one patient-derived model responded adequately to MAPK inhibition [112]. Still, even in a single patient-derived model, concurrent MEK and ALK inhibition gave markedly strong anti-proliferative effects. Also, decoding which components of the pathway can mediate resistance can be a worthwhile investigation. After these findings, a clinical trial protocol combining ceritinib + low-dose trametinib upfront for the treatment of EML4-ALK patients has been initiated (trial no.

NCT03087448). The outcomes of this trial will be pivotal for the concept of upfront combinations of TKIs with other compounds that aim to prevent drug resistance.

Recently, another key finding was made regarding the importance of the MAPK pathway. The protein phosphatase SHP2 was shown to be necessary for MAPK re-activation [119]. Accordingly, treatment of EML4-ALK patient-derived xenografts with the SHP2 inhibitor SHP099 was synergistic and led to durable responses in combination with ceritinib. Further, in a xenograft model from a patient who became refractory to ceritinib, treatment with SHP099 restored ceritinib sensitivity and led to the suppression of tumour growth. Given the enormous complexity of the potential mechanisms of resistance that can arise from TKI treatment, a compound that is effective irrespectively of the mechanism of resistance can be of profound clinical usefulness. There are currently 2 on-going clinical trials that will evaluate the activity of SHP2 inhibitors in cancers with MAPK overactivation (trial no. NCT03634982, NCT03114319). Should these trials prove safe dosing and adequate target engagement in monotherapy, this would open the road to quicker testing of these compounds in combination with ALK inhibitors.

4.1.2.10 Treatments that eliminate resistant cells without addressing a particular mechanism

Certain drugs seem to be particularly active in a certain context without a molecular alteration as the rational basis for a new therapy. In this case, while basic research tries to understand the reasons behind this phenomenon, it is without a doubt that for the benefit of patients, clinical testing of these compounds should be encouraged.

An example of this in EML4-ALK lung cancer is the use of the heat-shock protein 90 (HSP90) inhibitors ganetespib. EML4-ALK has long been known to be a client of HSP90 which ensures proper protein folding. It has been shown before that inhibiting HSP90 activity with ganetespib can be as effective as, or even more effective than, crizotinib. An upfront combination of ganetespib and crizotinib can greatly delay the emergence of resistant clones, while the use of single-agent ganetespib in cells that have already acquired resistance can effectively suppress their proliferation [54,120]. However, all the clinical trials for ganetespib have been terminated due to lack of efficacy *in vivo*, so it is unlikely that this combination will be tested in the future, at least until an HSP90 inhibitor with better pharmacological properties is discovered. Also, as expanded before, the potential upfront use of a combination of trametinib with ALK inhibitors should be noted [37].

4.1.2.11 Epithelial-to-mesenchymal transition

The epithelial-to-mesenchymal transition is a well-documented feature of cancer cells and it is postulated to alter their invasive and metastatic properties [121]. In cell models of acquired resistance to ALK inhibitors, differential expression of EMT-related genes, as well as mesenchymal characteristics, have been consistently noted. In H2228 crizotinib-resistant cells, TGF-β upregulation induced Vimentin upregulation and loss of E-Cadherin, suggesting a mesenchymal phenotype [122]. Also, knockdown of Vimentin in combination with crizotinib synergistically reduced cell proliferation, indicating that drug resistance was, at least in part, mediated by EMT. The same effect for TGF-β was recapitulated in a later report, where the authors showed that it mediated AXL-induced EMT [123]. AXL inhibition with the small molecule R428 was enough to

rescue the EMT phenotype, however, the only functional data regarding cell proliferation were surprisingly supplied with HSP90 inhibitors instead of AXL inhibitors making it impossible to specifically assess EMT.

Interestingly, in a later report in crizotinib-resistant H3122 cells, EMT was shown to be mediated by AXL [124]. However, AXL knockdown did not restore crizotinib sensitivity, but it greatly affected migration and invasion capabilities *in vitro*. The authors concluded that EMT is only associated with but is not causal to ALK inhibition resistance. Furthermore, ALK^{mut} cell lines exhibited distinct enrichment in EMT genes and the authors showed that ectopic overexpression of EML4-ALK in normal epithelial cells initiates an EMT program via the epithelial splicing regulatory protein 1 (ESRP1) [123].

A cohort of pre- and post- ALK-TKI specimens showed that EMT markers can be detected in a subset of patients upon progression on ALK inhibitors. In [47], 3/11 resistant specimens concurrently had ALK kinase domain mutations as well as EMT phenotypes, while 2/11 specimens exhibited EMT only. While it was not possible to assess the role of EMT in these patients, it is conceivable that EMT exhibits synergism with another driver of resistance to prevent response to ALK inhibition.

Despite several publications researching the role of EMT in EML4-ALK lung cancer, it is still not clear whether its role is causative or correlative. The latest research addition showed that epithelial and mesenchymal cells can exist in independent populations in different tumour lesions [125]. While the examined patient acquired the L1196 gatekeeper mutation, it was shown that the mutation was predominantly detected in the epithelial lesion. While this suggests that this patient had 2 concurrent mechanisms of resistance to crizotinib, one caused by the gatekeeper mutation and one caused by EMT, the contribution of EMT to resistance was not experimentally addressed. A limitation of this study is that the different cell populations were detected in only one patient and that the rest of the functional studies came from a mouse cell line xenograft model which may not accurately reflect the human condition.

4.1.3 Residual-persister cells

It has been a long-standing observation that *in vitro* treatment of cells with a lethal dose of TKIs, does not result in the complete elimination of cancer cells. It has been repeatedly observed that after several days the remaining cells can recover and start proliferating again, or given more time, become resistant to this drug dose and start forming colonies [126]. There are several possible explanations for the lack of complete response to targeted therapies. Firstly, it is useful to differentiate between cytotoxic and cytostatic therapies. Highly cytotoxic therapies like targeted therapies, rapidly select for resistant clones. However, cytostatic therapies will allow most cells to remain and occupy space and resources, minimising the evolutionary potential of resistance. Moreover, by suppressing cell division, cytostatic drugs minimise the emergence of de novo mutations [127].

One hypothesis is that there are always cancer stem cells that survive the treatment and after some time can differentiate and give rise to resistant clones. This state may be a plastic state, which can be initiated or ended depending upon extracellular signals. For example, in bladder cancer, chemotherapy-killed cells release prostaglandins which result in the increased survival of cancer stem cells [128]. However, the existence of cancer stem cells depends on the tumour context and it can't be easily assessed [129].

There is significant work in a variety of oncogene-driven cell lines that has shed more light on the existence of persistent or drug-tolerant cells. Specifically, the cancer stem cell marker ALDH1A1 was overexpressed in persister cells and was further shown to be strictly required for their survival. Pharmacological inhibition of ALDH1A1 led to preferential apoptosis of persister cells and its combination with the primary TKI led to a profound and durable response [130]. More vulnerabilities of drug-tolerant cells have been described, such as the histone demethylase KDM5 [131]. Interestingly, in this study, it was shown that the drug-tolerant population was pre-existing and this vulnerability could successfully be targeted before the commencement of the primary TKI treatment.

Lately, in EGFR-mutant NSCLC it was observed that the drug-tolerant state may not be clearly defined initially but is rather a transient state that cells can acquire upon strong selective pressure from TKI treatment. Furthermore, this transient population can provide a starting point for the emergence of incredibly diverse mutations that promote drug resistance, as observed from single-cell derived pools [132]. It is therefore likely that resistance mutations both pre-exist and arise later in oncogene-driven cells. The fact that even the highest initial drug doses can leave a number of cells unharmed, suggests that there is always a subpopulation of cells with the intrinsic capacity to enter a quiescent state and give rise to a drug-resistant population eventually.

Another ground-breaking finding in the battle against surviving persister cells came from studying HER2-amplified breast cancer. Through a large-scale small molecule inhibitor screening, it was discovered that persister cells are sensitive to the inhibition of the lipid hydroperoxidase GPX4 [133]. This inhibition could eliminate persister cells *in vitro* by induction of ferroptotic cell death as well as prevent tumour relapse in mice, however, there is reasonable doubt that the RSL3 compound that was used is not suitable for human testing. As a result, clinical testing of the combination of GPX4 inhibition with other TKIs has not been scheduled yet, at least to my knowledge.

4.1.4 Intrinsic resistance & tumour heterogeneity

The previous discussion regarding persister cells suggests that in some oncogene-driven cancers, a subset of the tumour population may be resistant to the therapy used from the start. Being a non-mutational mechanism, this would explain intrinsic or primary drug resistance instead of acquired. Another phenomenon that may mix up the distinction between primary and acquired resistance is tumour heterogeneity. Possibly, in an ALK^{mut} tumour, the majority of cells are ALK^{mut}, but a minority of them are ALK^{wt} and driven by another oncogenic mutation. In this case, ALK-directed therapy will deplete the ALK^{mut} fraction and allow the ALK^{wt} population to dominate the tumour. This is arguably conceptually closer to intrinsic resistance. This is clearly relevant in lung cancer, as the TRACERx study showed that driver mutations in lung cancer specimens are almost always clonal when examined in samples from different areas of the same tumour [134].

At this stage, it may be useful to draw an analogy to blood malignancies. In acute myeloid leukaemia, it is well-known that the existence of cancer stem cells leads to relapses. As discussed before, cancer stem cells may represent a plastic state, with cells entering in and out of it freely, which greatly complicates their detection. Despite the fact that cancer stem cells are not generally accepted in lung cancer, the paradigm of phenotypic plasticity can lead to the hypothesis that there is a nuanced contribution of both adaptive and intrinsic drug resistance in solid tumours. Supporting this hypothesis, a recent analysis of the evolution of $EGFR^{mut}$ tumour volume in the clinic shows that the only mathematical model that fits the observed evolution is a combination of an intrinsically-resistant population and a slow-growing, resistant population through adaptation [135]. Also, in confirmation of such plastic phenotypic state, in $EGFR^{mut}$ tumours, persister cells clearly contribute to relapse and have been shown to be driven by a transcriptional program, which is largely adaptive [136].

In an EML4-ALK-specific context, a way for drug-tolerant cells to survive ALK inhibition has been shown to slow their proliferation in the presence of the drug, which despite not being enough to support tumour re-population, can be easily augmented upon the acquisition of new mutations. Through the introduction of DNA barcodes and subsequent sequencing, the authors showed that these drug-tolerant populations are pre-existing, and the selective pressure applied by different ALK inhibitors leads to different adaptive drug resistance [137]. Lastly, focusing only on the tumour cells *per se* would discount the, increasingly identified as important, role of the tumour microenvironment. In ALK-driven lung cancer, *in vitro* experiments have shown that the presence or absence of fibroblasts can greatly affect the emergence of resistance to ALK inhibitors [138].

Thus, lung-cancer specific data collectively point to a greatly complex path towards the acquisition of drug resistance, with contribution from intrinsic cell properties, clonality of mutations, adaptive responses driven by different oncogene inhibitors and input from the tumour environment.

4.1.5 Cell cycle in NSCLC

Dysregulation of the cell cycle is an important hallmark of carcinogenesis [139] as it is a fundamental aspect of growth and proliferation. However, in different types of cancer, alterations

in cell cycle genes do not have the same significance. Cell cycle progression relies on the kinase activity of Cyclin-Dependent Kinases (**Figure 5**). A great review of their individual roles can be found in [140]. In humans, 21 genes have been discovered which code for serine/threonine kinases and comprise the CDK family [141].

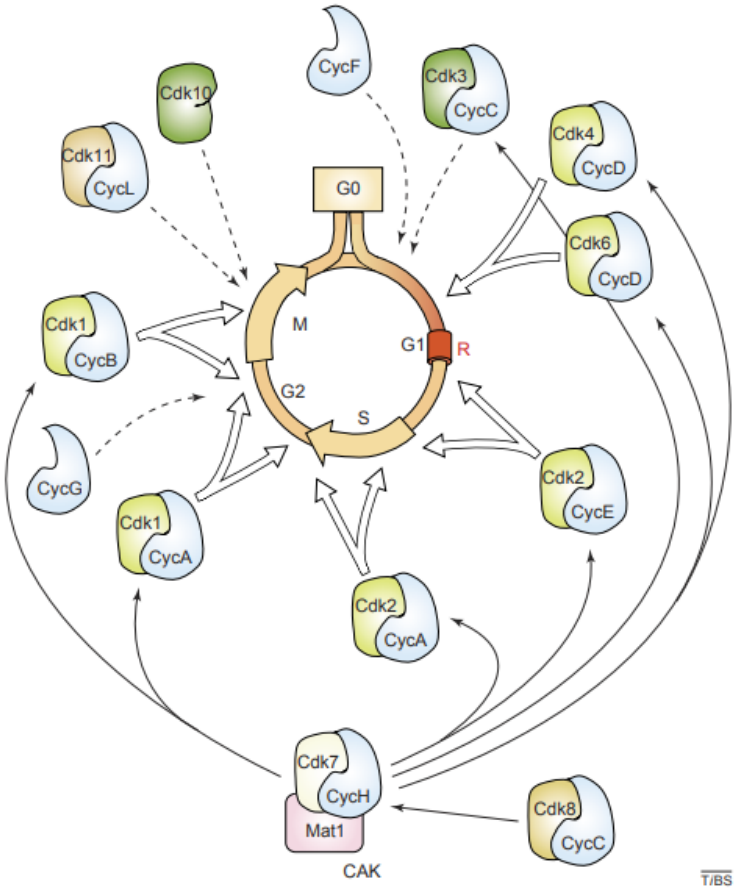

Figure 5: The role of CDKs in each phase of the cell cycle

Cell cycle progression is dependent upon the activity of CDKs and their partner cyclins. Generally, proliferative signals stimulate CDK4 and CDK6 to initiate cell cycle entry. Later, transcription of type A and type E cyclins lead CDK2 to initiate DNA replication. After the association of CDK1 with cyclin B or cyclin A, CDK1 phosphorylates protein targets necessary for G2/M progression. Lastly, the degradation of cyclin B is necessary for anaphase to occur. Other CDKs such as CDK7 seem to have less of a stage-specific role but are overarching activators of cyclins and transcription. Checkpoints are in place to ensure inhibition of CDK/Cyclin activity upon errors in cell division or DNA replication. A more extensive review of the process can be found in [140]. Image adapted from [140].

Mutations or copy number gains seem to preferentially accumulate in a subset of these CDK or cyclin genes, such as *CDK4/6* and *CCND1*. A splicing event has been shown to be oncogenic for cyclin D1, even in the absence of other somatic mutations [142,143]. Furthermore, *CCND1* appears altered in 6% of the TCGA pan-tumour cohort (http://cancergenome.nih.gov/). Cyclin E1 is similarly oncogenic. In high-grade serous ovarian cancer, overexpression of the *CCNE1* gene through copy number alteration or post-transcriptional regulation is a determinant of malignant transformation of fallopian tube cells. Furthermore, cyclin E1 overexpression was enough to induce anchorage-independent growth of primary human fallopian tube cells, suggesting that cyclin E1 is a *bona fide* oncogene in this context [144].

Given that CDK1 activity has to be reduced in order for cells to exit mitosis, it is not likely that direct CDK1 dysregulation will have oncogenic characteristics [145]. However, the expression of its partner cyclin, cyclin B1 has been shown to correlate with poor survival in breast cancer [146]. Of course, this does not guarantee a causal relationship, however to my knowledge artificial overexpression of cyclin B1 has not been functionally investigated for potential oncogenic action.

While all these mutations are widely considered oncogenic, to my knowledge, there is no formal proof that they can initiate tumours *in vivo*. Rather, they act as aids in the tumourigenic process, accelerating cell proliferation. Also, an effort to induce the most common human CDK mutations in mice and evaluate the tumourigenic effects has not yet been undertaken. Ultimately, evidence for the functional role of CDK mutations in cancer comes from the recent clinical success and FDA approval of the CDK4/6 inhibitors palbociclib, ribociclib and abemaciclib for the treatment of a molecularly-defined subset of advanced breast cancer. It is worth noting that in NSCLC, palbociclib trials have shown no improvement in patient response or survival compared to chemotherapy [147]. It would be interesting to dissect whether the reduced efficacy of this inhibitor was due to a poorly defined molecular signature of the selected patients.

4.1.6 CDK inhibitors

A multitude of CDK inhibitors has been developed to date. The naturally-occurring flavones gave birth to the pan-CDK inhibitor flavopiridol [148]. Later, dinaciclib was discovered by Merck, with selectivity towards CDK1, CDK2, CDK5 and CDK9, while achieving tumour regression at 80% of the maximum tolerated dose in mice [149]. The need to develop a CDK7-specific inhibitor led to the discovery of THZ1 [150], a CDK7/12 inhibitor which exhibited anti-tumour activity in a broad spectrum of tumour cells. To achieve CDK4/6 inhibition in breast cancer, palbociclib [151] was developed and was later granted FDA approval. In the clinic, none of the pan-CDK or CDK7 inhibitors have shown enough activity to warrant market approval [145]. The reasons for this are likely poor patient selection that was not guided by biomarkers and a lack of therapeutic window in

order to spare non-malignant cells and keep toxicity to a minimum. Of particular interest in ALK-driven cancers, ceritinib has been shown to synergise with the CDK4/6 inhibitor ribociclib as an upfront combination treatment in ALK-driven neuroblastoma [152]. A subsequent clinical trial in EML4-ALK patients (trial no NCT02292550) is still on-going, however, an initial phase I announcement suggests that there is no additional benefit from ribociclib, though this remains to be established in phase II.

4.1.7 Transcriptional addiction: An emerging pattern in tumours

Lately, increased transcriptional output as a feature of various cancers has gained increased attention. The addiction to transcription factors as driver oncogenes has been thoroughly reviewed in [153]. It appears that a multitude of solid tumours rely on high levels of transcription to support the expression of their oncogenes [154–156]. In the context studied herein, in EGFR- and EML4-ALK- mutant lung cancer cell lines, the authors showed that these cells rely on super enhancer-driven transcription for their oncogenic signalling, which can be specifically perturbed with low levels of transcriptional inhibition [156]. This suggests that a therapeutic window may exist, in which tumour cells can have transcriptional inhibition at a level sufficient so that it induces apoptosis, whereas normal, non-transcriptionally addicted cells are spared. Until a time comes that transcription factors are easily druggable, it appears that the best solution is to influence the transcriptional machinery indirectly, by targeting Cyclin-Dependent Kinases which control the RNA polymerase II. Specifically, CDK7 and CDK9 are known to control the elongation step of transcription by RNA pol II [157,158].

4.1.8 Transcription-associated CDKs

Phosphorylation of the RNA polymerase II C-terminal domain (CTD) is a crucial step for transcription initiation [159]. CDK7 along with cyclin H are parts of the transcription factor II (TFII) complex and phosphorylate the RNA pol II at the Ser5 and Ser7 sites [160]. CDK7 phosphorylates CDK9, which then phosphorylates the Ser2 site of the RNA pol II [161]. Thus, CDK7, directly and indirectly, affects the CTD of the RNA pol II. CDK9 along with cyclin T form the P-TEFb complex and control transcriptional elongation, phosphorylating Ser2 primarily, but also Ser5 and Ser7 [162]. By virtue of these facts, it has been shown that CDK7 inhibition with a covalent inhibitor affected RNA pol II occupancy at both promoters and gene bodies [150] while CDK9 inhibition increased occupancy at the promoters and decreased it at gene bodies, consistent with a role in transcriptional elongation. Very recently, it was discovered that modifications in the RNA pol II CTD are not CDK7 specific since there is a requirement for CDK12/13 activity in combination with CDK7 activity for Ser5 phosphorylation [163]. Interestingly, both CDK7 and CDK9 have been linked to epigenetic modifications [158,164], which raises concerns for cancer treatment. Specifically, prolonged CDK7 or CDK9 inhibition in cancer patients, may result in epigenetic changes that will have dire consequences after their therapy is completed, therefore these effects need to be taken into account and be better studied.

4.1.9 Apoptosis

It is evident that in terms of reducing tumour size in the clinic, a compound that eliminates tumour cells is preferable over one that simply inhibits their proliferation. While several forms of regulated cell death have been identified [excellently reviewed in 165], apoptosis is the most common form induced by anti-cancer cytotoxic therapies. Focusing on TKIs, different compounds seem to promote variable levels of apoptosis. In both HER2- driven breast cancer and EGFR-driven NSCLC, HER2 inhibition with lorlatinib or EGFR inhibition with erlotinib resulted in robust induction of apoptosis through the intrinsic mitochondrial pathway. The authors showed that BIM and Puma were essential to this process [166]. Similarly, in EML4-ALK NSCLC, knockdown of ALK with siRNA resulted in robust induction of apoptosis and BIM upregulation [38], suggesting that all ALK inhibitors will have the same effect.

4.1.9.1 The intrinsic apoptotic pathway

The intrinsic apoptotic pathway is initiated in response to various stimuli such as DNA damage or deprivation of growth factors. A key downstream event is the permeabilization of the outer mitochondrial membrane [167], followed by the release of cytochrome C and SMAC/DIABLO [168]. These and other molecules form the apoptosome, which leads to Caspase-9 activation [169]. Caspase-9 then cleaves and activates Caspase-3 and Caspase-7, the activation of which culminates in widespread protein degradation and eventual breakdown of the cytoplasmic membrane [170]. Another role for SMAC is to bind and sequester the Inhibitors of apoptosis-family (IAPs) proteins, which directly bind caspases and prevent the apoptotic cascade, such as the X-linked IAP (XIAP) [171].

Our current knowledge of the intrinsic pathway suggests a multi-levelled regulation of the initiation of apoptosis. Specifically, anti-apoptotic proteins are in balance with pro-apoptotic proteins and disruption of this balance is a necessary event for the induction of apoptosis. The final step required for permeabilization of the mitochondrial membrane is the activation of BAX and BAK, which form homo- or hetero-dimers [172], cause a further release of the BCL2 family anti-apoptotic proteins and result in conformational changes of the mitochondrial outer membrane [173]. This is supported by the finding that deletion of BAX and BAK simultaneously, results in profound insensitivity to apoptotic stimuli in a wide variety of cells [174].

BH3-domain proteins such as PUMA, NOXA, BIM and BID are pro-apoptotic proteins that have a single BH3 domain and are known to activate BAX and BAK to achieve mitochondrial permeabilization. Notably, these are induced both transcriptionally (mainly BIM, PUMA and NOXA) and post-translationally (Bid) [175]. The action of the BH3-domain proteins is counterbalanced by members of the BCL2-family such as BCL-X_L, BCL-W and MCL-1 [176]. These are anti-apoptotic proteins that antagonise BH3 domain pro-apoptotic proteins, but also bind to the mitochondria and sequester the membrane preventing BAX and BAK from forming oligomers [177].

4.1.9.2 Evasion of apoptosis as a tumour-promoting mechanism

The importance of individual apoptotic proteins in cancer treatment is well established. Related to oncogene-driven tumours and targeted therapies, the mRNA levels of BIM have been shown to be

particularly important for targeted therapies. Specifically, high BIM expression correlates with high levels of apoptosis upon oncogene disruption, in EGFR- and HER2-mutant cells [178]. The role of BIM is also clinically relevant since a genetic polymorphism of BIM has been shown to diminish the response to EGFR inhibition in NSCLC [74]. Also in EGFR-mutant NSCLC, an upregulation of MCL-1 in response to EGFR inhibition dampens the treatment effect and results in drug resistance, which can be overcome by MCL1 inhibition through siRNA or treatment with dinaciclib [179].

4.2 Results

4.2.1 Generation of drug-resistant ALK-rearranged cell lines

In order to investigate the mechanisms of resistance to ALK inhibition and to recapitulate the alterations which take place in tumours refractory to ALK inhibitors *in vitro*, drug-resistant cell lines were utilised. Crizotinib is the first FDA-approved inhibitor for the treatment of ALK-rearranged lung cancer. Using H3122 EML4-ALK cells [2] as the parental cell line, 3 clones were generated after long term exposure to crizotinib, namely CrizR1, CrizR4 and CrizR5 which were maintained in 1 μM crizotinib. Ceritinib (LDK378) is a second-generation ALK inhibitor [180] with activity against crizotinib-resistant ALK kinase domain mutations. After exposing H3122 cells to ceritinib, a clone named CeritR was generated and was maintained in 500nM ceritinib. The NCI-H2228 cell line was used in parallel as a model of primary resistance to ALK inhibitors. Indeed, CrizR1, CrizR4, CrizR5 and H2228 cells are more resistant to crizotinib treatment (**Figure 6A**) and CeritR and H2228 are more resistant to ceritinib treatment (**Figure 6B**) compared to H3122 cells. As a model of resistance to the new standard of care, alectinib, an additional EML4-ALK^{mut} cell line, STE-1 [3] was utilised, which were made resistant to alectinib, named AlecR and maintained in 500nM alectinib (**Figure 6C**). In all cell lines with acquired resistance, the ALK kinase domain was sequenced and found to be wild-type (data not shown).

In addition, some of the described findings were corroborated in EGFR-mutant lung cancer as well. To model this context, the PC-9 [181] and H1975 [182] cell lines have been used. PC-9 cells were exposed to increasing concentrations of osimertinib and afatinib, until they were resistant to 1μM dose of both drugs, generating the PC-9 OsimR clone (**Figure 6D**). PC-9 cells were exposed to increasing concentrations of erlotinib, until they were resistant to a dose of 1μM, generating the PC-9 ErlotR clone (**Figure 6E**). Both clones carry the T790M kinase domain mutation that makes them resistant to first-generation EGFR inhibitors. H1975 cells were exposed to increasing concentrations of osimertinib, until they were resistant to 1μM, generating the H1975 OsimR clone (**Figure 6F**). This clone has been reported to harbour SRC-family kinase amplification that compensates for EGFR inhibition [75].

As described in the methods, some of these cell lines presented with clinically relevant kinase domain mutations which promote drug resistance, such as F1174L for ALK and T790M for EGFR. However, due to the purpose of this study to unravel off-target mechanisms of resistance in EML4-ALK, only clones with ALK^{wt} kinase domain were used herein.

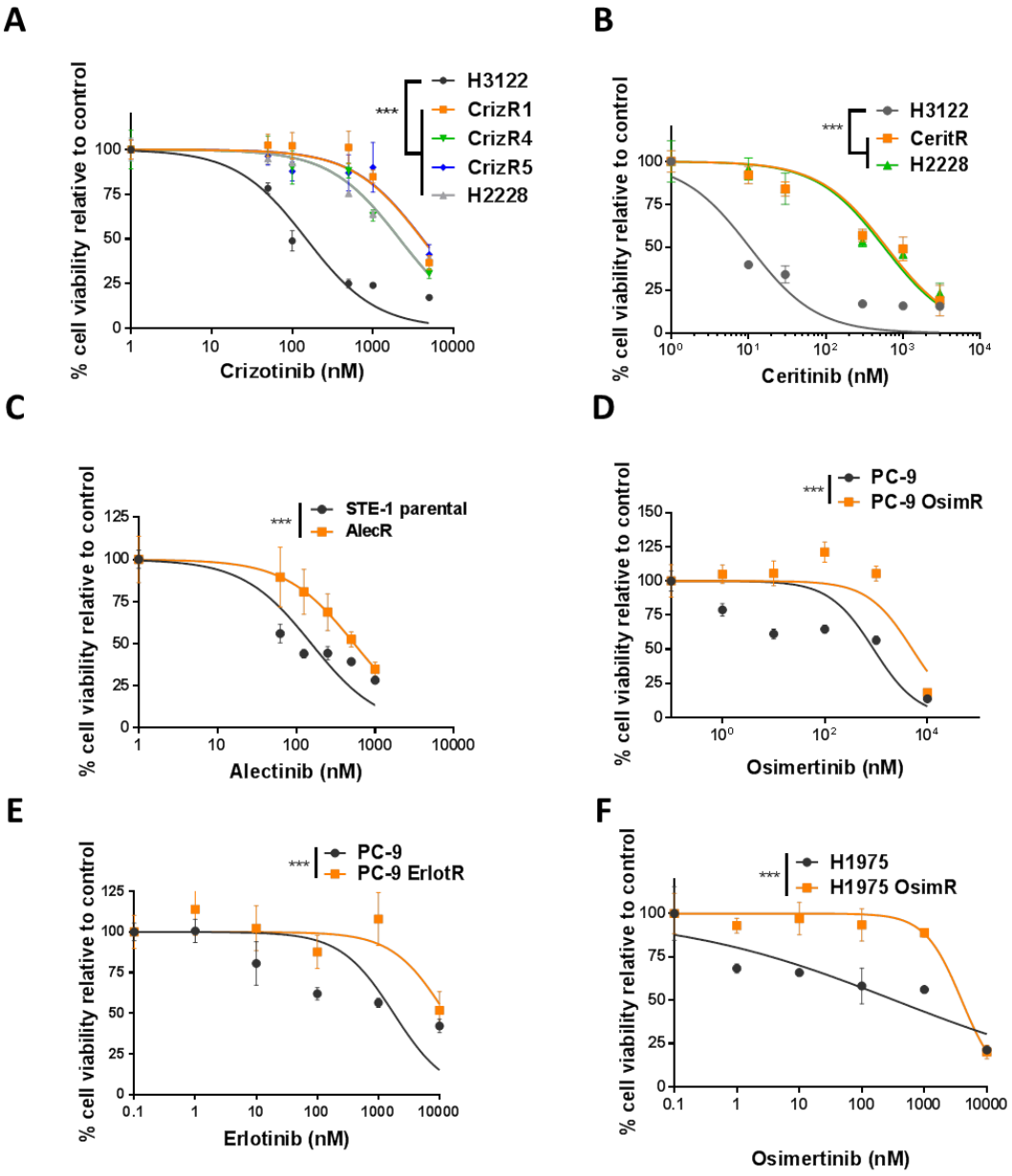

Figure 6: Cell line models of acquired resistance to TKIs

The indicated cell lines were treated with the indicated concentrations of:

- **A)** crizotinib, an ALK inhibitor
- **B)** ceritinib, an ALK inhibitor
- **C)** alectinib, an ALK inhibitor
- **D)** osimertinib, an EGFR inhibitor
- **E)** erlotinib, an EGFR inhibitor
- **F)** osimertinib, an EGFR inhibitor

72h later, cell viability was assessed with the use of the MTS proliferation assay. For each cell line, the vehicle control was transformed to 100% and the absorbance of other drug concentrations was normalized relative to this control. Data are presented as means ± SD from 2 (A, C, E) or 3 (B, D, F) biological replicates.

4.2.2 The expression of EML4-ALK and EGFR is dysregulated in drug-resistant clones

A multitude of studies regarding targeted therapies in lung cancer have proven that the mechanisms of resistance to TKIs are highly heterogeneous even within the same cellular clone [132,183]. Firstly, the expression of the driver oncogene was interrogated and ALK was found downregulated in crizotinib-resistant cells, most prominently in the CrizR1 clone (**Figure 7A**). Arguably the most common ALK-independent mechanism of resistance is an over-activation of EGFR, either at the receptor or the ligand (EGF) level [46]. To confirm the relevance of these cell line models, protein extracts were probed for the expression levels of EGFR. An over-activation of EGFR was then found in the CrizR1 and CrizR4 clones (**Figure 7B and C**) as well as increased phosphorylation of its downstream target AKT in CrizR1 cells. However, in this system, no evidence was found of EGFR compensating for EML4-ALK inhibition since knocking down EGFR with an siRNA (**Figure 7D**) combined with crizotinib resulted in no induction of apoptosis in CrizR1 cells (**Figure 7E**).

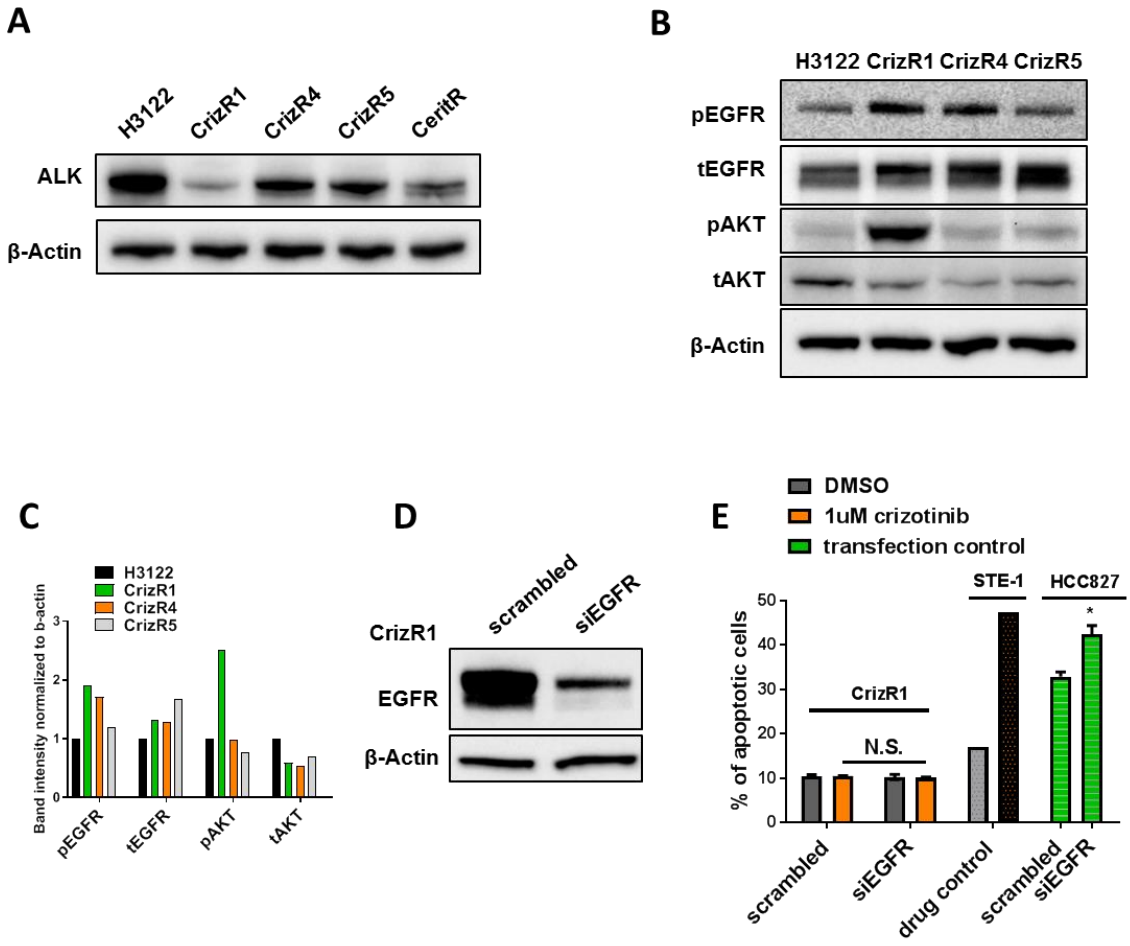

Figure 7: EGFR activation does not mediate resistance to crizotinib

- **A)** Protein extracts from H3122 parental and crizotinib-resistant cells were subjected to western blotting for the indicated proteins. ALK was downregulated in all drug-resistant cell lines. Shown is a representative blot of 2 independent experiments.
- **B)** As in **A),** activation of EGFR was detected at the protein level in crizotinib-resistant cells but particularly in the CrizR1 clone as evidenced by AKT phosphorylation.
- **C)** Quantification of the protein bands presented in B). Non-saturated ECL images were digitally quantified for signal intensity, which was subsequently normalised to the signal intensity of the loading control used (β-actin).
- **D)** CrizR1 cells were transfected with siEGFR and scrambled control for 48h. Then protein extracts were analysed by western blotting for EGFR expression. Shown is the western blot of one experiment.
- **E)** CrizR1 and HCC827 (EGFR-driven cells, as transfection control) cells were transfected with scrambled control and siEGFR for 72h in total. 24h post-transfection cells were treated with DMSO/1μM crizotinib. STE-1 parental cells were treated with crizotinib in parallel as drug control. 72h post-transfection apoptotic induction was assessed with the use of Annexin V/PI PI flow cytometry. EGFR knockdown in EGFR-driven cells increased apoptosis, whereas it did not increase apoptosis in crizotinib-resistant cells. Data are presented as means ± SD (n = 3 biological replicates).

4.2.3 Investigating the role of apoptotic genes identified from RNA-seq

In order to find genes whose up- or down-modulation is responsible for the resistance to crizotinib, poly-A RNA-seq was employed. Specifically, H3122 parental cells were cultured untreated and CrizR1 crizotinib-resistant cells were cultured in the presence of crizotinib and total RNA was extracted from 3 different passages. Then, a poly-A library was constructed to isolate mRNAs and this library was run on an Illumina sequencer as described in the methods. The reads were mapped to the human genome, quality checked and a bioinformatics pipeline (described in the methods) was run for statistical comparison. After a differential expression analysis, I considered genes differentially expressed only at an adjusted p-value < 0.05 and foldchange > 2, which led to 3,259 differentially expressed genes being found compared with the H3122 parental (dataset can be accessed at https://rebrand.ly/paliouras4). The long-term treatment of these cells with crizotinib would have resulted in a large transcriptomic diversity, only a minority of which would most likely contribute to drug resistance. Looking at individual genes from the RNA-seq and using the literature as a guide, several upregulated mRNAs that have the potential to mediate the resistance to crizotinib were identified.

A mechanism of resistance common to RTK inhibitors is a modulation of either pro- or anti-apoptotic proteins [179]. Interrogating the RNA-seq dataset for apoptotic genes, it was intriguing to find two members of the "Inhibitors of Apoptosis" protein family (IAP) to be dysregulated. The product of the anti-apoptotic BIRC5 gene, Survivin [171] was strikingly upregulated at the protein level in CrizR1 cells **(Figure 8A**), however, it was not feasible to knock down Survivin and investigate whether it can drive the resistance to crizotinib. The product of the BIRC3 gene, C-IAP2, [184] was upregulated in all the crizotinib-resistant cell lines (**Figure 8B**). However, silencing of c-IAP2 (**Figure 8C**) did not result in an increase in apoptosis in combination with crizotinib (**Figure 8D**) indicating that c-IAP2 does not have the potential to compensate for EML4-ALK inhibition in this clone.

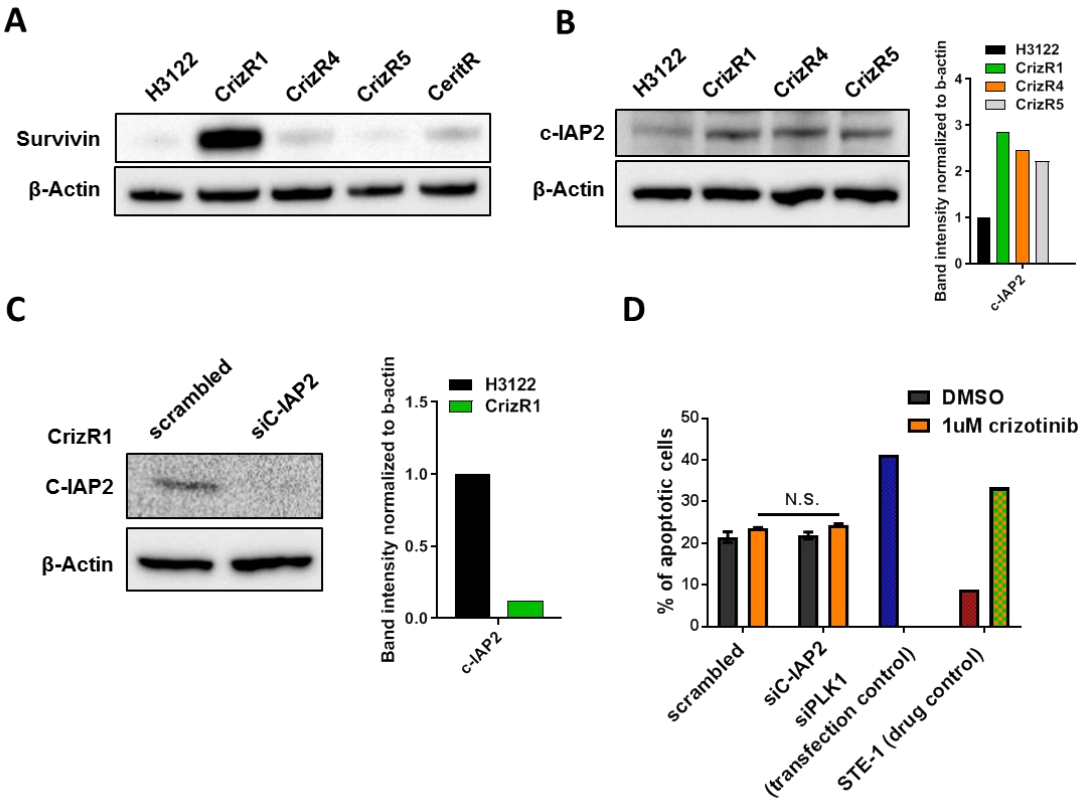

Figure 8: Survivin and c-IAP2 are dysregulated in crizotinib resistance

- **A)** Protein extracts from H3122 parental and crizotinib/ceritinib-resistant cells were subjected to western blotting for Survivin expression. Survivin is strikingly increased in CrizR1 cells. Shown is a representative blot of 2 independent experiments.
- **B)** As in A), cells were analysed for c-IAP2 expression which was found upregulated in all crizotinib-resistant clones. (right panel) Quantification of the protein bands presented on the left panel. Non-saturated ECL images were digitally quantified for signal intensity, which was subsequently normalised to the signal intensity of the loading control used (β-actin).
- **C)** CrizR1 cells were transfected with sic-IAP2 or scrambled oligos for 48h and protein extracts were then analysed for c-IAP2 expression by western blotting. Shown is a representative blot of 2 independent experiments. (right panel) Quantification of the protein bands presented on the left panel. Non-saturated ECL images were digitally quantified for signal intensity, which was subsequently normalised to the signal intensity of the loading control used (β-actin).
- **D)** As in C), cells were analysed for apoptosis by flow cytometry after siC-IAP2 transfection and no increase in apoptosis was observed. As transfection control, siPLK1 was used in CrizR1 cells which did lead to rapid induction of apoptosis. Data are presented as means ± SD (n = 3 biological replicates). P values were calculated by two-tailed student's t-test (*p < 0.05, **p<0.01, ***p<0.001).

4.2.4 The effect of TGFβ signalling on crizotinib resistance

Upon interrogation of the RNA-seq data, an upregulation of the TGFβ receptors 1 and 2 was also noticed, which was also observed at the protein level in CrizR1 and CrizR4 cells (**Figure 9A**). TGFβ-R2 has been shown before to be able to induce resistance to crizotinib [185]. These data are in agreement with this finding since treatment of CrizR1 cells with the TGFβ-R inhibitor galunisertib resulted in a decrease in proliferation in combination with crizotinib in CrizR1 cells (**Figure 9B**). However, this decrease was modest, which led us to hypothesise that different mechanisms of resistance may co-exist in the CrizR1 clone. Also, the requirement for a high concentration of galunisertib may mean an off-target effect rather than TGFβ-R inhibition.

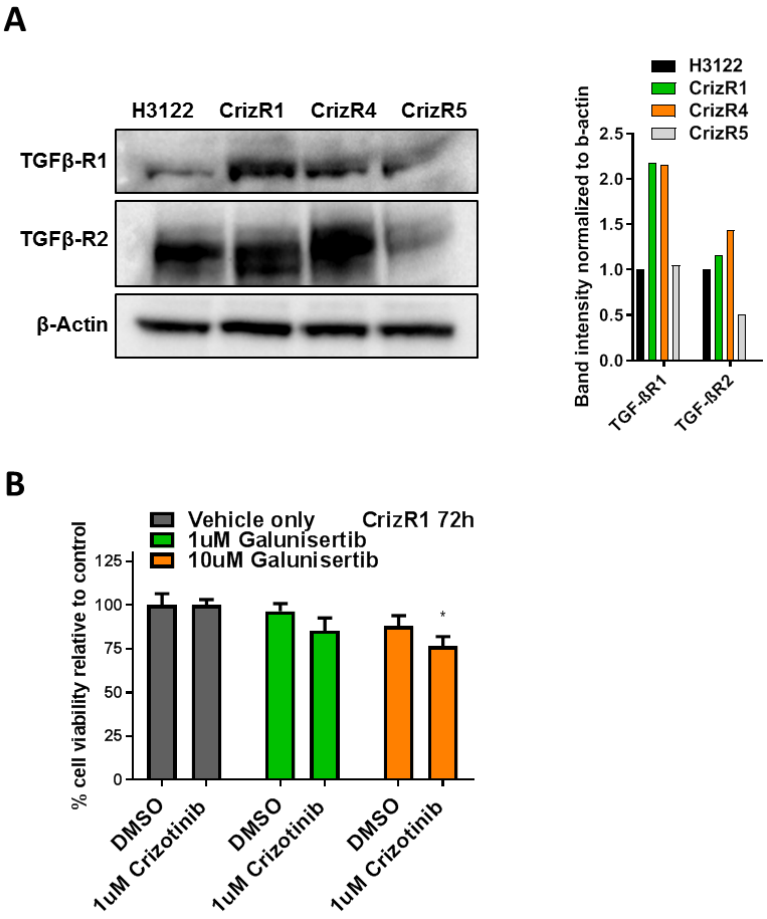

Figure 9: TGFβ-R1/2 inhibition can partially restore crizotinib sensitivity

A) Protein extracts from H3122 parental and crizotinib/ceritinib-resistant cells were subjected to western blotting for TGFβ-R1/2 expression. The expression of TGFβ-R1 was noticeably increased in CrizR1 and CrizR4 cells whereas TGFβ-R2 was only marginally increased. Shown is a representative blot of 2 independent experiments. (right panel) Quantification of the protein bands presented on the left panel. Non-saturated ECL images were digitally quantified for signal intensity, which was subsequently normalised to the signal intensity of the loading control used (β-actin).

B) CrizR1 cells were treated with vehicle control/1μM galunisertib/10μM galunisertib in the presence or absence of 1μM crizotinib. 72h post-transfection, cell proliferation was assessed by MTS. The absorbance of the vehicle control wells was transformed to 100% and the absorbance of other drug concentrations normalised to this control. Data points are presented as normalised means ± SD (n=3 biological replicates). P values were calculated by two-tailed student's t-test (*p < 0.05, **p<0.01, ***p<0.001).

4.2.5 The role of the transcription factors c-FOS and NF-κB

The transcription factor c-FOS was also found upregulated in the RNA-seq data. This observation was followed up on because, in a high-throughput screening, c-FOS overexpression was one of the hits that could render H3122 cells more resistant to crizotinib [1]. Western blot analysis confirmed the upregulation of c-FOS (**Figure 10A**). However, after knocking down c-FOS with siRNA (**Figure 10B**), there was no decrease in proliferation with or without crizotinib (**Figure 10C**). Again, a potentially oncogenic alteration was just a passenger rather than a driver in the resistance to crizotinib.

Data from EGFR-mutant lung cancer suggest that activation of the NF-κB pathway results in residual oncogenic signalling and resistance to EGFR inhibitors [117]. It was then hypothesised that this is the case for EML4-ALK lung cancer too. Western blot analysis of phosphorylated NF-κB identified an overactivation of the NF-κB p65 subunit in 2 clones, CrizR4 and CrizR5 (**Figure 10D**). In order to assess whether this activation was responsible for the differential drug response, p65 was silenced (**Figure 10E**) and cells were treated with crizotinib. After a proliferation assay, there was no synergism with p65 knockdown and crizotinib treatment (**Figure 10F**), therefore an NF-κB activation was not driving the resistance to crizotinib in this clone.

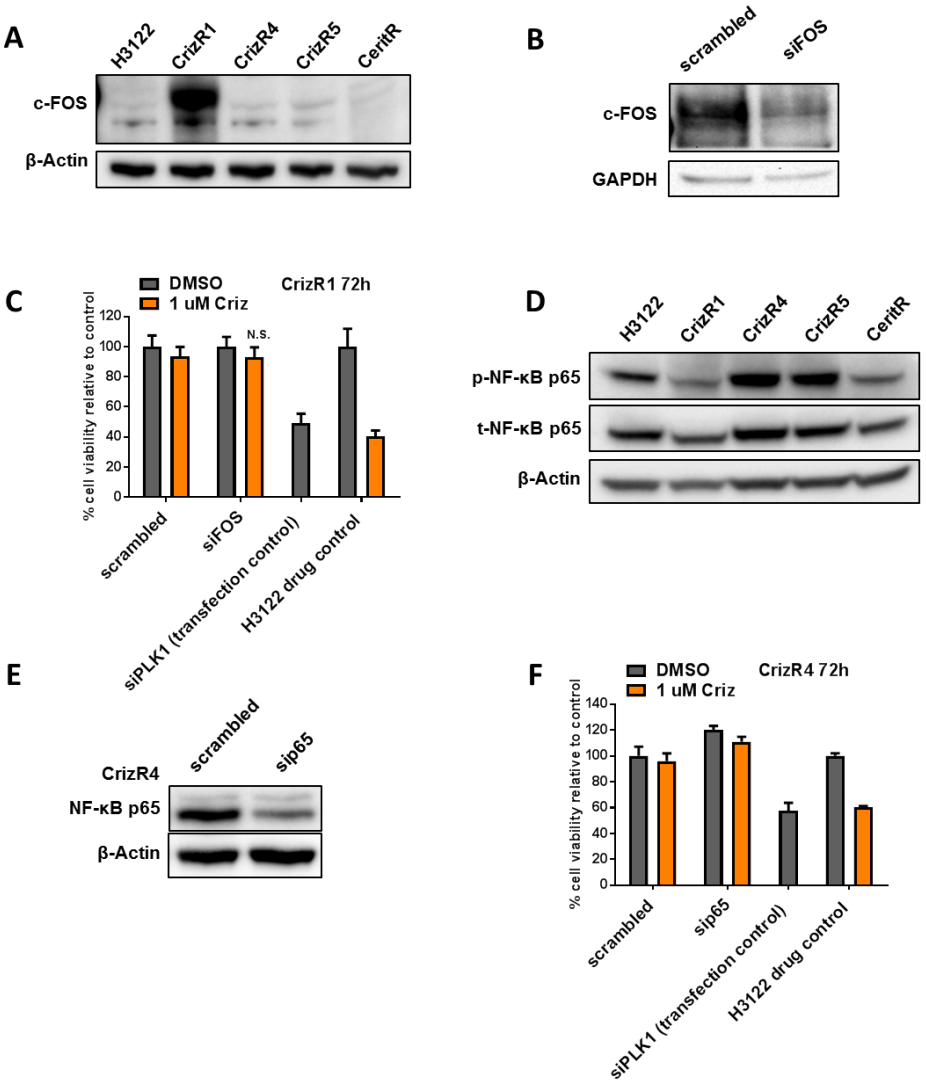

Figure 10: FOS and NF-κB upregulation is not oncogenic in this context

A) Protein extracts from H3122 parental and crizotinib/ceritinib resistant cells were subjected to western blotting for c-FOS expression. Shown is a representative blot of 2 independent experiments.

B) CrizR1 cells were transfected with siC-FOS and scrambled control for 72h. Then protein extracts were analysed by western blotting for c-FOS expression. Shown is a representative blot of 2 independent experiments.

C) CrizR1 cells were transfected with a scrambled control, siC-FOS and siPLK1 (as viability transfection control) for 72h in total. 24h post-transfection cells were treated with DMSO/1μM crizotinib. H3122 parental cells were treated with crizotinib in parallel as drug control. 72h post-transfection cell viability was assessed with the use of the MTS proliferation assay. The absorbance of the vehicle control wells was transformed to 100% and the absorbance of other drug concentrations normalised to this control. Data are presented as normalised means ± SD (n = 3 biological replicates).

D) Protein extracts from H3122 parental and crizotinib/ceritinib resistant cells were subjected to western blotting for NF-κB p65. Shown is a representative blot of 2 independent experiments.

E) CrizR4 cells were transfected with sip65 and scrambled control for 48h. Then protein extracts were analysed by western blotting for p65 expression. Shown is the western blot of one experiment. CrizR4 cells were transfected with a scrambled control, sip65, siPLK1 (as viability transfection control) for 72h in total. 24h post-transfection cells were treated with DMSO/1μM crizotinib. H3122 parental cells were treated with crizotinib in parallel as drug control. 72h post-transfection cell viability was analysed with the MTS proliferation assay. The absorbance of the vehicle control wells was transformed to 100% and the absorbance of other drug concentrations normalised to this control. Data are presented as normalised means ± SD (n = 2 biological replicates). P values were calculated by two-tailed student's t-test (*p < 0.05, **p<0.01, ***p<0.001).

4.2.6 Gene set enrichment data

After not being able to detect a single driving mechanism of resistance looking at individual genes it became apparent that a global overview of the transcriptome was needed. In order to find sets of genes that were significantly enriched in the drug-resistant condition, Gene-Set Enrichment Analysis (GSEA-described in the methods) was performed in the RNA-seq data. Briefly, this algorithm queries the overrepresentation of genes in a dataset based on pre-determined gene collections (corresponding to different pathways or experimental perturbations) [15]. I used the HALLMARK and KEGG gene collections which are manually curated for the most fundamental signalling and phenotypic gene collections based on published data. With the HALLMARK collection identified 12 significantly enriched pathways in up- or down-regulated genes (**Figure 11A**). The KEGG-based analysis is discussed in 4.2.8. It was interesting that EMT was the 2nd most enriched pathway in up-regulated genes (**Figure 11B**).

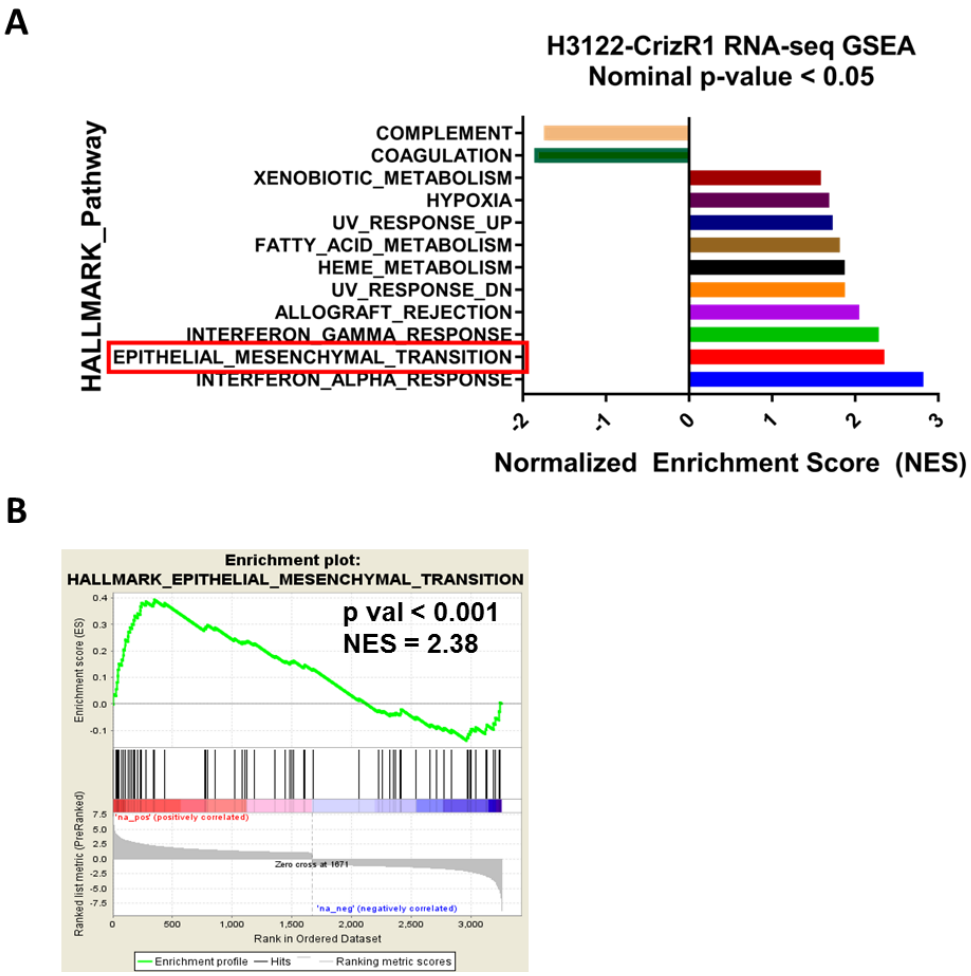

Figure 11: EMT-related genes are significantly enriched in crizotinib-resistant cells

A) H3122 parental and CrizR1 cells were subjected to poly-A RNA seq followed by differential expression analysis as described in 4.2.3. Using the Hallmark gene collection, gene-set enrichment analysis identified the plotted 12 significantly enriched pathways. An epithelial-to-mesenchymal transition signature was prioritised for follow-up studies.

B) As in A), a plot of EMT enrichment. NES stands for normalised enrichment score. Over 70 permutations are represented on the x-axis with clear enrichment in both positive (red-upregulation) and negative correlation (blue-downregulation).

4.2.7 Epithelial-to-mesenchymal transition as a mechanism of resistance

Recently in the literature, the epithelial-to-mesenchymal transition (EMT) has been described as a hallmark of resistance to crizotinib [125]. Except for the identified GSEA signature which shows >70 dysregulated genes involved in EMT, the crizotinib-resistant clones CrizR1, CrizR4 and CrizR5 exhibit a more mesenchymal-like morphology, while ceritinib-resistant cells remain epithelial-like (**Figure 12**).

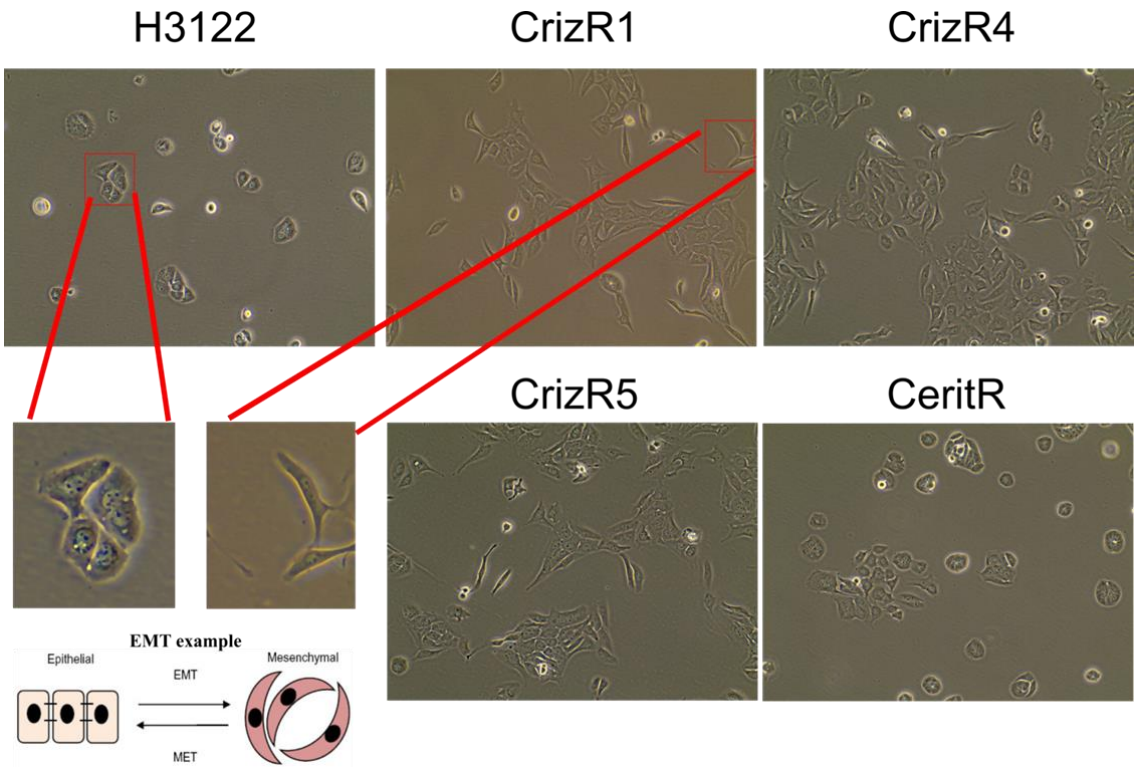

Figure 12: EML4-ALK cell crizotinib-resistant cell lines exhibit a mesenchymal morphology.

Cells were photographed at 20x magnification using an EVOS light microscope. H3122 and CeritR look distinctly like densely-packed, epithelial cells (at the bottom is a magnified example of H3122 cluster of cells compared to an example from the literature). CrizR1, CrizR4 and to a lesser degree CrizR5 cells look elongated-like, mesenchymal cells (at the bottom is a magnified example of 2 CrizR1 elongated cells compared to an example from the literature). EMT example adapted from [186].

The role of EMT in the resistance to crizotinib has been debated [124,187], raising the possibility that in some cases EMT has a causal role in crizotinib resistance, while in other cases it is just a marker of cells going through the process of acquiring resistance. I asked which was the case in this dataset and aimed to validate the results of the RNA-seq data via RT-qPCR. Four well-known EMT-related genes were selected and it was found that *AXL*, *LOX*, *SNAI2* and *Vimentin* were upregulated in the crizotinib-resistant clones CrizR1 and CrizR4 (CrizR5 only for LOX and SNAI2) at the mRNA level, while they were not upregulated in ceritinib-resistant cells, consistent with observed morphology (**Figure 13A**). AXL was particularly interesting since it is an RTK and RTKs are likely to mediate crizotinib resistance. Also, AXL-mediated activation of EMT has been described before [187]. Thus, upregulation of AXL was detected at the protein level in CrizR1 and CrizR4 cells (**Figure 13B**). Then, the small molecule inhibitor bemcentinib (R428) was used [188] to inhibit AXL and perform functional experiments. While other groups have shown that AXL inhibition does not restore sensitivity to crizotinib [124,187], in the data presented herein, AXL inhibition synergised with crizotinib and hindered the proliferation of crizotinib-resistant cells (**Figure 13C**). Furthermore, AXL inhibition resulted in the downregulation of LOX, SNAI2 and Vimentin at the mRNA level (**Figure 13D**), suggesting that AXL may be the driving force behind their upregulation. It was observed that bemcentinib treatment resulted in CrizR1 and CrizR4 acquiring a more epithelial-like morphology, however, a more carefully controlled experiment would be required to ascertain this. However, the combination of bemcentinib plus crizotinib did not result in an induction of apoptosis (**Figure 13E**) and I reasoned that further therapeutic interest in the combination may be limited because of this.

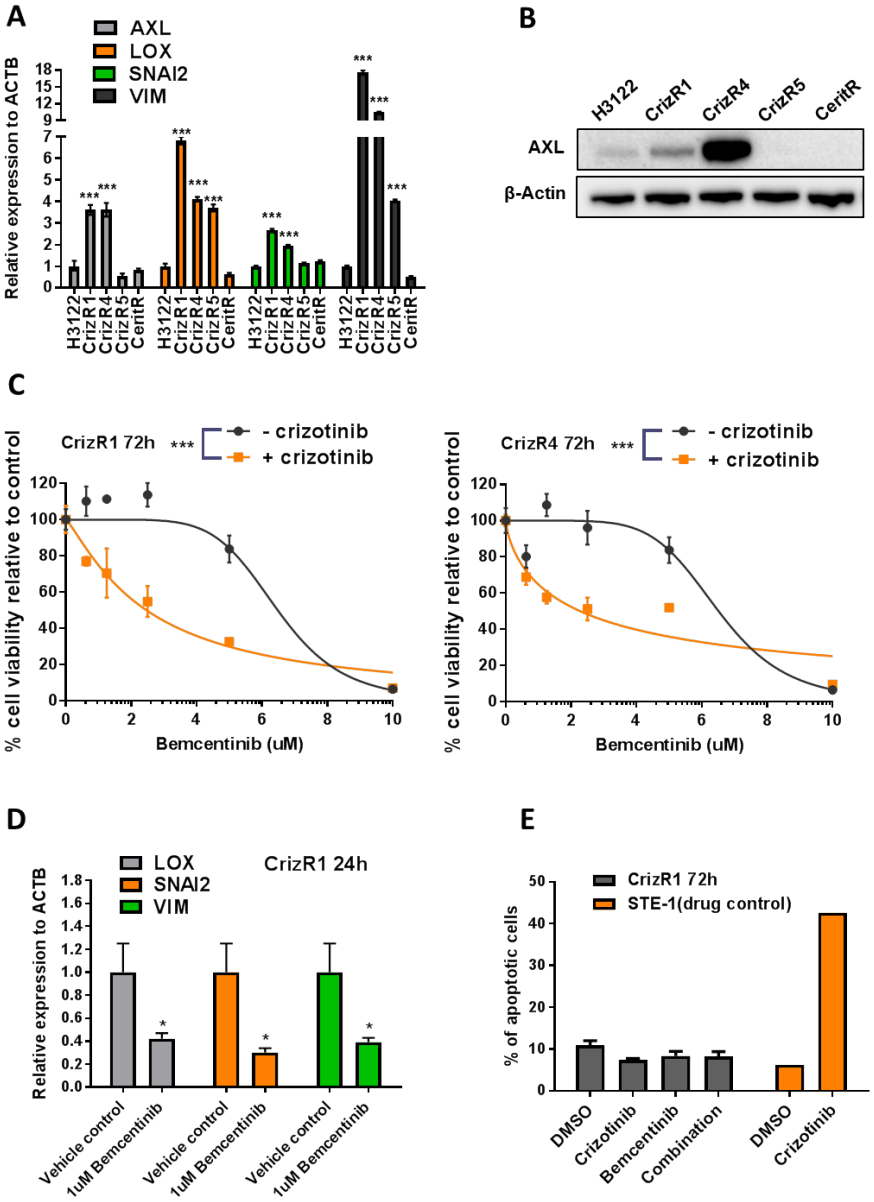

Figure 13: AXL upregulation contributes to EMT and to the resistance to crizotinib

A) RNA was extracted from H3122 parental and crizotinib/ceritinib resistant cells. The expression of the indicated genes was analysed via RT-qPCR. Data are presented as 2-ΔΔCT normalised means ± SD. (n = 4 biological replicates). P values were calculated by two-tailed student's t-test (*p < 0.05, **p<0.01, ***p<0.001).

B) Western blot for AXL protein expression in EML4-ALK cells, which was found increasingly expressed in CrizR1 and CrizR4 cells. Shown is a representative blot of 3 independent experiments.

C) CrizR1 and CrizR4 were treated with the indicated concentrations of bemcentinib ± 1μM crizotinib for 72h and cell proliferation was assessed by MTS. The absorbance of the vehicle control wells was transformed to 100% and the absorbance of other drug concentrations was normalized to this control. Data are presented as normalised means ± SD. (n = 3 biological replicates). P values were calculated for IC_{50} shift (*p < 0.05, **p<0.01, ***p<0.001).

D) CrizR1 cells were treated with 1μM bemcentinib or vehicle control for 24h. Then, RNA was extracted and the expression of the indicated genes was quantified by RT-qPCR. Data are presented as 2-ΔΔCT normalised means ± SD. (n = 3 biological replicates). P values were calculated by two-tailed student's t-test (*p < 0.05, **p<0.01, ***p<0.001).

E) CrizR1 cells were treated with 1μM crizotinib, 2.5μM bemcentinib, or combination for 72h. Then, apoptotic cells were quantified by Annexin V staining and flow cytometry. STE-1 parental cells were treated in parallel with crizotinib as drug control. Shown are means ± SD (n = 3 biological replicates).

4.2.8 The role of the cell cycle in the resistance to ALK inhibitors

In the previous RNA-seq data comparing crizotinib-resistant versus sensitive cells, an additional pathway analysis by GSEA using the KEGG collection aimed at more comprehensive coverage of biological pathways and revealed 9 pathways enriched in dysregulated genes (**Figure 14A**). Notably, among them, there was a significant enrichment in cell cycle-related genes (**Figure 14B**). To corroborate this finding, a previous dataset of EML4-ALK^{mut} STE-1 cells treated with 500nM crizotinib for 24 hours, followed by polyA-RNA-sequencing was interrogated. Specifically, parental STE-1 cells were cultured for 24 hrs in the presence of DMSO or crizotinib and RNA was extracted from 3 independent experiments. After the previously described sequencing and bioinformatics pipeline, differential expression analysis at adjusted $p < 0.05$ and foldchange > 2 identified 2,574 dysregulated genes (**https://rebrand.ly/paliouras2**). GSEA identified 9 pathways enriched in dysregulated genes, the most prominent of which featured a cell cycle dysregulation (**Figure 14C**). This suggests that cell cycle genes are essential for ALK-driven cell proliferation, are lost upon ALK inhibition and may be restored if another driver oncogene substitutes for ALK loss in drug resistance,

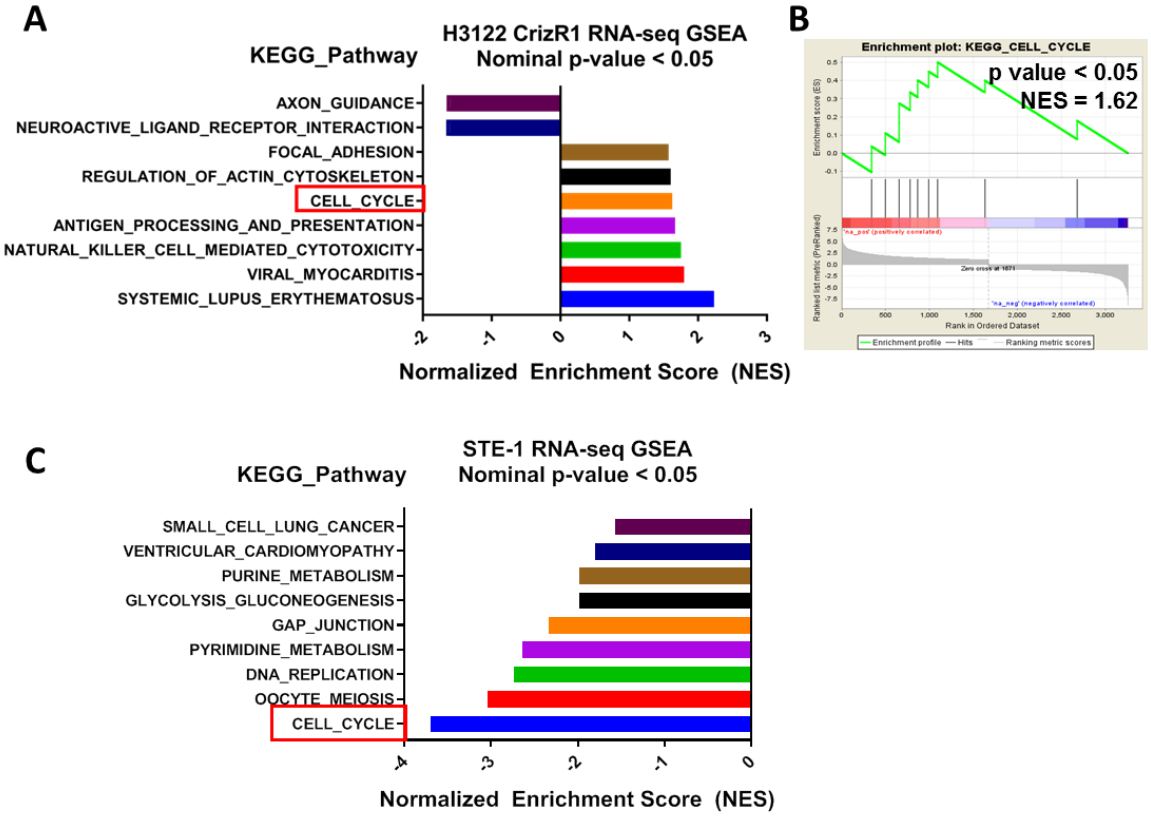

Figure 14: RNA-seq identifies a cell cycle dysregulation upon ALK inhibition

- **A)** H3122 parental and CrizR1 cells were subjected to poly-A RNA seq followed by differential expression analysis as described in 4.2.3. Using the KEGG gene collection, gene set enrichment analysis identified the plotted 12 significantly enriched pathways.
- **B)** Cell cycle enrichment plot from A). NES stands for normalised enrichment score. Nine permutations are represented on the x-axis with clear enrichment in only positive (red-upregulation) but not negative correlation (blue-downregulation).
- **C)** STE-1 cells were treated with vehicle control/crizotinib for 24h and RNA was extracted from 3 biological replicates. A poly-A cDNA library was constructed and sequenced, followed by differential expression analysis as described in 4.2.8. Using the KEGG gene collection, gene set enrichment analysis identified the plotted 9 significantly enriched pathways with cell cycle being the most significantly enriched.

The list of enriched genes highlighted important components of cell division, such as CCNB1, CCNE1, CDK1 and CDK2 (**Figure 15A**). The downregulation of cyclin B1, CDK1 and CDK2 was confirmed upon crizotinib treatment, but not of cyclin E1 at the protein level after 24h or 48h of crizotinib treatment (**Figure 15B**).

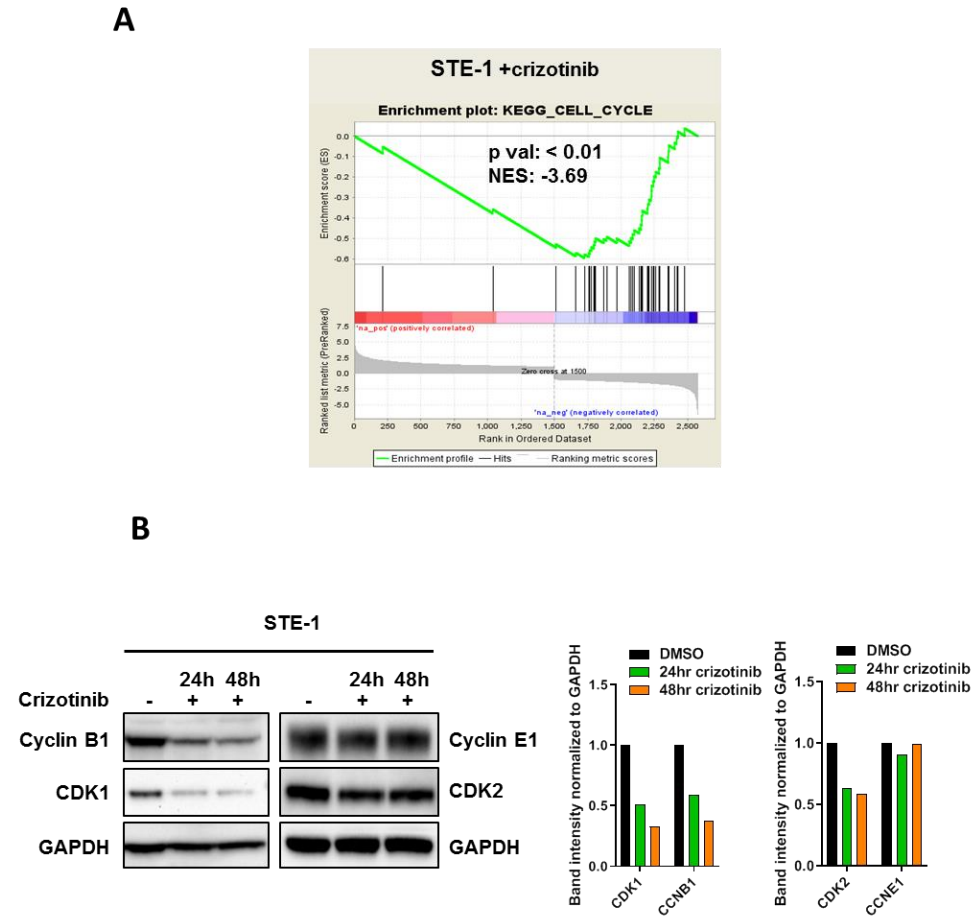

Figure 15: Cyclin-dependent kinases are downregulated upon crizotinib treatment

A) Expanded gene list from the GSEA analysis shown in (**Figure 14C**). NES stands for normalised enrichment score. Over 20 permutations are represented on the x-axis with clear enrichment in only negative correlation (blue-downregulation) but not positive (red-upregulation).

B) STE-1 cells were treated with vehicle control/crizotinib for 24h then protein extracts were subjected to western blotting for the indicated proteins. CCNB1, CDK1 and CDK2 are robustly downregulated after crizotinib treatment. Shown is a representative blot of 2 independent experiments. (right panel) Quantification of the protein bands presented on the left panel. Non-saturated ECL images were digitally quantified for signal intensity, which was subsequently normalised to the signal intensity of the loading control used (GAPDH).

This similarity of the response to crizotinib with the crizotinib-resistant cells raised the possibility that cell cycle genes may escape the initial crizotinib-induced downregulation and thus contribute to drug resistance. In crizotinib-resistant cells, the upregulation of several cell cycle proteins was confirmed by western blotting, such as CDK1, cyclin B1, cyclin E1 and CDK6 (**Figure 16A**). As expected, these genes are upregulated at different degrees in different drug-resistant clones. I asked whether the same was true for EGFR-mutant cells resistant to EGFR inhibitors. PC-9 and H1975 cells resistant to osimertinib had increased levels of cyclin E1 only (**Figure 16B**). The most common upregulation was of CDK6, in CrizR1, CrizR4 and CrizR5 cells. CDK6 mutations and copy-number alterations are occurring in patients who acquire resistance to EGFR inhibitors [78] even though there has not been experimental evidence that these mutations have a functional role (that is, in an EML4-ALK/EGFR context). Given the recent regulatory approval of cell cycle inhibitors for breast cancer treatment [189], I asked whether combined CDK4/6 inhibition can re-sensitise CrizR1 cells to crizotinib. Treatment of CrizR1 cells with the specific CDK4/6 inhibitor palbociclib resulted in only partial re-sensitisation to crizotinib, but only in clinically irrelevant [147] concentrations (**Figure 16C**).

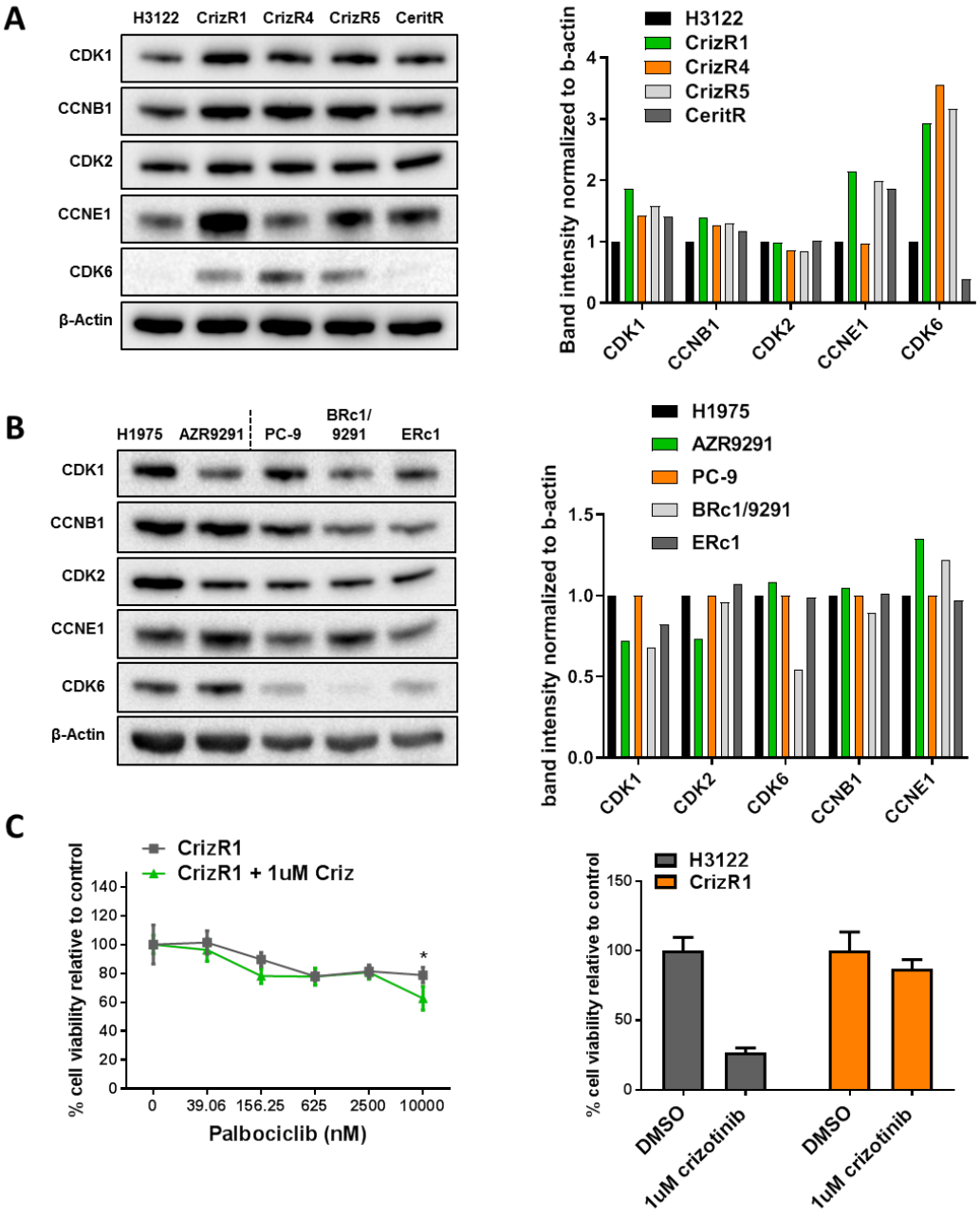

Figure 16: Cell cycle genes are dysregulated in EML4-ALK drug-resistant cells

A) Protein extracts from EML4-ALK^{mut} cells were analysed by western blotting for the expression of the indicated proteins. Shown is a representative blot from 3 independent experiments. (right panel) Quantification of the protein bands presented on the left panel. Non-saturated ECL images were digitally quantified for signal intensity, which was subsequently normalised to the signal intensity of the loading control used (β-actin).

B) As in A), for EGFR^{mut} cells, which present an upregulation of CCNE1 only. Shown is a representative blot from 3 independent experiments. (right panel) Quantification as in A).

C) (left panel) CrizR1 cells were treated with the indicated concentrations of palbociclib ± 1μM crizotinib for 72h. Then, cell proliferation was assessed by MTS. Data are presented as normalised means ± SD. (n = 3 biological replicates). P values were calculated by a two-tailed student's t-test (*p < 0.05, **p<0.01, ***p<0.001).
(Right panel) H3122 and CrizR1 cells were treated in parallel with 1μM crizotinib or vehicle control.

4.2.9 Pan-CDK inhibition is detrimental to the proliferation of drug-resistant EML4-ALK cells

The results from the palbociclib experiment leave open the possibility of several cell cycle genes cooperating to induce resistance to crizotinib. To test this, the pan-CDK inhibitor alvocidib was used, which by inhibiting the majority of human CDKs [190], also affects the action of their partner cyclins, allowing for the interrogation of this potential mechanism. While the combination of alvocidib and crizotinib did not synergise in decreasing cell proliferation in CrizR1 cells (**Figure 17A**), a particular sensitivity to alvocidib as a single agent was observed, previously seen only in haematological malignancies [191]. This finding was expanded in all the drug-resistant cell lines (**Figure 17B, C**), including the H2228 (EML4-ALK variant 3) cells (**Figure 17D**), all of which showed decreased proliferation with low nanomolar concentrations of alvocidib. Of note, the parental cells responded similarly as the drug-resistant clones, suggesting that CDK inhibition is not addressing a mechanism of resistance to ALK inhibition, but perhaps affects all EML4-ALK^{mut} cells.

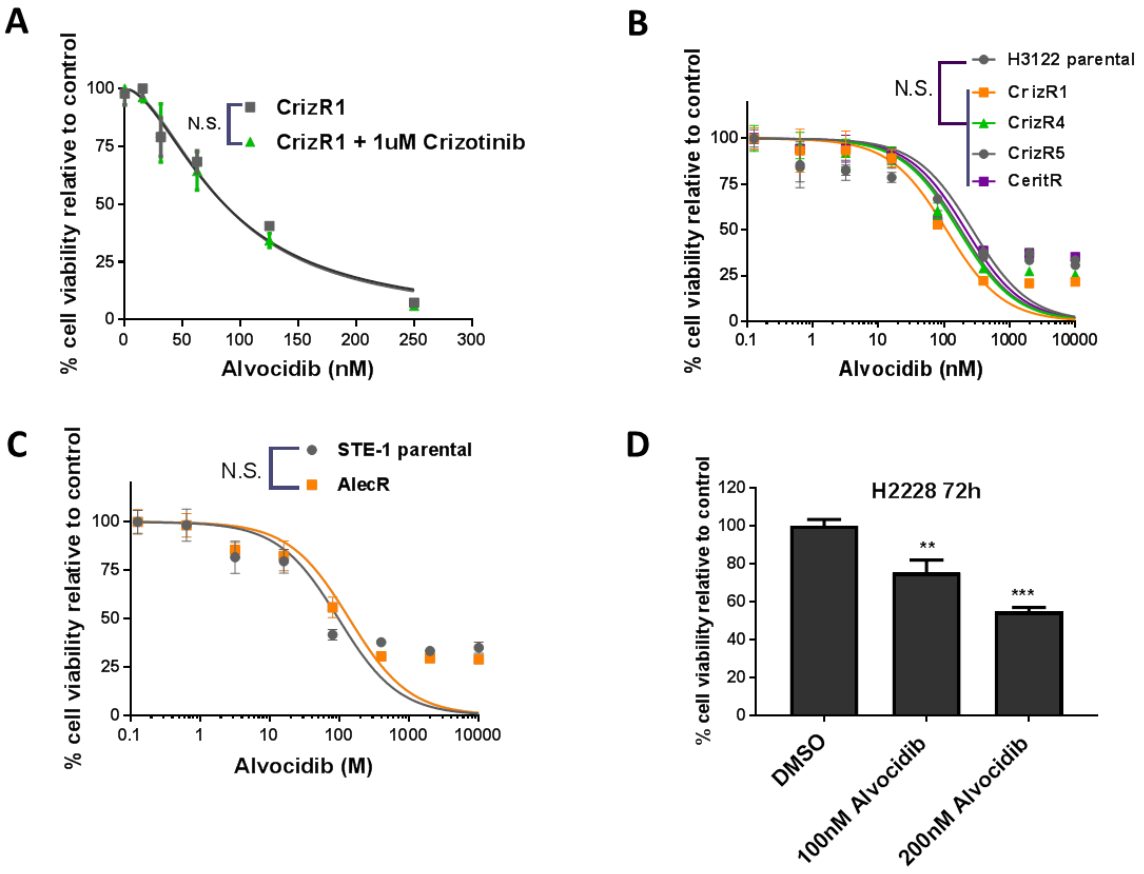

Figure 17: EML4-ALK^{mut} cells are sensitive to alvocidib treatment

A) CrizR1 cells were treated with the indicated concentrations of alvocidib ± 1µM crizotinib for 72h. Then, cell proliferation was assessed by MTS. Data are presented as normalised means ± SD. (n = 3 biological replicates). H3122 cells were treated with crizotinib in parallel as drug control (not shown). P values were calculated for IC_{50} shift (*p < 0.05, **p<0.01, ***p<0.001).

B) H3122 parental and drug-resistant cells were treated with the indicated concentrations of alvocidib for 72h. Then, cell proliferation was assessed by MTS. Data are presented as normalised means ± SD. (n = 3 biological replicates). P values were calculated for IC^{50} shift (*p < 0.05, **p<0.01, ***p<0.001).

C) As in B), for STE-1 parental and alectinib-resistant cells.

D) H2228 cells were treated with vehicle control, 100nM alvocidib or 200nM alvocidib for 72h. Then, cell proliferation was assessed by MTS. Data are presented as normalised means ± SD. (n = 3 biological replicates). P values were calculated by two-tailed student's t-test (*p < 0.05, **p<0.01, ***p<0.001).
The absorbance of the vehicle control wells was transformed to 100% and the absorbance of other drug concentrations was normalised to this control.

To follow up on the observed sensitivity to CDK inhibition I decided to test dinaciclib, a newer CDK1, CDK2, CDK5 and CDK9 inhibitor with better pharmacological properties [149]. Dinaciclib, like alvocidib, is not considered a selective probe, as it has activity against several members of the CDK family. Also, the recent discovery of the CDK7/12 inhibitor THZ1 has shown very promising anti-tumour activity [150] and in the context of EML4-ALK cancer, THZ1 has been shown to prevent the development of resistance to ALK inhibitors by suppressing adaptive transcriptional responses [156]. I was interested to see whether this inhibitor is also potently active against cells that have already acquired resistance to ALK inhibitors. After testing all these compounds, the proliferation of EML4-ALK cells resistant to crizotinib/ceritinib (**Figure 18A**) and alectinib (**Figure 18B**) was potently suppressed by low nanomolar concentrations of dinaciclib and similarly, of THZ1 (**Figure 18C, D**). This observation was expanded in EGFR-mutant cells, where the combination of erlotinib/osimertinib with CDK inhibitors was likewise not synergistic (data not shown), however, a marked sensitivity to alvocidib on its own was observed (**Figure 18E, F, G**).

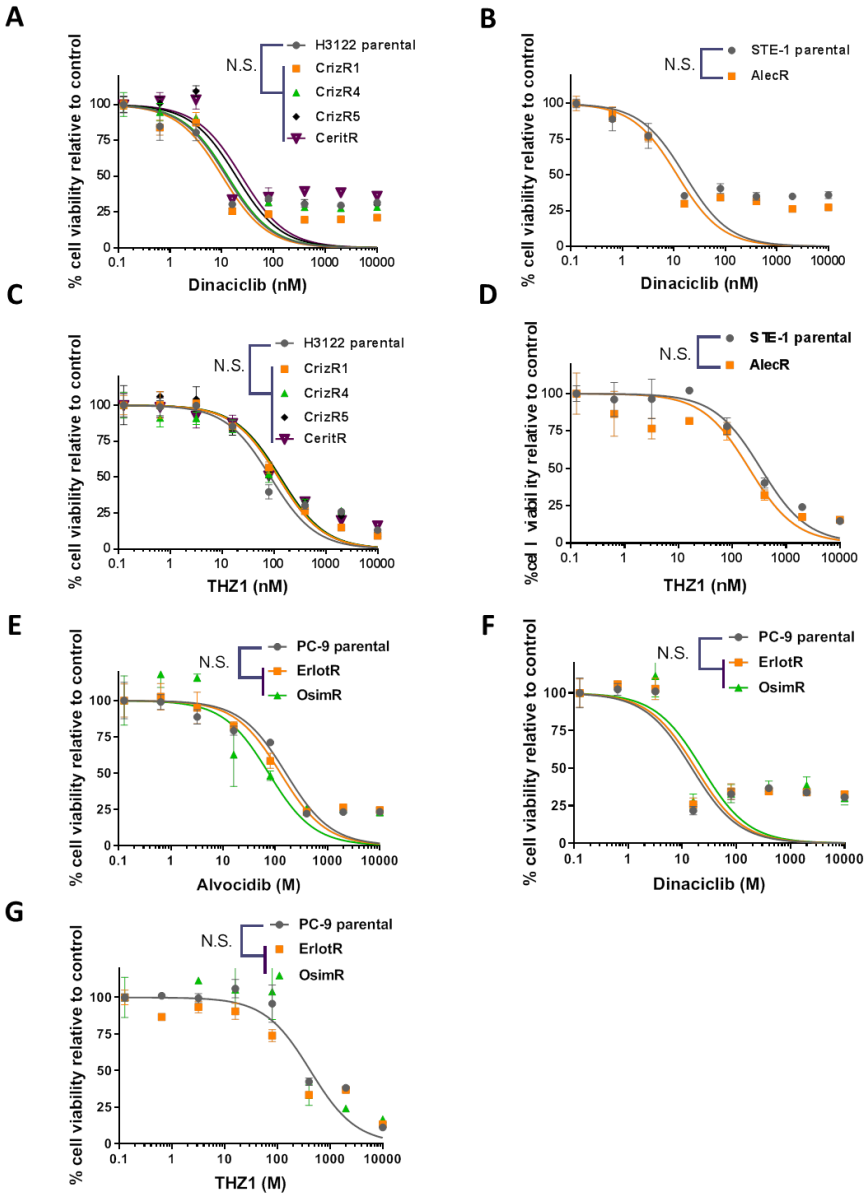

Figure 18: CDK inhibition effective suppresses cell proliferation of oncogene-driven NSCLC cells

A) H3122 parental and crizotinib-resistant cells were treated with the indicated concentrations of dinaciclib, a CDK1, CDK2, CDK5 and CDK9 inhibitor for 72h. Then, cell proliferation was assessed by MTS. Data are presented as normalised means ± SD. (n = 3 biological replicates). P values were calculated for IC_{50} shift (*p < 0.05, **p<0.01, ***p<0.001).

B) As above, for STE-1 parental and alectinib-resistant cells.

C) As in A), for THZ1, a CDK7/12 inhibitor.

D) As in C), for STE-1 parental and alectinib-resistant cells.

E) PC-9 parental, erlotinib-resistant and osimertinib-resistant cells were treated with the indicated concentrations of alvocidib for 72h. Then, cell proliferation was assessed by MTS. Data are presented as normalised means ± SD. (n = 3 biological replicates). P values were calculated for IC_{50} shift (*p < 0.05, **p<0.01, ***p<0.001).

F) As in A), for dinaciclib.

G) As in A), for THZ1.

In all experiments, the absorbance of the vehicle control wells was transformed to 100% and the absorbance of other drug concentrations was normalised to this control.

4.2.10 Assessing the effect of CDKi on long-term survival

The same potent effects were observed with a more prolonged CDK inhibitor treatment followed by crystal violet staining (**Figure 19A**) and it was apparent that STE-1 parental cells and cells resistant to the current standard of care, alectinib, did not respond to low doses of THZ1, however, they did respond to alvocidib or dinaciclib. Recently, it has been proven that after an *in vitro* initial high dose of TKIs, some cells survive the treatment and re-populate the culture dishes. These cells have been named 'persisters' [126] and recapitulate the context of primary, as opposed to acquired, resistance. To mimic this, H3122 sensitive cells were treated with high doses of crizotinib and alectinib, until the surviving cells repopulated the wells. At this point, cells were treated with alvocidib, and it was apparent that alvocidib is effective with persister cells as well **(Figure 19B**). Furthermore, I reasoned that as with any single agent molecule, resistance to alvocidib or dinaciclib would eventually appear. It was thus tested whether an upfront combination of ALK inhibition with low dose alvocidib or dinaciclib can prevent the emergence of resistant clones. In a crystal violet assay, single-agent alectinib, alvocidib or dinaciclib all led to a number of surviving cells and development of drug-resistant colonies. However, the combination of alectinib with low-dose alvocidib or dinaciclib led to complete elimination of all cells, suggesting that such a combination may be highly effective, provided that the correct dose could be identified to minimise *in vivo* toxicity (**Figure 19C**). This experiment was only performed once, so additional repeats would be required for a confident conclusion.

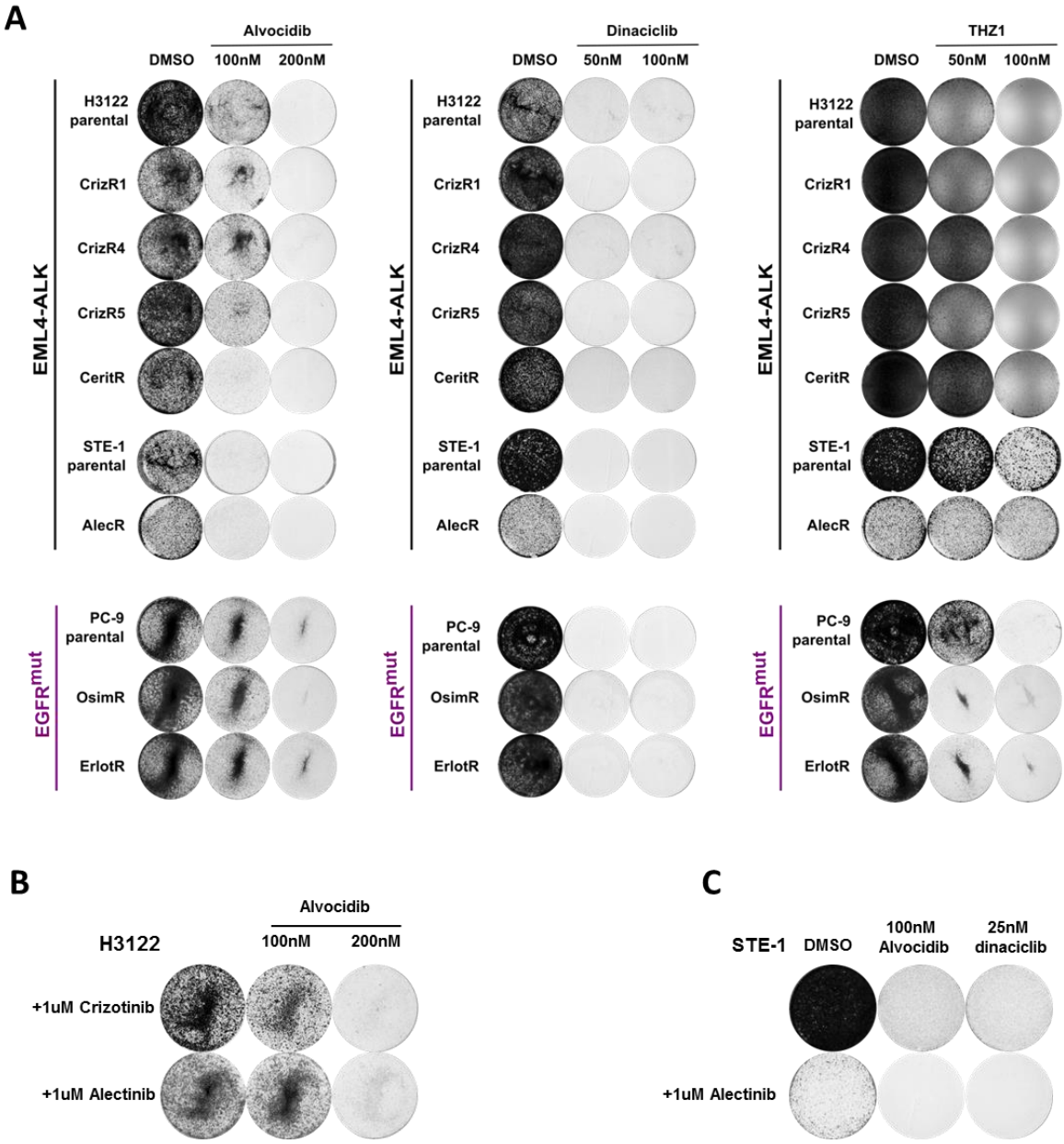

Figure 19: Long-term treatment with CDKi suppresses persister cells

A) All the indicated cell lines were treated with the indicated compounds until the vehicle control well reached confluence (7-10 days). Then, cells were fixed and stained with crystal violet to assess cell viability. Alvocidib treatment modestly inhibits the survival of EML4-ALK^{mut} or EGFR^{mut} cell at 100nM while completely inhibits it at 200nM for EML4-ALK^{mut} cells. Dinaciclib treatment modestly inhibits the survival of EML4-ALK^{mut} or EGFR^{mut} cell at 50nM while completely inhibits it at 100nM. Lastly, THZ1 has similar effects at 50 and 100nM but with STE-1 cells being more resistant to long-term THZ1 treatment. Shown are representative wells of at least 2 independent experiments.

B) As in A), H3122 cells were treated with 1μM crizotinib or alectinib until persister cells emerged and started to proliferate. Then cells were treated long-term with the indicated concentrations of alvocidib (~3 weeks). Clearly, upon the addition of 100nM alvocidib, persister cells show decreased survival over 3 weeks, while at 200nM they are largely eliminated. Shown are representative wells of 2 independent experiments.

C) STE-1 cells were treated with vehicle control, 100nM alvocidib or 20nM dinaciclib in the presence or absence of 1μM alectinib. After 10 days, cells were fixed and stained with crystal violet to assess cell viability. While single-agent alvocidib, dinaciclib or alectinib all result in residual cells that will lead to drug resistance, a combination of low-dose alvocidib or dinaciclib with maximum dose alectinib eliminates all cells. Shown are the wells of 1 experiment.

4.2.11 CDK inhibition results in a potent apoptotic response in EML4-ALK cells

I then aimed to identify the reason for decreased proliferation upon alvocidib treatment. Cell cycle analysis was only possible at the 24h time point due to observed cell death and during that time point, an arrest at the G2/M phase of the cell cycle was observed in CrizR1 cells (**Figure 20A**). The marked cell death led us to question whether apoptosis was induced. Annexin/PI flow cytometry analysis uncovered a marked induction of apoptosis in all the crizotinib-resistant cell lines tested, with the CrizR1 clone showing the highest levels (**Figure 20B**). The high amount of apoptotic cells raised concerns for toxicity; however, it was found that this induction of apoptosis is preferential towards EML4-ALK cells, as the normal lung epithelial cells HBEC remained unaffected after alvocidib treatment (**Figure 20C**).

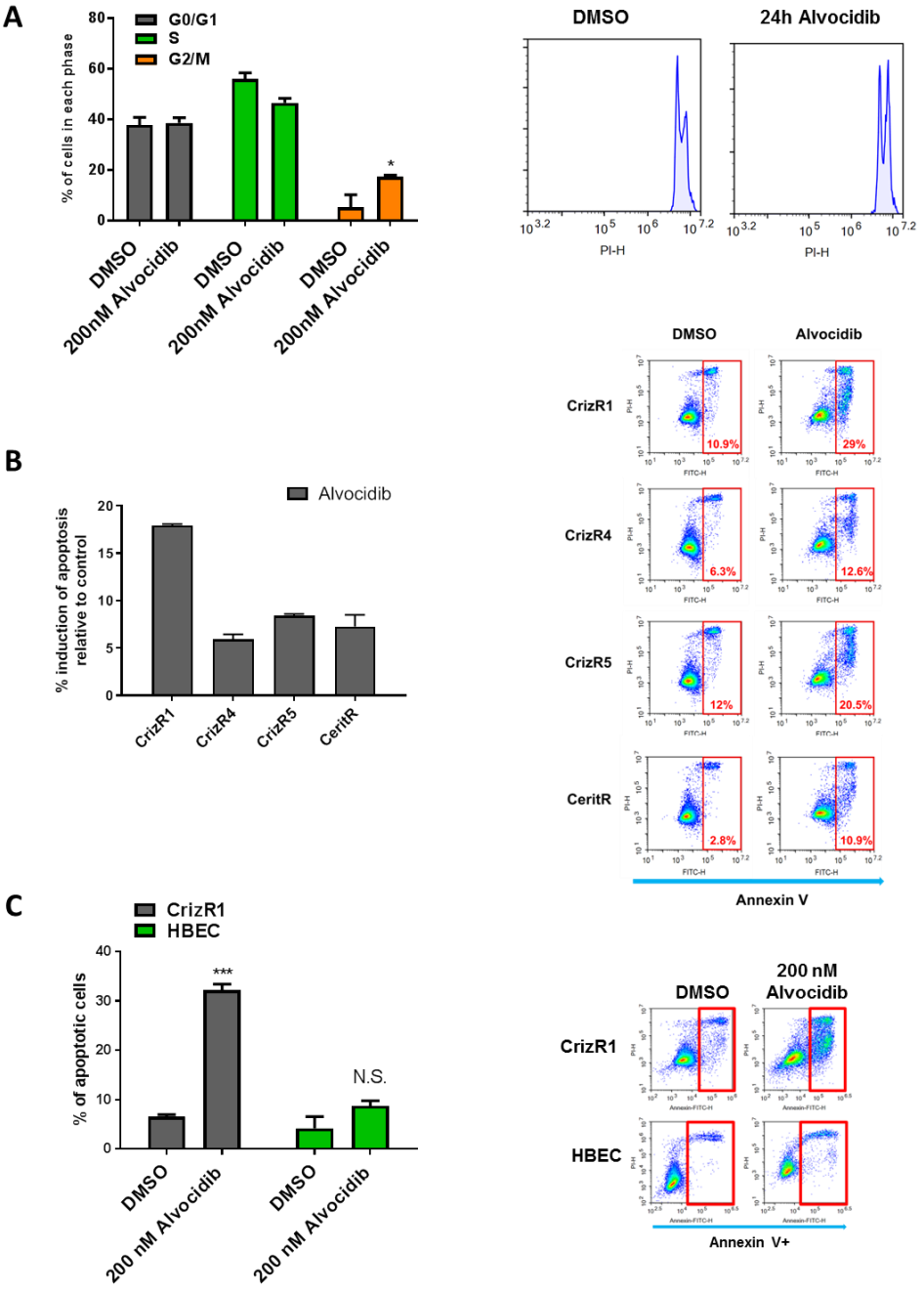

Figure 20: Alvocidib causes apoptosis with minimal cell cycle arrest

A) CrizR1 cells were treated with vehicle control or 200nM alvocidib for 24h. Then, cells were fixed and stained with PI, followed by flow cytometry. Shown on the right are the DNA content peaks generated by the flow cytometer.

B) The indicated cell lines were treated with vehicle control or 200nM alvocidib for 48h. Then, cells were stained with Annexin V/PI, followed by flow cytometry analysis. Before plotting the percentage of Annexin+ cells, the percentage of apoptosis induced by the vehicle control was subtracted to show the percentage of apoptotic cells purely due to drug treatment. Shown on the right are the gated flow cytometry graphs, gated after single stain, no-stain and double-stain controls.

C) CrizR1 and HBEC cells were treated with vehicle control or 200nM alvocidib for 72h. Then, cells were stained with Annexin V/PI, followed by flow cytometry analysis. Shown on the right are the gated flow cytometry graphs, gated after single stain, no-stain and double-stain controls.

Data are presented as means ± SD. (n = 3 biological replicates). P values were calculated by two-tailed student's t-test (*p < 0.05, **p<0.01, ***p<0.001).

I asked whether dinaciclib or THZ1 treatment also results in the induction of apoptosis. Dinaciclib at concentrations as low as 50nM and THZ1 at 100nM caused robust apoptotic cell death as assessed by Annexin V staining and flow cytometry in all EML4-ALK cells tested (**Figure 21A**). The drug-resistant EML4-ALK cells exhibit different degrees of apoptosis, suggesting that each clone is susceptible to a different degree to CDK inhibition.

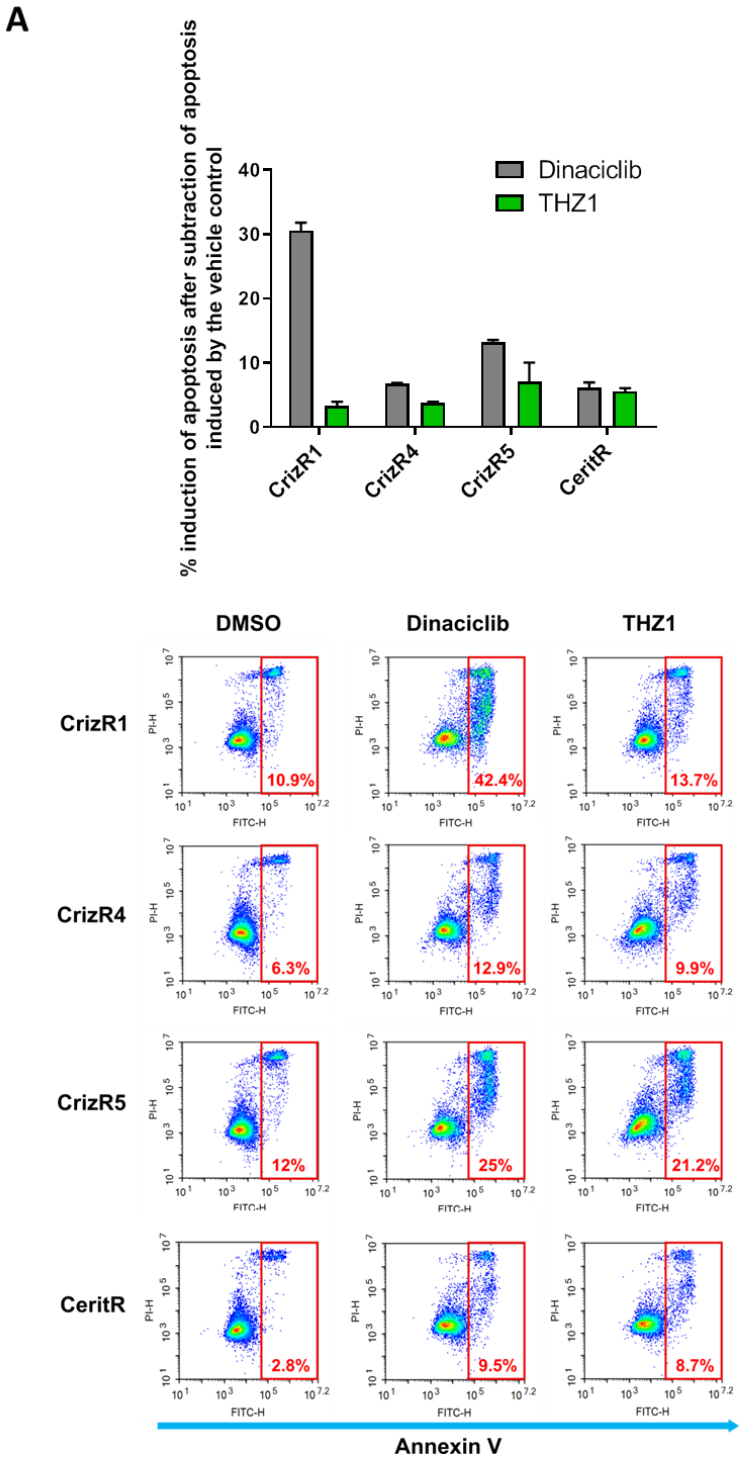

Figure 21: Apoptotic induction by dinaciclib and THZ1

A) The indicated cell lines were treated with vehicle control, 50nM dinaciclib, or 100nM THZ1 for 48h. Then, cells were stained with Annexin V/PI, followed by flow cytometry analysis. Data are presented as means of Annexin V^+ cells ± SD. Before plotting the percentage of Annexin+ cells, the percentage of apoptosis induced by the vehicle control was subtracted to show the percentage of apoptotic cells purely due to drug treatment. (n = 3 biological replicates). P values were calculated by two-tailed student's t-test (*p < 0.05, **p<0.01, ***p<0.001). Shown on the bottom are the gated flow cytometry graphs, gated after single stain, no-stain and double-stain controls for each cell line.

Lastly, the differential response to alvocidib and dinaciclib was examined in a panel of NSCLC cell lines with different genetic backgrounds. H3122 CrizR1 cells and STE-1 AlecR exhibited the highest levels of apoptosis with low dose alvocidib or dinaciclib (**Figure 22**), suggesting a selectivity of these compounds towards EML4-ALK drug-resistant cells.

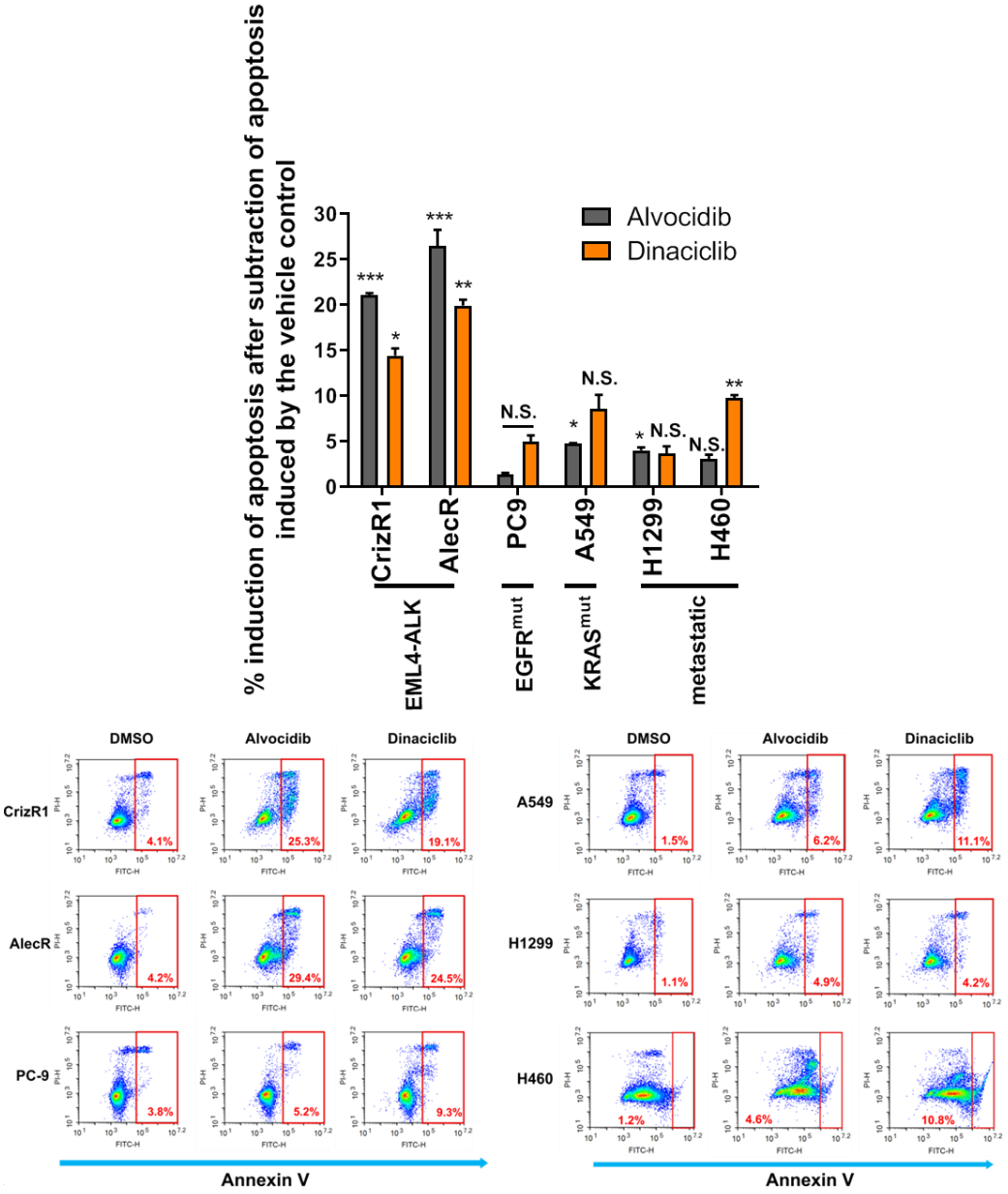

Figure 22: Pan-CDK inhibition shows selectivity towards EML4-ALK drug-resistant cells

A) The indicated cell lines were treated with vehicle control, 200nM alvocidib or 25nM dinaciclib for 48h. Then, cells were stained with Annexin V/PI, followed by flow cytometry analysis. Data are presented as means of Annexin V+ cells ± SD. Before plotting the percentage of Annexin+ cells, the percentage of apoptosis induced by the vehicle control was subtracted to show the percentage of apoptotic cells purely due to drug treatment (n = 3 biological replicates). P values were calculated by two-tailed student's t-test (*p < 0.05, **p<0.01, ***p<0.001). Shown below are the gated flow cytometry graphs, gated after single stain, no-stain and double-stain controls for each cell line.

4.2.12 Mechanism of apoptosis following CDKi treatment

I aimed to understand how pan-CDK inhibition results in cell death. The fact that there is minimal cell cycle arrest led me to hypothesise that the induction of apoptosis is largely cell cycle-independent. Furthermore, H3122 cells carry a TP53 E285V mutation (COSMIC project, Sanger Institute) which renders p53 inactive [192]. Therefore, these cells should initiate p53-independent apoptosis. To approach this in an unbiased fashion, an apoptotic protein array which simultaneously profiles 43 apoptotic proteins was used (**Figure 23A**). After 24h of alvocidib treatment, several dysregulated proteins were detected, some of these changes, however, were not robust (**Figure 23B**). A significant upregulation was found for the pro-apoptotic proteins BIM, BID, SMAC and as expected Caspase 3 and Caspase 8 (**Figure 23C**). These findings suggest an induction of the mitochondrial apoptotic pathway.

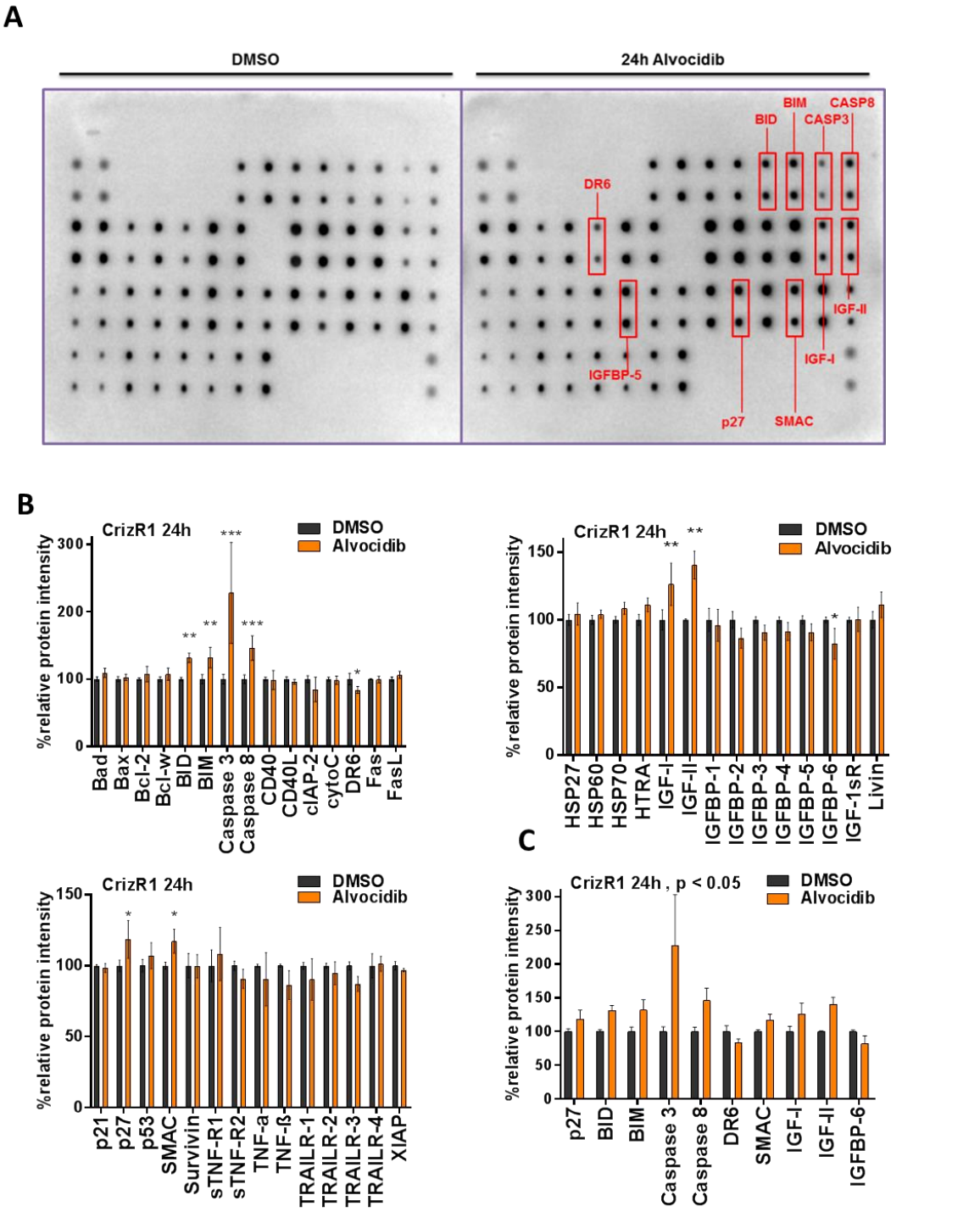

Figure 23: The intrinsic mitochondrial apoptotic pathway is induced by alvocidib treatment

A) CrizR1 cells were treated with vehicle control or 200nM alvocidib for 24h. Then, protein extracts were hybridised to an Abcam 43-protein apoptotic array and chemiluminescence was detected according to the manufacturer's instructions and as detailed in 2.5.1. Increased or decreased signal upon alvocidib treatment indicates increased or decreased protein expression respectively, for this particular membrane spot. The luminescence signal was recorded and normalized to loading controls. Shown is a representative blot of 2 independent experiments.

B) Quantification of the signal from A), with DMSO pixel values having been transformed to represent 100%. Graphs show normalised means ± SD. (n = 3 biological replicates). P values were calculated by a two-tailed student's t-test (*p < 0.05, **p<0.01, ***p<0.001).

C) Plotted are only the significant changes from B).

Looking in the literature it was found that alvocidib caused a suppression of the anti-apoptotic protein MCL-1 in lung carcinoma cells [193]. The loss of MCL-1 was confirmed in all EML4-ALK drug-resistant cell lines after alvocidib and dinaciclib treatment (**Figure 24A**). The anti-apoptotic protein Survivin has also been linked to the response to alvocidib before [194]. A downregulation of Survivin was detected upon alvocidib and dinaciclib treatment at the protein level. In addition, alvocidib is known to decrease transcriptional output by inhibiting CDK9 and consequently, elongation by the RNA Polymerase II [195]. It was then reasoned that all three inhibitors affect transcriptional regulation and subsequently, the mRNA levels of pro- and anti-apoptotic proteins. Indeed, in this system, alvocidib and dinaciclib treatment decreased phosphorylation at the Ser2 repeat of the RNA Polymerase II (**Figure 24B**).

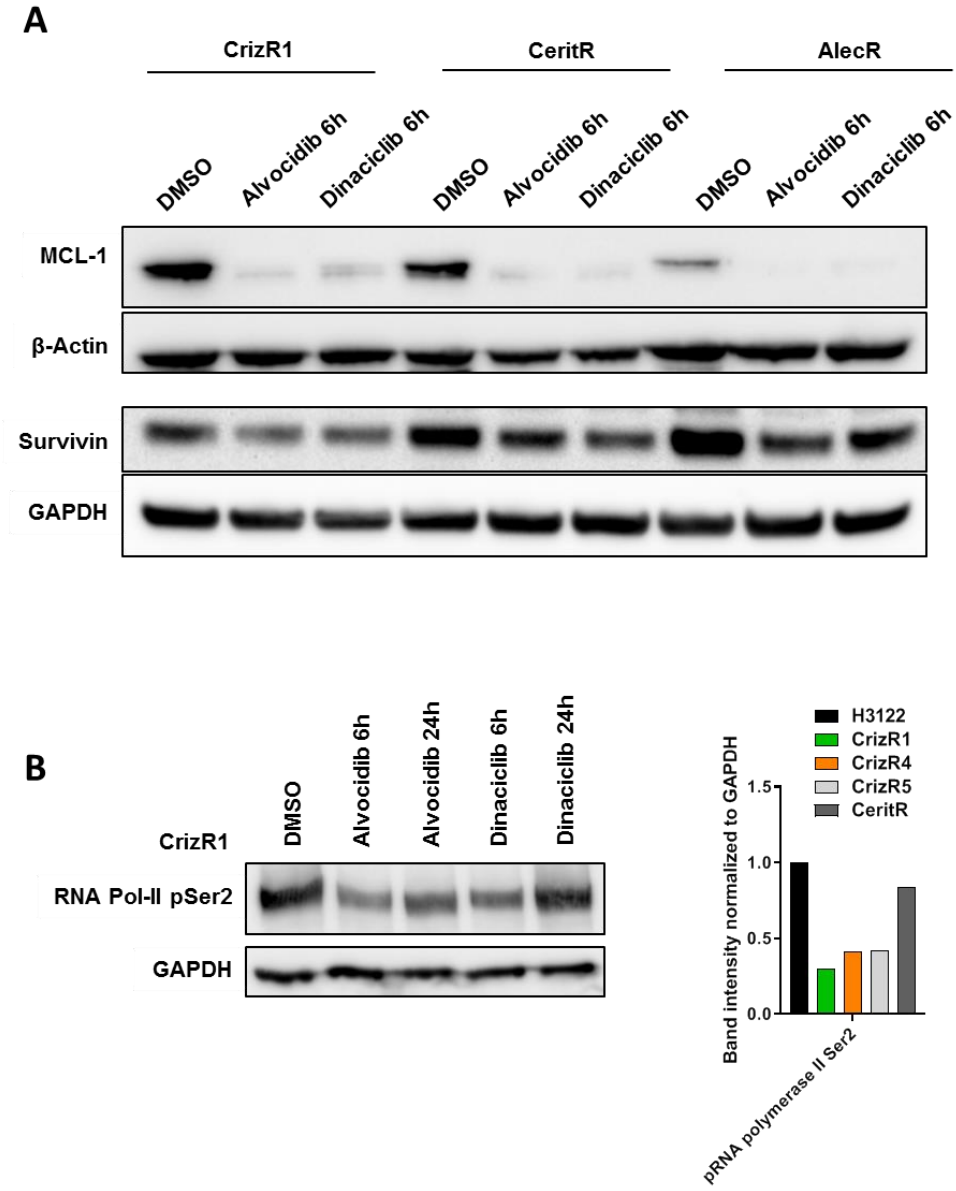

Figure 24: MCL-1 and Survivin are downregulated upon alvocidib treatment

A) The indicated cell lines were treated with vehicle control, 25nM dinaciclib or 200nM alvocidib, for 6h, after which point protein extracts were analysed by western blotting for the expression of MCL-1/Survivin with β-Actin/GAPDH as housekeeping control. Both MCL-1 and Survivin are downregulated in response to alvocidib or dinaciclib treatment, in all drug-resistant EML4-ALK cells. Shown is a representative blot of 3 independent experiments.

B) CrizR1 cells were treated with vehicle control, 25nM dinaciclib or 200nM alvocidib for 6h and 24h, after which point protein extracts were analysed by western blotting for the expression of the indicated proteins. The phosphorylation of RNA polymerase II at the Ser2 repeat is decreased upon alvocidib or dinaciclib treatment, indicating a CDK9-specific effect. Shown is a representative blot of 2 independent experiments. (right panel) Quantification of the protein bands presented on the left panel. Non-saturated ECL images were digitally quantified for signal intensity, which was subsequently normalised to the signal intensity of the loading control used (GAPDH).

To test the specificity of these inhibitors, siRNA oligos for CDK7 and CDK9 were used (**Figure 25A**). Only a modest knockdown of CDK9 was enough to induce apoptosis (**Figure 25B**), reinforcing the transcriptional hypothesis. Conversely, CDK7 knockdown on its own did not lead to apoptosis, suggesting a need for combined inhibition of CDK7/12/13. This reinforces the likelihood of a CDK9-mediated RNA polymerase II inhibition that ultimately results in apoptosis. While it is possible that the effect of the CDK9 siRNA may be due to off-target activity, a mixed sequence of 4 different oligos was used (Dharmacon), to minimise this possibility.

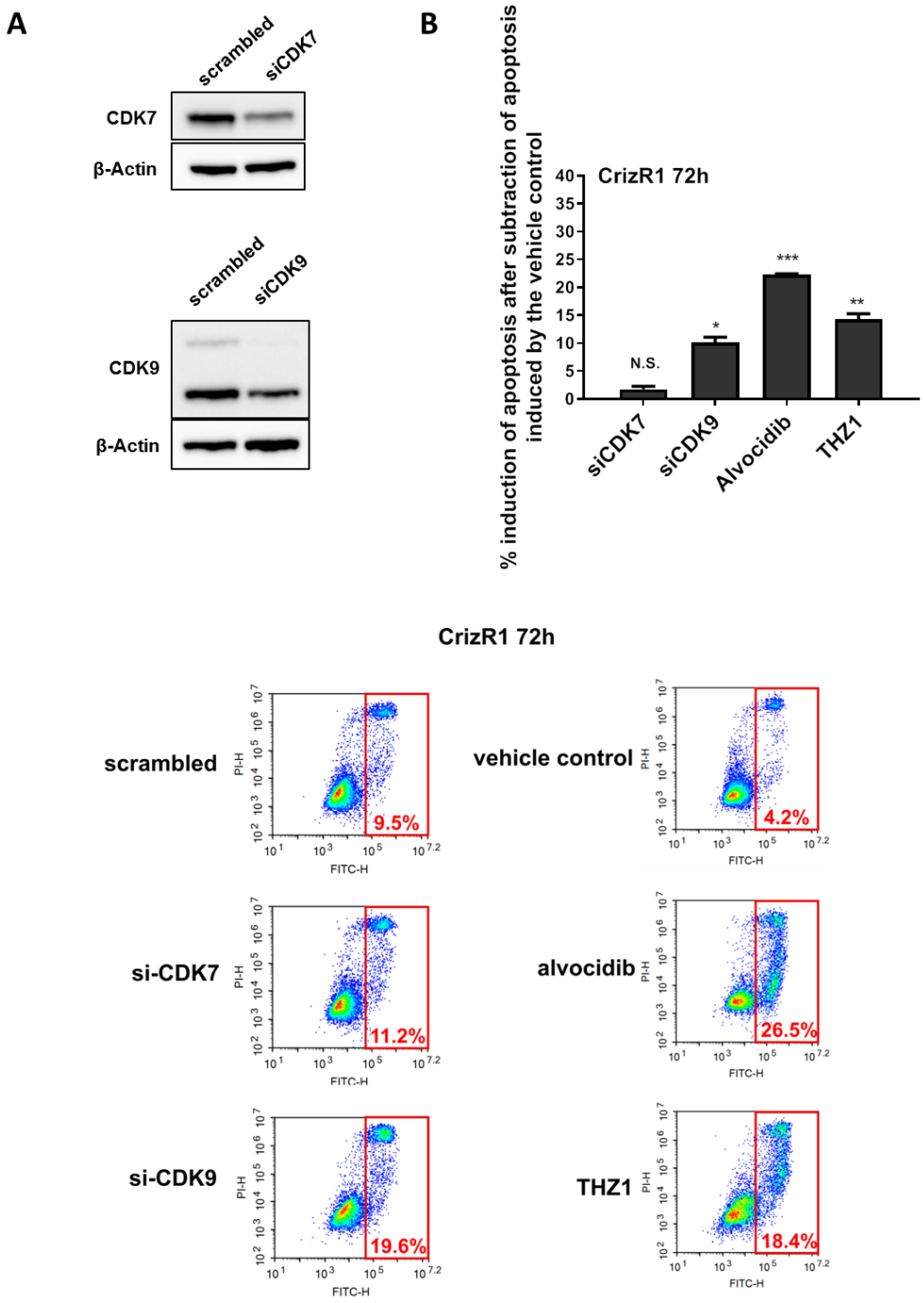

Figure 25: CDK9 knockdown induces apoptosis

A) Western blot analysis of CrizR1 cells treated with scrambled or siRNA for CDK7 or CDK9 for 72h shows a modest knockdown with CDK9 and a more effective knockdown with CDK7. Shown are representative blots of 2 independent experiments.

B) CrizR1 were treated as above, or with DMSO/100nM alvocidib/50nM THZ1 and cells were stained with Annexin V/PI and analysed by flow cytometry for Annexin V+ cells 72h post-transfection. (Gate plots are shown at the bottom, gated after no-stain, single-stain and double stain apoptotic controls). Before plotting the percentage of Annexin+ cells, the percentage of apoptosis induced by the vehicle control was subtracted to show the percentage of apoptotic cells purely due to drug treatment. Data are presented as normalised means ± SD. (n = 3 biological replicates). P values were calculated by a two-tailed student's t-test (*p < 0.05, **p<0.01, ***p<0.001).

To add more confidence to the mechanistic basis of CDK7 or CDK9 inhibition, we performed Chip-seq for RNA polymerase II after treating CrizR1 cells with alvocidib or THZ1. A global overview of RNA pol II peaks suggested that alvocidib treatment dramatically increased occupancy at the TSS, while THZ1 slightly decreased it (**Figure 26A**). We performed GSEA analysis with the HALLMARK gene collection based on the core enrichment of the mapped peaks and found 6 differentially enriched signatures with alvocidib (**Figure 26B**) and 11 with THZ1 (**Figure 26C**). Notably, both drugs induced different RNA pol II occupancy in the transcription start site (TSS) of MYC targets.

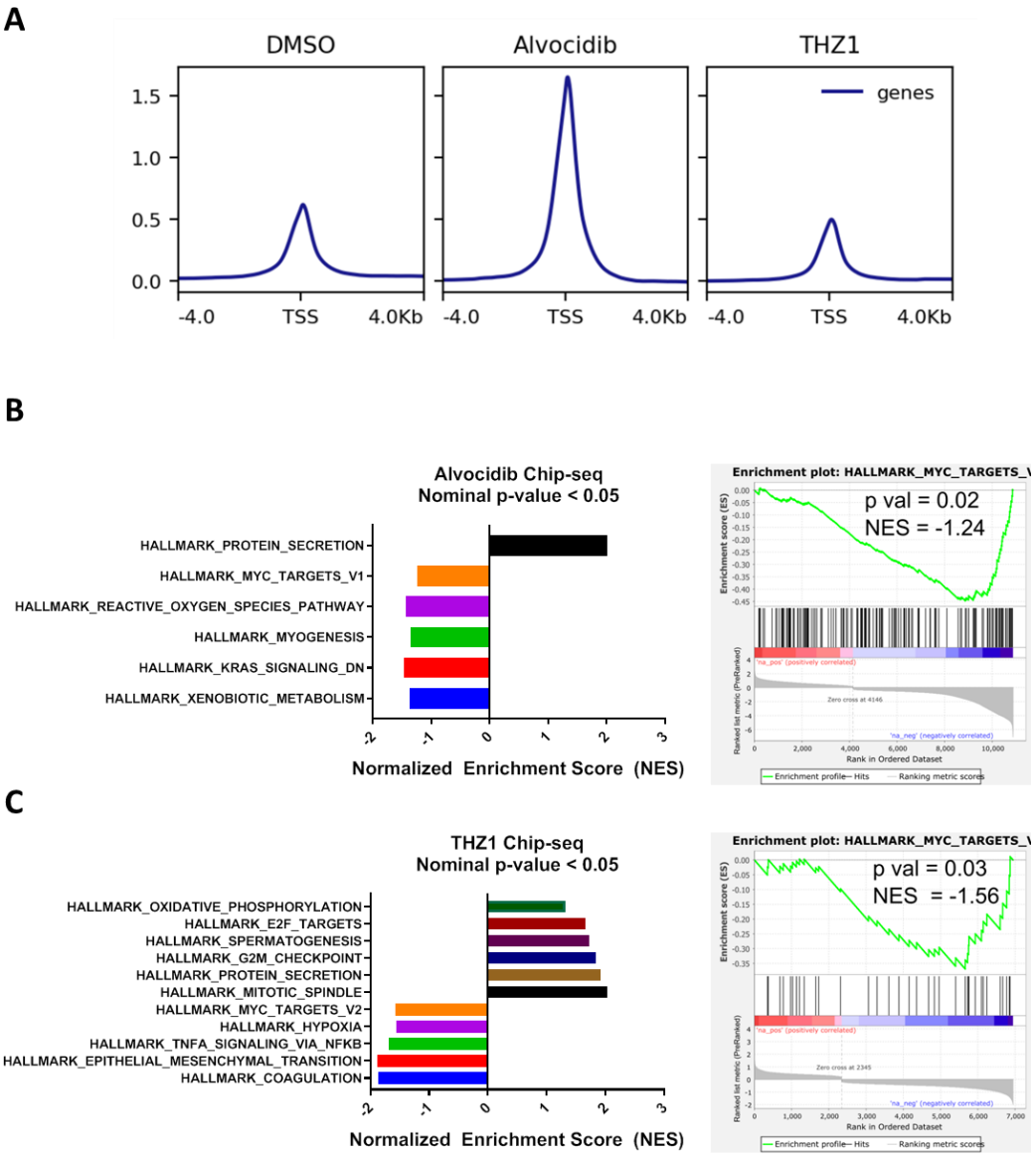

Figure 26: Alvocidib or THZ1 treatment is concordant with CDK7 or CDK9 inhibition based on RNA polymerase II Chip-seq

A) CrizR1 cells were treated with vehicle control, 200nM alvocidib or 100nM THZ1 for 6 hrs, then chromatin was precipitated with an anti-RNA polymerase II antibody and sequenced. Plotted is the average number of peaks per condition, showing increased RNA pol II occupancy at the transcription start site (TSS) with alvocidib treatment and decreased occupancy with THZ1 treatment.
B) GSEA analysis using the HALLMARK gene collection for the differentially enriched peaks around the TSS (±1kb) with alvocidib shows a significant change in MYC targets. Shown on the right are the plots of the "MYC targets"-enriched signatures. NES stands for normalised enrichment score. Over 100 permutations are represented on the x-axis with clear enrichment in both negative (blue-downregulation) and positive (red-upregulation) correlation.
C) As above, for THZ1 treatment, GSEA shows a significant change in MYC targets. Shown on the right are the plots of the "MYC targets"-enriched signatures. NES stands for normalised enrichment score. Over 30 permutations are represented on the x-axis with enrichment in both negative (blue-downregulation) and positive (red-upregulation) correlation.

Lastly, we looked at the RNA pol II peaks of the previously examined genes *MCL1* and *Survivin* and we also included *MYC*. From the gene tracks, it was evident that alvocidib treatment results in pausing of the RNA pol II at the Transcription Start Site (TSS) while reducing the occupancy across the gene body and THZ1 results in reduced binding of RNA pol II at the TSS (**Figure 27A**, **B** and **C**). This is highly concordant with previous findings which suggest that CDK7 mediates the binding of the RNA pol II at the promoters, while CDK9 regulates the release and elongation steps [150].

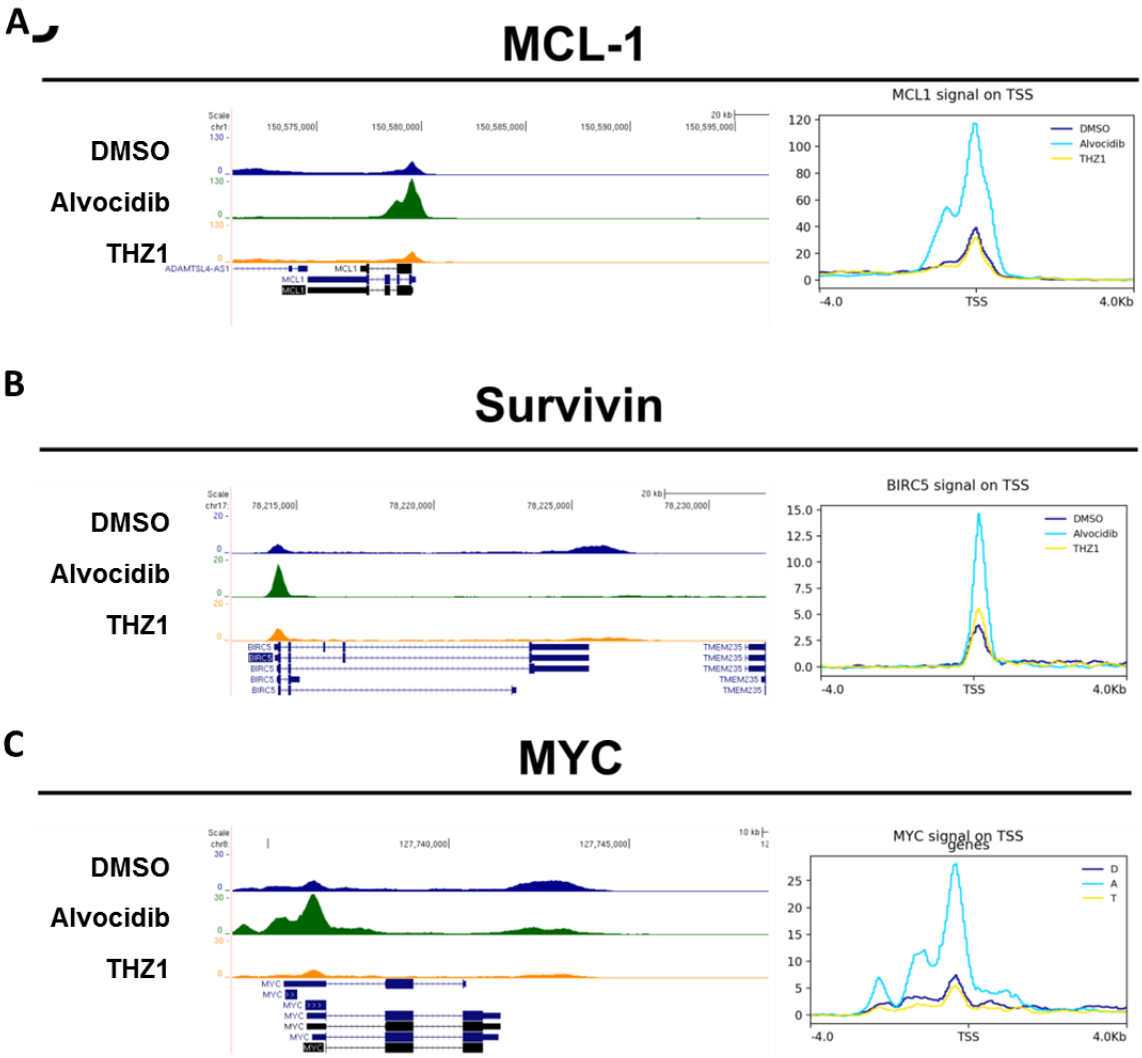

Figure 27: Alvocidib reduces the RNA pol II occupancy across the gene body while THZ1 at promoter sites

A) Background-subtracted gene tracks of RNA polymerase II occupancy at the *MCL1* locus using the UCSC genome browser.
B) As above, for the *BIRC5* locus.
C) As above, for the *MYC* locus.
Evidently, for all the above loci, RNA polymerase II peak intensity is reduced across the gene body with alvocidib treatment, while it is increased around the TSS indicating an inhibition of the elongation step of transcription. THZ1 treatment on the other hand marginally reduces RNA polymerase II peak intensity around the TSS, indicating inhibition of RNA polymerase II recruitment at the promoter.

Subsequently, it was hypothesised that short-lived, anti-apoptotic mRNAs such as *MCL-1* and *Survivin* are degraded after transcriptional inhibition. Consistently, *MCL-1* and *Survivin* were downregulated at the mRNA level after treatment with all the compounds (**Figure 28A**). I asked whether MCL-1 downregulation is enough to induce apoptosis and to account for alvocidib-induced cell death. MCL-1 was silenced using two different siRNAs, (**Figure 28B**), however, there was no significant induction of apoptosis (**Figure 28C**), suggesting that there is a contribution of other apoptotic proteins to initiate alvocidib-induced cell death.

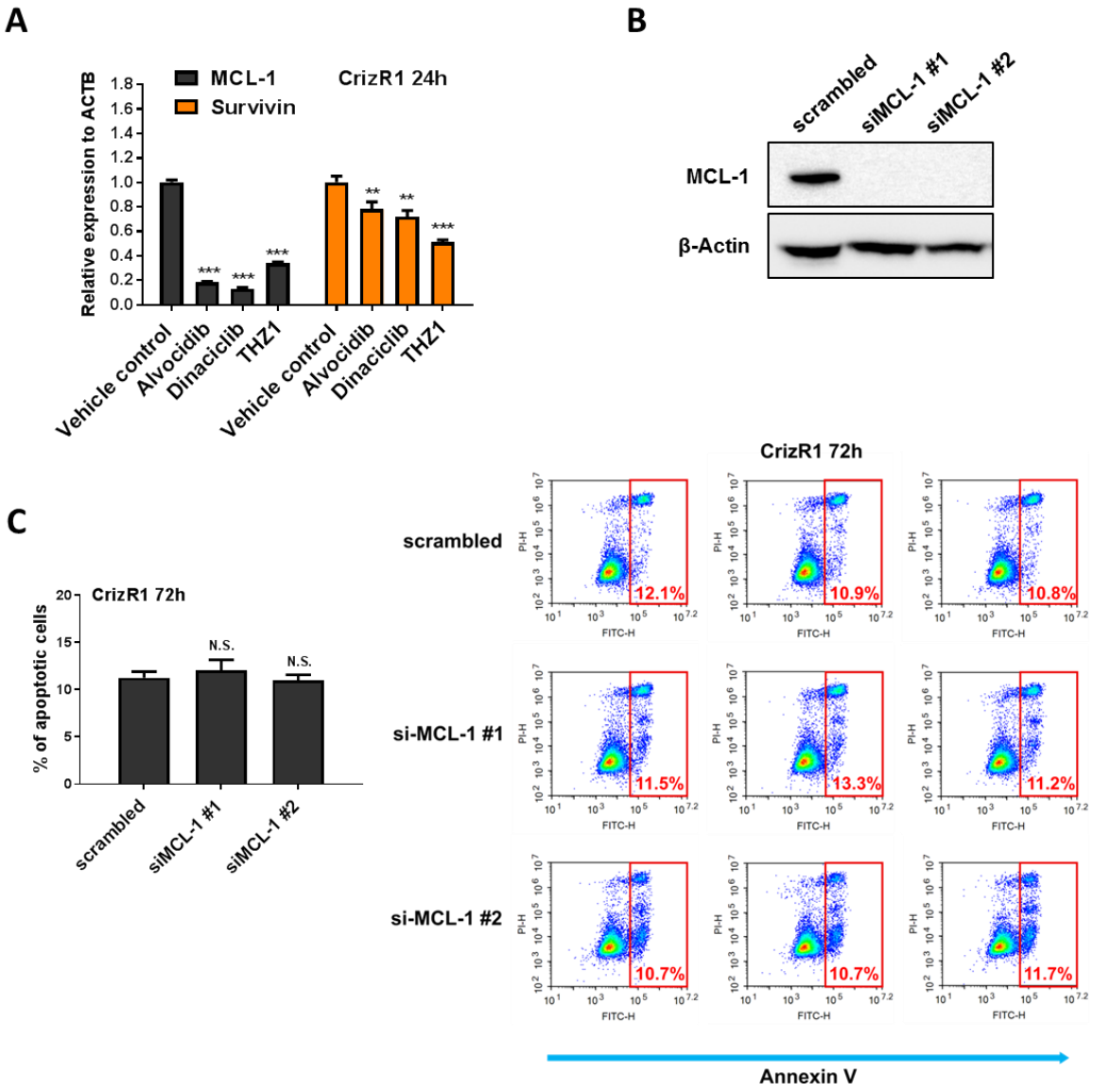

Figure 28: MCL-1 downregulation is not enough to initiate apoptosis

A) CrizR1 cells were treated with 200nM alvocidib, 25nM dinaciclib, 100nM THZ1 or vehicle control for 24h. Then, RNA was extracted and the expression of the indicated genes was quantified by RT-qPCR. Data are presented as 2-ΔΔCT normalised means ± SD. (n = 3 biological replicates).

B) Western blot analysis for MCL-1 expression of CrizR1 cells treated with scrambled (50nM) or siRNA for MCL-1 (50nM) for 72h. Shown is a representative blot of 2 independent experiments.

C) CrizR1 were treated as above, for 72h and cells were stained with Annexin V/PI and analysed by flow cytometry for Annexin V+ cells 72h post-transfection. Data are presented as means ± SD (n = 3 biological replicates). Shown on the right are the gated flow cytometry plots after single-stain, no-stain and double-stain apoptotic controls.
P values were calculated by a two-tailed student's t-test (*p < 0.05, **p<0.01, ***p<0.001).

Furthermore, I was interested to see if the expression of cell cycle genes is affected by transcriptional inhibition. The mRNA levels of some of the previously examined cell-cycle related genes were upregulated in CrizR1 cells compared to the H3122 parental. Alvocidib treatment partially or completely restored their expression to the parental levels or lower (**Figure 29**). Additionally, in the same experiment, treatment with the transcriptional inhibitor actinomycin D had an almost identical effect on the cell cycle mRNAs, reinforcing the notion that alvocidib does indeed act through transcriptional inhibition.

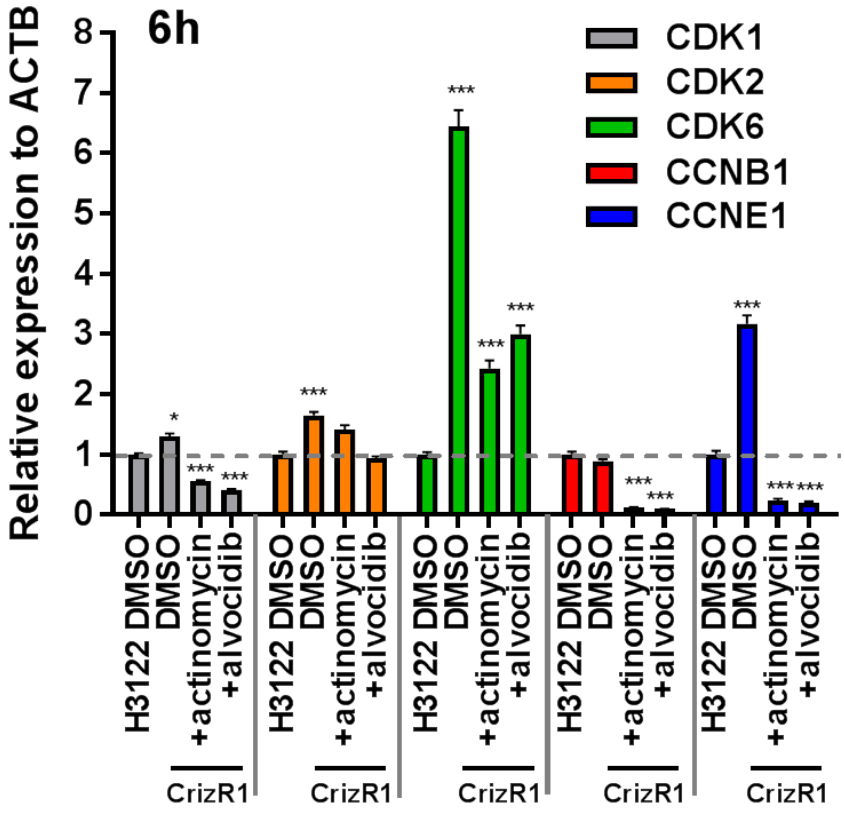

Figure 29: Alvocidib treatment results in the loss of key cell cycle-related mRNAs

H3122 parental and CrizR1 cells were treated with DMSO, 200nM alvocidib or 250ng/ml actinomycin D for 6 hours. Then, RNA was extracted and the expression of the indicated genes was quantified by RT-qPCR. Data are presented as 2-ΔΔCT normalised means ± SD. The DCq values of H3122 parental cells were transformed to 100% and the rest of the treatment conditions were normalised to this, clearly indicating that CDK1, CDK2, CDK6 and CCNE1 are upregulated in CrizR1 compared with H3122 parental cells at the mRNA level. Alvocidib or actinomycin D treatment greatly reduces their mRNA levels (n = 4 biological replicates). P values were calculated by a two-tailed student's t-test (*p < 0.05, **p<0.01, ***p<0.001).

4.2.13 EML4-ALK specificity

While it was demonstrated that EML4-ALK cells are more sensitive to CDK inhibitors compared with other NSCLC cell lines, it was still not clear why. To shed light on this, data from a comprehensive RNA-seq effort of the Cancer Cell-Line Encyclopaedia were utilised (CCLE) [16]. The only EML4-ALK v1 cell line that was available in this cohort was the parental H3122 cells. The normalised RNA-seq expression data were downloaded for only the lung-adenocarcinoma cells (LUAD). Then, the HALLMARK apoptosis gene collection was used and the z-score of the apoptotic genes in all the LUAD cells was plotted (**Figure 30**).

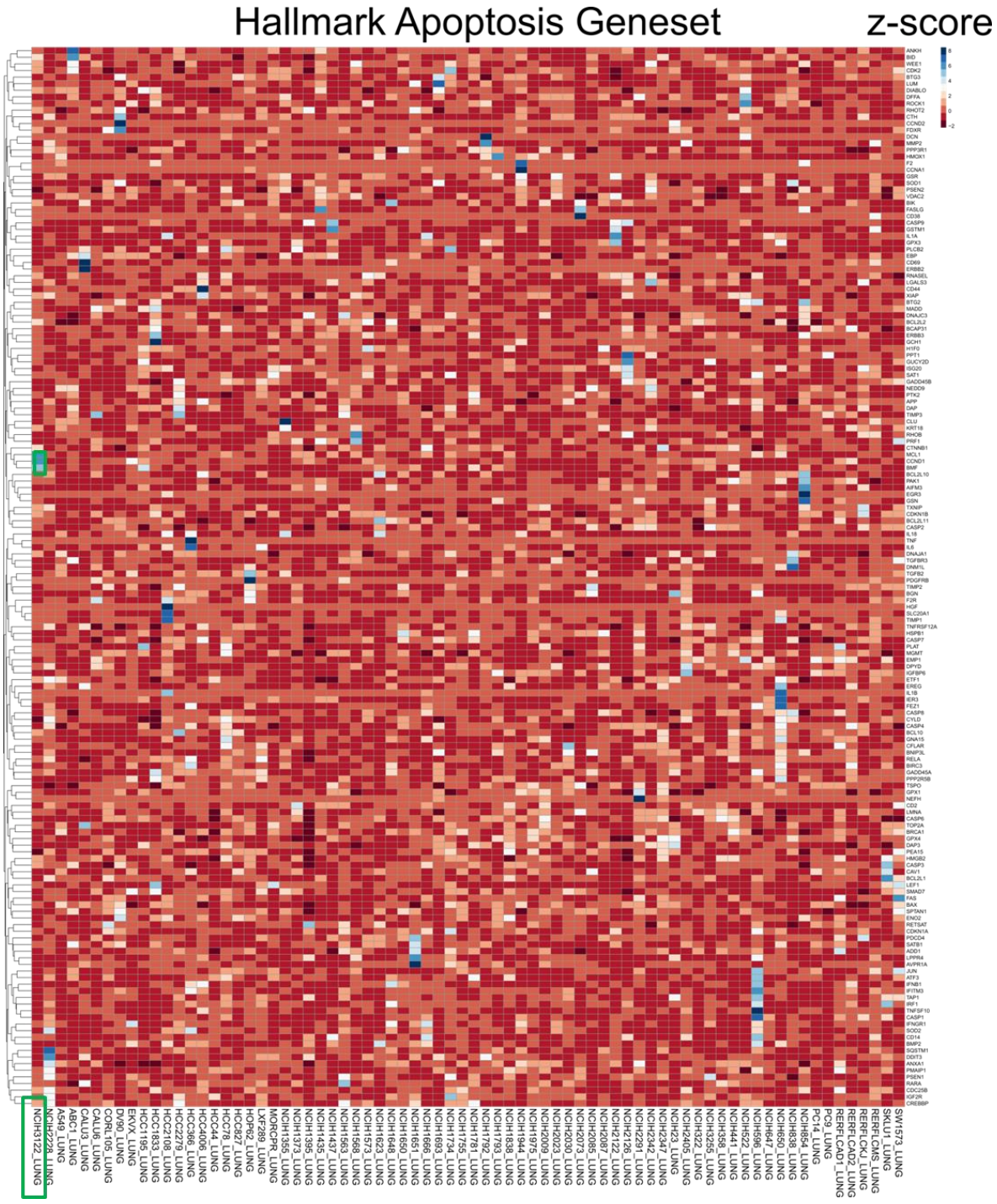

Figure 30: Cluster analysis reveals high expression levels of MCL1 and CCND1 in H3122 cells

Sequencing data from the CCLE project were utilised, specifically the RPKM (Reads Per Kilobase of transcript, per Million mapped reads) values which represent a uniform, normalized way of looking at transcript expression across cell lines [16]. Then, the gene expression data of only the lung adenocarcinoma cell lines were isolated. To visualise these data, the values were transformed to z-score, indicating how many standard deviations above the mean is the expression of a single gene. After isolating only the apoptosis-related genes using the HALLMARK gene collection, the z-score was plotted on a heatmap using Euclidian distance clustering. Looking at the cell line of interest, H3122 EML4-ALK^{mut} cells, it is evident that there is a cluster of distinctly upregulated genes, highlighted with a green square. This blue colour intensity represents an expression of more than 6 standard deviations above the lung adenocarcinoma mean for the genes MCL1 and CCND1.

There was a distinct clustering of up-regulated apoptotic genes, which were *MCL-1* and *CCND1***.** *Survivin* was not part of the HALLMARK gene set, but when it was examined separately, it was found that H3122 cells also had the highest mRNA levels. The normalised RPKM values for these genes are plotted (**Figure 31**). These data raise the possibility that a collective dysregulation of these genes renders EML4-ALK cells particularly susceptible to transcriptional perturbation.

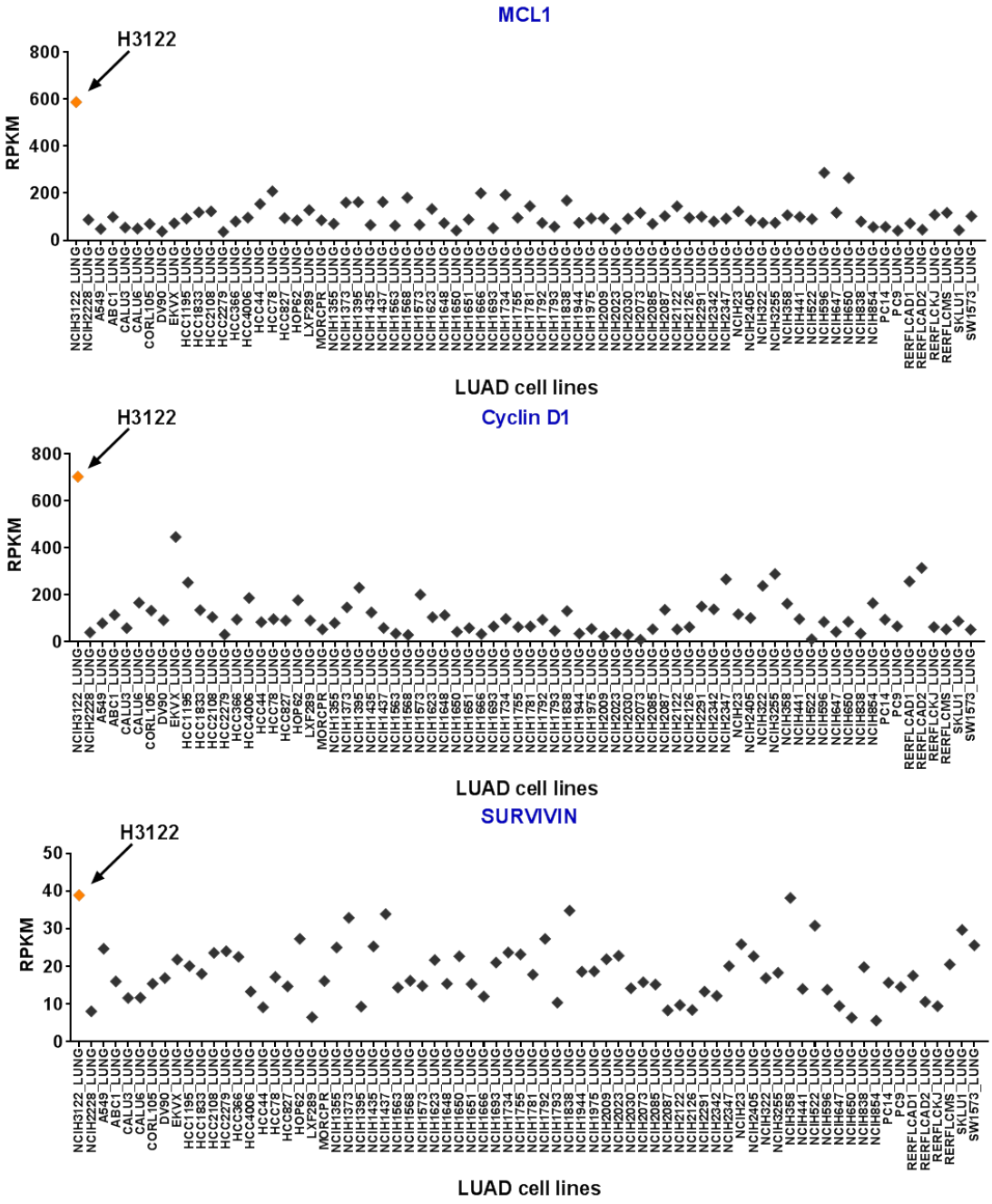

Figure 31: RPKM values from RNA-seq comparing H3122 with other LUAD cell lines

As described in **(Figure 30),** the normalised RPKM values (Reads Per Kilobase of transcript, per Million mapped reads) values which represent a uniform, normalized way of looking at transcript expression across cell lines [16] were downloaded from CCLE. These normalized gene expression values are plotted in a graph comparing H3122 with the rest of the LUAD cell lines. Arrows indicate the highest expression levels for the mRNAs of *MCL-1, Survivin* and *CCND1.*

Lastly, in an effort to test whether there is a differentiating gene signature of H3122 cells, the RNA-seq data were ordered according to z-score. Then, only genes that were at least 1.5 standard deviations above or below the LUAD mean were isolated. Upon a GSEA analysis, a significant enrichment in STAT1 targets was uncovered (**Figure 32A**), as well as genes that have been previously described as amplified in lung cancer (**Figure 32B**). These data may suggest that an aberration related to STAT1 activity has rendered EML4-ALK cells distinctly sensitive to transcriptional perturbation. Interestingly, the previously identified candidate *CCND1* is a STAT1 target as indicated in the gene set list.

A

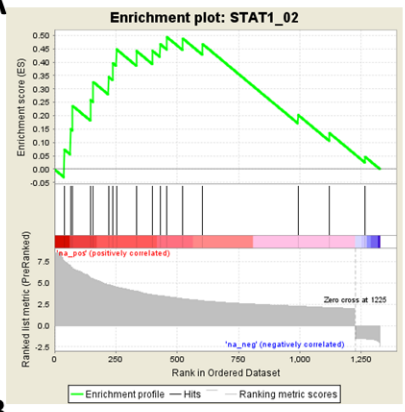

GENE SYMBOL	RANK IN GENE LIST	RANK METRIC SCORE	CORE ENRICHMENT
SCNM1	39	7.55	Yes
PI4KB	65	6.99	Yes
RGS17	74	6.67	Yes
CCND1	147	5.60	Yes
POGZ	158	5.46	Yes
SF3B4	220	4.78	Yes
FOXG1	237	4.66	Yes
GABPB2	252	4.53	Yes
AKIRIN2	334	4.03	Yes
NKX2-8	399	3.61	Yes
SRSF2	430	3.50	Yes
PABPN1	458	3.39	Yes
ZNF385A	523	3.14	No
VEZF1	603	2.91	No
SKA2	992	2.27	No
HNRNPH2	1120	2.11	No
LRRC41	1266	-1.56	No

B

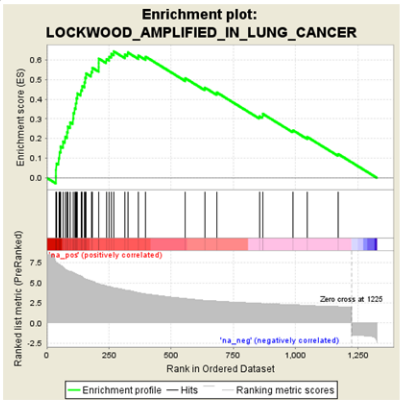

GENE SYMBO	RANK IN GENE LIS	RANK METRIC SCOR	CORE ENRICHMEN
MRPL9	36	7.62	Yes
ILF2	37	7.60	Yes
S100A13	38	7.55	Yes
SNAPIN	48	7.35	Yes
RPS27	51	7.29	Yes
PSMB4	56	7.15	Yes
PI4KB	65	6.99	Yes
SLC39A1	73	6.76	Yes
PIP5K1A	82	6.56	Yes
TDRKH	84	6.55	Yes
SETDB1	94	6.43	Yes
DENND4B	105	6.28	Yes
S100A11	108	6.27	Yes
EAPP	112	6.21	Yes
MBIP	117	6.10	Yes
PPFIA1	119	6.10	Yes
PPP2R3C	123	6.04	Yes
SNX6	137	5.87	Yes
ARNT	143	5.72	Yes
CERS2	152	5.55	Yes
STRN3	154	5.52	Yes
POGZ	158	5.46	Yes
FADD	179	5.24	Yes
PNN	183	5.19	Yes
AP4S1	208	4.86	Yes
JTB	209	4.85	Yes
SRP54	210	4.84	Yes
BAZ1A	239	4.64	Yes
ARHGAP5	251	4.54	Yes
KIAA0391	259	4.47	Yes
GEMIN2	269	4.39	Yes
MIPOL1	314	4.13	No
FAM177A1	325	4.08	No
PAX9	368	3.78	No
TUFT1	397	3.62	No
CFL2	557	3.05	No
S100A6	635	2.82	No
NKX2-1	683	2.73	No
NFKBIA	854	2.45	No
FOXA1	867	2.44	No
SEC23A	868	2.44	No
FASTKD3	989	2.28	No
SIVA1	1047	2.20	No
TARS	1171	2.05	No

Figure 32: H3122 cells are significantly enriched in STAT1 targets and genes previously identified as amplified in lung cancer

A) GSEA enrichment in H3122 transcripts expressed at least 1.5 standard deviation above the lung adenocarcinoma average shows enrichment in STAT1 targets. NES stands for normalised enrichment score. Over 15 permutations are represented on the x-axis with clear enrichment in positive (red-upregulation) but not negative correlation (blue-downregulation). On the right is the expanded list of permutations.

B) As in A), the Lockwood set of genes amplified in lung cancer was identified. NES stands for normalised enrichment score. Over 40 permutations are represented on the x-axis with clear enrichment in positive (red-upregulation) but not negative correlation (blue-downregulation). On the right is the expanded list of permutations. On the right is the expanded list of genes

4.2.14 *In vivo* studies & clinical modelling

Given the impressive activity of alvocidib, dinaciclib and THZ1 *in vitro*, I decided to test whether they would be equally effective in a mouse xenograft model of these drug-resistant cell lines. Subsequently, CrizR4 cells resistant to crizotinib were injected in the right flank of nude mice. When tumours reached between 100-200 mm^3, mice were randomised to different groups. Mice were treated with crizotinib daily at a dose of 50 mg/kg P.O. with the corresponding vehicle control group. As expected, crizotinib-resistant cells formed tumours that were not significantly delayed by crizotinib treatment (**Figure 33A**). THZ1 at a dose of 10mg/kg twice per day I.P. exhibited significant weight loss/toxicity (**Figure 33B**) which led to premature termination of the study according to the pre-defined humane endpoints. This is in contrast with previous studies, where this dose of THZ1 showed minor weight loss [150,156]. In this study, after 5 daily treatments, mice had lost more than 20% weight and became hunched and inactive. A similar observation took place for dinaciclib treatment, at 48mg/kg by I.P. injection twice a week, as per the published protocol [149]. In this study, after only one injection of dinaciclib, all mice lost weight (**Figure 33C**), some of which at the 20% limit and were thus sacrificed and the study terminated. A protocol with lower drug doses was subsequently initiated.

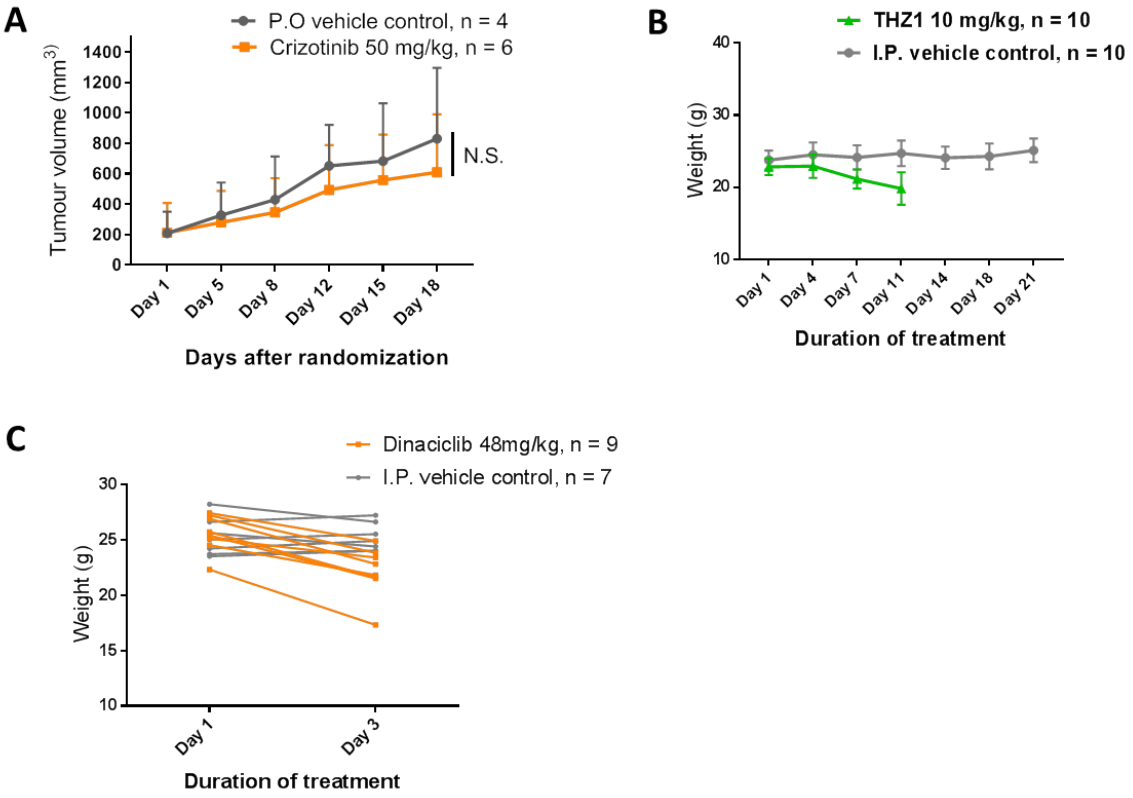

Figure 33: Immunocompromised xenograft model of crizotinib-resistant cells

A) CrizR4 cells were injected in the right flank of nude athymic mice, and mice were randomised in different groups, with 7 mice per group initially. When tumour average size reached 200mm^3, mice were treated with vehicle control or crizotinib at 50mg/kg by oral gavage. Plotted are the tumour size means ± SD. Due to tumour ulceration or reaching the maximum allowed size, by the end of the experiment, there were n = 4 mice in the vehicle control group and n = 6 mice in the crizotinib group.

B) As in A), mice were treated with vehicle control or THZ1 at 10mg/kg by 2x daily I.P. injection. Plotted are the mouse weight means ± SD, n = 10 mice per group.

C) As in A), mice were treated with vehicle control or THZ1 at 10mg/kg by daily I.P. injection. Plotted are the individual mouse weight measurements, n = 7 mice for the control group, n = 9 mice for the treatment groups.

Alvocidib treatment at 10mg/kg, using daily I.P. injections resulted in a significant delay in tumour growth (**Figure 34A**). After 2 weeks weight loss was observed, at which point the treatment was interrupted and all mice but one, recovered fully. Interestingly, even with a week without treatment, tumours did not grow significantly, suggesting that there is room for improving the dose scheduling as daily injections may not be required. Unfortunately, this study could not be kept monitored for longer, as progressively more tumours in the control group became ulcerated and mice had to be sacrificed. Then, tumour sections were stained for cleaved caspase-3 in order to assess the levels of apoptosis. A trained pathologist quantified the expression levels of cleaved caspase-3 and concluded that there is a marginally significant increase in apoptosis (**Figure 34B**). These data were expanded with alectinib-resistant cells. Unlike CrizR4 cells, these cells despite remaining resistant in culture lost resistance to alectinib during the ~3 week inoculation period in mice (**Figure 34C**). Even though alectinib dramatically reduced tumour growth, alvocidib or dinaciclib treatment at 10mg/kg or 20mg/kg 3x/week also significantly reduced tumour growth. Alvocidib was more effective, highlighting again the translational relevance of these data and pointing to alvocidib testing in all EML4-ALK patients despite their prior use of ALK inhibitors. Subsequent staining for cleaved caspase 3 was initiated but was unfortunately beyond the time frame of this thesis.

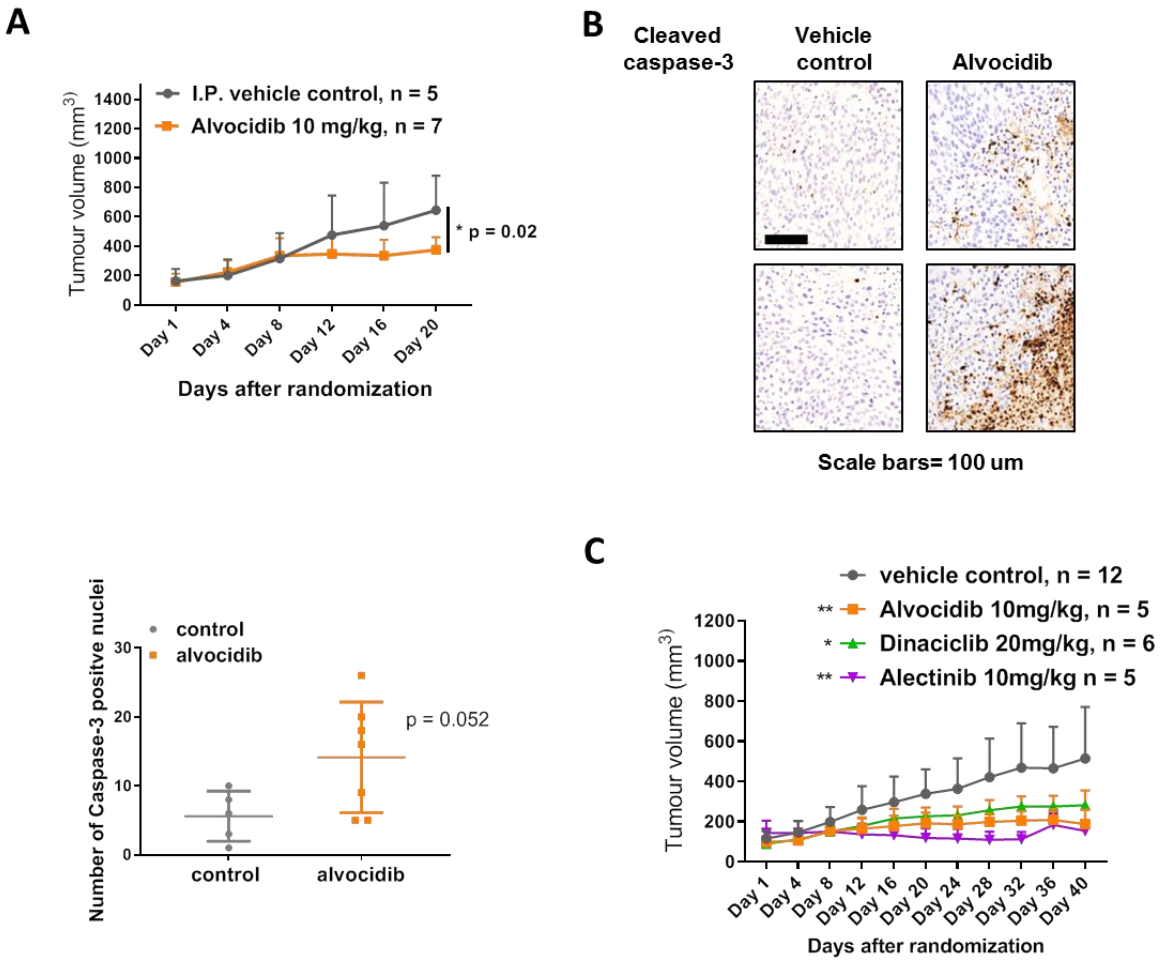

Figure 34: Alvocidib or dinaciclib treatment delays tumour growth *in vivo*

A) CrizR4 cells were injected in the right flank of nude athymic mice, and mice were randomised in different groups, n = 7 mice/group. When tumour average size reached 200mm^3, mice were treated with vehicle control or alvocidib at 10mg/kg by I.P. injection. Plotted are the tumour size means ± SD. Due to tumour ulceration or reaching the maximum allowed size, by the end of the experiment there were n = 5 mice in the vehicle control group and n = 7 mice in the alvocidib group. P values were calculated at the last time point by a two-tailed student's t-test (*p < 0.05, **p<0.01, ***p<0.001).

B) Paraffin blocks of harvested tumours were stained with IHC for cleaved caspase-3. The quantification was kindly performed by Dr Matteo Fassan.

C) AlecR cells were injected in the right flank of NOD-SCID mice and mice were randomised in different groups. When the average size of tumours reached 200mm^3, mice were treated with vehicle control P.O. / I.P. at 10ml/kg 3x/week, 10mg/kg alectinib P.O. 3x/week, 10mg/kg alvocidib I.P. 3x/week or 20mg/kg dinaciclib I.P. 3x/week. Plotted are the tumour size means ± SD, n = 5 for the alvocidib group, n =5 mice for the alectinib group, n = 6 mice for the dinaciclib group, n = 12 (6+6) mice for the control groups. P values were calculated at the last time point by a two-tailed student's t-test (*p < 0.05, **p<0.01, ***p<0.001).

Taken together, these data suggest that alvocidib or dinaciclib may be viable therapeutic options in the clinic for patients with ALK-independent mechanisms of resistance. For this cohort of patients with only chemotherapy left as a treatment option, it could be argued that lorlatinib, the most recently approved ALK inhibitor [92] should be used. Therefore, I decided to test this kind of clinical sequencing in the *in vitro* models of acquired resistance. As expected, the H3122 parental cells were very sensitive to lorlatinib and equally sensitive to alvocidib or dinaciclib (**Figure 35A**). Crizotinib-resistant cells were completely resistant to lorlatinib but remained very sensitive to alvocidib or dinaciclib. Lastly, while ceritinib- or alectinib- resistant cells had a partial response to lorlatinib, they were significantly more sensitive to alvocidib or dinaciclib. The same was observed by long-term treatment and survival assay (**Figure 35B**). Should these data be translated in the clinic, lorlatinib would have no activity in patients with wild-type ALK kinase domain and it is possible that transcriptional inhibition would be beneficial to these patients.

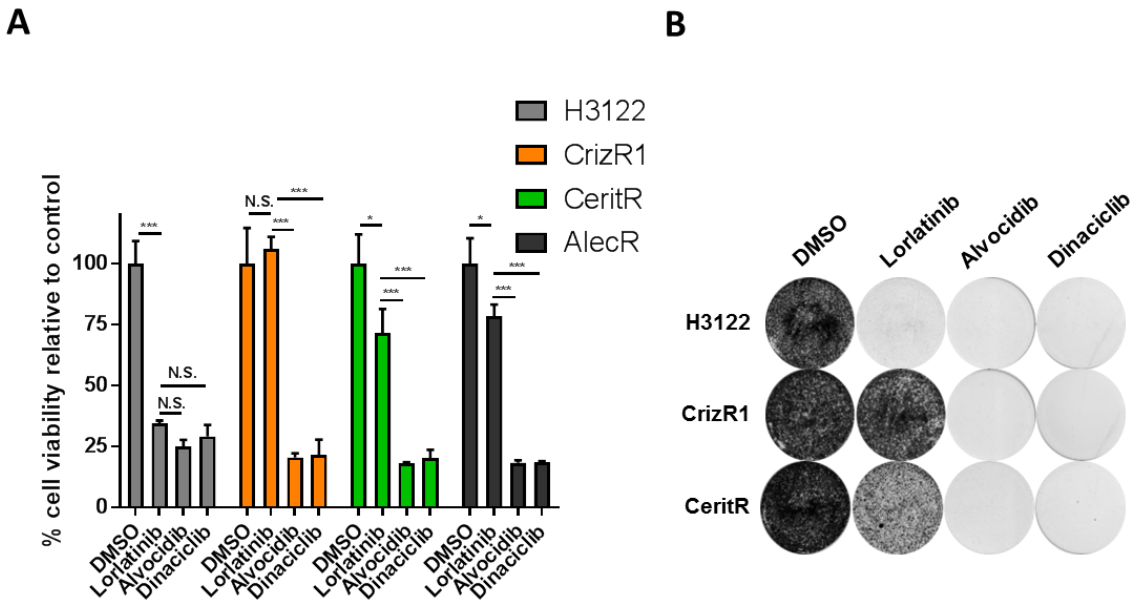

Figure 35: CDKi may be effective in a lorlatinib-resistant context

A) The indicated EML4-ALK cell lines were treated with 100nM lorlatinib, 200nM alvocidib, 25nM dinaciclib or vehicle control for 72h. Then, cell proliferation was assessed by an MTS proliferation assay. Plotted are normalised means ± SD (n = 3 biological replicates). P values were calculated by a two-tailed student's t-test (*p < 0.05, **p<0.01, ***p<0.001).

B) All the indicated cell lines were treated with 100nM lorlatinib, 200nM alvocidib, 25nM dinaciclib or vehicle control until the vehicle control well reached confluence (7-10 days). Then, cells were fixed and stained with crystal violet to assess cell viability. Shown are representative wells of 3 independent experiments.

4.3 Discussion

4.3.1 Selection of the model system used

To study the development of drug resistance in a clinically-relevant fashion, systems that can be used are: Clinical specimens (either biopsy samples or blood samples), patient-derived xenograft (PDX) models, primary cultures generated from tumour biopsies or cell lines that were made drug-resistant through exposure in culture. While clinical specimens provide direct proof for the clinical condition, they can only be used for the identification of potential mechanisms, which then need to be functionally interrogated with cell lines or mice. Thus, they are frequently used to confirm findings that were generated *in vitro*. In this study, the only clinical samples that could be obtained were blood samples and were used to confirm the relevance of miRNA-related findings, as discussed in the next chapter. PDX models are invaluable to monitor drug response. For example, as it relates to this thesis, CDK inhibition tested in a PDX model generated from a patient that acquired resistance to ALK inhibitors would provide additional confidence to the usefulness of CDKi in the clinic. Primary cultures generated from excised tumours have been used before to interrogate both mechanisms of acquired resistance to ALK inhibitors as well as functionally test ways to combat these [112,196]. While this is a very desirable model, the MGH series of cell lines referenced earlier were proprietary and thus I was not able to acquire them. Furthermore, through collaboration with clinicians, there was no clinical specimen that could be cultured in order to generate a new primary model.

Thus, for the purpose of initiating this project, EML4-ALK^{mut} cell lines that acquired resistance through long-term exposure were used. This system has the advantage of rapid growth which allows interrogation of all desired questions and also allows for rapid drug screening upon successful identification of mechanisms of resistance. An obvious disadvantage is that cells that have been cultured in plastic for several years may have drifted from the human condition as it presents in the clinic. Therefore, any discovery in this model should be validated with patient-relevant material to increase confidence in the findings. Despite this disadvantage, cell line models of acquired resistance have been successfully used for over a decade in EGFR- and ALK-driven lung cancers and still produce very robust findings [132,197–199]. The relevance of the model used is also strengthened by the fact that we have detected alterations that recurrently appear in the literature, such as EGFR activation (despite not driving crizotinib resistance) [113], AXL upregulation and EML4-ALK loss [197].

4.3.2 Several genes contribute to crizotinib resistance

Generally, it has been established that one way to avoid the induction of cell death in response to targeted therapies would be to modulate the levels of pro- or anti-apoptotic proteins. In fact, BIM deletion has been shown to affect the response to targeted therapies [74]. While the gene expression data set was interrogated for apoptotic proteins, an upregulation of c-IAP2 (BIRC3) was identified. It is an anti-apoptotic protein that has been shown to promote resistance to radiotherapy in oesophagal adenocarcinoma [184] and its deletion in mice is enough to induce caspase-8 driven apoptosis followed by embryonic death [200]. Moreover, the anti-apoptotic

protein Survivin was increased in the RNA-seq dataset. Survivin is typically induced by the EML4-ALK-STAT3 axis [38], with the disruption being key for apoptotic cell death upon ALK inhibition. In a similar context, in EGFR-mutant NSCLC, co-targeting of Survivin along with EGFR leads to pronounced durable responses to erlotinib treatment in mice [201]. While a functional role for c-IAP2 was ruled out in this context, it is not clear whether Survivin had such a role. In the future, I intend to knock out endogenous Survivin in H3122 cells and examine how this affects the development of resistance to crizotinib.

Strikingly, while an EGFR over-activation is the most common mechanism of resistance to crizotinib in the clinic [115], EGFR did not mediate resistance to ALK inhibition in this system. Knocking down EGFR did not re-sensitise cells to crizotinib, which is consistent with a previous finding where EGFR and ERBB2/3 amplification co-existed in the same clone but only ERBB2/3 were functional [113]. In the diagnostic setting, the same finding would complicate treatment decisions, especially if other potential mechanisms of resistance were simultaneously present.

The transcription factor c-FOS has been shown to confer resistance to crizotinib when overexpressed in H3122 EML4-ALK cells [1]. However, to my knowledge, no data that show the spontaneous emergence of c-FOS as a driver of acquired resistance to crizotinib exist. In the transcriptomic comparison of H3122 and CrizR1 cells, a prominent upregulation of c-FOS was detected and confirmed at the protein level. However, silencing of this gene had no impact on cell proliferation with or without crizotinib, ruling out that c-FOS had an oncogenic role in this instance. These questions were limited by the fact that the effects of c-FOS upregulation were not investigated in terms of cell motility, migration or invasion. Given a report which shows the importance of c-FOS in regulating EMT downstream of KRAS and YAP1 signalling [202], it is likely that the effects of c-FOS upregulation would only be evident in a metastatic context.

Overexpression of TGFβ-R2 has been shown to make H3122 cells more resistant to crizotinib [185]. Thus, after observing an upregulation of the TGFβ-R1 and TGFβ-R2 in the described data set, I set out to investigate whether these receptors are mediating resistance to crizotinib. Inhibition of TGFβ-R1/2 led to only a modest re-sensitisation to crizotinib, making it unlikely that these receptors are a main driver of resistance in this clone. Future siRNA experiments targeting each receptor individually should shed more light on whether TGFβ-R1 or R2 are required. It was therefore clear that these cells had co-existing mechanisms of resistance, each contributing at various degrees. According to this hypothesis, several oncogenes were upregulated in the NGS which were not pursued further, like MYB, c-KIT, ERBB4 and FGFR. Furthermore, the ETV- family transcription factors, have already been associated with the resistance to crizotinib [1] and in this dataset, CrizR1 cells exhibited an upregulation of ETV2 at the mRNA level.

In this work, the potential contribution by drug transporter proteins that may pump small molecule compounds out of the drug-resistant cells has not been thoroughly tested. Despite their rare contribution to ALK inhibition resistance, p-glycoproteins such as ABCB1 have been detected as

upregulated in the clinic [196]. While this gene was not upregulated in the RNA-seq data of CrizR1 cells, a lack of investigation of other members of this family is a limitation of the current approach.

4.3.3 The epithelial to mesenchymal transition promotes crizotinib resistance

After RNA-seq, a GSEA enrichment analysis was also performed and enrichment of EMT-related genes became apparent. The involvement of EMT in the resistance to crizotinib has been studied before, with somewhat controversial findings. There are reports that show that EMT is not causal in making EML4-ALK cells resistant to ALK inhibition [124] but also reports which show that targeting EMT is detrimental to crizotinib-resistant cell proliferation [187]. In these findings, I focused on the overactivation of AXL and showed that its inhibition can partially restore crizotinib sensitivity. Recent work has shown that overexpressing AXL in crizotinib-sensitive cells can promote drug resistance [1], however, to my knowledge, this is the first time that spontaneous AXL activation has been shown to allow cell proliferation in the presence of crizotinib. Since the combination of bemcentinib and crizotinib did not result in apoptotic cell death, it is not clear that such combination would be clinically useful, particularly given the fact that the far more potent effects of alvocidib, dinaciclib or THZ1 were discovered later.

Lastly, while I did not have access to patient samples to probe for potential AXL dysregulation, these findings build upon the results from melanoma patients, where AXL activation is evident upon tyrosine kinase inhibitor treatment [203]. Whether AXL is the master controller of EMT is not yet clear from these data, which are limited in the sense that examine only the proliferation- and apoptosis-related roles of EMT. However, EMT has been long associated with properties such as invasion, migration and ultimately, metastasis (Reviewed in : 187). I have set up a pre-requisite for further studies that could examine the implications of targeting AXL and other EMT proteins in an EML4-ALK mouse model of metastasis. This is particularly important in this context, where brain metastases are frequent and can be found in around 60% of patients [204].

4.3.4 Cell cycle-guided investigation

Experimental data from the response to crizotinib but also from the resistance to crizotinib agree on the modulation of cell cycle genes. While it has been shown before that cell-cycle genes are dysregulated upon ALK inhibition [112], this finding was corroborated in the presented cell lines and a loss of CDK1, CDK2 and Cyclin B1 was further shown. It stands to reason that the disruption of proliferative signalling should result in the loss of cell cycle genes that would otherwise allow continued cellular replication. Furthermore, CDK1 and CDK2 are established targets of E2F1 and MYC, which are downregulated in response to ALK inhibition [34], which may explain their repression.

Regarding the cell cycle dysregulation in the resistance to crizotinib, an upregulation of CDK1, CDK6, CCNB1 and CCNE1 was reported here. Whether these alterations arise from a genomic amplification or are a result of increased upstream signalling remains to be determined. Even though the effects of a knockdown for all the cell cycle genes that arose from the GSEA were tested, a limitation of the present study is that not every cyclin-dependent kinase and its partner

cyclin has been investigated. Driven by the prominent upregulation of CDK6 it was found that inhibition of CDK6 with the specific inhibitor palbociclib does not robustly decrease cell proliferation. Clearly, CDK6 upregulation is not a driver of resistance to crizotinib, as its inhibition (or knockdown) did not restore sensitivity to crizotinib. It cannot, however, be excluded that the striking upregulation of CDK6 primes drug-resistant cells for cell cycle progression upon some unidentified stimuli. Interestingly, in ALK-driven neuroblastoma, the combination of ceritinib and palbociclib was synergistic [152]. While this synergistic potential was not examined in H3122 drug-sensitive cells, the disappointing activity of palbociclib led me to abandon this compound.

While it cannot be excluded that these transcriptomic changes are present only *in vitro*, recent findings in a large cohort of patients who acquired resistance to ALK inhibitors show that mutations in cell cycle genes such as CDK4 and CDKN2A do arise in the clinic [47]. Furthermore, similar findings have been observed in EGFR-mutant cancer [78]. In hepatocellular carcinoma, cyclin E1 but not cyclin E2 correlates with resistance to sorafenib. Interestingly, alvocidib treatment re-sensitised cells to sorafenib [205]. In addition, cyclin E1 copy number gain has been reported in a case of EGFR-mutant NSCLC patient following the development of resistance to osimertinib [79].

4.3.5 Transcriptional inhibition

It does not appear that a cell cycle-related vulnerability renders crizotinib-resistant cells sensitive to CDK inhibitors since in these data H3122 parental cells are as sensitive as their drug-resistant isogenic clones. This raised the possibility that all EML4-ALK cells have an intrinsic vulnerability to CDK inhibitors. It was then proposed that this is due to inhibition of high levels of transcription by CDK inhibitors. Specifically, alvocidib and dinaciclib potently inhibit CDK9 which regulates the RNA polymerase II [149] while THZ1 inhibits CDK7/12/13 which also regulate the RNA polymerase II [163]. CDK7/12 and CDK9 regulate transcription by phosphorylating the RNA-Polymerase II [206]. While phosphorylation of RNA pol II at the Ser5 and Ser7 sites by CDK7 has been shown to be important for the recruitment of the complex at the TSS [207], phosphorylation at Ser2 by CDK9 is important for the release and the elongation step [208]. Indeed, through means of Chip-seq, we have shown that alvocidib results in high occupancy of TSS with RNA pol II while THZ1 in reduced occupancy. This suggests that in the described cellular context, CDK inhibition of CDK7 and CDK9 has a widespread transcriptional effect. With siRNA experiments, we were able to induce apoptosis by partial CDK9 downregulation while as expected, CDK7 downregulation was not enough on its own, likely requiring synergism with CDK12/13 [163]. The fact that oncogene-driven cancers rely on high levels of transcription to accumulate genes necessary for their oncogenicity has recently been shown to occur through reliance on super-enhancers, whose activity can be inhibited with low levels of CDK7/12 inhibition [156].

4.3.6 Characteristics of individual CDK inhibitors

A question can be raised why cell cycle inhibitors have not been identified as potent hits in previous, high throughput drug screens in EML4-ALK cancer. In the report by [112], alvocidib and palbociclib were included in the screen but did not qualify as hits. An explanation for this is that the authors were looking for synergistic drugs and only took into account a synergistic index with the

primary ALK inhibitors, while in the present findings alvocidib is active as a single agent and is not synergistic.

4.3.6.1 Alvocidib

In crizotinib-resistant cells, treatment with the pan-CDK inhibitor alvocidib resulted in a cell cycle arrest in the G2/M phase and a much more prominent induction of apoptosis. In terms of the mechanism, it has been corroborated that an E2F1-MCL-1 axis is downstream of alvocidib-induced cell death [193]. Furthermore, evidence was provided that there is a rapid activation of the mitochondrial apoptotic pathway. This is evident through an upregulation of BIM, Bid and SMAC. This model is entirely consistent with a recent report which suggests a requirement for RB-proficiency for apoptotic induction upon cell cycle inhibition, mediated by an upregulation of SMAC and repression of FOXM1/Survivin [209]. In fact, repression of Survivin upon alvocidib treatment was detected in the present study. Furthermore, it has been shown before that overexpressing Survivin in H3122 cells can protect them from ALKi-induced apoptosis [38]. While it was shown that MCL-1 downregulation is not sufficient to induce apoptosis, a limitation of these data is that the same question was not asked for Survivin or a combination of MCL-1/Survivin knockdown.

It is known that alvocidib is a promiscuous inhibitor with several off-target effects. In fact, at 1μM alvocidib inhibits at least 179 kinases (www.chemicalprobes.org). Alvocidib has also been shown to target SRC [149]. Interestingly, SRC inhibitors have been shown to be the most prominent re-sensitisers to crizotinib [112], potentially because of a preferential re-activation of SRC upon parallel RTK activation. While the low concentrations used in my experiments make this unlikely, it is still possible that alvocidib may have off-target activity through SRC inhibition. Furthermore, the very similar data obtained with three different CDK inhibitors make the possibility of the same off-target effect from all of them improbable. I do not view the previously reported off-target effects of this compound as a limitation, but rather as an opportunity to take advantage of a poly-pharmacology based drug treatment, in line with other recent approaches [210]. This way, old drugs can be re-purposed for a different use than the one they were originally intended for.

In terms of safety, it was shown that there is preferential induction of apoptosis in EML4-ALK-mutant cells and no induction of apoptosis in non-transformed epithelial cells. This is in line with the original reports of alvocidib. Also, in human studies, alvocidib has almost universally shown a manageable safety profile. For example, in patients with late-stage NSCLC, it was deemed safe in phase I 2001 trial, however, there was no cytotoxic activity observed in patients and the trial was halted [211]. The authors note that there was prolonged non-progression, which may suggest a cytostatic instead of a cytotoxic effect. Since the trial cohort was not representative of patients with EML4-ALK or EGFR mutations, the activity of alvocidib in a more targeted, oncogene-driven cohort of patients cannot be predicted. Dosing regimen and scheduling appear to be determining factors in the efficacy of alvocidib, given that after the initial disappointing trials, a trial using a new schedule reported clinical efficacy with 45% partial responses in high-risk CLL [212]. Lastly, even though alvocidib has not seen approval for any cancer indication, there are still at the time of writing 6 active clinical trials with alvocidib, most of them in acute myeloid leukaemia.

4.3.6.2 Dinaciclib

After the failure of alvocidib in the clinic, newer CDK inhibitors with better pharmacological properties were developed. Dinaciclib was developed by Merck [149] and subsequently showed great activity in mouse models of NSCLC [179]. Specifically, dinaciclib seems to achieve potent target engagement, resulting in tumour growth suppression at 80% of the maximum tolerated dose, likely due to better pharmacokinetics *in vivo*. These data about the potency of dinaciclib have been corroborated in this thesis, as a potent block of cell proliferation was evidenced and induction of apoptosis with low nanomolar concentration of the drug. Similarly with alvocidib, it was hypothesised that the anti-tumour effects of this drug are due to perturbing the reliance of EML4-ALK cells on high levels of transcription.

A clinical trial of dinaciclib in NSCLC patients as second-line treatment after erlotinib failure was not successful [213]. However, this trial was run when EGFR or ALK mutation testing was not being used in the clinic, therefore, these patients had unknown ALK status. The data in this thesis propose testing of this inhibitor in a well-validated cohort of patients with ALK mutations after patients develop resistance to TKI inhibitors. Additionally, I have shown that upfront combination of dinaciclib with crizotinib can prevent the emergence of crizotinib resistance, supporting the case for a trial with upfront low-dose dinaciclib. At the time of writing, there are 5 active clinical trials with dinaciclib in various advanced solid tumours as well as in acute myeloid leukaemia.

4.3.6.3 THZ1

New findings regarding CDK7/12 inhibition suggest the potential for preferential anti-tumour activity. The THZ1 compound [150] showed broad anti-tumour effects in various cells which correlate with the expression levels of oncogenic transcription factors. Likely, in low nanomolar doses, transcriptional programs are inhibited just enough to block highly expressed oncogenes, but not enough to affect normal cellular functions. This was later shown to be through the preferential targeting of super-enhancers and their dependent genes [156]. Furthermore, I am not aware at this moment of any data examining the off-target effects of the THZ1 compound, but as with any kinase inhibitors, off-target effects likely exist. Therefore no claim should be made for the importance of CDK7/12 inhibition but rather for the potency of the compound itself in conferring anti-proliferative and apoptotic responses in oncogene-addicted NSCLC cells. The presented findings suggest an investigation of this compound as subsequent therapy in EML4-ALK- and EGFR-mutant lung cancer, where ALK- and EGFR- inhibitors have failed. In terms of clinical efficacy, at the time of writing there is one clinical trial of a THZ1-modified compound, initially in ovarian cancer and later expanding to metastatic breast cancer (NCT03134638). However no Phase I/II data have been released in order to evaluate the safety profile.

4.3.7 Selectivity of EML4-ALK cells/patients

While it is apparent that EML4-ALK cells are more sensitive to CDKi compounds compared with other NSCLC cell lines, I am aware that this specificity window has not been clearly elucidated. The presented hypothesis regarding high levels of transcription is not likely to be conclusively demonstrated. However, it has been shown before that EML4-ALK cells are prone to high levels of

super enhancer-driven transcription [156]. Furthermore, other differentiating factors were uncovered that may actually result in dissimilar drug response. Specifically, the *MCL-1* and *cyclin D1* mRNAs in EML4-ALK cells were expressed at levels more than 5 standard deviations above the LUAD mean. As an anti-apoptotic protein, MCL-1 is well known to promote tumourigenic activity in oncogene-driven cancers [179] and is, for this reason, an established anti-cancer drug target [214]. Cyclin D1 is a critical modulator of proliferation, evident through cell cycle and transcriptional control [142]. It has also been shown to be downregulated in response to alvocidib [215]. Given the increased proliferative signals in tumours, it would be reasonable to hypothesise that increased levels of cyclin D1 in EML4-ALK cells are linked to their oncogenicity. It is therefore tempting to posit that reliance on the anti-apoptotic activity of MCL-1 and Survivin and the pro-proliferative activity of cyclin D1 has rendered EML4-ALK cells sensitive to transcriptional inhibition by CDK inhibitors. Future experiments could look at the downregulation of cyclin D1 in response to CDKi, as well as the effect of combined knockdown of these genes in EML4-ALK-driven cancer cells and xenograft models. Lastly, a STAT1 transcriptional signature that may differentiate EML4-ALK from the rest of lung adenocarcinoma cells was identified and future experiments will look at the effects of STAT1 knockdown in this context.

4.3.8 *In vivo* outcomes of CDKi treatment

Alvocidib, dinaciclib and THZ1 have all been successfully tested in mouse xenograft models in previous publications. Specifically, alvocidib slowed tumour growth in a breast cancer xenograft mouse model [194], reversed sorafenib resistance in a hepatocellular carcinoma xenograft mouse model [205] and reversed venetoclax resistance in an acute myeloid leukaemia mouse model [216]. I am not aware of a study that has looked into the activity of alvocidib in lung cancer xenograft models.

Dinaciclib was first tried in an ovarian carcinoma xenograft model, where it eliminated tumour growth at the maximum tolerated dose [149]. There is a plethora of data from various tumour types, in which dinaciclib showed complete or partial inhibition of tumour growth in mouse models of T-cell acute lymphoblastic leukaemia [217], MYCN-amplified neuroblastoma [218], KRAS-mutant pancreatic cancer [219] and BRAF-mutant colorectal cancer [220]. Lastly, in a recent study of EGFR-mutant NSCLC, dinaciclib delayed tumour growth and eliminated tumours in combination with gefitinib [179]. All these data suggest that dinaciclib has a favourable toxicity & activity profile relative to alvocidib *in vivo.*

The most relevant data for EML4-ALK lung cancer come from THZ1. In a genetically engineered mouse model of EML4-ALK, the upfront combination of THZ1 with crizotinib resulted in the elimination of tumours, therefore preventing the emergence of resistance and the same was true for EGFR-mutant tumours and erlotinib treatment [156]. Prior to this, THZ1 was highly effective in a xenograft mouse model of T-cell acute lymphoblastic leukaemia [150] and of small-cell lung cancer [155].

Given the impressive activity of the above compounds *in vitro,* I asked whether they are effective in a mouse model of crizotinib and alectinib resistance. Regarding alvocidib, a higher dose than previously published was safely used, which resulted in anti-tumour activity, strengthening the case for the use of alvocidib to target EML4-ALK drug-resistant cells. Notably, this anti-tumour activity was also evident *in vivo* with cells resistant to the current standard of care, alectinib. Dinaciclib was also effective in alectinib-resistant cells, even though the dosing protocol requires further optimization in the future.

However, it was surprising to see that dosing of THZ1 was toxic to nude athymic mice. While the published dosage of 10 mg/kg twice per day by I.P. injection was safe in [150,156], in my study even 10 mg/kg once per day led to more than 20% weight loss and premature termination of the protocol. Since a toxicity protocol was not integrated with this study I did not have the data to assess why this happened. It is likely that the genetic background of the mice or the origin of the compound played a role in this. I, however, do not suggest that this necessarily negates the published well-established mouse safety profile of THZ1 and it is possible that some unidentified difference in the described protocol was what caused this toxicity. Therefore an argument in favour of or against using THZ1 *in vivo* cannot be made given the conflict between the mouse data. In the end, only safety data in humans can conclusively settle this discrepancy.

4.3.9 Applicability of these findings in patients

The ideal assay to determine mechanisms of resistance would be to compare biopsy samples from patients taken before treatment, and after the development of resistance to ALK inhibitors. There was severe difficulty in securing those samples, resulting in the use of the only publicly available dataset [1]. Differential expression analysis of these RNA-seq data (kindly performed by Dr Sudhakar Sahoo, data not shown), disappointingly showed very high differences in gene expression with few genes being robustly differentially expressed. This is because of the fact that this data set contains a mixed cohort of treatment-naïve and progression samples from different patients, without them being matched. For this approach to be beneficial, a larger cohort of patients would be needed to help minimise the variability in gene expression among individuals. The only material that could be obtained was plasma samples but it was only possible to look into circulating miRNAs and thus not possible to confirm or reject the *in vitro* results for this chapter.

Regarding the clinical usefulness of CDK inhibitors, it is evident that pan-CDK inhibitors will always be associated with toxicity. CDK1 is the only essential mitotic kinase [221] therefore even off-target CDK1 inhibition will likely be intolerable in the clinic. A case can be made for specific CDK2 inhibitors, which could indirectly target malignancies with CCNE1 amplification [145]. It can be envisioned that specific CDK inhibition is one way to avoid toxicity. For example, in malignancies associated with transcriptional addiction, specific CDK7/12 or CDK9 inhibitors may provide enough of a therapeutic window to offer minimal toxicity. Until specific CDK9 inhibitors reach the clinic, it is suggested that dinaciclib should be tested as the next available option, with the hope that a

therapeutic window exists, where low-dose dinaciclib targets transcriptionally-addicted cancer cells while sparing normal cells.

4.3.10 Conclusions

ALK kinase domain mutations that cause resistance to ALK inhibitors are well studied and can be successfully treated with sequential use of different inhibitors. Complications arise when drug resistance is caused by parallel pathway alterations or new oncogenic mutations. Through an overwhelming amount of data, we now begin to realise that the heterogeneity in the potential mechanisms of resistance that can arise in response to TKIs is enormous. Simultaneous mechanisms of resistance in the same tumour do occur, as a recent study reported a patient who presented both the L1196M ALK domain mutation, as well as significant EMT markers, found only upon progression to crizotinib [125]. Moreover, these mechanisms of resistance cannot be predicted, nor do they correlate with other biomarkers, and can only be identified through laborious pathway screening. While in the research lab such screening can take place with cultured cells with ample material, in the clinic with little material this would be unrealistic. Resistance to TKIs can appear rapidly and patients need to be treated quickly, which limits the time for potential expansion of patient material and subsequent personalised screening.

Again, I take this opportunity to reinforce that the appearance of a mutation or amplification typically classified as oncogenic does not always drive the resistance to ALK inhibition. Therefore, screening for rare, heterogeneous mechanisms of resistance can be inefficient and inconclusive. A conceivable solution to this would be to identify where all these parallel pathways converge and then inhibit this target. This led to the testing of the upfront combination of crizotinib and the MEK inhibitor trametinib [37] since the majority of resistance mechanisms converge on the MAPK pathway. While this solution may be successful for the upfront treatment of patients, I propose the potential to globally treat patients who are refractory to ALK inhibitors with the CDK inhibitors alvocidib, dinaciclib or THZ1, regardless of their (ALK-independent) mechanism of resistance. Along the same line of thinking, recently, the convergence of ALK-independent mechanisms of resistance on the MAPK pathway was exploited therapeutically. Specifically, the SHP2 protein phosphatase was found essential for MAPK pathway activity. By inhibiting SHP2 with a small molecule inhibitor, the authors were able to re-sensitise drug-resistant cells to ceritinib or crizotinib [119].

This idea of a central master regulator that can be the key to treatment has been proposed before for targeting transcription factors [70]. While targeting transcription factors themselves has proven challenging, new tools now allow us to indirectly interfere with transcriptional regulation. In the presented data set, the CDK7/12 inhibitor THZ1 can robustly inhibit the proliferation of EML4-ALK cells resistant to ALK inhibitors. The activity of alvocidib and dinaciclib against CDK9 also results in indirect transcriptional silencing. Taking into account the alvocidib data, it is suggested that it should be further investigated as second-line therapy where even third-generation ALK inhibitors have failed. I have provided experimental evidence to this fact since lorlatinib had no activity in crizotinib-resistant cells with wild-type ALK and very little activity in ceritinib- or alectinib-resistant cells. These patients are in dire need of immediate treatment upon disease progression and it is

hypothesised that the global activity of alvocidib or dinaciclib can be of benefit in this context. The ineffectiveness of chemotherapy, or of the recent addition of immunotherapy agents [57] upon failure of ALK inhibition suggests that any regimen with a sound rational basis should be tested as an alternative. It is evident that the use of an inhibitor which does not require testing for the particular mechanism of resistance can be enormously beneficial in the clinic, especially in a limited-resources context.

4.3.11 Future work

I have shown the dysregulation of a multitude of genes in an *in vitro* model of acquired resistance. Future work could address whether these alterations occur in patients who became resistant in the clinic. To this end, core biopsies should be obtained before treatment and upon progression. Likely, a new recruitment protocol would have to be made specifically for this purpose, since to my knowledge, in already established archives such matched samples are not available.

Regarding the epithelial to mesenchymal transition, new data have been introduced that add to the conflicting arguments in the literature. A comprehensive way to study the contribution of EMT would be to take established EMT-related genes, such as AXL or ZEB1, introduce them to H3122 crizotinib-sensitive cells and investigate whether these cells become resistant to crizotinib. This investigation should take into account the role of EMT in metastasis, therefore both proliferation, as well as metastatic capacity, should be interrogated. Two parallel mouse models would be effective, one simple xenograft model with crizotinib treatment to check tumour cell proliferation and one orthotopic model followed long enough to develop metastases. If this hypothesis holds true, then mice injected with H3122-EMT cells treated with crizotinib should develop more metastases. Alternatively, a crizotinib-resistant cell line with a stable knockdown of AXL can be injected orthotopically and metastases monitored compared to the non-knockdown control.

To determine whether there is generalized drug resistance through increased drug efflux, future experiments should address the question whether the parental and drug-resistant cells respond similarly to standard chemotherapeutic agents. Lack of response of the drug-resistant cells would indicate the potential contribution of drug transporter proteins to crizotinib or alectinib resistance.

In terms of the mechanistic results with CDK inhibitors, future experiments should address whether the induction of apoptosis follows the same pathway *in vivo*. Tumours from mice treated with CDKi could be harvested and protein extracts could be probed for induction of BIM/BID and downregulation of MCL-1/Survivin. The *in vitro* data are supportive of the notion that alvocidib, dinaciclib or THZ1 are highly potent in the context of acquired resistance in EML4-ALK lung cancer. To strengthen these conclusions future experiments may be performed in patient-derived xenografts (PDX), given that cell-line xenograft models are often known to not translate to humans. To this end, more than one patient samples should be obtained and transplanted to mice in parallel, since PDX models have a high failure rate prior to establishment.

Finally, previous work with trametinib and THZ1 [37,156] suggests that the upfront drug combination with ALK inhibitors is the best approach to minimise or at least greatly delay the

emergence of resistance. It would be of immense interest to have a trial of low-dose alvocidib, dinaciclib or THZ1 in combination with alectinib upfront compared with these compounds used sequentially as single agents when patients become resistant to ALK inhibitors.

5 The role of ncRNAs in EML4-ALK cancer

5.1 Introduction

After the complete sequencing of the human genome, it became apparent that only a small fraction of the genome codes for proteins. As years went by, more and more evidence accumulated, showing that genomic regions are usually transcribed to RNA, irrespectively of their content in protein-coding genes. The ENCODE project concluded that probably more than 75% of the human genome can give rise to primary transcripts [222]. So initially thought of as ”junk” DNA has now transformed into transcriptome-level thinking and indeed RNA has now a more central role in cell function than ever [223]. Always transcribed, but lacking open reading frames and thus not translated to polypeptides, ncRNAs can be subdivided according to their size in small ncRNAs (<200bp) and long ncRNAs. Long ncRNAs are generally poorly studied and their mechanism of action can be as diverse as it can be crucial to a cell’s fate [224]. In the nucleus, they typically guide protein complexes to specific chromatin sites, via nucleic acid interactions. In the cytoplasm, the function of lncRNAs is not as well defined yet but it has been demonstrated that they can modulate mRNA expression, the mechanisms of which are under intense investigation [225].

5.1.1 Biogenesis of microRNAs and mechanism of action

MicroRNAs, members of the small ncRNA family, were first discovered in *Caenorhabditis elegans* [226]. After about a decade of that discovery, the field started to realise that miRNAs act to coordinate gene expression in large scale, each miRNA having the potential to control hundreds of genes. Specifically, they are oligonucleotides of ~22 bp length, which bind to the 3’ UTR of their target mRNA(s) and cause degradation of the target mRNA, or translational repression [227]. The traditional view is that miRNAs can only bind to the 3’ UTR of target mRNAs. A recent study proves that as far as mechanics are concerned, miRNAs can bind equally well to the 5’ UTR of target mRNAs [228], but this does not necessarily reflect the *in vivo* function. Furthermore, miRNA binding sites can also exist inside the coding region of an mRNA [229].

High-throughput analysis of miRNA-mRNA interactions now challenges the pre-existing model even more, since it suggests that the majority of the interactions are non-canonical and can include bases outside the seed region of the miRNA [230]. Initial data suggested that the translational repression of mRNA targets, accounts only for a small fraction of the miRNA interactions, while mRNA decay represents the majority of interactions at a percentage of about 84%. This was shown utilising the method of ribosome profiling, which unlike other proteomics methods, is not biased towards highly expressed genes [231]. A limitation of this study is that it draws its conclusions from steady-state interactions. Accordingly, a more recent and dynamic approach, reports that the translational repression of targets takes place first and subsequently leads to mRNA de-adenylation and decay [232]. From these studies, it can be inferred that the depth of miRNA-mRNA interactions hasn’t allowed for a definite elucidation of the mechanisms as of yet. Most probably, mRNA decay and translational repression both account significantly for the downregulation of a target’s expression and the exact involvement of each may never be fully

understood. Adding to the ambiguity, conclusions about miRNA-mediated target suppression are largely based on experiments done on a limited number of transformed cell lines, therefore methods that substantiate these findings *in vivo* are always well-received.

As far as their genomic location is concerned, miRNAs can be found in independent genome regions and they are usually regulated by their own promoter, in which case are classified as intergenic. They can also be located inside introns of coding genes, following the host gene's regulation and are considered intronic. In some cases, there is evidence that even intronic miRNAs can be transcribed as independent units [233]. The RNA polymerase II is typically carrying out the task of their transcription, as long primary miRNAs [234]. Then, DROSHA and DGCR8 cleave the primary transcript to free small, hairpin structured precursor miRNAs. It is worth noting that this function predisposes several miRNAs to accumulate in clusters [235]. The precursors are exported to the cytoplasm by exportin 5 and further processed by the RNAse DICER to form the mature miRNA strand, which associates with Argonaute proteins to form the RISC complex (the mechanism is reviewed in [236]) which, guided by the miRNA's complementarity, attaches to the target. Degradation of mRNA targets usually happens after the mRNA is deadenylated and then decapped. Following decapping, an exoribonuclease can attack the mRNA molecule, in a classic 5' -> 3' decay reaction [237]. A model for miRNA biogenesis can be found in (**Figure 36**).

5.1.2 MicroRNAs in cancer

Even though miRNAs' roles in cancer were first unearthed in the case of chronic lymphocytic leukaemia [238], it is now accepted that they are dysregulated in virtually every cancer type. What is not always clear, is when a miRNA has a causative role in tumourigenesis, or is just a by-product of the malignant process. In the first case, a miRNA can be classified as either tumour suppressing or tumour promoting, albeit in a strict tissue-specific manner. A role as a *bona fide* driver oncogene was first established for the loci of miR-15/16, deletion of which in mice is enough to give rise to acute myeloid leukaemia [239].

It is very intriguing that early on, the total miRNA pool was shown to be down-regulated in many types of cancer, when compared to the healthy tissue profile, indicating that one or multiple biogenesis events are altered during carcinogenesis [240]. This is not surprising, granted that very frequently miRNAs are located in genomic sites that exhibit instability and as a result, are prone to undergo genetic loss, amplification or translocation [241]. Later it was established that perturbing the miRNA processing machinery can accelerate tumourigenesis [242], but to what extent this phenomenon occurs in each type of human cancer requires further investigation.

MiRNAs do not always succeed in suppressing their targets; a very interesting phenomenon has been observed, where oncogenes seem to shorten their 3' untranslated regions so as to avoid downregulation by miRNAs. This results in an increased expression of many oncogenes, without altering the transcription of the mRNA *per se* [243]. When it comes to oncogenicity, some miRNAs are now validated as oncogenes. A causative role in maintaining a malignant phenotype was first demonstrated for miR-21, overexpressed *in vivo* [244]. In this mouse model of pre-B cell

lymphoma, miR-21 overexpression was enough to initiate and maintain tumour growth. Conversely, its withdrawal resulted in reinstating the healthy state, in a context termed by the authors as ”Oncomir addiction”.

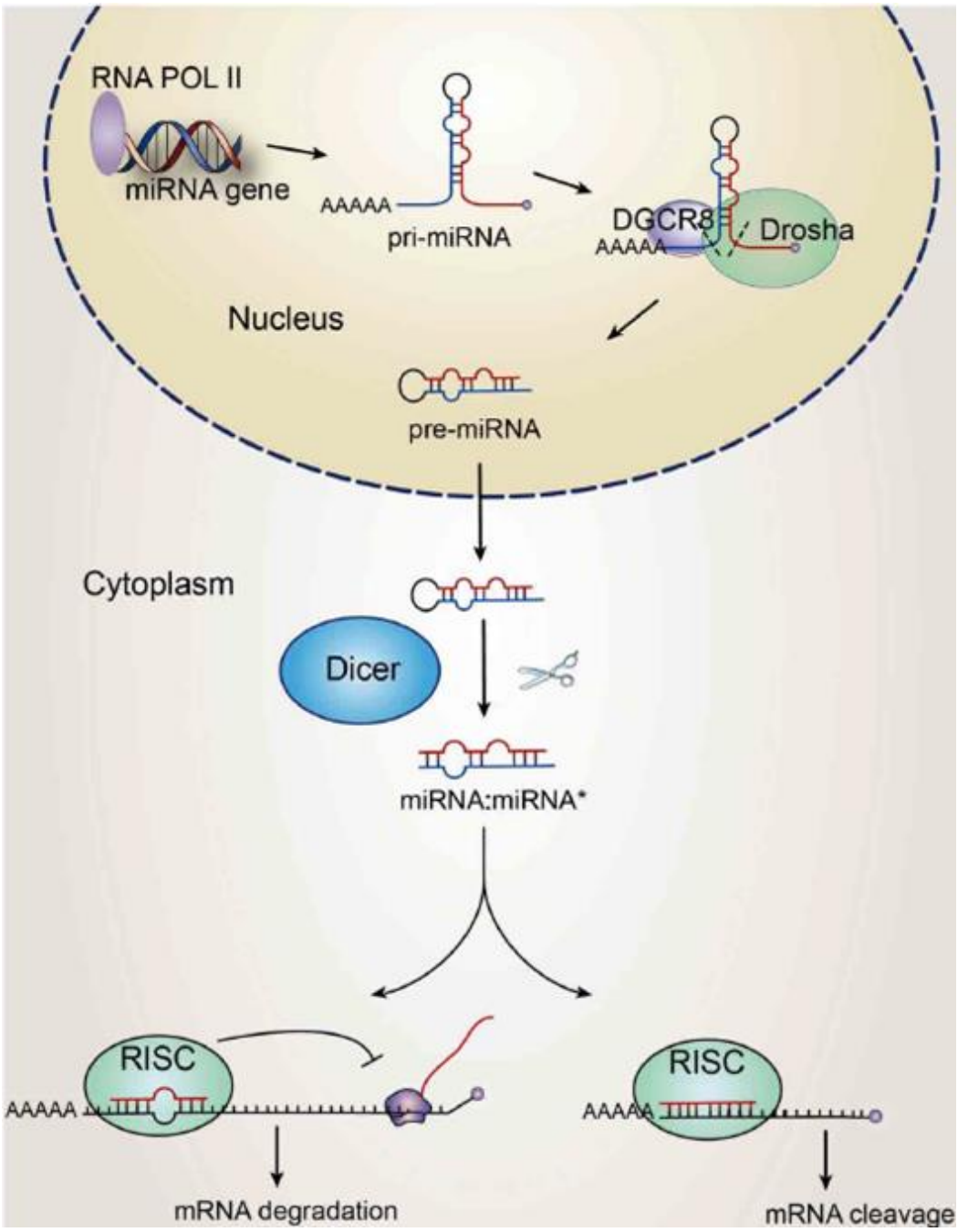

Figure 36: The canonical miRNA biogenesis pathway.

The RNA polymerase II transcribes miRNAs as long primary transcripts (pri-miRNA). While still in the nucleus, a complex of DROSHA with DGCR8 (microprocessor complex) cleaves the primary transcript into shorter, precursor miRNAs that form hairpins (pre-miRNA). Then, the precursors are exported to the cytoplasm, where the RNase Dicer cleaves the precursor further into a single-stranded RNA molecule of 19-25 nt (mature miRNA). The mature miRNAs can then associate with proteins of the Argonaute family to form the RNA-induced silencing complex (RISC) which is guided to the 3’UTR of its target mRNA based on complementarity between the miRNA and a 7- or 8-mer in the 3’ UTR. Degradation of the mRNA or translation repression ensues. Image adapted from [245].

5.1.3 MicroRNAs in lung cancer

The roles of miRNAs in lung cancer are under intense investigation, both *in vivo* and *in vitro.* One of the best-characterized miRNAs, let-7, has been shown to act as a tumour suppressor in lung cancer, along with other miRNAs such as miR-34, miR-145, miR-200. On the other hand, equally well characterized; miR-21, miR-221/222 and the cluster miR-17-92 have all shown oncogenic properties [246]. Not lacking therapeutic potential, and having demonstrated such in preclinical models, miRNA-based therapeutics are currently in development. These strategies utilise either the replacement of depleted tumour-suppressing miRNAs or the inhibition of overexpressed tumour-promoting ones. In a lung cancer context, concurrent administration of the powerful tumour suppressors let-7 and miR-34 using lipid-based nanoparticles led to increased survival in a NSCLC mouse model [247].

5.1.4 The miR-17-92 cluster

The overexpression of the oncogenic miR-17-92 cluster in lung cancer was first described in 2005 [248]. It was then established that this cluster can increase cell proliferation, but its mechanism of action was not discovered until later. The cluster has been shown to be under the control of C-MYC and it can target and regulate the levels of the transcription factor E2F1 [249]. All the evidence points to the cluster being oncogenic, both in solid tumour and in haematological malignancies [250]. An interesting exception to this is that only one member of this cluster, miR-92a is actually anti-angiogenic, therefore it has the potential to act as a tumour suppressor [251]. It was later shown that differential post-transcriptional processing results in the miR-92a antagonizing the stability of the rest of the members of the cluster [252]. To strengthen this, inhibition of miR-92a resulted in the upregulation of miR-18a and miR-20a [253], providing evidence that even though the cluster is transcribed as a single primary transcript, there are regulatory elements that result in different expression levels of this cluster. Since DROSHA cleaves individual pre-miRNAs that are afterwards processed by DICER, in theory, all the individual miRNAs may act independently [254]. Interestingly, despite the oncogenic cooperation between these miRNAs, some are more important than the others, depending on the context. In a mouse model of MYC-driven lymphoma, deletion of miR-19, but not of the other members of the cluster, actually impairs MYC-driven tumourigenesis [255].

5.1.5 MicroRNAs and drug resistance

Being involved in all tumourigenic processes, miRNAs can also modulate aspects of the response to certain drugs. Microtubule-targeting agents, such as the taxanes paclitaxel and docetaxel are very frequent therapeutic options for advanced NSCLC. However, given time, both primary and secondary resistance has rendered taxane therapy ineffective. One of the first miRNAs that were found to affect the response to paclitaxel, miR-135a, was enough to confer resistance, partially acting through the downregulation of the known tumour suppressor APC [256]. Still extensively used as a first-line treatment for NSCLC, the platinum agent cisplatin prompts apoptosis after

causing extensive DNA damage through cross-linking. Resistance to this agent has been shown to be affected by miR-31 overexpression, which targets the drug transporter protein ABCB9, resulting in decreased uptake of the drug [257]. Given that the majority of the studies are done *in vitro* or in mouse models, whether they depict the interactions actually taking place in human malignancies will be further corroborated as more data from patient samples accumulate.

Of particular interest to lung cancer therapy, miRNAs have been shown to modulate the response to RTK inhibitors. The small-molecule inhibitor gefitinib is used to treat $EGFR^{mut}$ NSCLC. In a comprehensive investigation, the inhibition of miR-221 and miR-30 was enough to re-sensitise drug-resistant cell lines and mouse models to gefitinib treatment. Furthermore, overexpression of MET-controlled miR-103 and miR-203 greatly improved sensitivity to gefitinib [258]. This provides an excellent example of how better drug response can be achieved by manipulating the levels of endogenous miRNAs. Even more evidence that microRNAs can have important roles in acquired resistance is provided by a recent study [259], where miR-21, miR-30c and miR-100 were shown to enhance resistance to TRAIL (TNF-related apoptosis-inducing ligand) by strengthening the NF-kB pro-survival pathway. Notably, these miRNAs are transcriptionally activated by NF-kB, which creates a positive feedback loop that affects tumour aggressiveness. This has obvious implications for improving NSCLC therapy, as shown by combination therapy with NF-kB inhibitors and TRAIL in mice. Many of the potential ways of involvement of miRNAs in chemoresistance are not listed in this manuscript, but these have been thoroughly reviewed elsewhere (**Figure 37**) [260,261].

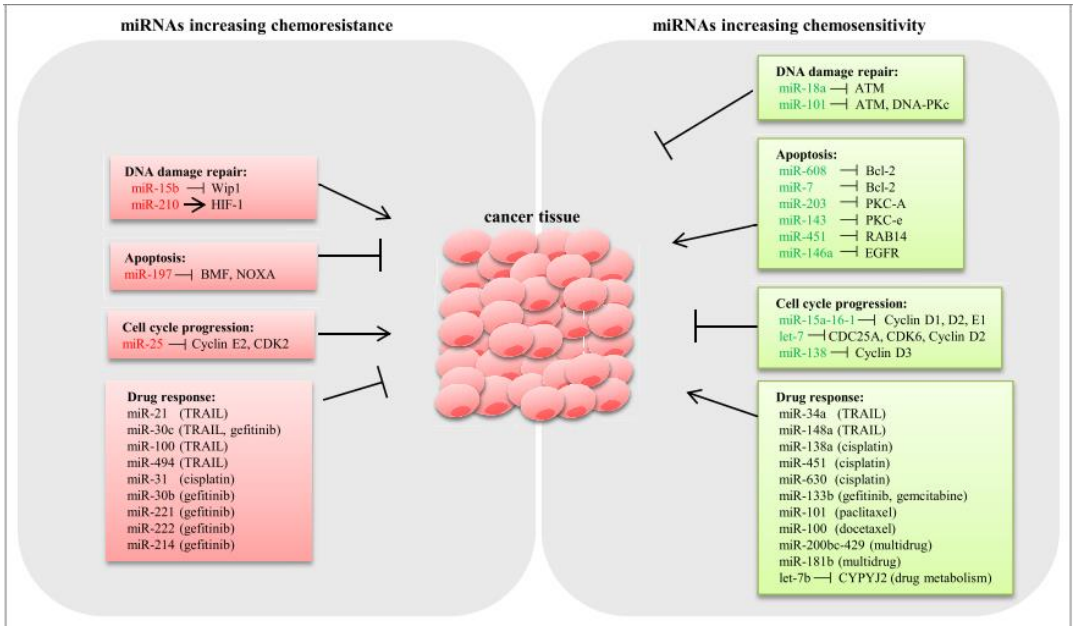

Figure 37: Examples of miRNAs affecting drug response

MiRNAs have been shown to affect all aspects of drug response. Tumour-suppressing miRNAs that are lost will typically promote chemoresistance, such as miR-31, the loss of which promotes SRC upregulation and cisplatin resistance [262]. On the other hand, upregulated tumour-suppressing miRNAs can lead to chemosensitivity, such as let-7b which suppresses the expression of the drug efflux protein CYPY12. In the case of oncogenic miRNAs, increased or decreased expression also affects drug response. For example, miR-100 leads to TRAIL resistance when upregulated but to TRAIL sensitivity when it is downregulated. Image adapted from [260].

5.1.6 MicroRNAs as biomarkers

MiRNAs can be detected in all bodily fluids and are extremely stable, being able to withstand prolonged storage in room temperature as well as multiple freeze-thaw cycles [263]. In lung cancer, several miRNAs from lung tissue samples have been able to help initial diagnosis or even distinguish the tumour subtype [246]. However, the real value of miRNAs as biomarkers will likely be realised when extracellular circulating miRNAs will be routinely used for cancer screening. A scenario where with a minimally invasive procedure, such as blood sample screening, we will be able to identify patients, has been the goal of cancer researchers for decades. Promising in that aspect, miRNA-based classifiers for early detection in the plasma are already under testing, some of which are achieving impressive sensitivity of as much as 90% [264,265]. Furthermore, miRNAs in the sputum have been shown to be more sensitive than cytology for the diagnosis of lung malignancies [266].

While at the moment miRNA-profiling tests are not routinely used for diagnosis in the clinic, we can envision that pending prospective validation and FDA approval, they can replace invasive biopsies. For initial diagnosis, a CT scan is not invasive and easy to perform. However, the challenge arises when the physician needs to genotype or extract more information about the tumour. There, a biopsy is an invasive procedure that carries risk. On the other hand, a blood sample can be taken frequently and with very limited risk. This highlights the opportunities for miRNAs circulating in the blood to be used as liquid biopsies.

One additional feature of miRNA profiling would be to identify the driver oncogene if such an oncogene exists. It is likely that each driver oncogene affects signalling in a way that results in a very specific miRNA signature. A recent study has shown that the expression levels of miR-1253, miR-504, and miR-26a-5p are enough to accurately identify if a lung tumour is KRAS+, EGFR+ or ALK+ [267]. While this study was performed with RNA from core biopsies, it would be feasible to retrospectively test whether this holds true in circulating miRNAs as well. Also, this study started with only 67 patients. A big cohort of hundreds of patients accompanied by a machine learning algorithm would likely yield significantly more sensitivity and accuracy.

5.1.7 LncRNAs: Molecules with extremely diverse functions

Until only recently, how lncRNAs exert their function, as well as their biological relevance, eluded us. In the past years though, ground-breaking research has shed light on the mechanistic action of lncRNAs and has uncovered novel functions in cancer development. LncRNAs can interact with mRNAs, with microRNAs, with other lncRNAs, as well as proteins. This plethora of interactions leads to a multitude of potential functions (examples given in **Figure 38**) that cannot be predicted by the sequence or structure of the lncRNA. Interestingly, a bioinformatics approach of RNA-seq data shows that analysis of co-expression data can often predict the function of lncRNAs [268]. This is predicated upon the assumption that tightly co-expressed transcripts often have very similar functions.

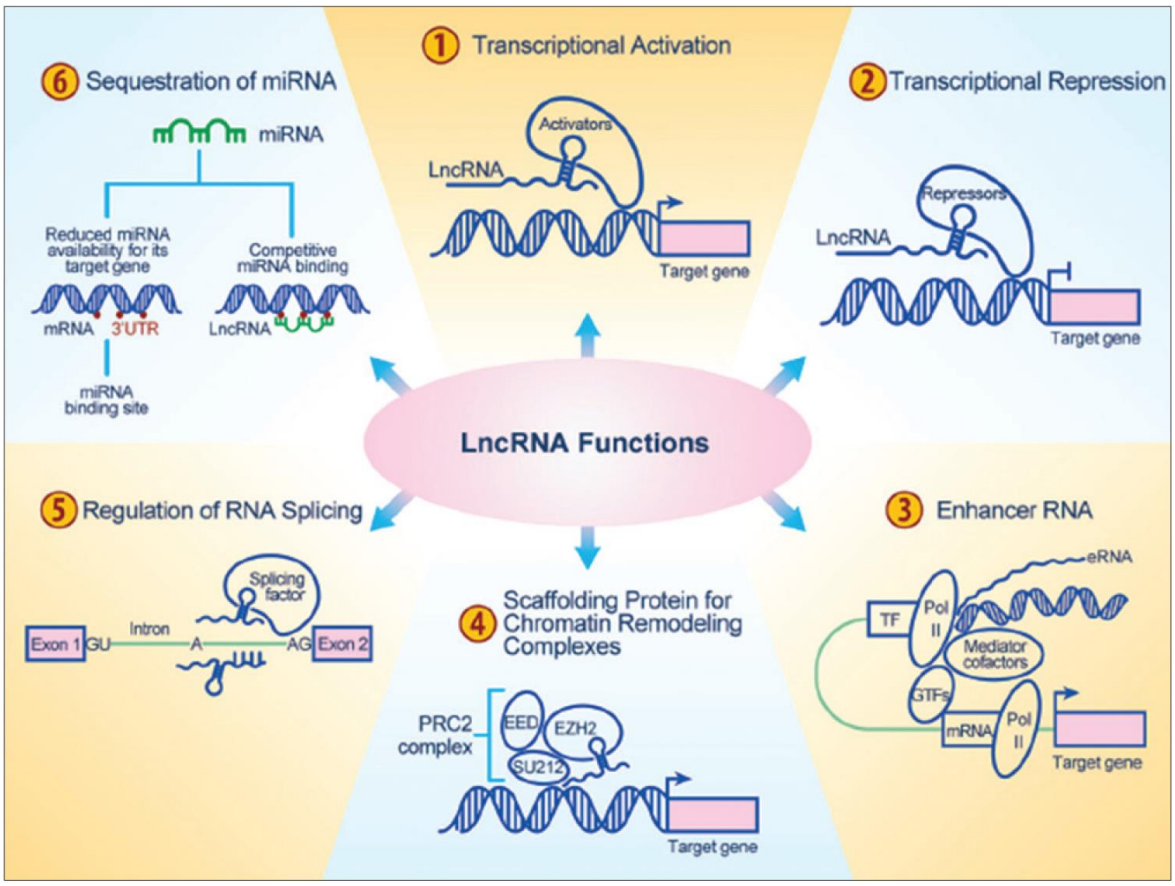

Figure 38: Long non-coding RNAs interact with proteins and other RNA molecules

Provided are six examples of the ways lncRNAs exert their biological effects. By interacting with transcription factors or other transcription-regulating proteins, they can activate or repress the transcription of specific genes. Similarly, by interacting with proteins at enhancer regions they can promote or decelerate the transcription of target genes. Acting as scaffolds, they can affect the way chromatin remodelling complexes change gene expression. Post-transcriptionally, they may interact with splicing factors or the mRNA itself to produce different splicing outcomes. Lastly, they may complementarily bind to miRNAs, sequestering them and preventing them from downregulating their target genes, indirectly influencing gene expression. Given the limitless interactions with proteins and other DNA or RNA molecules, there are almost certainly more unidentified lncRNA functions in a cell. Image adapted from [269].

Similar to miRNAs, lncRNAs can affect virtually every aspect of cancer, including initiation, progression and metastasis [270]. The most compelling pre-clinical evidence regarding the necessity of a lncRNA for tumour initiation would be lncRNA depletion followed by tumour regression (or absence of growth) in a genetically engineered mouse model. While to my knowledge this has not been demonstrated before, there is still compelling evidence for the importance of lncRNA dysregulation as a driving force of tumour growth. For example, in MYC-driven cancers, it was shown that MYC relies at least in part, on the lncRNA PVT-1. Ablation of PVT-1 in a colon cancer MYC-driven cell line resulted in complete suppression of tumour growth in mice, highlighting the importance of this lncRNA for early stages of tumour establishment *in vivo* [271]. In hepatocellular carcinoma (HCC), the lncRNA-ATB was found to be up-regulated in a metastatic cohort of patients and to be induced by TGF-β signalling. Upon silencing of this lncRNA there was a significant decrease in metastatic nodules in a mouse model of HCC, suggesting that this lncRNA has a crucial role in the metastatic process [272].

5.1.8 Examples of dysregulated lncRNAs in cancer

Numerous sequencing efforts have discovered dysregulated lncRNAs that have an active role in cancer development, as well as several lncRNAs which are dysregulated as a by-product of disease. Initial observations claimed that the very low expression levels of most lncRNAs cannot possibly result in substantial functional relevance. However, this was later disproved by the discovery that the lncRNA VELUCT can modulate the proliferation of NSCLC cells despite its very low abundance [273]. Also highlighted in the same study, the differential localisation of lncRNAs (cytoplasmic vs nuclear) can have profound effects on cellular functions as well as make detection challenging. Specifically, while the total expression levels of this lncRNA were very low, upon cellular fractionation, the nuclear fraction was significantly enriched in VELUCT.

Absence of a tumour-suppressing lncRNA may be enough to contribute to tumourigenesis. A single-nucleotide polymorphism in the *LINC00673* lncRNA locus was found to be associated with pancreatic ductal adenocarcinoma (PDAC) in a genome-wide association study (GWAS) [274]. Intriguingly, a G > A mutation in this locus renders LINC00673 susceptible to binding by miR-1231 (followed by downregulation). This prevents the interaction with PTPN11 and its regulation through ubiquitination, which results in subsequent increased SRC-ERK signalling which promotes tumour growth and proliferation. Finally, LINC00673 was a *bona fide* tumour suppressor, as its overexpression in xenograft mouse models could delay tumour growth, an effect which could be rescued by introducing the G>A mutation. This study provides another example of how a mutation in a silent area of the genome can still have important phenotypic consequences. One of the most well-studied lncRNAs, HOTAIR, has been found to be up-regulated in a variety of different tumour sites compared with their normal counterparts. As a regulator of chromatin dynamics, it utilises several different mechanisms of action, through which it contributes to tumour progression and these have been thoroughly reviewed in [275]. In melanoma, a powerful dependence on the lncRNA SAMMSON was demonstrated [276]. This lncRNA is co-expressed with the oncogenic transcription factor MITF in a subset of melanomas and treatment with an anti-sense RNA led to tumour regression in PDX mouse models.

Lastly, lncRNAs have been demonstrated to affect aspects of DNA damage and subsequently the response to radiotherapy. In triple-negative breast cancer (TNBC), a genetic screening led to the discovery that knockdown of the lncRNA LINP1 led to induction of apoptosis in TNBC cells. The authors found that LINP1 is recruited to double-strand breaks and stabilized DNA repair proteins. This functional relevance was confirmed *in vivo*, as upon silencing of LINP1 with shRNA, a mouse xenograft model treated with radiation showed prolonged tumour regression compared with shRNA control [277].

5.1.9 LncRNAs in drug resistance

In cancer-related lncRNAs, an addiction that results in resistance to small-molecule inhibitors has been convincingly demonstrated. In head & neck squamous cell carcinomas gefitinib is often a treatment option. In a recent study, exceptional responders to gefitinib revealed a single-nucleotide polymorphism (SNP) that results in profound gefitinib sensitivity [278]. This silent SNP resulted in decreased levels of the lncRNA EGFR-AS1 which the authors convincingly demonstrate that causes addiction to EGFR signalling, both *in vitro* and *in vivo*. Therefore, patients with this silent SNP have low levels of EGFR-AS1, followed by increased EGFR signalling and are prone to respond well to EGFR inhibition. These results suggest that trying to predict protein function from the genomic sequence will often fail. Instead, robust assays that rely on protein readout could be utilised to detect increased EGFR signalling in the above example.

LncRNAs can also affect the response to EGFR inhibition with the monoclonal antibody cetuximab in colorectal cancer. Whole-exome sequencing of cetuximab-resistant cells revealed an upregulation of the lncRNA miR-100HG and its intronic miRNAs miR-100 and miR-125b [279]. Combined inhibition of miR-100 and miR-125b greatly sensitised mice xenograft models to cetuximab treatment. Furthermore, it was shown that this particular miR-100/125b activity happens because of a downregulation of key components of the Wnt pathway such as DKK1 and DKK3.

In an effort to discover mediators of resistance to sunitinib in renal cell carcinoma (RCC), [280] a study found that the lncRNA lncARSR can promote resistance to multiple-RTK inhibition. Knockdown of lncARSR was able to restore sensitivity to sunitinib in a mouse xenograft model of renal carcinoma. Mechanistically, the authors found that this lncRNA is normally a competing endogenous RNA (ceRNA) for the tumour suppressing miR-34 and miR-449a. These data suggest that high-throughput approaches to identify drivers of drug resistance should incorporate ncRNA-examining methods as well. Clearly, whole-exome sequencing misses information from the majority of the genome and should well be replaced by whole-genome sequencing. Furthermore, in the absence of RNA-seq data, the functional impact of detected mutations is harder to assess.

5.2 Results

5.2.1 The response of transcriptional networks to ALK inhibition

MiRNAs downstream of ALK signalling have the potential to mediate cell death in response to crizotinib. Oncogenic miRNAs induced by EML4-ALK would be expected to contribute to EML4-ALK carcinogenesis and therefore be downregulated or lost upon EML4-ALK inhibition. On the other hand, tumour-suppressing miRNAs should be repressed by EML4-ALK and thus, loss of EML4-ALK signalling should restore the expression of such miRNAs.

Therefore, I aimed to identify any miRNAs that might be modulated by ALK and which accordingly might affect the response to ALK inhibition. The drug-responsive EML4-ALK cell line H3122 (variant 1, E13;A20) was used as the initial screening model for dysregulated miRNAs, with the aim to check for generalisable dysregulation in the drug-responsive STE-1 (variant 1, E13;A20) cell line. This experiment would culminate in the identification of the most robustly-changing miRNAs and subsequent analysis for their potential targets followed by functional assays (pipeline in **Figure 39A**).

Thus, H3122 cells were treated with DMSO or 100nM crizotinib for 24 hrs and high-throughput miRNA profiling performed in collaboration with the Ohio State University core facility revealed over 100 differentially expressed miRNAs upon ALK inhibition, the top 20 of which can be found in (**Figure 39B**). The whole dataset can be accessed in (https://rebrand.ly/paliouras1).

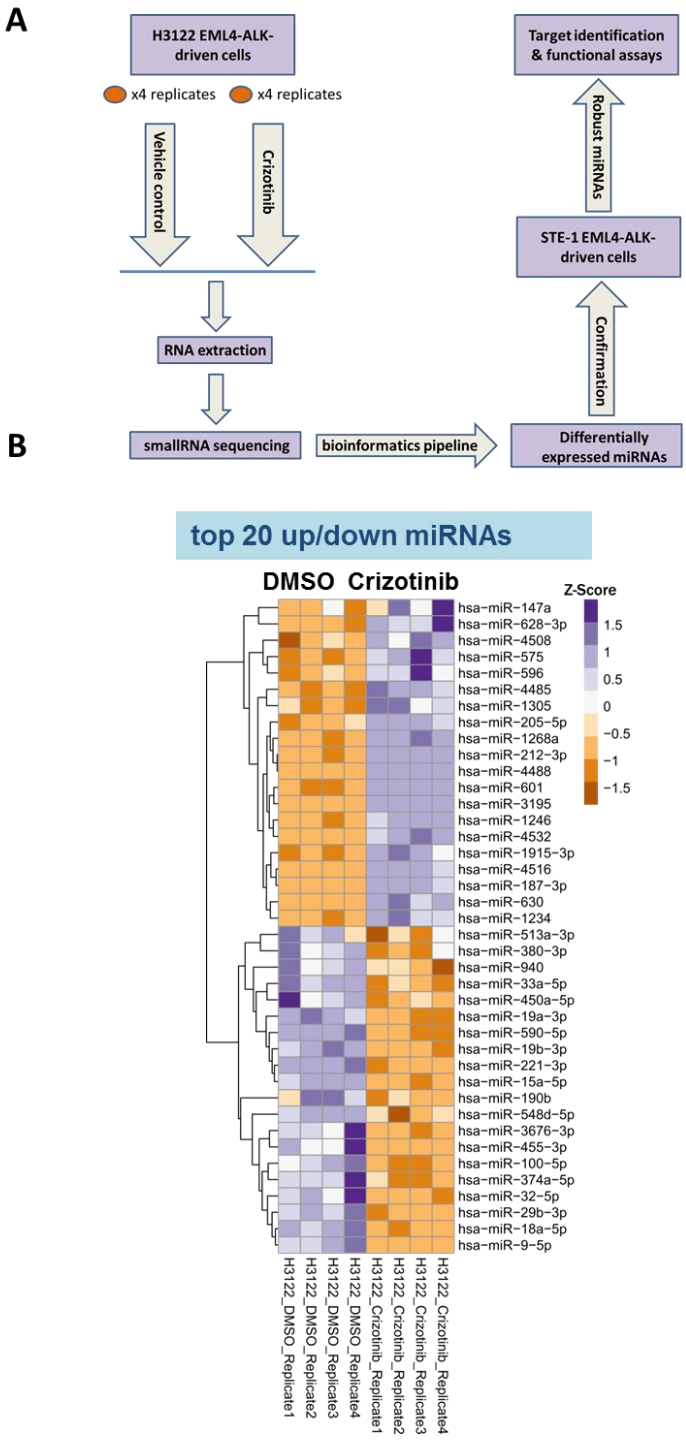

Figure 39: Pipeline for miRNA identification and top 20 differentially expressed miRNAs upon ALK inhibition

A) H3122 EML4-ALK cells were used as the basis to identify differentially expressed miRNAs upon crizotinib treatment. To this end, cells were treated with DMSO /100nM crizotinib for 24hrs. Then, RNA was extracted and small RNA libraries were prepared, size-selected and sequenced. After a differential expression analysis, .candidates from the top 20 up/down regulated miRNAs would be confirmed via qPCR in another EML4-ALK-driven cell line (STE-1). Given the identification of robustly dysregulated miRs, target prediction and confirmation would follow.
B) H3122 parental cells were RNA extracted and were sequenced for small RNAs as described in A). The differential expression analysis was kindly performed by Dr Gianpiero Di Leva. Cut-off p adj < 0.01. n = 4 biological replicates. The top20 up/down modulated miRNAs are plotted in the heatmap shown comparing the different replicates. Members of the oncogenic miR-17-92 cluster and miR-221/222 cluster can be observed among the top-20 up/down modulated miRs.

Two major miRNA clusters were found to be down-regulated upon crizotinib treatment: The miR-17-92 cluster which is comprised of miR-17, miR-18a, miR-19a, miR-19b, miR-20a and miR-92a [248], and the miR-221/222 cluster comprised of miR-221 and miR-222 [281]. Given the potential inaccuracies of small-RNA seq [282], I aimed to confirm the dysregulation of these miRNAs with the more accurate method of RT-qPCR. A downregulation of members of the miR-17-92 cluster was confirmed in H3122 (**Figure 40A**) and STE-1 (**Figure 40B**) cells upon treatment with crizotinib. The same was true for miR-221 and miR-222, which comprise the miR-221/222 cluster (**Figure 40C**). Interestingly, the miR-221/222 cluster has been shown to target the pro-apoptotic protein PUMA [283] and PUMA is a known mediator of the response to crizotinib [284]. This suggests that downregulation of the miR-221/222 cluster may allow the activation of PUMA and the induction of cell death in this context.

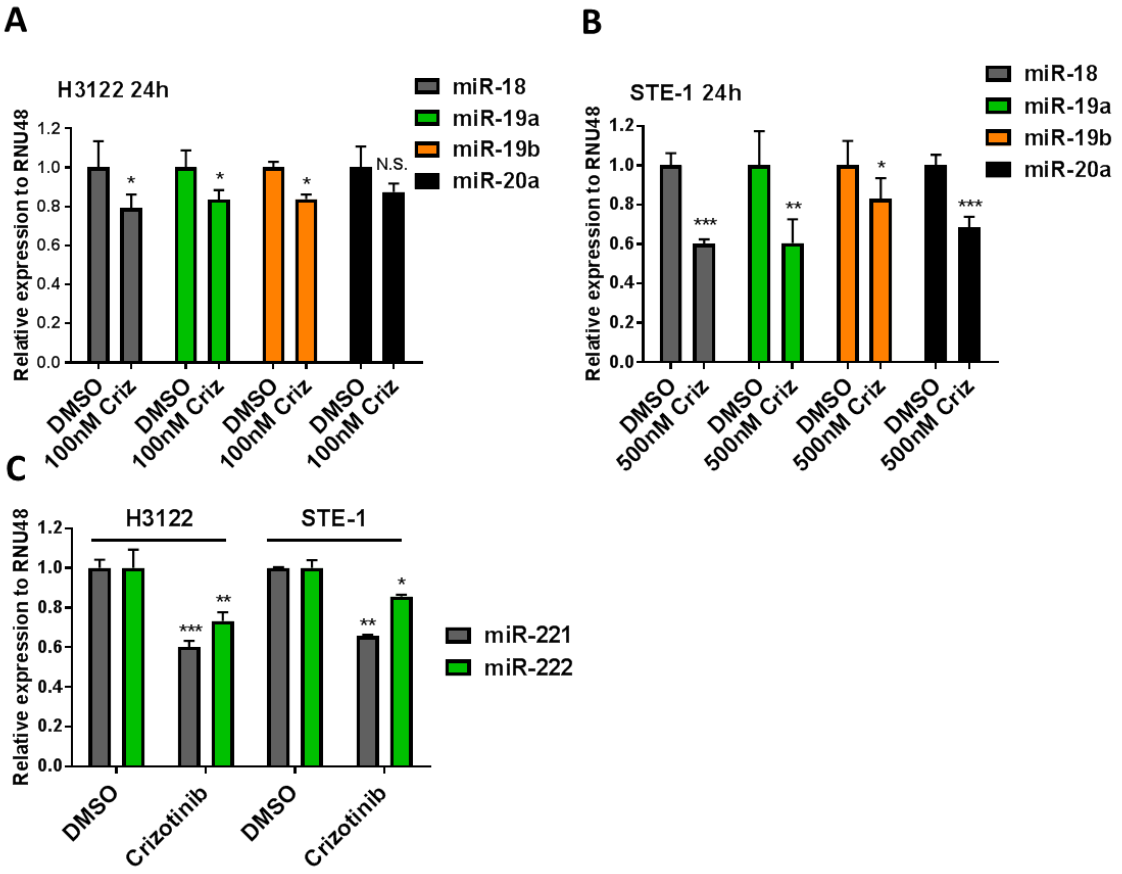

Figure 40: The miR-17-92 and miR-221/222 clusters are repressed upon ALK inhibition

A) H3122 cells were treated with crizotinib and vehicle control for 24h and RNA was extracted. RT-qPCR for miR-18a, miR-19a, miR-19b and miR-20a. Data are presented as 2-ΔΔCT-normalised means ± SD (n=3 biological replicates)

B) As in A), reproduced in STE-1 cells.

C) In the same samples, qPCR for miR-221 and miR-222 was performed in H3122 and STE-1 cells. Data are presented as 2-ΔΔCT-normalised means ± SD (n=3 biological replicates) and p values were calculated by two-tailed student's t-test (*p < 0.05, **p<0.01, ***p<0.001).

5.2.1.1 MiR-19b targets BIM

To identify mRNAs that are regulated by the miR-17-92 cluster, Targetscan target prediction analysis was performed. The pro-apoptotic protein BIM was a recurrently predicted 3'UTR as a target for miR-18a, 19b and miR-20a. In lymphoblastic leukaemia, BIM is a confirmed target of the miR-17-92 cluster [285]. Given the special importance of the induction of BIM and PUMA as a response to oncogene inhibition in oncogene-driven cancers [166], it was then decided to test miRNAs that target BIM, the loss of which might explain its upregulation. First, the induction of BIM in an EML4-ALK system after crizotinib treatment was confirmed (**Figure 41A**). Then miR-18a, miR-19b and miR-20a synthetic mimics were transfected (**Figure 41B**), but a downregulation of BIM was observed only after miR-19b overexpression (**Figure 41C**). MiR-19b also resulted in a partial rescue of the overexpression of BIM after crizotinib, (**Figure 41D**) suggesting that the downregulation of miR-19b has a functional role in the induction of BIM followed by cell death upon crizotinib treatment. These data indicated that BIM is either a direct or an indirect target of miR-19b.

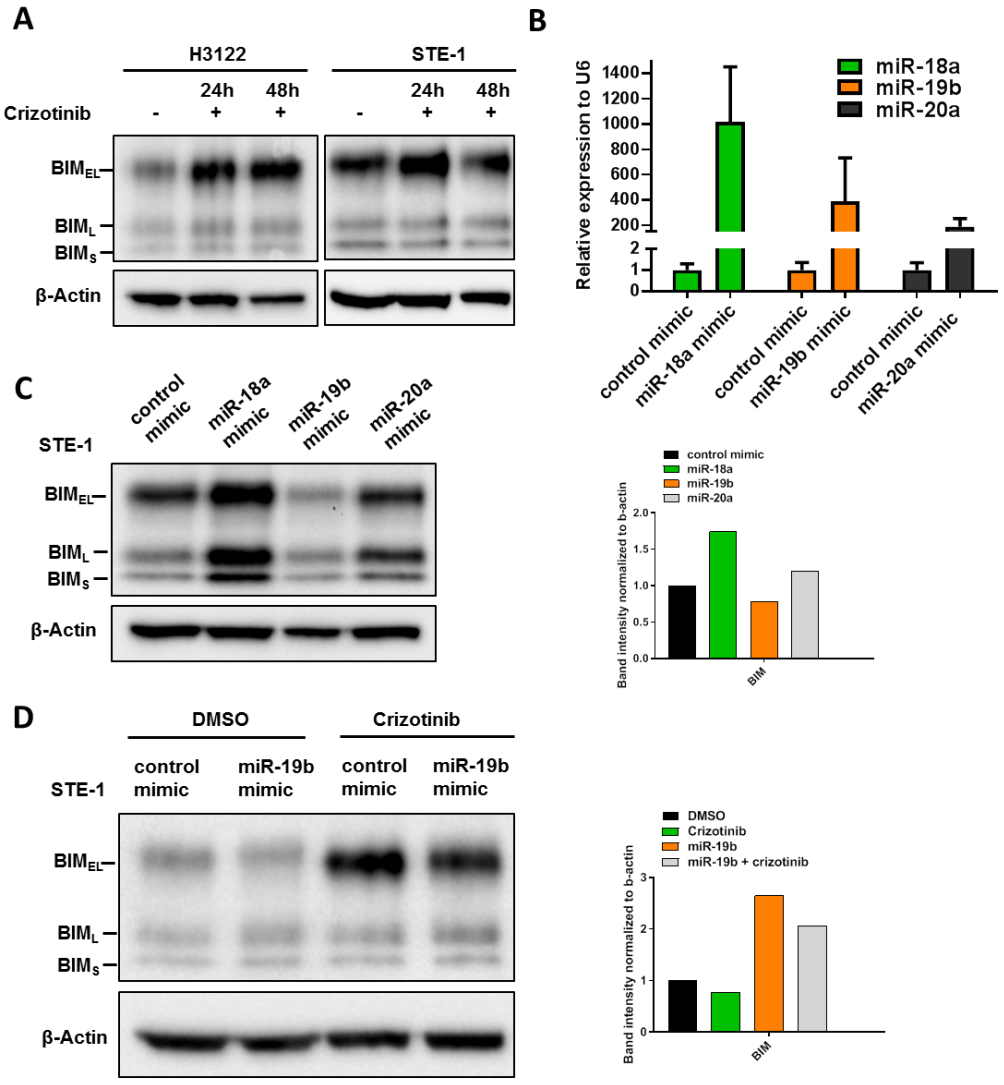

Figure 41: BIM is a miR-19b target downstream of ALK signalling

A) H3122/STE-1 cells were treated with vehicle control/crizotinib for 24h then protein extracts were subjected to western blotting for the 3 major isoforms of BIM. Shown is a representative blot of 2 independent experiments.

B) STE-1 cells were transfected with miRNA mimics for 48h and RNA-extracted. RT-qPCR for the indicated miRNAs was performed and data are presented as 2-ΔΔCT-normalised means ± SD (n=2 biological replicates).

C) STE-1 cells were transfected with the specified miRNA mimics for 72h then protein extracts were subjected to western blotting for the 3 major isoforms of BIM. Shown is a representative blot of 2 independent experiments. (right panel) Quantification of the protein bands presented on the left panel. Non-saturated ECL images were digitally quantified for signal intensity, which was subsequently normalised to the signal intensity of the loading control used (β-actin).

D) STE-1 cells were transfected with the specified miRNA mimics. 48h post-transfection cells were additionally treated with vehicle control/crizotinib. 72h post-transfection, protein extracts were harvested and subjected to western blotting for the 3 major isoforms of BIM. Shown is a representative blot of 2 independent experiments. (right panel) Quantification as in C).

To clarify this, the part of the 3' UTR that contains the miR-19b binding site was cloned (**Figure 42A**) in a luciferase reporter vector. Co-transfection of a miR-19b mimic along with the luciferase reporter vector led to a decrease in luciferase activity. This decrease was rescued upon deletion of the miR-19b binding site, confirming that the interaction between miR-19b and the BIM 3' UTR is indeed direct (**Figure 42B**). Thus, I identified a new miR-19b target in EML4-ALK^{mut} cells.

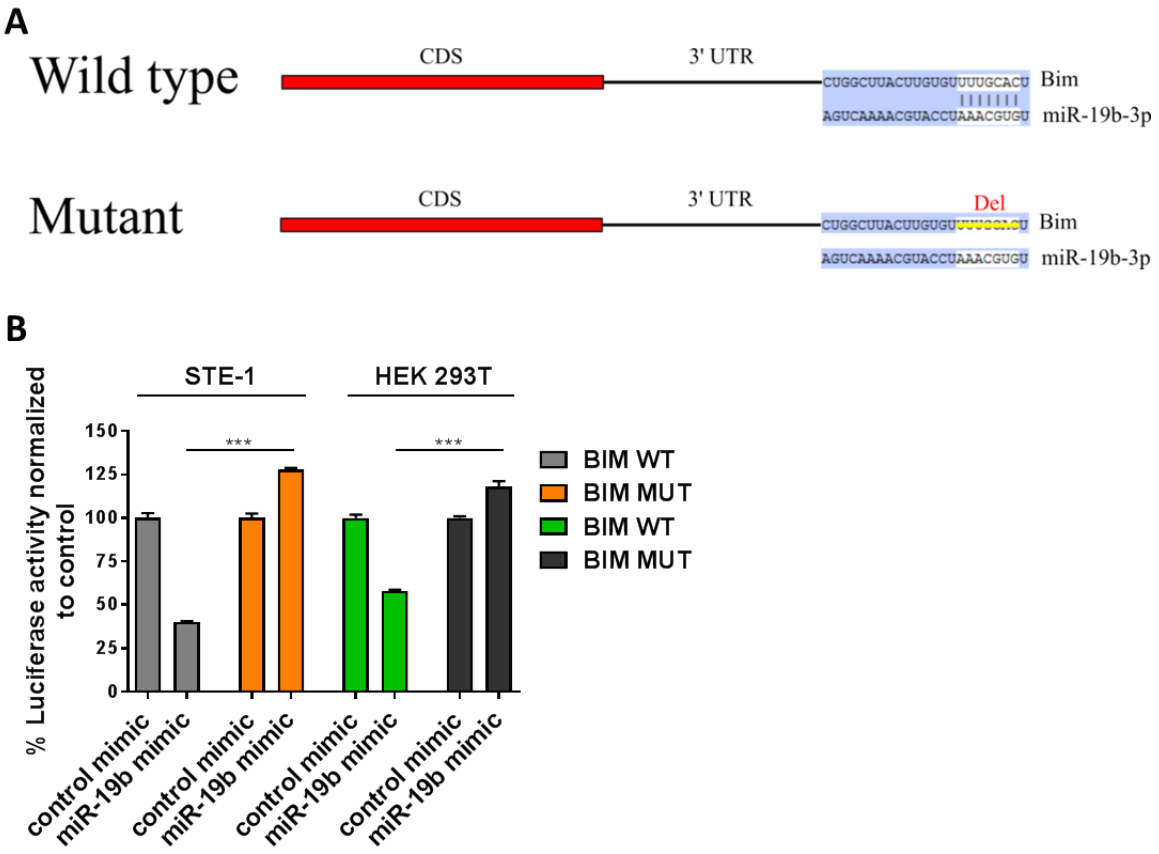

Figure 42: MiR-19b directly targets the BIM 3' UTR

A) Representation of the position of a miR-19b binding site in the BIM 3′ UTR (position no. 4092). The binding site was deleted with the use of site-directed mutagenesis to interrogate the specificity of the interaction with miR-19b.
B) STE-1 and HEK293T cells were transfected with pGL3 control 3′ UTR BIM plasmid (WT/MUT for the miR-19b predicted binding site) and co-transfected with control or miR-19b mimic. 24h post-transfection, luminescence was recorded and normalised according to the Firefly: Renilla ratio. Error bars indicate mean ± SD (n=3 biological replicates) and p values were calculated by a two-tailed student's t-test (*p < 0.05, **p<0.01, ***p<0.001).

5.2.1.2 The role of STAT3 signalling in the response to crizotinib

I sought to further investigate the signalling changes that might contribute to miR-17-92 downregulation in response to crizotinib treatment. There is evidence that activation of STAT3 and the subsequent expression of downstream targets may lead to increased proliferation upon ALK inhibition [37]. Interestingly, there has been evidence of STAT3 signalling regulating the miR-17-92 cluster in the context of ALCL [286]. A loss of STAT3 phosphorylation was indeed confirmed upon ALK inhibition in two cell lines (**Figure 43A-B**), as observed before [38]. In addition, using a STAT3 siRNA (**Figure 43C**) it was observed that downregulation of STAT3 results in reduced expression of the miR-17-92 cluster and of miR-221 (**Figure 43D**). Thus, STAT3 regulates the miR-17-92 cluster and miR-221, however, miR-222 does not appear to be regulated by STAT3. It should be noted that more prolonged STAT3 inhibition may have more pronounced effects on miRNAs, due to their stable nature.

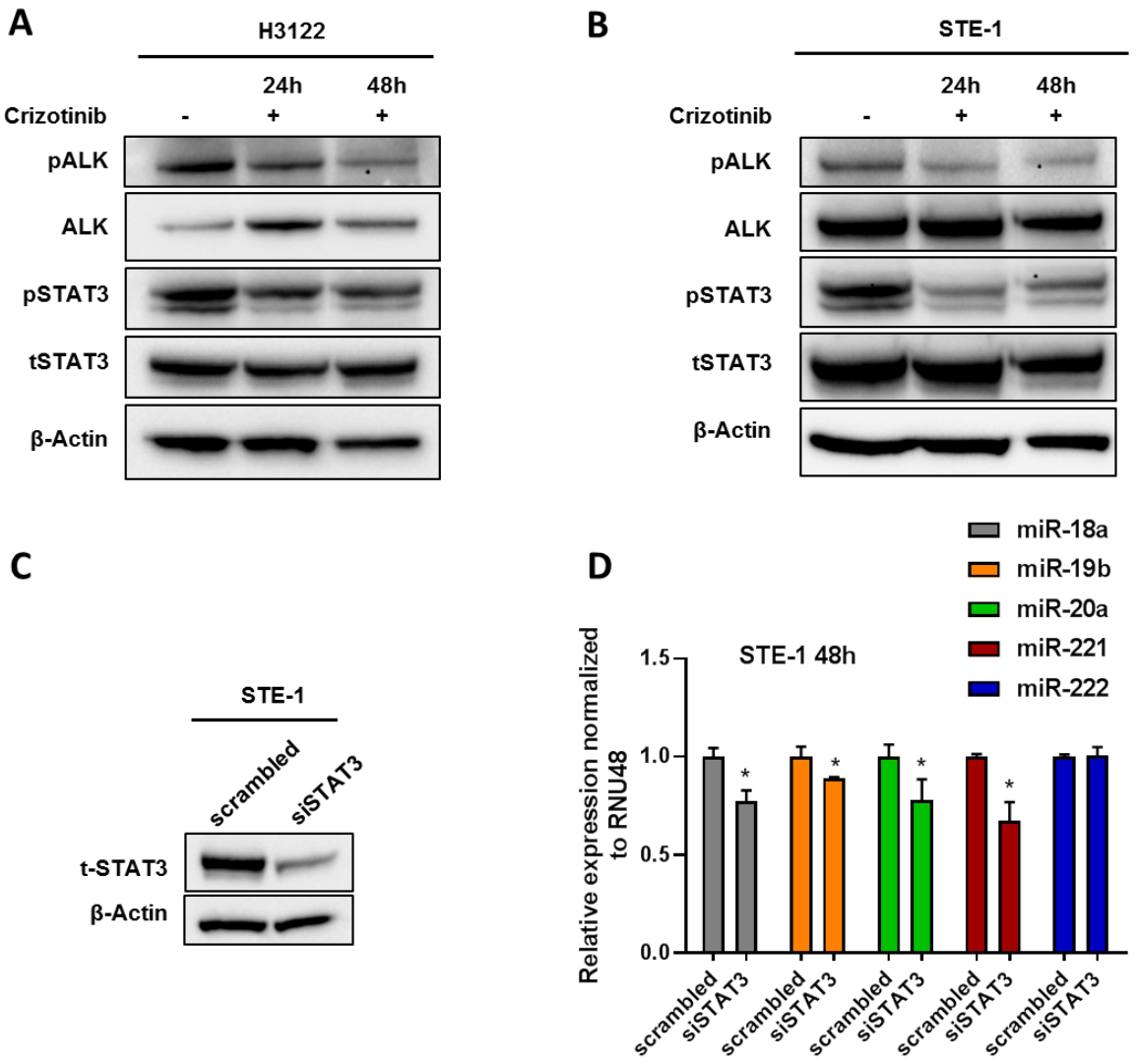

Figure 43: STAT3 is downstream of ALK signalling and partially regulated the miR-17-92 cluster

A) H3122 cells were treated with vehicle control/crizotinib for 24h then protein extracts were subjected to western blotting for the indicated proteins, evidencing reduced phosphorylation of STAT3 upon crizotinib treatment. Shown is a representative blot of 2 independent experiments.

B) As in A), reproduced in STE-1 cells.

C) STE-1 cells were transfected with scrambled control or siSTAT3 for 48h. Then protein extracts were analysed by western blotting for the expression levels of STAT3. Shown is a representative blot of 2 independent experiments.

D) STE-1 cells were transfected with scrambled control or siSTAT3 for 48h. Then, RNA was extracted and the expression of the indicated miRNAs was assessed by RT-qPCR. Error bars indicate mean ± SD (n=3 biological replicates) and p values were calculated by a two-tailed student's t-test (*p < 0.05, **p<0.01, ***p<0.001).

5.2.1.3 Contribution of miR-18a to STAT3 signalling

The fact that the total STAT3 levels do not change after crizotinib, led to the hypothesis that the reduction in phosphorylated STAT3 might be due to an interaction with one of the negative regulators of the JAK-STAT pathway. One of the most common proteins that negatively regulate this pathway is PIAS3 [287], which was found to be slightly increased after crizotinib treatment (**Figure 44A**). It was reasoned that the upregulation of PIAS3 could be due to the loss of a miRNA that would normally suppress its expression. After bioinformatics analysis, a binding site for miR-18a was identified in the PIAS3 3' UTR. To investigate whether miR-18a has the capacity to decrease the PIAS3 protein levels, a synthetic mimic of miR-18a was overexpressed in STE-1 cells and downregulation of PIAS3 was observed at the protein level (**Figure 44B**). With a luciferase reporter system, the direct binding of miR-18a to the PIAS3 3' UTR was measured and was partially rescued upon deletion of the miR-18a binding site, proving the specificity of the interaction (**Figure 44C**). However, after knocking down PIAS3, no changes in STAT3 phosphorylation were observed (**Figure 44D**) and the hypothesis that the loss of STAT3 phosphorylation comes from an interaction with PIAS3 was rejected.

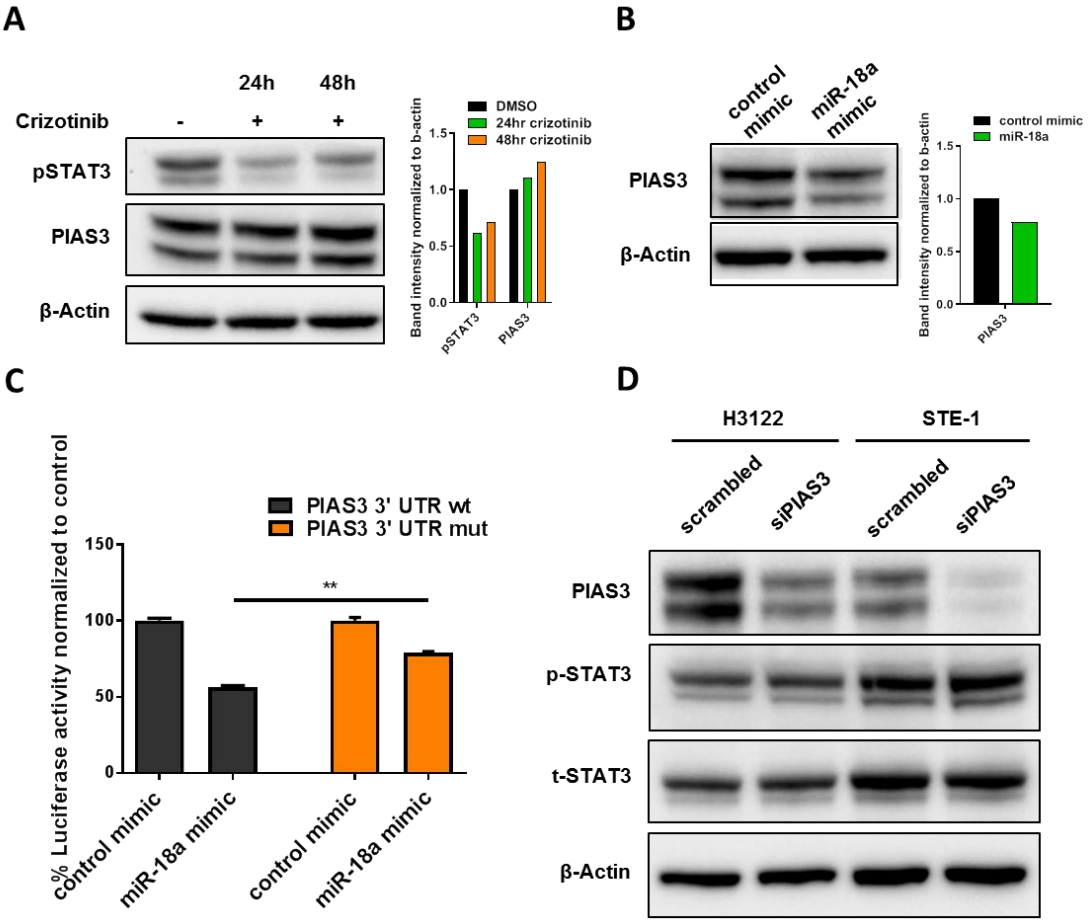

Figure 44: PIAS3 does not contribute to loss of STAT3 phosphorylation

A) STE-1 cells were treated with vehicle control/crizotinib for 24h or 48h then protein extracts were subjected to western blotting for the indicated proteins. Shown is a representative blot of 2 independent experiments. (right panel) Quantification of the protein bands presented on the left panel. Non-saturated ECL images were digitally quantified for signal intensity, which was subsequently normalised to the signal intensity of the loading control used (β-actin).

B) STE-1 cells were transfected control mimic/miR-18a mimic for 72h then protein extracts were subjected to western blotting for the indicated proteins. Shown is a representative blot of 2 independent experiments. (right panel) Quantification as in A).

C) HEK293T cells were transfected with pGL3 control 3' UTR PIAS3 plasmid (WT/MUT for the miR-18a binding site) and co-transfected with control/ miR-18a mimic. 24h post-transfection, luminescence was recorded and normalised according to the Firefly: Renilla ratio. Plotted are the normalised means ± SD (n=3 biological replicates). P values were calculated by two-tailed student's t-test (*p < 0.05, **p<0.01, ***p<0.001).

D) STE-1 or H3122 cells were transfected with the scrambled siRNA/ siRNA STAT3 for 48h then protein extracts were subjected to western blotting for the indicated proteins. Shown is a representative blot of 2 independent experiments.

5.2.2 Potential role of miRNAs in drug resistance

The next hypothesis was that during the process of developing resistance to ALK inhibitors, a cell may undergo a reprogramming of its miRNA signalling network. Therefore, miRNA deregulation might form a mechanism of resistance to ALK inhibitors. To test this, the miRNA expression of H3122 and CrizR1 cells was profiled using small RNA Next Generation Sequencing (NGS) (the dataset can be accessed on https://rebrand.ly/paliouras3).

After small-RNA sequencing and differential expression analysis, a pronounced miRNA dysregulation was found in the CrizR1 clone (**Figure 45A**). Then, the NGS data were verified or rejected by RT-qPCR. MiR-381 was reported as the most up-regulated miRNA in the NGS data. This, however, was not confirmed after RT-qPCR and its expression was undetectable (data not shown).

Initially, several potentially up-regulated miRNAs were selected to be screened by RT-qPCR. MiR-30c was robustly up-regulated in all drug-resistant clones, while miR-25 was up-regulated in CrizR1 and CrizR5 cells (**Figure 45B**)**.** Surprisingly, another miRNA member of the miR-25 cluster, miR-106b, was not robustly dysregulated (**Figure 45C**), indicating differential processing of the primary miRNA transcript.

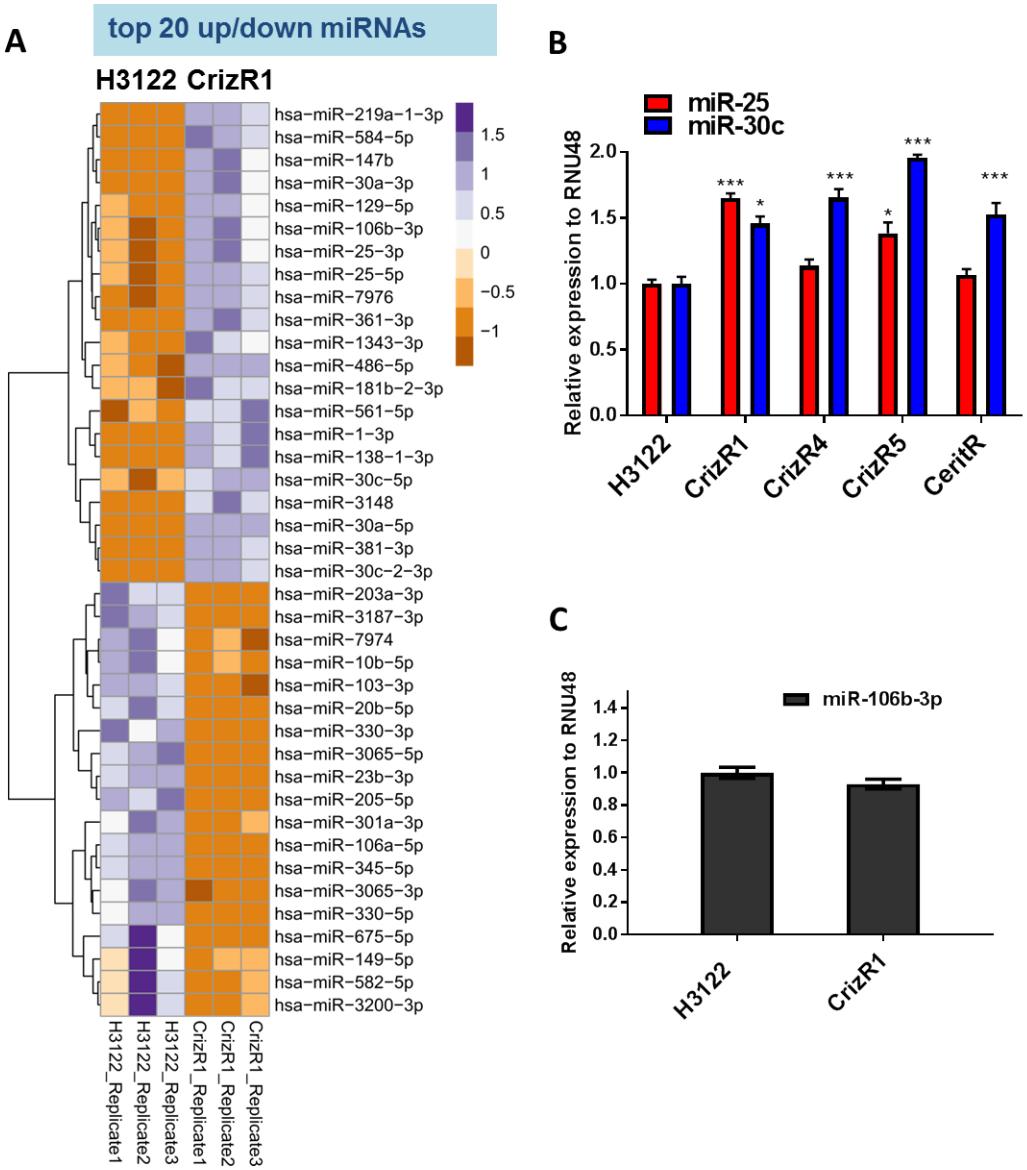

Figure 45: MiR-25 and miR-30c are robustly upregulated in drug-resistant EML4-ALK cells

A) RNA was extracted from H3122 and CrizR1 cells and small RNA libraries were prepared and size selected. The libraries were then sequenced and the data processed to map human miRNAs, followed by differential expression analysis. Z-score is depicted, cut-off p adj < 0.05. n = 3 biological replicates. MiRNAs such as the oncogenic miR-25 and miR-30c are upregulated in CrizR1 cells compared with their H3122 parental.

B) RNA was extracted from H3122 and CrizR1 cells. RT-qPCR for the indicated miRNAs was performed and data are presented as 2-ΔΔCT-normalised means ± SD (n=3 biological replicates). The H3122 parental values were transformed to 1 and the values of the drug-resistant cell lines were normalised to this. Compared with the parental, miR-30c is upregulated in all drug-resistant clones whereas miR-25 only in CrizR1 and CrizR5. P values were calculated by two-tailed student's t-test (*p < 0.05, **p<0.01, ***p<0.001).

C) As in B), RT-qPCR analysis for miR-106b expression in CrizR1 cells which did not differ significantly from its expression in H3122 parental cells, n = 2 biological replicates.

In this data set, the most down-regulated miRNA in CrizR1 cells is miR-205. This was confirmed by RT-qPCR (**Figure 46A**), where miR-205 was down-regulated almost to the limit of non-detection in CrizR1 cells. Moreover, the downregulation of the well-studied tumour suppressing miR-23b cluster was confirmed (**Figure 46B**) [288], as well as the downregulation of miR-103, miR-149, miR-345 and miR-3065, with the exception of the ceritinib-resistant clone, in which only miR-149 was down-regulated (**Figure 46C**).

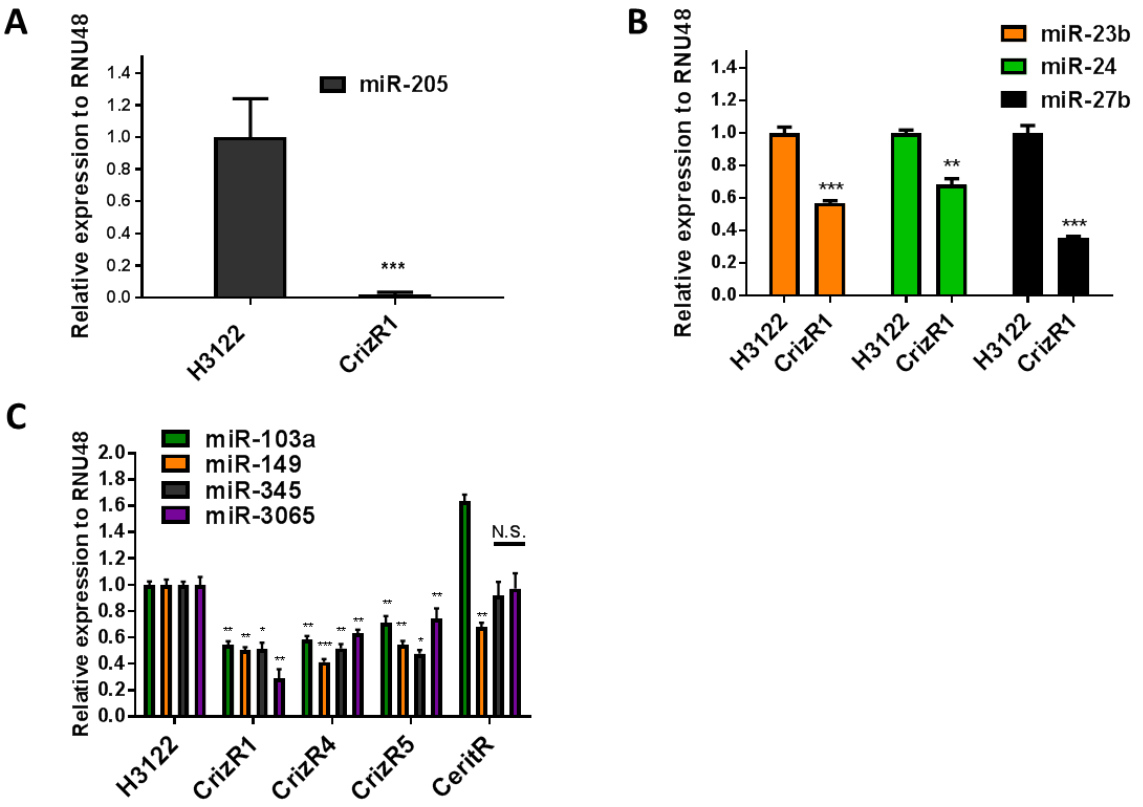

Figure 46: QPCR confirmation of the downregulation of potential tumour suppressing miRNAs

A) RNA was extracted from H3122 and CrizR1 cells. RT-qPCR for miR-205 was performed and data are presented as 2-ΔΔCT-normalised means ± SD (n=3 biological replicates).

B) As in A), RT-qPCR for miR-23b, miR-24 and miR-27b (n=3 biological replicates).

C) RNA from the indicated cell lines was analysed for the expression of the indicated miRNAs. Data are presented as 2-ΔΔCT-normalised means ± SD (n=3 biological replicates).

The H3122 parental values were transformed to 1 and the values of the drug-resistant cell lines were normalised to this. P values were calculated by two-tailed student's t-test (*p < 0.05, **p<0.01, ***p<0.001).

5.2.2.1 MiR-149 induces apoptosis while miR-25 and miR-30c inhibition affect the cell cycle

Dysregulated miRNAs in crizotinib-resistant cells may form a mechanism of resistance, or they may simply reflect signalling changes due to parallel pathway alterations. To shed light on this, functional studies with these miRNAs were performed. For the down-regulated miRNAs, re-introduction of miR-205 in the form of a synthetic mimic (**Figure 47A**) did not result in a robust re-sensitisation to crizotinib, therefore this miRNA was rejected as a potential mediator of resistance (**Figure 47B**). The only down-regulated miRNA from this screen which had a functional effect was miR-149. Upon re-introduction of miR-149 in CrizR1 cells, (**Figure 47C**), a decrease in proliferation was observed (**Figure 47D**), as well as apoptotic induction (**Figure 47E**). However, there was no synergism with crizotinib, suggesting that this miRNA is indeed a tumour suppressing one, albeit not mediating the resistance to crizotinib.

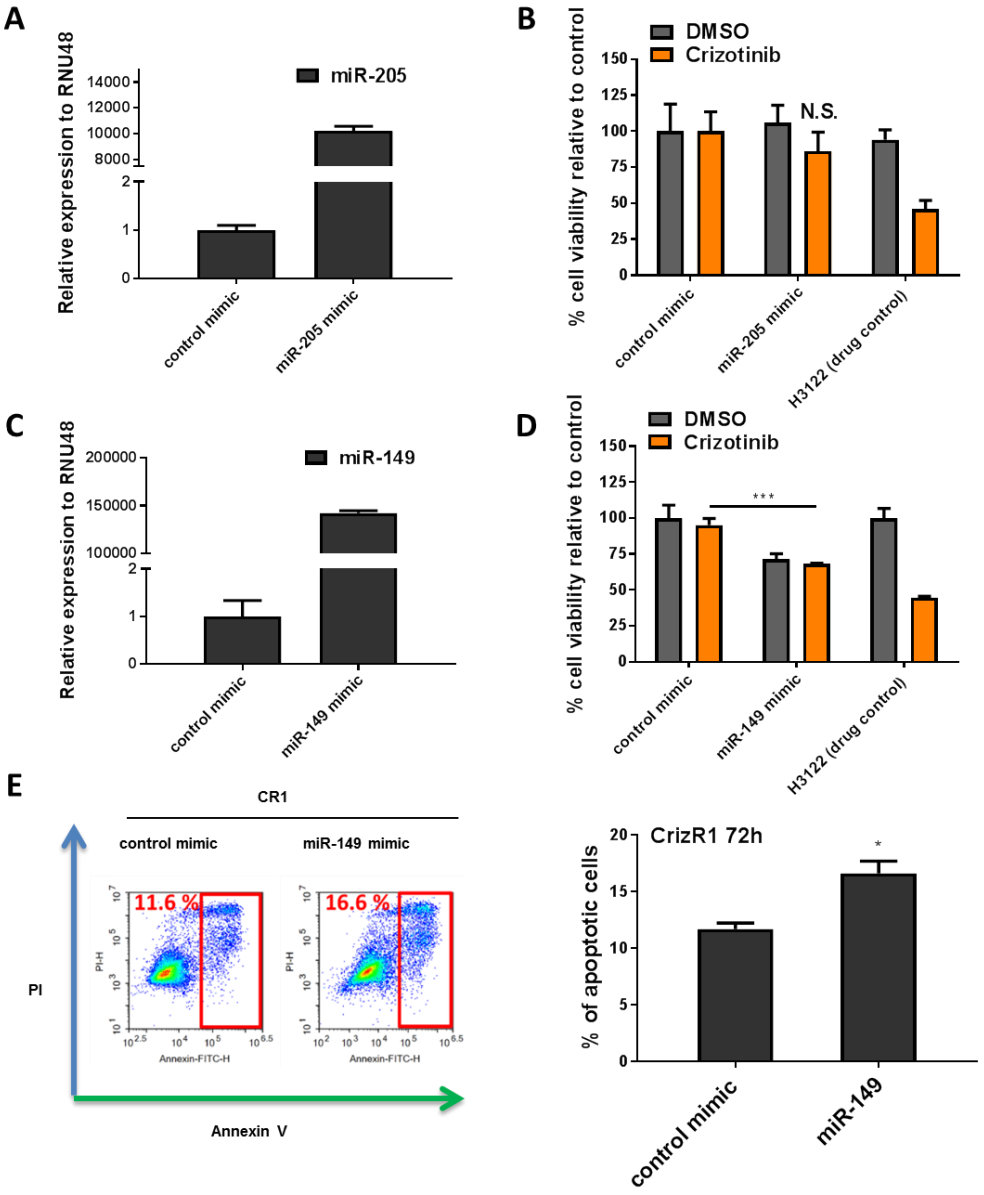

Figure 47: MiR-149 promotes apoptosis in EML4-ALK cells

A) CrizR1 cells were transfected with non-targeting control and miR-205 mimic for 72h and RNA-extracted. RT-qPCR for miR-205 was performed and data are presented as 2-ΔΔCT-normalised means ± SD (n=2 biological replicates).

B) CrizR1 cells were transfected with non-targeting control and miR-205 mimic for 72h, in the presence or absence of the indicated concentrations of crizotinib. 72h post-transfection, cell proliferation was assessed by MTS. H3122 cells were used in parallel as crizotinib control. Data are presented as normalised means ± SD (n=3 biological replicates).

C) CrizR1 cells were transfected with non-targeting control and miR-149 mimic for 72h and RNA-extracted. RT-qPCR for miR-149 was performed and data are presented as 2-ΔΔCT-normalised means ± SD (n=2 biological replicates).

D) CrizR1 cells were transfected with non-targeting control and miR-149 mimic for 72h, in the presence or absence of 1μM crizotinib. 72h post-transfection, cell proliferation was assessed by MTS. H3122 cells were used in parallel as crizotinib control. Data points are presented as normalised means ± SD (n=3 biological replicates).

E) CrizR1 cells were transfected with non-targeting control and miR-149 mimic for 72h. Then, cells were stained with Annexin V and PI and analysed by flow cytometry. Annexin V+ cells are depicted (left) and quantified (right). N = 3 biological replicates. P values were calculated by two-tailed student's t-test (*p < 0.05, **p<0.01, ***p<0.001).

To investigate the role of the up-regulated miRNAs, hairpin inhibitors were used that resulted in partial knockdown of miR-25 and miR-30c (**Figure 48A**). It became apparent that the downregulation of miR-25 and 30c led to a G2/M cell cycle arrest in CrizR1 cells (**Figure 48B**), while miR-30c knockdown had the additional effect of inducing cell death in combination with crizotinib (**Figure 48C**).

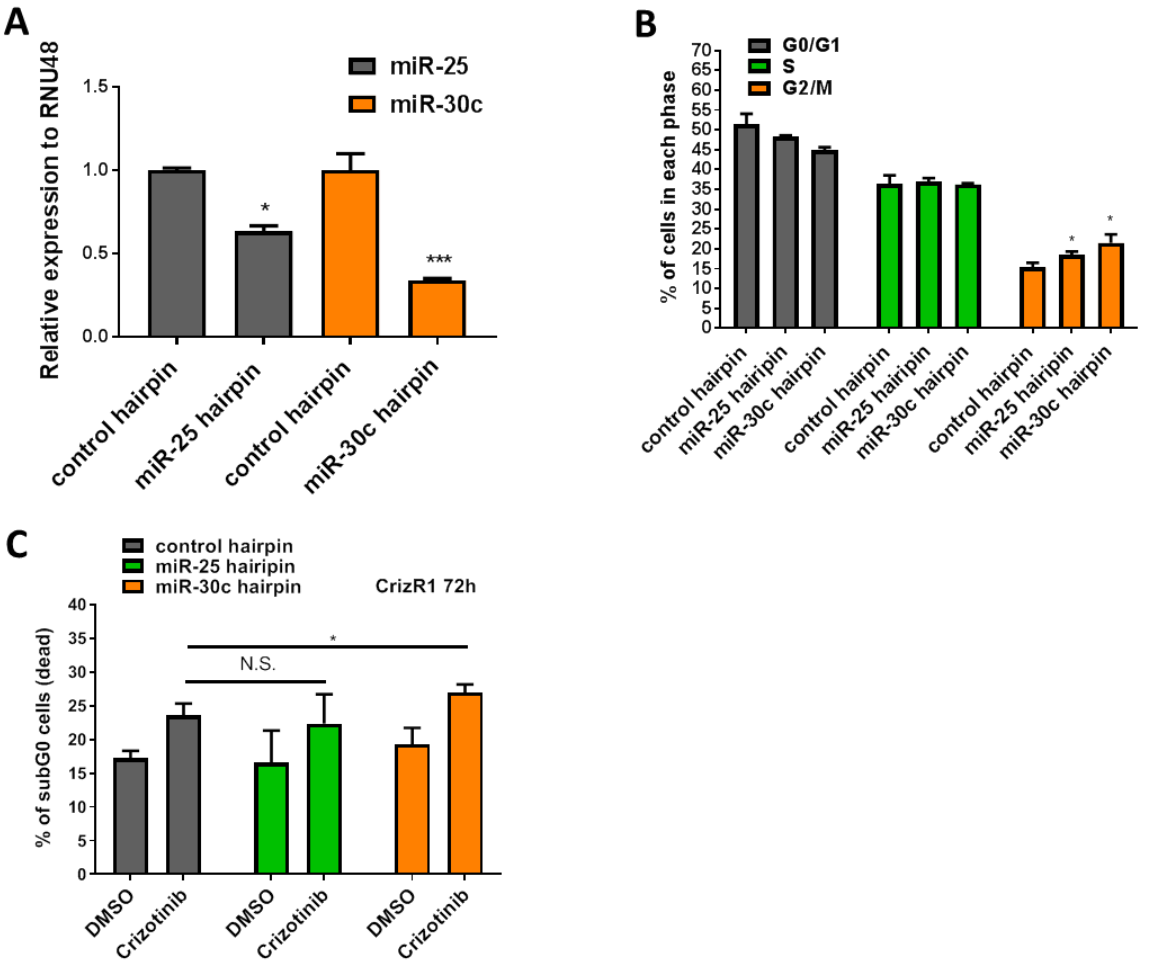

Figure 48: MiR-25/30c inhibition has functional consequences in CrizR1 cells

A) CrizR1 cells were transfected with non-targeting hairpin inhibitor, miR-25 hairpin and miR-30c hairpin for 72h and RNA-extracted. RT-qPCR for the indicated miRNAs was performed and data are presented as 2-ΔΔCT-normalised means ± SD (n=3 biological replicates). The control hairpin values were transformed to 1 and the values of the miR-25 and miR-30c inhibitors were normalised to this.

B) CrizR1 cells were transfected with non-targeting hairpin inhibitor, miR-25 hairpin and miR-30c hairpin for 72h. Then, cells were fixed and stained with PI. The cells were analysed by flow cytometry for DNA content and cell cycle phase. Data points are presented as means ± SD (n=3 biological replicates).

C) As in B), subG0 cells were quantified for cell death in the presence or absence of 1μM crizotinib. P values were calculated by two-tailed student's t-test (*p < 0.05, **p<0.01, ***p<0.001).

5.2.2.2 Analysis of potential transcription factors regulating miR-149, miR-25 and miR-30c

To identify whether the changes in miRNA expression levels are a result of regulation at the transcriptional level, the publicly available database JASPAR was used [289]. The promoters of miR-25, miR-30c and miR-149 all shared motifs that could be recognised by the transcription factors NF-κB, C-FOS and STAT5A. Then, siRNA oligos were used to knock down NF-κB (**Figure 49A**), C-FOS (**Figure 49B**) and STAT5A (**Figure 49C**) but no robust changes in miRNA levels were detected by qPCR. It was thus concluded that these miRNAs are not subject to regulation by these transcription factors.

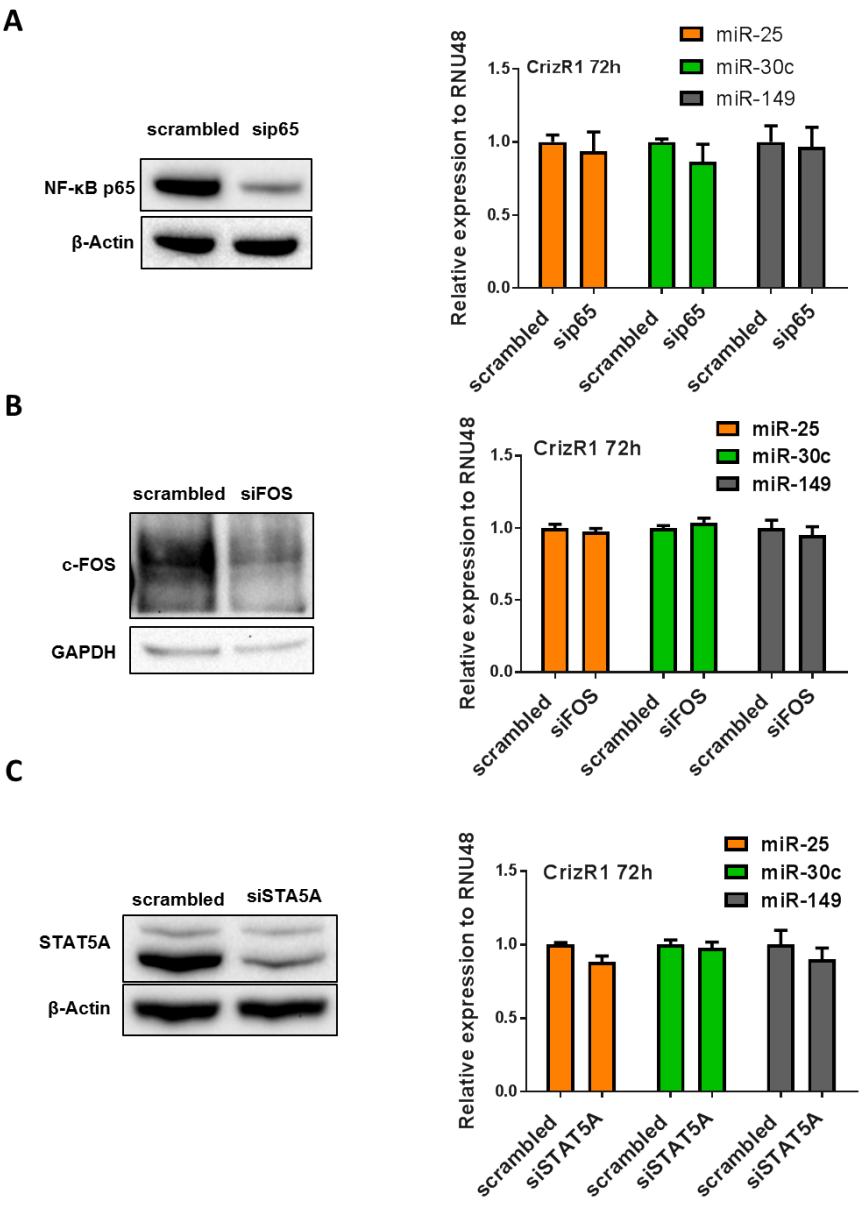

Figure 49: Analysis of transcription factor interactions with validated miRNAs

- **A)** CrizR1 cells were transfected with scrambled oligo or sip65. After 72h, protein and RNA were extracted. Protein extracts were analysed for the indicated proteins (left, n=2 independent experiments), while RNA was analysed via RT-qPCR for miR-25, miR-30c and miR-149 (n=3 biological replicates). The scrambled control values for each experiment were transformed to 1 and the values of the other treatment conditions were normalised to this.
- **B)** As in A), siRNA for C-FOS.
- **C)** As in A), siRNA for STAT5A.

5.2.2.3 Binding prediction analysis for potential targets of miR-25, miR-30c and miR-149

Given the prominent dysregulation of cell cycle-related genes in the previous chapter, I decided to investigate whether the increased levels of these genes were due to a loss of regulation by miRNAs. Then, 3′ UTR prediction analysis for the identified miRNAs was performed using a cell cycle gene set as input for potential targets. Regarding the up-regulated miRNAs, the CDKN1A gene (p21) was identified as a potential target of miR-25, while no other cell cycle-related genes were identified as potential targets of miR-30c. Accordingly, miR-25 inhibition in CrizR1 cells resulted in an upregulation of p21 (**Figure 50A**), which may account for the cell cycle arrest observed in (**Figure 48B**). However, after careful analysis of the 3′ UTR (data not shown), a strong binding site for miR-25 was not identified and the interaction was concluded to be indirect.

Regarding the down-regulated miRNAs, bioinformatics analysis identified 2x and 1x potential binding sites for miR-103 and miR-149 in the *CDK6* 3′ UTR respectively and one binding site for miR-103 in the *CCNE1* 3′ UTR. Furthermore, the *CDK6* 3′UTR contains 1x binding site for miR-345 and miR-3065. Functional studies were then performed, initially with miR-149. Overexpression of miR-149 in the CrizR1, CrizR4 and CrizR5 cells resulted in a downregulation of CDK6 (**Figure 50B**). Except for *CDK6*, *CDK1* also has a binding site for miR-3065 in its 3′ UTR. However, after overexpressing miR-345 (**Figure 51A**) and miR-3065 (**Figure 51B**) no downregulation of CDK6 or CDK1 was observed. On the contrary, overexpression of miR-103 potently down-regulated CDK6 at the protein level (**Figure 51C**).

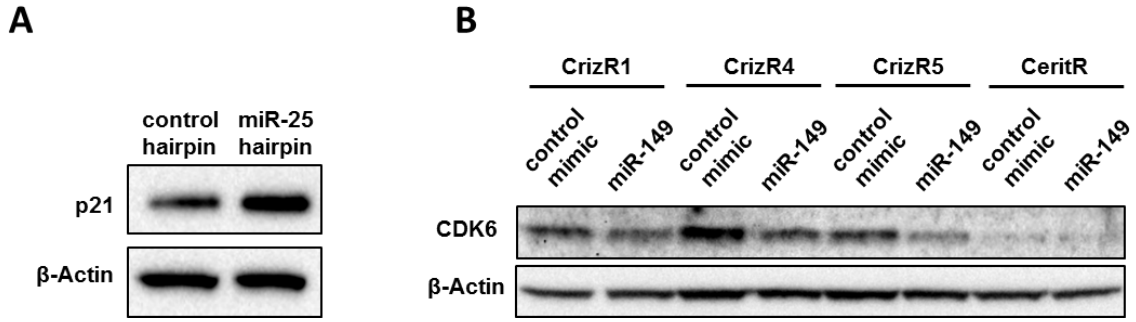

Figure 50: P21 is an indirect target of miR-25 and CDK6 of miR-149

- **A)** CrizR1 cells were transfected with control or miR-25 hairpin inhibitor for 72h. Then, protein extracts were analysed for the indicated proteins. Shown is a representative blot from 2 independent experiments.
- **B)** As in A), the indicated cell lines were transfected with miR-149 mimic. While CrizR1, CrizR4 and CrizR5 cells have high expression levels compared with the H3122 parental as shown in **4.3.4**, transfection of miR-149 reduces such expression.

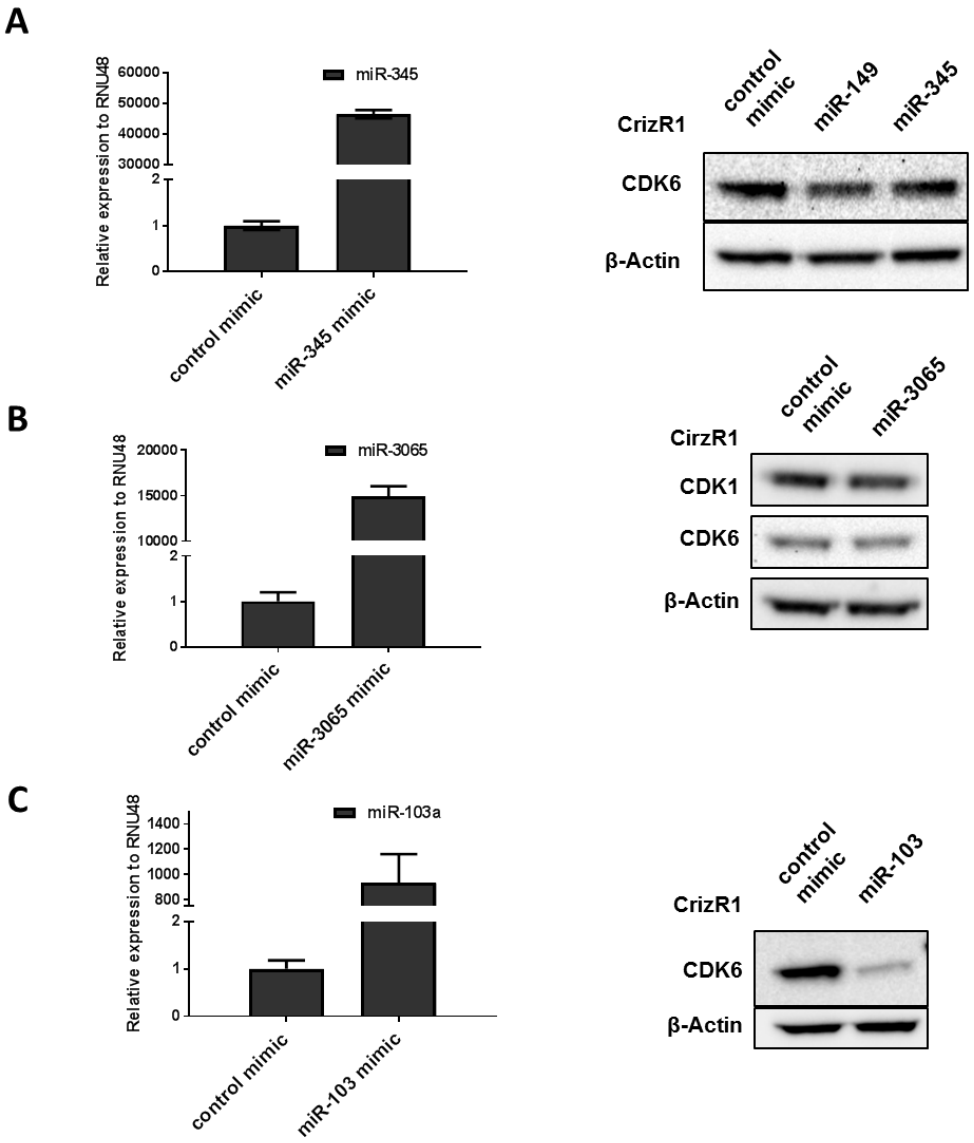

Figure 51: CDK6 is a target of miR-103 but not of miR-345 or miR-3065

A) CrizR1 cells were transfected with control or miR-345 mimic for 72h and then protein and RNA was extracted. RT-qPCR analysis for miR-345 presented as 2-ΔΔCT normalised means ± SD (left, n =2 biological replicates). On the right side, protein extracts were analysed for the indicated proteins (miR-149 as positive control). Shown is a representative blot of 2 independent experiments.

B) As in A), cells were transfected with miR-3065 mimic.

C) As in A), cells were transfected with miR-103 mimic.

To determine if *CDK6* or *CCNE1* were direct targets of these miRNAs, their 3' UTRs (**Figure 52A**) were cloned in a luciferase reporter vector. Co-transfection of the CDK6 3' UTR with miR-149 and CCNE1 3' UTR with miR-103 did not result in decreased luminescence (**Figure 52B**) suggesting that the interaction is indirect. However, co-transfection of miR-103 revealed a decrease in luminescence for the CDK6 3' UTR, suggesting that CKD6 is a direct target (**Figure 52C**). Upon mutating the 2 different miR-103 binding sites in the CDK6 3' UTR it became apparent that the 1st binding site is the main mediator of the interaction, as its mutation partially restored luminescence.

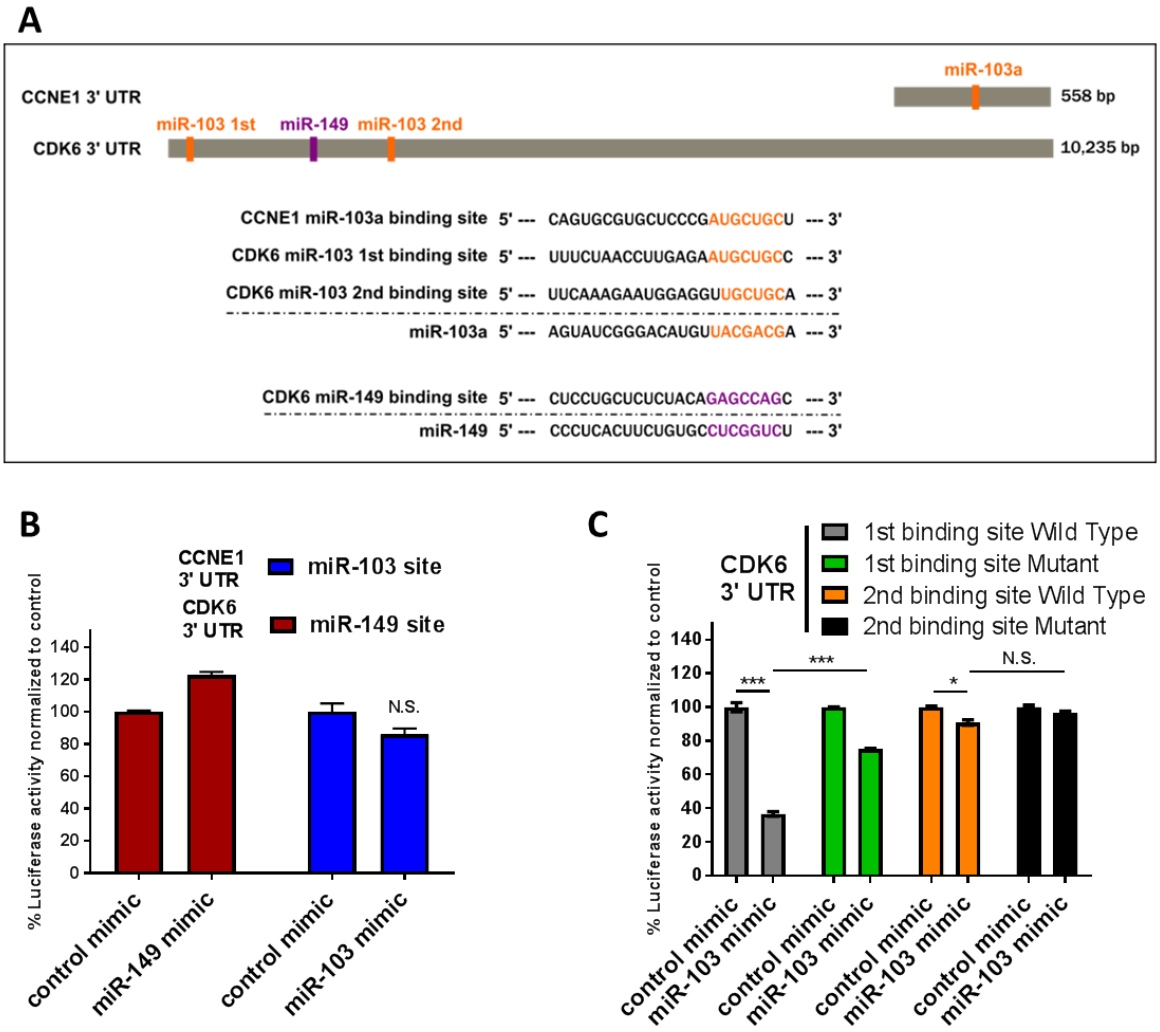

Figure 52: CDK6 is a direct target of miR-103

A) Schematic representation of the CDK6 and CCNE1 3' UTRs with the corresponding miRNA binding sites.

B) HEK293T cells were transfected with pGL3 control 3' UTR CDK6 and CCNE1 plasmid (WT for the miR-103/149 predicted binding sites) and co-transfected with control, miR-103 and miR-149 mimic. 24h post-transfection, luminescence was recorded and normalised according to the Firefly: Renilla ratio.

C) HEK293T cells were transfected with pGL3 control 3' UTR CDK6 plasmid (WT/MUT for the miR-103 predicted binding sites) and co-transfected with control or miR-103. 24h post-transfection, luminescence was recorded and normalised according to the Firefly: Renilla ratio.
Data are presented as normalised means ± SD (n=3 biological replicates) and p values were calculated by a two-tailed student's t test (*p < 0.05, **p<0.01, ***p<0.001).

5.2.2.4 MiRNAs in response to CDK inhibition

In the previous chapter, a potent downregulation of oncogenic transcripts was identified in response to CDK inhibition. I asked whether oncogenic miRNAs are similarly affected by the same drug treatment. Treatment of CrizR1 cells with alvocidib for 6h or 24h resulted in the downregulation of miR-25 and miR-30c, to levels comparable to those of the H3122 parental cells (**Figure 53**). These data, taken together with the previous chapter, suggest a transcriptional sensitivity of EML4-ALK cells that is also evident through, among other oncogenic transcripts, a miRNA dysregulation.

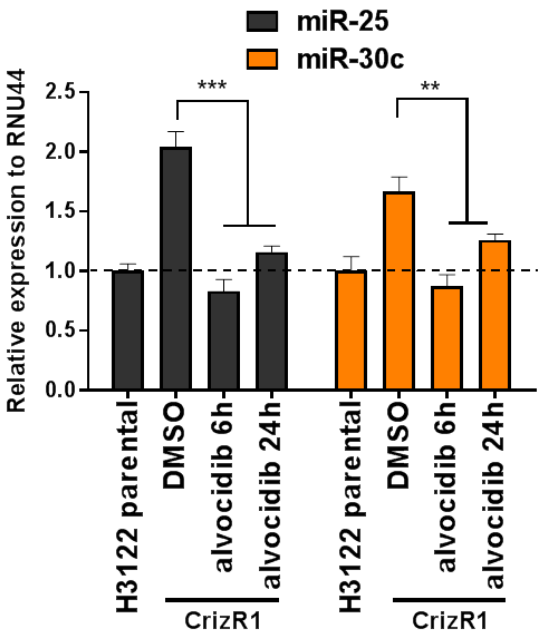

Figure 53: MiR-25 and miR-30c are down-regulated upon CDK inhibition

H3122 and CrizR1 cells were treated with the indicated compounds for 6 or 24h and then RNA was extracted and subjected to RT-qPCR analysis for miR-25 and miR-30c, presented as 2-ΔΔCT normalised means ± SD (n =3 biological replicates). The H3122 parental values were transformed to 1 and the values of the drug-resistant cell lines treated with DMSO or alvocidib were normalised to this. While miR-25 and miR-30c were overexpressed in CrizR1 cells, alvocidib treatment restores their expression to the H3122 parental levels. P values were calculated by a two-tailed student's t-test (*p < 0.05, **p<0.01, ***p<0.001).

5.2.2.5 MiRNA expression levels in patient samples refractory to ALK inhibitors

While experimental data were obtained from EML4-ALK^{mut} cell lines, it is not necessary that the same findings should apply to patients who developed resistance to ALK inhibitors in the clinic. Unfortunately, it was not feasible to obtain matched core biopsies. MiRNAs are inherently stable in the plasma, thus in collaboration with Professor Fiona Blackhall, we obtained plasma samples from 8 ALK^{+} NSCLC patients, 1 EGFR^{+} NSCLC patient and 2 NSCLC patients with an unidentified driver mutation. Samples were obtained at baseline, and upon progression on one or more ALK inhibitors. Then, the expression of these miRNAs in the plasma was analysed by RT-qPCR for miR-25 and miR-30c. Setting a threshold of 2-fold upregulation compared to baseline, it was evident that 5 patients had increased levels of miR-25 or miR-30c on progression with various ALK inhibitors (**Figure 54**). Furthermore, control patient 2, upon acquired resistance to gefitinib treatment, also had elevated levels of miR-30c in the plasma sample, which is in line with previous findings [258]. These data confirm the existence of the studied miRNA dysregulation *in vivo*. Given the heterogeneity in the mechanisms of resistance, it is not surprising that such upregulation is detected only in a subset of patients.

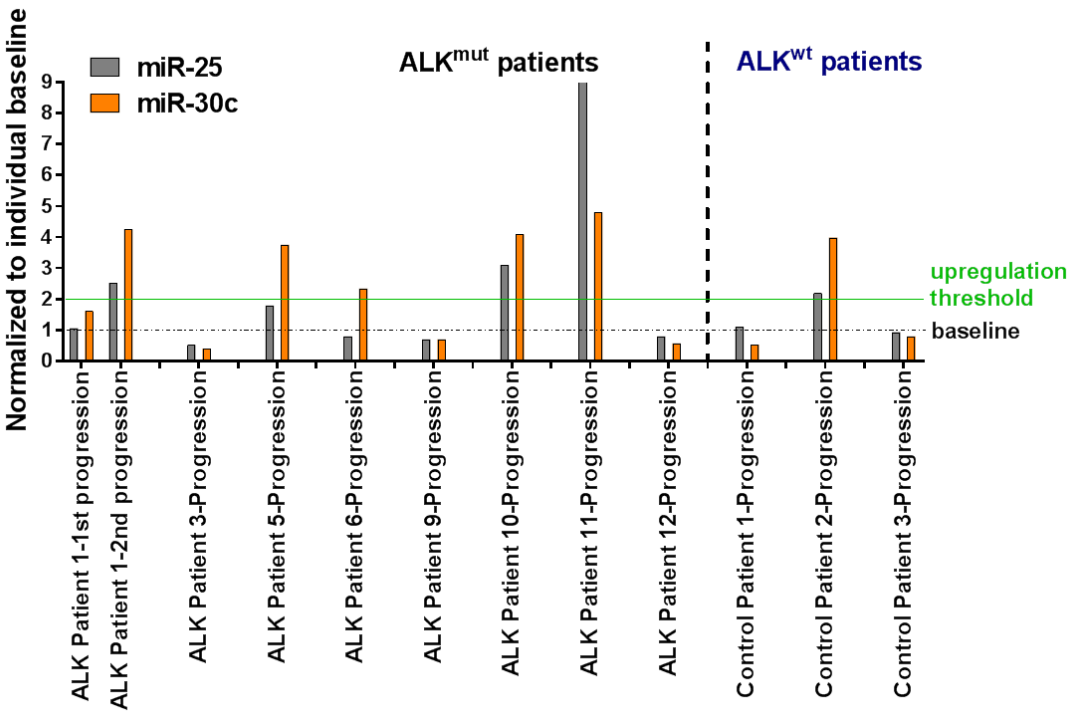

Figure 54: MiR-25 and miR-30c are repeatedly dysregulated in the plasma of patients upon progression on TKIs

Patient plasma was separated in 3 aliquots. After performing 3 different RNA extractions with the addition of miRNA spike-in, RT-qPCR for miR-25 and miR-30c was performed. Graphs represent the mean of the 3 independent RNA extractions followed by RT-qPCR normalised to the individual baseline sample.

5.2.3 LncRNAs as a mechanism of resistance

5.2.3.1 Identification and validation of dysregulated lncRNAs

The unexplored landscape of lncRNAs in EML4-ALK lung cancer led us to interrogate the dataset that was obtained from total RNA-seq of H3122 parental versus CrizR1 cells for dysregulated lncRNAs. It was found that 171 lncRNAs change their expression levels in crizotinib resistance (**Figure 55A**). This list was narrowed down by asking which lncRNAs are also dysregulated after crizotinib treatment, and could, therefore, be downstream of ALK signalling. This way, the switch from ALK-dependence to another oncogene-dependence in CrizR1 cells may have restored or suppressed the expression levels of these lncRNAs in resistant cells. In the data set of crizotinib-naïve STE-1 cells treated with vehicle control versus treated with crizotinib, 143 lncRNAs were found to be dysregulated after crizotinib treatment (**Figure 55A**). Looking at the overlap between these 2 data sets, 12 lncRNAs were common (**Figure 55B**). I decided to validate these candidates and see if their expression levels by RT-qPCR reflect the expression levels by NGS.

To this end, RT-qPCR primers were designed in exonic regions visualised through the UCSC Genome Browser, validated for specificity (data not shown), and RNA from H3122 and CrizR1 cells was used as input. It became evident that 8/12 lncRNAs were robustly dysregulated in independent experiments (**Figure 55C**) and should be subsequently investigated. Only one lncRNA, LINC00704 was up-regulated in CrizR1 cells, while the other 7 lncRNAs were suppressed in CrizR1 cells. Interestingly, LINC00704 was the only lncRNA at the time of writing that has been studied in the literature [290]. The next step was to ask whether these lncRNAs have a functional role in crizotinib resistance.

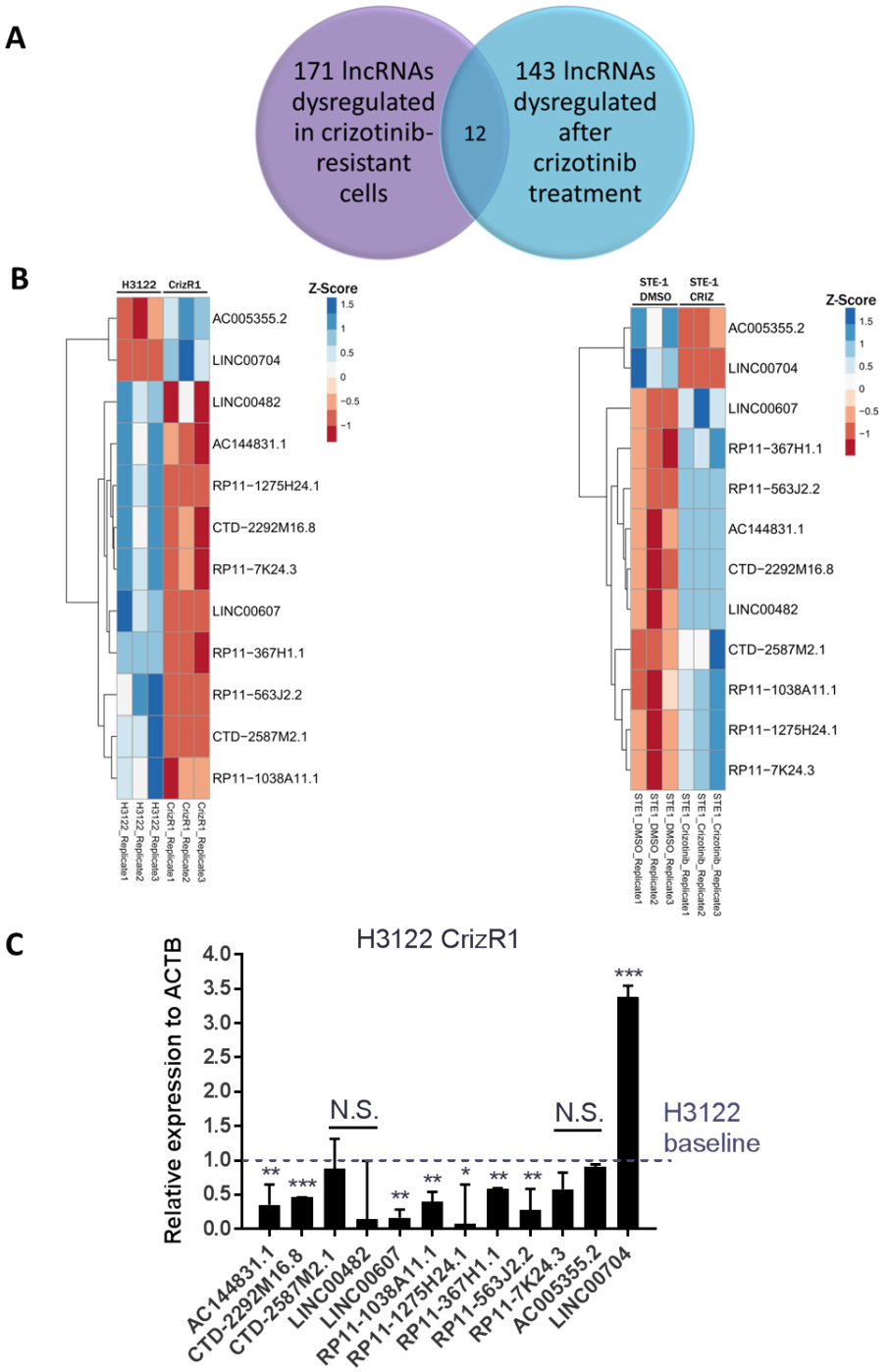

Figure 55: A subset of lncRNAs may be involved in the resistance to crizotinib

A) RNA-seq data were analysed from previously described sequencing experiments. to identify lncRNAs that are significantly dysregulated after ALK inhibition in STE-1 parental cells and lncRNA significantly dysregulated in crizotinib-resistant cells compared with H3122 parental. Pie chart representing the common lncRNAs that are dysregulated upon crizotinib treatment in STE-1 parental cells, but also in crizotinib-resistant cells. This overlap narrows down to lncRNAs downstream of EML4-ALK signalling, that may also functionally affect the resistance to ALK inhibition.

B) Heatmaps representing the expression levels of the indicated lncRNAs in CrizR1 vs H3122 parental (left) or STE-1 treated with crizotinib versus vehicle control (right).

C) H3122 and CrizR1 cells were RNA-extracted. Custom primers were designed for the indicated lncRNAs and used in an RT-qPCR assay to determine the lncRNA expression levels. Data are presented as 2-ΔΔCT normalised (using the H3122 parental expression levels as baseline transformed to 1) means ± SD (n = 3 biological replicates). P values were calculated with a two-tailed student's t-test (*p < 0.05, **p<0.01, ***p<0.001).

5.2.3.2 Knockdown experiments of chosen lncRNAs

Investigating the only up-regulated lncRNA that was shortlisted, LINC00704, I asked whether it is also up-regulated in the rest of these cell lines resistant to ALK inhibitors. Then, an upregulation of MANCR (LINC00704) was detected in CrizR1, CrizR5 and CeritR cells (**Figure 56A**). I decided to knock down this lncRNA with custom-designed Gapmers [291] and 2 Gapmers were designed, targeting 2 different exons. After transfecting these Gapmers in CrizR1 cells, Gapmer #2 led to a robust knockdown of LINC00704, at 24 or 48h, as detected by RT-qPCR (**Figure 56B**). It was hypothesised that knockdown of LINC00704 in combination with crizotinib treatment would re-sensitise CrizR1 cells to crizotinib. However, after Annexin V/PI staining and flow cytometry analysis there was no difference in cell death or apoptosis with this combination (**Figure 56C**). Therefore this hypothesis was rejected and it was concluded that the LINC00704 dysregulation does not reflect a functional role in these cells.

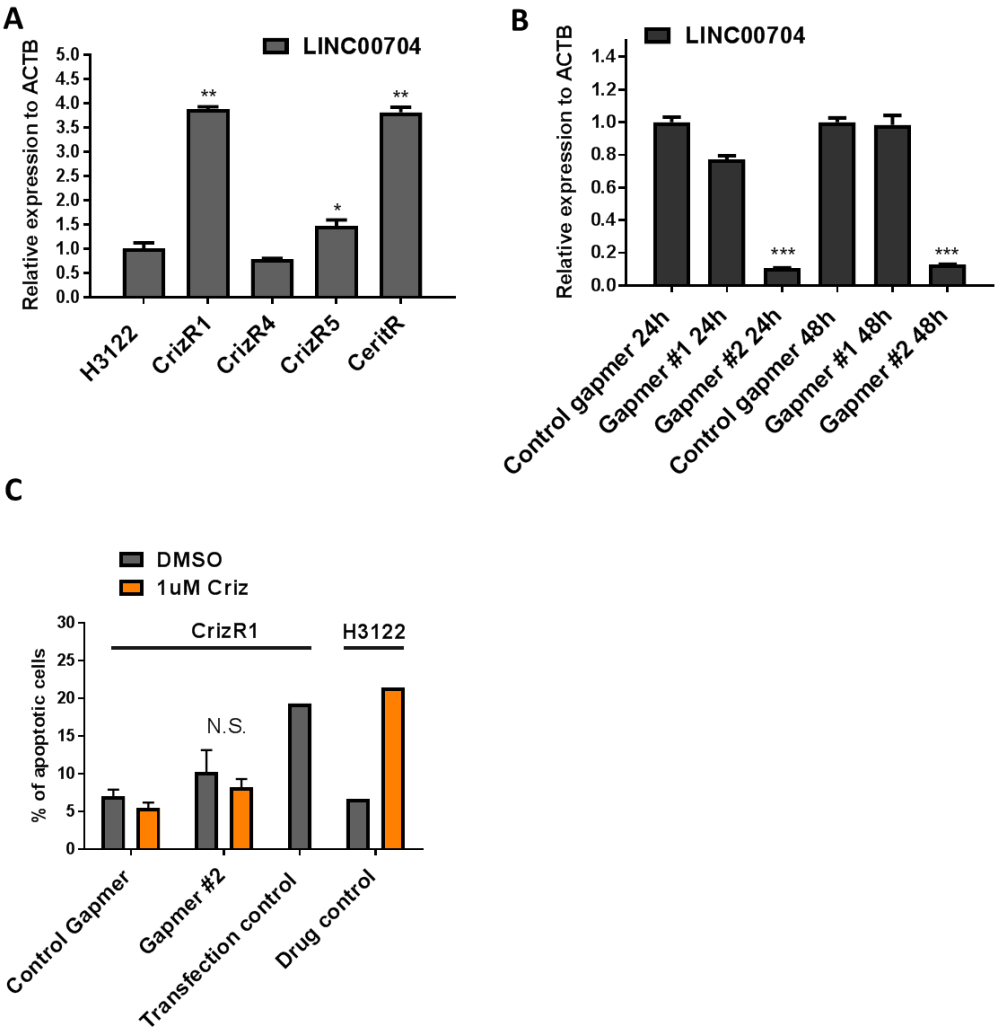

Figure 56: MANCR is not functional in CrizR1 cells

A) RNA from the indicated cell lines was extracted. The expression levels of LINC00704 were analysed by RT-qPCR. Data are presented as 2-ΔΔCT normalised (to ACTB) means ± SD (n = 3 biological replicates).

B) CrizR1 cells were transfected with non-targeting Gapmer control / Gapmer #1 / Gapmer #2 for 24h or 48h. Then, RNA was extracted and the expression levels of LINC00704 were analysed by RT-qPCR. Data are presented as 2-ΔΔCT normalised (to ACTB) means ± SD (n = 3 biological replicates).

C) CrizR1 cells were transfected with Gapmer control and Gapmer #2 for 48h, in the presence or absence of 1 µM crizotinib. Then, apoptosis was assessed by an Annexin V/PI assay and flow cytometry. H3122 cells were used in parallel as crizotinib control. SiPLK1 was used as a positive transfection control (apoptosis-inducing). Data points are presented as normalised means ± SD (n=3 biological replicates for Gapmers, n =1 for controls).
P values were calculated with a two-tailed student's t test (*p < 0.05, **p<0.01, ***p<0.001).

5.2.3.3 Overexpression experiments of down-regulated lncRNAs

To study the 7 down-regulated lncRNAs, I decided to clone and overexpress them in CrizR1 cells, investigating a possible tumour-suppressing role. However, 3/7 are tens of thousands of base pairs long and thus not feasible to be cloned in an expression vector, so only 4/7 lncRNAs were taken forward. Their downregulation was tested in the rest of the cell lines resistant to ALK inhibitors and lncRNA CTD-2292M16.8 was excluded from further analysis, as it was only lost in CrizR1 cells but not the other clones (**Figure 57A**). The 3 remaining lncRNAs were then cloned in a pCDH-CMV-MCS-EF1-copGFP vector. The RP11-367H1.1 (**Figure 57B**), AC144831.1 and RP11-1275H24.1 (**Figure 57C**) lncRNAs were successfully cloned and overexpressed in CrizR1 cells. However, after a proliferation assay, it became apparent that restoration of these lncRNAs had no effect on the proliferation of crizotinib-resistant cells, with- or without crizotinib (**Figure 57D**). A potential role for these lncRNAs in the resistance to ALK inhibitors was therefore rejected.

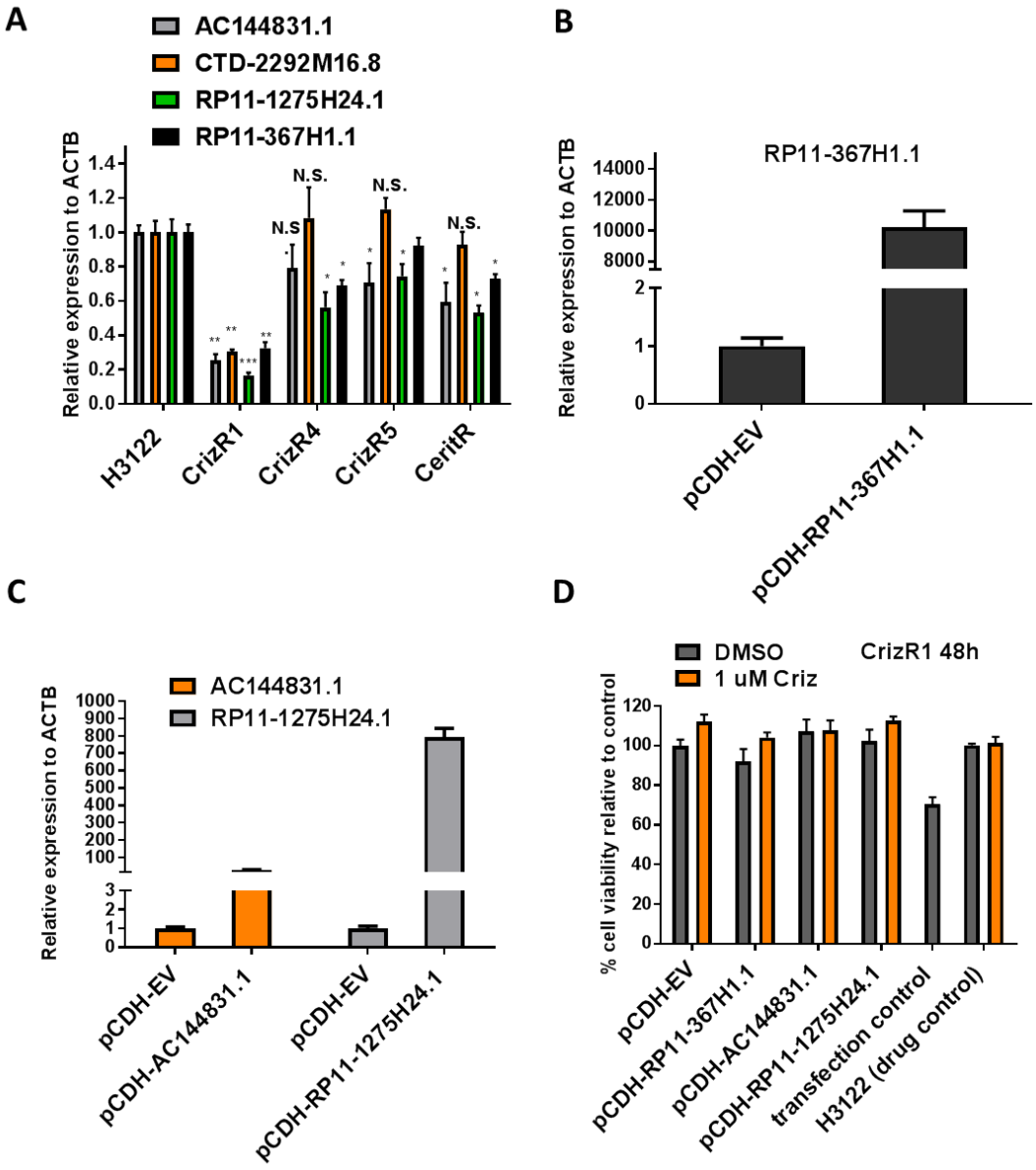

Figure 57: Overexpression of selected lncRNAs does not restore sensitivity to crizotinib

A) RNA from the indicated cell lines was extracted. The expression levels of the indicated lncRNAs were analysed by RT-qPCR. Data are presented as 2-ΔΔCT normalised (to ACTB) means ± SD (n = 3 biological replicates).

B) CrizR1 cells were transfected with pCDH empty vector (EV) or pCDH containing the indicated lncRNA inserts. 48h post-transfection, RNA was extracted. The expression levels of the indicated lncRNAs were analysed by RT-qPCR. Data are presented as 2-ΔΔCT normalised (to ACTB) means ± SD (n = 2 biological replicates).

C) As in A). CrizR1 cells were transfected with pCDH empty vector (EV) or pCDH containing the indicated lncRNA inserts, in the presence or absence of 1μM crizotinib. Then, cell proliferation was assessed by the MTS proliferation assay. H3122 cells were used in parallel as crizotinib control. SiPLK1 was used as a positive transfection control (apoptosis-inducing). Data points are presented as normalised means ± SD (n=2 biological replicates). P values were calculated with a two-tailed student's t-test (*p < 0.05, **p<0.01, ***p<0.001).

5.3 Discussion

5.3.1 Oncogene-driven miRNA regulation

A recurrent theme in oncogene-driven cancers is the downstream engagement of miRNAs in signalling. Oncogenic miRNAs that potentiate the oncogene's action are often directly controlled by it. In cases where tumour-suppressing miRNAs antagonise the oncogene's action, they are often repressed by it. We have previously reviewed the relationship between some of the most common oncogenes and miRNAs in [292]. The discovery of signalling downstream of driver oncogenes benefits our understanding of the malignant transformation process. For example, very frequently, changes in response to RTK inhibition feedback negatively and are the cause of acquired resistance [113,114]. It is therefore reasonable that the discovery of such feedback signalling can be used to create combinational inhibition strategies to restrict tumour adaptation.

5.3.1.1 Signalling changes upon oncogene interruption

The mechanisms of cell death in response to oncogene inhibition are incompletely understood and knowledge in this area can offer new rational drug combinations. It is known that in response to oncogene inhibition with gefitinib or crizotinib in lung cancer, the result is a combination of cell cycle arrest [53,293] and apoptotic induction [166]. While it can be presumed that the deprivation of growth/proliferative signalling triggers this response, the exact process remains unknown. Recently, loss of CDK2 upon ALK inhibition has been shown to occur due to enhancer remodelling and loss of H3K27 acetylation in the proximal promoter [198].

Except for constitutively active proliferative signalling, oncogenes also tend to suppress pro-apoptotic pathways. For example, cell death after crizotinib treatment is a combination of BIM induction caused by repression of ERK and a loss of STAT3-induced expression of the anti-apoptotic protein Survivin [38]. The functional role of these is evident in studies such as [178], where low levels of the pro-apoptotic protein BIM are enough to cause a poor response to EGFR inhibition. Expanding these findings, we and others have observed that the H2228 cell line, which carries the EML4-ALK 3a/b variant, is much more resistant to ALK inhibition compared to the variant 1-carrying cell lines H3122 and STE-1 [37,294]. A reason for this differential drug sensitivity may be that even though ALK phosphorylation is inhibited in H2228, these cells do not up-regulate BIM or induce apoptosis (evidenced by lack of PARP cleavage) like the H3122 [59].

5.3.1.2 MiRNAs downstream of oncogene-driven cancers

The relationship between ALK-driven cancers and miRNAs has been investigated before, albeit in different contexts. Firstly, in patient samples, a subset of miRNAs were able to distinguish EML4-ALK lung cancer from EGFR- and KRAS- mutant patients [267]. Interestingly, there is an overlap between these dysregulated miRNAs, rendering the common miR-1253, miR-504 and miR-26a-5p indicators of an oncogene mutation.

Furthermore, in ALK+ Anaplastic Large Cell Lymphoma (ALCL), 14 miRNAs were commonly regulated by an ALK knockdown as well as STAT3 knockdown, identifying the miRNAs that are downstream of the ALK-STAT3 signalling node. The miR-17-92 cluster was a prominent hit in this

assay and was demonstrated to have a functional role in mediating ALCL cell proliferation [286]. Thereafter, I aimed to characterise the signalling changes that involve miRNAs upon ALK inhibition. A combination of RNA-seq in STE-1 cells and miRNA-seq in H3122 cells produced an overlap of genes that could be downregulated in response to miRNA upregulation and vice versa, which I explored further. However, a clear limitation is that the use of 2 different cell lines introduced heterogeneity and limited the pool of potential targets that could be investigated. Still, the findings described in this thesis recapitulate the literature since a marked dysregulation of the miRnome was detected in response to ALK inhibition. Hypothesising that some of these miRNAs should be downstream of ALK signalling, the miR-17-92 cluster was then validated as a downstream effector of ALK activity.

5.3.1.3 Regulation of BIM by the miR-17-92 cluster

In EML4-ALK^{mut} cells, there is a modest targeting of BIM by miR-19b. It can be reasoned that there are several miRNAs whose combined loss results in the upregulation of BIM and which were not detected. Therefore the loss of miR-19b is partially responsible for the upregulation of BIM and the induction of apoptosis. It can be deduced then that BIM downregulation after crizotinib treatment should rescue the induction of apoptosis, at least in part, and this has been confirmed before [38]. It is thus possible that a compound which would result in the overexpression of BIM in combination with crizotinib may lead to more potent initial responses. In fact, this has been recently demonstrated in EGFR-mutant lung cancer, where a combination of a BIM-mimetic with erlotinib, overcame the deletion of BIM as a resistance mechanism [74]. Future experiments will investigate whether the miR-17-92 cluster is necessary for the oncogenicity of EML4-ALK and whether other miRNAs are responsible for targeting BIM.

5.3.1.4 EML4-ALK-STAT3 signalling

The JAK-STAT3 pathway has been ubiquitously shown to be a major component of ALK signalling. However, its importance for cell proliferation has been debated in the literature. In a study of genetic activation of STAT3 [37], it modestly protected H3122 cells from crizotinib-induced cell death. However, in earlier work, pharmacological inhibition of STAT3 did not affect H3122 cell proliferation [54], rendering the evidence for the STAT3 importance inconclusive. In EML4-ALK^{mut} cells, STAT3 knockdown with siRNA had no effect on cell proliferation. My hypothesis that the loss of STA3 phosphorylation is due to a negative interactor of STAT3 was incorrect since STAT3 was shown directly to form a complex with ALK [295]. Thus ALK directly phosphorylates STAT3 and this interaction is abrogated by crizotinib. Then, PIAS3 was confirmed as a direct target of miR-18a in EML4-ALK^{mut} cells, however, this interaction in response to ALK inhibition is probably biologically inconsequential in terms of STAT3 regulation. It cannot be excluded that in physiological conditions, the ALK-STAT3 axis up-regulates the miR-17-92 cluster in order to suppress negative interactors of STAT3, such as PIAS3.

5.3.2 Findings of miRNAs affecting drug resistance

Relevant findings regarding miRNAs and the resistance to targeted therapies mainly come from different types of cancer since at the beginning of my thesis this had not been studied in EML4-ALK NSCLC. Later, however, a report examined crizotinib- and ceritinib-resistant cells and identified a loss of miR-34a and miR-449a through enhancer remodelling, which contributes to AXL upregulation and drug resistance [198]. These findings were recapitulated in samples from patients who acquired resistance to ceritinib or crizotinib in the clinic.

In data obtained from crizotinib-resistant cells after a global miRNA profiling, a striking loss of miR-205 was observed in these cells which exhibited the most mesenchymal-like characteristics. Previously in the literature, miR-205 downregulation was shown to be an early event upon the malignant transformation of lung epithelial cells, which allows EMT as well as stem cell-related properties [296]. While in these cells restoring miR-205 did not functionally affect the resistance to crizotinib, it is tempting to posit that the striking AXL-induced EMT characteristics are in part mediated by miR-205 and future experiments could examine the impact of the re-introduction of miR-205 on *SNAI2* and *Vimentin*. Also, the expression levels of miR-205 in other drug-resistant cell lines were not examined and I intend to perform these experiments in the future.

5.3.2.1 Tumour-promoting miRNAs

In the small-RNA sequencing data, some of the miRNAs were expressed at a very low level, which makes them unlikely to be functional candidates as mediators of resistance. Several of these miRNAs turned out to be by-products of dysregulated signalling, while others showed a functional role, with the capacity to affect the response to crizotinib. Specifically, the inhibition of miR-25/30c could partially re-sensitise cells to crizotinib. The literature is supportive of these findings, as explained below.

MiR-25 arises from the miR-106b~25 polycistron, along with miR-93 and miR-106b. These clustered miRNAs would be expected to be concomitantly regulated, but this was not the case. While upregulation of miR-25 was detected in crizotinib-resistant cells, the levels of miR-106b did not change. A similar phenomenon has been observed before [233], where miR-106b and miR-25 were up-regulated after hypoxia in MCF-7 cells but miR-93 was not, highlighting once more the potential for differential regulation of clustered miRNAs. In gastric cancer, this polycistron was shown to affect the proliferation of cells *in vitro* and *in vivo.* MiR-93 and miR-106b targeted p21, while miR-25 targeted BIM [297]. In prostate cancer, the miR-106b~25 cluster can cooperate with its host gene MCM7 in the transformation of cells, by targeting PTEN [298]. In a drug-treatment context, doxorubicin-induced senescence in breast cancer can be overcome by upregulation of the miR-106b~25 cluster. Specifically, all three clustered miRNAs can cause drug resistance by targeting the regulator of E-Cadherin, EP300 [299].

MiR-30c has been implicated in the resistance to gefitinib in EGFR-mutant lung cancer [258] by targeting BIM. Given the similarities with EML4-ALK^{MUT} cancer, this is not surprising. In the same dataset, miR-103 was shown to be tumour-suppressing in NSCLC by targeting PKC-ε. Uncovering the biological mechanism of the increased expression of miR-25 and miR-30c was not possible.

Even though transcription factor binding analysis showed several potential transcription factors, functional experiments did not conclusively show an upregulation through increased transcription factor activity. Future experiments looking at the methylation profile of these promoters could help clarify whether this is an epigenetic phenomenon.

Lastly, the described findings were not a cell culture artefact, as it was possible to detect elevated levels of circulating-free miR-25 and miR-30c in plasma samples of ALK^{MUT} patients upon progression on ALK inhibitors. Also, in one patient treated with gefitinib, there were increased levels of circulating miR-30c, which supports a previous study [258]. This analysis was retrospective, from archived samples, therefore to estimate the clinical usefulness of these miRNAs, a prospective analysis would be needed.

5.3.2.2 Tumour-suppressing miRNAs

MiR-149 is a known tumour-suppressing miRNA. It has been reported to act by targeting ZBTB2 in order to suppress the proliferation of gastric cancer cells [300] and by targeting GIT1 to prevent metastasis in breast cancer [301]. In NSCLC, to my knowledge, there are no data of high confidence that prove a tumour suppressing role for this miRNA. It was shown in the previous 'Results' section that the downregulation of miR-149 in CrizR1 is functional as re-introduction of this miRNA induces apoptosis in these cells. No direct targets for this miRNA were identified, and it would be useful to elucidate this in the future, possibly by a combination of miR-149 overexpression and RNA-seq. Furthermore, its mechanism of downregulation was not examined in this context. However, a previous report in breast cancer suggested that the miR-149 is prone to CpG island-methylation proximal to its promoter, which may also account for its downregulation in CrizR1 cells [302].

MiR-103 is known to be a tumour-suppressing miRNA in NSCLC, examined in a gefitinib-resistance context [258]. It can also greatly affect metastatic breast cancer cells by targeting Dicer [303]. As examined in the previous chapter in crizotinib-resistant cells CDK6 was amplified. The presented data point to a novel regulation of CDK6 by miRNAs. MiR-149 indirectly targets CDK6 and its restoration has a suppressive role in CrizR1 cells, whereas miR-103 targets CDK6 directly but is not relevant to cell viability. Other miRNAs that were investigated were not involved with the modulation of cell cycle genes.

5.3.2.3 MiRNAs acting in unity

While the mechanism through which these miRNAs are dysregulated was not uncovered, it can be speculated that a genomic event which results in aberrant transcriptional output could be the reason. As mentioned earlier, enhancer remodelling has been shown to promote the dysregulation of several miRNAs in this context [198]. While in other drug-resistant contexts, a single miRNA can be the sole driver of resistance, this was not the case in the drug-resistant cell lines, or if it was, it was not detected with the methods used. Driven by the effectiveness of cell-cycle inhibitors in crizotinib-resistant cells, it is tempting to speculate that a collective loss/downregulation of cell-cycle targeting miRNAs is what allows the amplification of cyclins and cyclin-dependent kinases. This was further augmented by the large overlap observed between miRNAs down-regulated in

CrizR1 cells and miRNAs that potentially target CDK1, CDK6, CCNB1 and CCNE1. However, only a pooled miRNA overexpression screen would give the answer to this hypothesis. In a recent paper [304], a large cohort of CDK-targeting miRNAs was identified, and this could be used to guide a selection of miRNAs whose expression would be restored in CrizR1 cells.

5.3.3 Long non-coding RNAs

LncRNAs mediating resistance to targeted therapies have been identified before, as was the case for the MIR100HG lncRNA (which acts by regulating miR-100 and miR-125b), whose upregulation is a cause of resistance to cetuximab in squamous cells carcinomas [279]. In the presented data set, lncRNAs with the potential to affect resistance to ALK inhibitors were chosen on the basis of their dysregulation in crizotinib-resistant cells. Some of them were not robustly dysregulated, suggesting a temporary nature of changes in their expression. Nevertheless, the majority of them were robustly down-regulated in CrizR1 cells. Since functional experiments with the identified lncRNAs did not show differences in cell proliferation and lead to the conclusion that these lncRNAs were not responsible for the resistance to ALK inhibition. It is still likely that lncRNAs which were not studied in this thesis play a role in terms of ALKi sensitivity and that is a clear limitation of this approach. The differential expression data from *in vitro* experiments should be confirmed in samples from patients with EML4-ALK-driven lung cancer. However, while trying to utilise a publicly available dataset from crizotinib-naïve and crizotinib-resistant patients there was a significant challenge. This cohort did not have matched patients, but rather a mix of samples from different patients, which resulted in significant heterogeneity in the expression of all RNA transcripts [1, kindly analysed by Dr Sudhakar Sahoo]. Therefore it could not be conclusively assessed whether the differentially expressed lncRNAs did appear in the clinical setting.

5.3.3.1 Translational aspects of lncRNA findings

While mechanistically, the involvement of lncRNAs in the resistance to oncogene inhibitors can be of immense interest, biomarker-based applications are closer to routine clinical use at the moment. From a biomarker point of view, lncRNA detection requires sophisticated equipment as well as highly trained personnel. Thus, global detection of lncRNA alterations would be inefficient in the clinical setting as it requires high-depth RNA sequencing. However, a few lncRNAs the dysregulation of which would be detected in a high enough number of patients who are refractory to ALK inhibitors could lead to the development of a diagnostic kit, likely PCR-based. High frequency of a particular permutation is a prerequisite to justify the screening of patients.

From a therapeutic point of view, clinically meaningful *in vivo* modulation of lncRNAs has not been achieved to date even though several products are under development. For oncogenic lncRNAs, anti-sense RNA technologies promise efficient knockdown of any RNA, but their preferential localisation to the liver and the elicitation of immune responses has limited their use to date [305]. The field is in dire need of a formulation that will allow the efficient packaging of RNA oligonucleotides and will guarantee their delivery to the desired tissue and ideally, desired cell population. The existence of lncRNAs who are primarily nuclear, complicates their modulation, as knockdown of nuclear RNA has traditionally been much more challenging.

For tumour-suppressing lncRNAs, the technologies to reverse their loss also exist. Frequent delivery of synthetic lncRNAs is not the optimal approach for a lot of lncRNAs as their size is prohibitive. Instead, *in vivo* genome engineering has the capacity to re-introduce lost lncRNAs or to alter regulatory elements that will allow for higher expression levels. CRISPR, in particular, is the most promising technology in that regard, and the results of the first *in vivo* uses of CRISPR will instruct whether or not it should be used for lncRNA modulation *in vivo.*

Ultimately, the strengths of lncRNAs for cancer treatment may well lie in the characteristics that make them tough to study and experiment with. Since lncRNA levels are exquisitely balanced within a cell, one would have to achieve a minimal level of perturbation to observe a phenotypic change. The wealth of data curated over the years from sequencing thousands of tumours provides a unique opportunity for functional biology to uncover the underlying mechanisms of action for all these RNA molecules. As more research starts to yield relevant data, hopefully, patterns will start to emerge which will make studying lncRNAs easier and allow us to more readily reach the ones that truly matter in a disease context.

5.3.4 Conclusions

In the present study, miRNAs are up- or down-regulated in most of the crizotinib/ceritinib resistant cell lines but not in all of them. This should come as no surprise as different clones will acquire different mechanisms of resistance. In particular, DUSP6 loss was detected only in some of the resistant clones examined [37] and EGFR inhibitor-resistant cells acquire entirely unique mechanisms of resistance even after limiting single-cell dilution [132]. Despite this, even if a particular protein dysregulation is detected in only one cell line, this finding can still be clinically relevant, as patients will be equally divergent in their underlying causes of resistance to the inhibitor used. While this complicates diagnosis and interpretation in the clinical setting, it also highlights the importance of continuing research in this context, in order to have as complete an understanding of the reasons of failure of ALK inhibitors as possible.

A global change in crizotinib-resistant cells, which could be detected and warn for the emergence of resistance, would be invaluable as a biomarker. However, this is unlikely to happen as after all these years of research something as profound would have been picked up on from the existing EML4-ALK-focused studies. However, given that most efforts focus on transcriptomic approaches, it could be conceived that there is an epigenetic or non-transcribed modification that unequivocally happens when EML4-ALK cells acquire resistance to ALK inhibitors. These findings raise the possibility that a collective dysregulation of the miRNome in combination with several oncogenes is the driving force behind resistance to ALK inhibition. This cannot be conclusively tested due to the number of potential alterations involved, but even if it could, would be translationally impractical.

Thereby, I propose a model where miRNAs are key downstream players of parallel pathway alterations that lead to the resistance to ALK inhibitors. Following up on my experiments, a miRNA mimic/inhibitor high-throughput screen should be performed, taking into account which miRNAs are either up- or down-regulated. MiRNAs whose experimental perturbation results in re-

sensitisation to crizotinib should be explored further. In a similar context in other cancer types such as melanoma, miRNA manipulation has been effective in suppressing resistance to targeted therapies, at least *in vitro* [306].

Given that different mechanisms of resistance can modulate different miRNAs, it would be clinically impractical to screen for all the potential mechanisms of resistance and intervene by modulating miRNAs. This study's findings have value as mechanistic insights regarding the way cancer cells alternate pathways to modulate their response to targeted therapies. While of little therapeutic value, it is possible that the described data set can still have translational value. Specifically, a targeted miRNA panel that could inform about the emergence of resistance (due to parallel pathway alterations) would be highly beneficial to these patients. The detection of miR-25 and 30c overexpression was associated with ALK-independent mechanisms of resistance and could be valuable to identify the patients that will not benefit from switching ALK inhibitors. We and others have shown the power of miRNAs in stratifying patients [307] and predicting the response to EGFR inhibition [308]. This would allow rapid treatment without the need for repeat biopsies. Eventually, this would be paired excellently with the discovery of a small molecule inhibitor that can effectively address all mechanisms of resistance.

5.3.5 Future work

While individual miRNAs that are associated with the resistance to crizotinib were successfully identified, a more comprehensive approach could identify many more such miRNAs. Specifically, a high-throughput miRNA overexpression library would have the advantage of identifying potential powerful tumour suppressing miRNAs. A tumour suppressing miRNA can have the advantage of potently suppressing cell proliferation upon artificial overexpression, without a requirement for it being differentially expressed in the original cell (such as the well-studied miR-34).

It was shown that miR-25 and miR-30c circulate more in the plasma of some patients who became refractory to ALK inhibitors. While for oncogenic miRNAs such testing is feasible, for tumour-suppressing ones it is not recommended, as these miRNAs may not circulate in the plasma even at baseline and therefore can't be detected. More complexity is introduced by the fact that exosomes in the blood seem to contain different miRNA species compared to free miRNAs in the plasma [309]. While my approach was deterministic, a no-hypothesis screening in a large number of patient samples could be highly beneficial to diagnosis. Specifically, a trial should be designed to obtain patient blood sample before treatment, after the first treatment and on several time points after progression. Then, RNA would be extracted from the plasma of these samples and subjected to deep RNA-sequencing. Comparing matched samples before treatment and after treatment would yield valuable information on early signalling events that may lead to compensatory feedback mechanisms that result in early, primary resistance, or later contribute to ALK inhibition resistance. Furthermore, comparing matched samples at baseline and on progression could lead to the development of a non-coding RNA biomarker panel that could inform clinicians about the emergence of resistance before it manifests with clinical symptoms. This would have the

advantage of switching treatment regimen early before tumours grow again significantly, which presumably could lead to more durable responses.

Evidently, the presented work regarding lncRNAs in EML4-ALK lung cancer requires several subsequent experiments in order to be complete. Specifically, I have looked at the intersection between dysregulated RNAs after crizotinib treatment and in crizotinib resistance. While this was to ensure that there were more chances of confidently identifying an oncogenic or tumour-suppressing lncRNA, it also meant that some potentially interesting lncRNAs that were not present in one of the two RNA-seq experiments would be missed. Furthermore, the high attrition rate in the validation phase of lncRNAs means that it would be better to utilise a global approach instead of validating individual lncRNAs. Of course this will be limited by the fact that high-throughput libraries cannot be as easily designed for lncRNAs, however, one can envision that the top-50 or even top-100 lncRNAs could be screened in an efficient fashion. To better inform this approach, any patient-derived data should be taken into account to minimise cell culture artefacts. Specifically, RNA-seq from even one patient, before ALK inhibitor treatment and after the appearance of resistance, would be invaluable in identifying lncRNAs that may have a driving role in this context. Lastly, I have shown that the lncRNA MANCR is up-regulated and several lncRNAs are down-regulated in more than one drug-resistant cell lines. Future work would address the potential of these lncRNAs as biomarkers by interrogating patient material via qPCR.

6 Final discussion

The field of EML4-ALK-mutant lung cancer advances rapidly and it is nowadays common to see patients that surpass the 5-year survival mark by cycling through different ALK inhibitors [310]. However, despite the latest impressive evidence for alectinib activity, which has shown an average progression-free survival of 35 months [311], patients do develop resistance to alectinib and progress, resulting in no difference in overall long-term survival compared with other ALK inhibitors. Due to the heterogeneity of the mechanisms of resistance, which can be both on-target (ALK) or off-target, new therapeutics are needed that do not require extensive screening to identify this mechanism. Specifically, if at the time of progression a core (or liquid) biopsy is negative for ALK kinase domain mutations, clinicians are left with few treatment options. If enough biopsy material is present, then clinicians can pursue a potential identification of the mechanism of resistance, mainly through whole-exome or RNA sequencing. However, this will rarely be fruitful. Indeed, there are several recent attempts in the field to target a global mediator of drug resistance in oncogene-driven lung cancer, such as Aurora Kinase A inhibition or SHP2 inhibition [76,119] or the repurposing of metformin [312], which was recently shown to increase survival in combination with EGFR inhibitors in a clinical trial [313]. This is a necessary effort, as ALK+ patients represent the only NSCLC cohort that categorically does not benefit from immunotherapy at all and are in dire need of other options [314].

The lack of a single driver of ALK inhibition resistance is a recurrent finding in the literature. This was evident in the cell culture models of acquired resistance described herein, where oncogenes such as EGFR, TGFβ-R1/2, c-FOS, NF-κB and Survivin were just passengers and not drivers of acquired resistance. Furthermore, in a previous evolutionary-guided approach to determine the origin of resistance, the authors described their cell models as presenting a "complex, multifactorial nature of resistance" [137]. This thesis echoes the above finding, utilising a multitude of cell line models that recapitulate the emergence of resistance to ALK inhibitors. While ideally, I should like to perform this analysis starting with patient-derived drug-resistant cell lines, specifically the MGH-series [112], I was not able to obtain these proprietary cells. Nevertheless, resistance to ALK inhibitors was effectively suppressed by CDK inhibition. Equally important, an upfront combination of low-dose CDK inhibitors with ALK inhibitors may greatly delay the emergence of resistance. The potential for upfront combinations of different compounds has generated a lot of interest in oncogene-driven lung adenocarcinomas lately [37,156,315] and has started to be tested in the clinic. This is predicated upon the conclusion that it is better to prevent the development of resistance to a single drug, rather than try to predict one of the myriads of mechanisms of resistance that can potentially appear.

AXL-mediated EMT as a mechanism of resistance to targeted therapies is well demonstrated in the literature. In melanoma, targeting EMT via an anti-AXL antibody could effectively suppress tumour subpopulations that were high in AXL expression in mice, resulting in re-sensitisation to MAPK pathway inhibitors [203]. In this thesis, data that show the importance of AXL activation in drug resistance were presented. The combination of crizotinib and bemcentinib, while only cytostatic

and not cytotoxic, could be further studied in order to find a meaningful combination that could be used in the clinic to target EMT. Specifically, a potential benefit in a metastatic context is likely. Bemcentinib has been shown before to diminish metastatic properties of breast cancer cells *in vitro* and *in vivo* [188].

In the context of EML4-ALK drug resistance, transcriptional sensitivity is a previously unappreciated way to induce apoptosis. This method is not toxic to normal epithelial cells and also exhibits a degree of selectivity towards EML4-ALK cells among other NSCLC cells. Not only do EML4-ALK cells express disproportionately high levels of the anti-apoptotic proteins MCL-1 and Survivin, but these proteins are also severely downregulated upon treatment with alvocidib, dinaciclib or THZ1. Through Chip-seq, it was demonstrated that transcriptional inhibition is indeed the outcome of treatment with alvocidib or THZ1, as expected due to their hypothesised inhibition of CDK9 and CDK7/12 respectively.

The role of the non-coding genome has been examined in multiple ways in this thesis. MiR-19b was shown to be part of the response to ALK inhibition, allowing an apoptotic induction through BIM upregulation. In the resistance to ALK inhibitors, miR-25 and miR-30c were upregulated and partly contributing to crizotinib resistance, whereas a miR-103 and miR-149 downregulation contributed to the observed upregulation of CDK6. Most importantly, miR-25 and miR-30c appear to circulate in higher levels in plasma samples from patients who progressed after treatment with ALK inhibitors in the clinic. While several future studies are needed, these data pave the way for a multi-miRNA biomarker panel that can notify the physician for an upcoming clinical progression. The last examined non-coding element in drug resistance were lncRNAs, even though none of the ones I tested were functional in this context.

Using a different paradigm, a critique of the approach described herein would be that trying to combat mechanisms of resistance after they arise is, due to their enormous complexity, counter-productive. Thus, a more impactful approach would have been to perform a drug screen for FDA-approved compounds which may in low dose, in combination with crizotinib, delay the emergence of resistance. In parallel, I could have asked what differentiates persister cells that survive initial ALK inhibition from the responding cells. The same transcriptomic approach used in drug-resistant clones could have been used in persister cells, in order to identify a vulnerability that may be actionable. This could have led to the use of another small molecule inhibitor in combination with ALK inhibition to suppress persister cells, an approach which has been fruitful in other contexts [133].

Despite remaining unanswered questions in the described sensitivity of EML4-ALK cells to CDK inhibitors, I was able to demonstrate that crizotinib- and alectinib-resistant lung cancer cells grow significantly less in mice when treated with alvocidib. Not only is this the first time that this has been shown in a model of lung adenocarcinoma, but it is also directly relevant to the clinic. Alectinib is currently the standard of care, and ALK-independent alectinib resistance will leave only chemotherapy available as a treatment option, as it was demonstrated here that newer inhibitors

such as lorlatinib would be ineffective in this context. Thus, I have presented a potential new alternative to chemotherapy for a defined cohort of patients, which may be clinically tested promptly.

6.1 Main points

- Several oncogenic markers may appear as drivers of resistance to ALK inhibitors, some of them falsely.
- AXL activation is a *bona fide* driver of crizotinib resistance and may be therapeutically exploited upon future studies.
- Re-purposing older compounds can be effective as a fall-back solution upon the inevitable resistance to RTK inhibition.
- MicroRNAs are an integral part of acquired resistance and careful selection of them can lead to useful biomarker panels.
- The first time that alvocidib has been demonstrated to be effective in a mouse model of lung adenocarcinoma.
- The CDK inhibitors alvocidib and THZ1 exhibit primarily anti-transcriptional activity in EML4-ALK cells, likely due to an inherent sensitivity of this oncogene-driven cancer.

7 References

[1] F.H. Wilson, C.M. Johannessen, F. Piccioni, P. Tamayo, J.W. Kim, E.M. Van Allen, S.M. Corsello, M. Capelletti, A. Calles, M. Butaney, T. Sharifnia, S.B. Gabriel, J.P. Mesirov, W.C. Hahn, J.A. Engelman, M. Meyerson, D.E. Root, P.A. Jänne, L.A. Garraway, A Functional Landscape of Resistance to ALK Inhibition in Lung Cancer, Cancer Cell. 27 (2015) 397–408. doi:10.1016/j.ccell.2015.02.005.

[2] C.M. Lovly, J.M. Heuckmann, E. De Stanchina, H. Chen, R.K. Thomas, C. Liang, W. Pao, Insights into ALK-driven cancers revealed through development of novel ALK tyrosine kinase inhibitors, Cancer Res. 71 (2011) 4920–4931. doi:10.1158/0008-5472.CAN-10-3879.

[3] C.M. Lovly, N.T. McDonald, H. Chen, S. Ortiz-Cuaran, L.C. Heukamp, Y. Yan, A. Florin, L. Ozretić, D. Lim, L. Wang, Z. Chen, X. Chen, P. Lu, P.K. Paik, R. Shen, H. Jin, R. Buettner, S. Ansén, S. Perner, M. Brockmann, M. Bos, J. Wolf, M. Gardizi, G.M. Wright, B. Solomon, P. a Russell, T.-M. Rogers, Y. Suehara, M. Red-Brewer, R. Tieu, E. de Stanchina, Q. Wang, Z. Zhao, D.H. Johnson, L. Horn, K.-K. Wong, R.K. Thomas, M. Ladanyi, W. Pao, Rationale for co-targeting IGF-1R and ALK in ALK fusion–positive lung cancer, Nat. Med. 20 (2014) 1027–1034. doi:10.1038/nm.3667.

[4] C.B. Meador, H. Jin, E. de Stanchina, C.A. Nebhan, V. Pirazzoli, L. Wang, P. Lu, H. Vuong, K.E. Hutchinson, P. Jia, X. Chen, R. Eisenberg, M. Ladanyi, K. Politi, Z. Zhao, C.M. Lovly, D.A.E. Cross, W. Pao, Optimizing the Sequence of Anti-EGFR-Targeted Therapy in EGFR-Mutant Lung Cancer, Mol. Cancer Ther. 14 (2015) 542–552. doi:10.1158/1535-7163.MCT-14-0723.

[5] K.J. Livak, T.D. Schmittgen, Analysis of Relative Gene Expression Data Using Real-Time Quantitative PCR and the 2−ΔΔCT Method, Methods. 25 (2001) 402–408. doi:10.1006/meth.2001.1262.

[6] M.I. Love, W. Huber, S. Anders, Moderated estimation of fold change and dispersion for RNA-seq data with DESeq2, Genome Biol. 15 (2014) 550. doi:10.1186/s13059-014-0550-8.

[7] Y. Liao, G.K. Smyth, W. Shi, The Subread aligner: fast, accurate and scalable read mapping by seed-and-vote, Nucleic Acids Res. 41 (2013) e108–e108. doi:10.1093/nar/gkt214.

[8] Y. Liao, G.K. Smyth, W. Shi, featureCounts: an efficient general purpose program for assigning sequence reads to genomic features, Bioinformatics. 30 (2014) 923–930. doi:10.1093/bioinformatics/btt656.

[9] J.D. Nelson, O. Denisenko, K. Bomsztyk, Protocol for the fast chromatin immunoprecipitation (ChIP) method, Nat. Protoc. 1 (2006) 179–185. doi:10.1038/nprot.2006.27.

[10] K.T. Huang, Y.H. Chen, A.M. Walker, Inaccuracies in MTS assays: major distorting effects of medium, serum albumin, and fatty acids, Biotechniques. 37 (2004) 406–412. doi:10.2144/04373ST05.

[11] Y.L. Choi, M. Soda, Y. Yamashita, T. Ueno, J. Takashima, T. Nakajima, Y. Yatabe, K. Takeuchi, T. Hamada, H. Haruta, Y. Ishikawa, H. Kimura, T. Mitsudomi, Y. Tanio, H. Mano, EML4-ALK Mutations in Lung Cancer That Confer Resistance to ALK Inhibitors, N. Engl. J. Med. 363 (2010) 1734–1739. doi:10.1056/NEJMoa1007478.

[12] I.S. Vlachos, K. Zagganas, M.D. Paraskevopoulou, G. Georgakilas, D. Karagkouni, T. Vergoulis, T. Dalamagas, A.G. Hatzigeorgiou, DIANA-miRPath v3.0: deciphering microRNA function with experimental support, Nucleic Acids Res. 43 (2015) W460–W466. doi:10.1093/nar/gkv403.

[13] V. Agarwal, G.W. Bell, J.W. Nam, D.P. Bartel, Predicting effective microRNA target sites in mammalian mRNAs, Elife. 4 (2015) 1–38. doi:10.7554/eLife.05005.

[14] D. Betel, A. Koppal, P. Agius, C. Sander, C. Leslie, Comprehensive modeling of microRNA targets predicts functional non-conserved and non-canonical sites, Genome Biol. 11 (2010) R90. doi:10.1186/gb-2010-11-8-r90.

[15] A. Subramanian, P. Tamayo, V.K. Mootha, S. Mukherjee, B.L. Ebert, M.A. Gillette, A. Paulovich, S.L. Pomeroy, T.R. Golub, E.S. Lander, J.P. Mesirov, Gene set enrichment analysis: A knowledge-based approach for interpreting genome-wide expression profiles, Proc. Natl. Acad. Sci. 102 (2005) 15545–15550. doi:10.1073/pnas.0506580102.

[16] M. Ghandi, F.W. Huang, J. Jané-Valbuena, G. V. Kryukov, C.C. Lo, E.R. McDonald, J. Barretina, E.T. Gelfand, C.M. Bielski, H. Li, K. Hu, A.Y. Andreev-Drakhlin, J. Kim, J.M. Hess, B.J. Haas, F. Aguet, B.A. Weir, M. V. Rothberg, B.R. Paolella, M.S. Lawrence, R. Akbani, Y. Lu, H.L. Tiv, P.C. Gokhale, A. de Weck, A.A. Mansour, C. Oh, J. Shih, K. Hadi, Y. Rosen, J. Bistline, K. Venkatesan, A. Reddy, D. Sonkin, M. Liu, J. Lehar, J.M. Korn, D.A. Porter, M.D. Jones, J. Golji, G. Caponigro, J.E. Taylor, C.M. Dunning, A.L. Creech, A.C. Warren, J.M. McFarland, M. Zamanighomi, A. Kauffmann, N. Stransky, M. Imielinski, Y.E. Maruvka, A.D. Cherniack, A. Tsherniak, F. Vazquez, J.D. Jaffe, A.A. Lane, D.M. Weinstock, C.M. Johannessen, M.P. Morrissey, F. Stegmeier, R. Schlegel, W.C. Hahn, G. Getz, G.B. Mills, J.S. Boehm, T.R. Golub, L.A. Garraway, W.R. Sellers, Next-generation characterization of the Cancer Cell Line Encyclopedia, Nature. (2019). doi:10.1038/s41586-019-1186-3.

[17] E. Brambilla, W.D. Travis, T.V. Colby, B. Corrin, Y. Shimosato, The new World Health Organization classification of lung tumours, Eur. Respir. J. 18 (2001) 1059–1068. doi:10.1183/09031936.01.00275301.

[18] Z. Chen, C.M. Fillmore, P.S. Hammerman, C.F. Kim, K.-K. Wong, Non-small-cell lung cancers: a heterogeneous set of diseases, Nat. Rev. Cancer. 14 (2014) 535–546.

doi:10.1038/nrc3775.

[19] F. Skoulidis, J. V. Heymach, Co-occurring genomic alterations in non-small-cell lung cancer biology and therapy, Nat. Rev. Cancer. (2019). doi:10.1038/s41568-019-0179-8.

[20] A.D. Cox, S.W. Fesik, A.C. Kimmelman, J. Luo, C.J. Der, Drugging the undruggable RAS: Mission Possible?, Nat. Rev. Drug Discov. 13 (2014) 828–51. doi:10.1038/nrd4389.

[21] P.E. Postmus, K.M. Kerr, M. Oudkerk, S. Senan, D.A. Waller, J. Vansteenkiste, C. Escriu, S. Peters, Early and locally advanced non-small-cell lung cancer (NSCLC): ESMO Clinical Practice Guidelines for diagnosis, treatment and follow-up†, Ann. Oncol. 28 (2017) iv1–iv21. doi:10.1093/annonc/mdx222.

[22] S. Novello, F. Barlesi, R. Califano, T. Cufer, S. Ekman, M.G. Levra, K. Kerr, S. Popat, M. Reck, S. Senan, G. V. Simo, J. Vansteenkiste, S. Peters, Metastatic non-small-cell lung cancer: ESMO Clinical Practice Guidelines for diagnosis, treatment and follow-up†, Ann. Oncol. 27 (2016) v1–v27. doi:10.1093/annonc/mdw326.

[23] R.S. Herbst, P. Baas, D.-W. Kim, E. Felip, J.L. Pérez-Gracia, J.-Y. Han, J. Molina, J.-H. Kim, C.D. Arvis, M.-J. Ahn, M. Majem, M.J. Fidler, G. de Castro, M. Garrido, G.M. Lubiniecki, Y. Shentu, E. Im, M. Dolled-Filhart, E.B. Garon, Pembrolizumab versus docetaxel for previously treated, PD-L1-positive, advanced non-small-cell lung cancer (KEYNOTE-010): a randomised controlled trial, Lancet. 387 (2016) 1540–1550. doi:10.1016/S0140-6736(15)01281-7.

[24] N.A. Rizvi, J. Mazières, D. Planchard, T.E. Stinchcombe, G.K. Dy, S.J. Antonia, L. Horn, H. Lena, E. Minenza, B. Mennecier, G.A. Otterson, L.T. Campos, D.R. Gandara, B.P. Levy, S.G. Nair, G. Zalcman, J. Wolf, P.-J. Souquet, E. Baldini, F. Cappuzzo, C. Chouaid, A. Dowlati, R. Sanborn, A. Lopez-Chavez, C. Grohe, R.M. Huber, C.T. Harbison, C. Baudelet, B.J. Lestini, S.S. Ramalingam, Activity and safety of nivolumab, an anti-PD-1 immune checkpoint inhibitor, for patients with advanced, refractory squamous non-small-cell lung cancer (CheckMate 063): a phase 2, single-arm trial, Lancet Oncol. 16 (2015) 257–265. doi:10.1016/S1470-2045(15)70054-9.

[25] M. Reck, D. Rodríguez-Abreu, A.G. Robinson, R. Hui, T. Csőszi, A. Fülöp, M. Gottfried, N. Peled, A. Tafreshi, S. Cuffe, M. O'Brien, S. Rao, K. Hotta, M.A. Leiby, G.M. Lubiniecki, Y. Shentu, R. Rangwala, J.R. Brahmer, Pembrolizumab versus Chemotherapy for PD-L1–Positive Non–Small-Cell Lung Cancer, N. Engl. J. Med. 375 (2016) 1823–1833. doi:10.1056/NEJMoa1606774.

[26] L. Gandhi, D. Rodríguez-Abreu, S. Gadgeel, E. Esteban, E. Felip, F. De Angelis, M. Domine, P. Clingan, M.J. Hochmair, S.F. Powell, S.Y.-S. Cheng, H.G. Bischoff, N. Peled, F. Grossi, R.R. Jennens, M. Reck, R. Hui, E.B. Garon, M. Boyer, B. Rubio-Viqueira, S. Novello, T. Kurata, J.E. Gray, J. Vida, Z. Wei, J. Yang, H. Raftopoulos, M.C. Pietanza, M.C. Garassino, Pembrolizumab plus Chemotherapy in Metastatic Non–Small-Cell Lung Cancer, N. Engl. J.

Med. 378 (2018) 2078–2092. doi:10.1056/NEJMoa1801005.

[27] R. Pagliarini, W. Shao, W.R. Sellers, Oncogene addiction: pathways of therapeutic response, resistance, and road maps toward a cure, EMBO Rep. 16 (2015) 280–296. doi:10.15252/embr.201439949.

[28] M. a. Lemmon, J. Schlessinger, Cell Signaling by Receptor Tyrosine Kinases, Cell. 141 (2010) 1117–1134. doi:10.1016/j.cell.2010.06.011.

[29] W. Pao, N. Girard, New driver mutations in non-small-cell lung cancer, Lancet Oncol. 12 (2011) 175–180. doi:10.1016/S1470-2045(10)70087-5.

[30] R. Rosell, N. Karachaliou, Large-scale screening for somatic mutations in lung cancer, Lancet. 387 (2016) 1354–1356. doi:10.1016/s0140-6736(15)01125-3.

[31] P. Clinical Lung Cancer Genome, M. Network Genomic, A genomics-based classification of human lung tumors, Sci Transl Med. 5 (2013) 209ra153. doi:10.1126/scitranslmed.3006802.

[32] B. Witek, A. El Wakil, C. Nord, U. Ahlgren, M. Eriksson, E. Vernersson-Lindahl, A. Helland, O.A. Alexeyev, B. Hallberg, R.H. Palmer, Targeted disruption of ALK reveals a potential role in hypogonadotropic hypogonadism, PLoS One. 10 (2015) e0123542. doi:10.1371/journal.pone.0123542.

[33] P.B. Murray, I. Lax, A. Reshetnyak, G.F. Ligon, J.S. Lillquist, E.J. Natoli, X. Shi, E. Folta-Stogniew, M. Gunel, D. Alvarado, J. Schlessinger, Heparin is an activating ligand of the orphan receptor tyrosine kinase ALK, Sci. Signal. 8 (2015) ra6. doi:10.1126/scisignal.2005916.

[34] B. Hallberg, R.H. Palmer, Mechanistic insight into ALK receptor tyrosine kinase in human cancer biology., Nat. Rev. Cancer. 13 (2013) 685–700. doi:10.1038/nrc3580.

[35] R. Chiarle, C. Voena, C. Ambrogio, R. Piva, G. Inghirami, The anaplastic lymphoma kinase in the pathogenesis of cancer, Nat. Rev. Cancer. 8 (2008) 11–23. doi:10.1038/nrc2291.

[36] M. Soda, Y.L. Choi, M. Enomoto, S. Takada, Y. Yamashita, S. Ishikawa, S. Fujiwara, H. Watanabe, K. Kurashina, H. Hatanaka, M. Bando, S. Ohno, Y. Ishikawa, H. Aburatani, T. Niki, Y. Sohara, Y. Sugiyama, H. Mano, Identification of the transforming EML4–ALK fusion gene in non-small-cell lung cancer, Nature. 448 (2007) 561–566. doi:10.1038/nature05945.

[37] G. Hrustanovic, V. Olivas, E. Pazarentzos, A. Tulpule, S. Asthana, C.M. Blakely, R.A. Okimoto, L. Lin, D.S. Neel, A. Sabnis, J. Flanagan, E. Chan, M. Varella-Garcia, D.L. Aisner, A. Vaishnavi, S.-H.I. Ou, E.A. Collisson, E. Ichihara, P.C. Mack, C.M. Lovly, N. Karachaliou, R. Rosell, J.W. Riess, R.C. Doebele, T.G. Bivona, RAS-MAPK dependence underlies a rational polytherapy strategy in EML4-ALK–positive lung cancer, Nat. Med. 21 (2015) 1038–1047. doi:10.1038/nm.3930.

[38] K. Takezawa, I. Okamoto, K. Nishio, P.A. Janne, K. Nakagawa, Role of ERK-BIM and STAT3-Survivin Signaling Pathways in ALK Inhibitor-Induced Apoptosis in EML4-ALK-Positive Lung Cancer, Clin. Cancer Res. 17 (2011) 2140–2148. doi:10.1158/1078-0432.CCR-10-2798.

[39] M. Soda, S. Takada, K. Takeuchi, L.C. Young, M. Enomoto, T. Ueno, H. Haruta, T. Hamada, Y. Yamashita, Y. Ishikawa, Y. Sugiyama, H. Mano, A mouse model for EML4-ALK-positive lung cancer, Proc. Natl. Acad. Sci. U. S. A. 105 (2008) 19893–19897. doi:10.1073/pnas.0805381105.

[40] K. Ota, K. Azuma, A. Kawahara, S. Hattori, E. Iwama, J. Tanizaki, T. Harada, K. Matsumoto, K. Takayama, S. Takamori, M. Kage, T. Hoshino, Y. Nakanishi, I. Okamoto, Induction of PD-L1 Expression by the EML4-ALK Oncoprotein and Downstream Signaling Pathways in Non-Small Cell Lung Cancer, Clin. Cancer Res. 21 (2015) 4014–4021. doi:10.1158/1078-0432.CCR-15-0016.

[41] L. O'Regan, G. Barone, R. Adib, C.G. Woo, H.J. Jeong, E.L. Richardson, M.W. Richards, P.A.J. Muller, S. Collis, D. Fennell, J. Choi, R. Bayliss, A. Fry, EML4-ALK V3 Drives Cell Migration Through NEK9 and NEK7 Kinases in Non-Small-Cell Lung Cancer, SSRN Electron. J. (2019). doi:10.2139/ssrn.3377373.

[42] S.A. Forbes, D. Beare, P. Gunasekaran, K. Leung, N. Bindal, H. Boutselakis, M. Ding, S. Bamford, C. Cole, S. Ward, C.Y. Kok, M. Jia, T. De, J.W. Teague, M.R. Stratton, U. McDermott, P.J. Campbell, COSMIC: exploring the world's knowledge of somatic mutations in human cancer, Nucleic Acids Res. 43 (2015) D805–D811. doi:10.1093/nar/gku1075.

[43] T. Sasaki, S.J. Rodig, L.R. Chirieac, P.A. Jänne, The biology and treatment of EML4-ALK non-small cell lung cancer, Eur. J. Cancer. 46 (2010) 1773–1780. doi:10.1016/j.ejca.2010.04.002.

[44] D.W.S. Wong, E.L.H. Leung, K.K.T. So, I.Y.S. Tam, A.D.L. Sihoe, L.C. Cheng, K.K. Ho, J.S.K. Au, L.P. Chung, M.P. Wong, The EML4-ALK fusion gene is involved in various histologic types of lung cancers from nonsmokers with wild-type EGFR and KRAS, Cancer. 115 (2009) 1723–1733. doi:10.1002/cncr.24181.

[45] J.F. Gainor, A.M. Varghese, S.-H.I. Ou, S. Kabraji, M.M. Awad, R. Katayama, A. Pawlak, M. Mino-Kenudson, B.Y. Yeap, G.J. Riely, a J. Iafrate, M.E. Arcila, M. Ladanyi, J. a Engelman, D. Dias-Santagata, A.T. Shaw, ALK Rearrangements Are Mutually Exclusive with Mutations in EGFR or KRAS: An Analysis of 1,683 Patients with Non-Small Cell Lung Cancer, Clin. Cancer Res. 19 (2013) 4273–4281. doi:10.1158/1078-0432.CCR-13-0318.

[46] R.C. Doebele, A.B. Pilling, D.L. Aisner, T.G. Kutateladze, A.T. Le, A.J. Weickhardt, K.L. Kondo, D.J. Linderman, L.E. Heasley, W.A. Franklin, M. Varella-Garcia, D.R. Camidge, Mechanisms of Resistance to Crizotinib in Patients with ALK Gene Rearranged Non-Small Cell Lung Cancer, Clin. Cancer Res. 18 (2012) 1472–1482. doi:10.1158/1078-0432.CCR-11-

2906.

[47] J.F. Gainor, L. Dardaei, S. Yoda, L. Friboulet, I. Leshchiner, R. Katayama, I. Dagogo-Jack, S. Gadgeel, K. Schultz, M. Singh, E. Chin, M. Parks, D. Lee, R.H. DiCecca, E. Lockerman, T. Huynh, J. Logan, L.L. Ritterhouse, L.P. Le, A. Muniappan, S. Digumarthy, C. Channick, C. Keyes, G. Getz, D. Dias-Santagata, R.S. Heist, J. Lennerz, L. V. Sequist, C.H. Benes, A.J. Iafrate, M. Mino-Kenudson, J.A. Engelman, A.T. Shaw, Molecular Mechanisms of Resistance to First- and Second-Generation ALK Inhibitors in ALK-Rearranged Lung Cancer, Cancer Discov. 6 (2016) 1118–1133. doi:10.1158/2159-8290.CD-16-0596.

[48] A. Kron, C. Alidousty, M. Scheffler, S. Merkelbach-Bruse, D. Seidel, R. Riedel, M. Ihle, S. Michels, L. Nogova, J. Fassunke, C. Heydt, F. Kron, F. Ueckeroth, M. Serke, S. Krüger, C. Grohe, D. Koschel, J. Benedikter, B. Kaminsky, B. Schaaf, J. Braess, M. Sebastian, K.-O. Kambartel, R. Thomas, T. Zander, A.M. Schultheis, R. Büttner, J. Wolf, Impact of TP53 mutation status on systemic treatment outcome in ALK-rearranged non-small-cell lung cancer, Ann. Oncol. (2018). doi:10.1093/annonc/mdy333.

[49] K. Takeuchi, L.C. Young, Y. Togashi, M. Soda, S. Hatano, K. Inamura, S. Takada, T. Ueno, Y. Yamashita, Y. Satoh, S. Okumura, K. Nakagawa, Y. Ishikawa, H. Mano, KIF5B-ALK, a novel fusion oncokinase identified by an immunohistochemistry- based diagnostic system for ALK-positive lung cancer, Clin. Cancer Res. 15 (2009) 3143–3149. doi:10.1158/1078-0432.CCR-08-3248.

[50] T. Yoshida, Y. Oya, K. Tanaka, J. Shimizu, Y. Horio, H. Kuroda, Y. Sakao, T. Hida, Y. Yatabe, Differential Crizotinib Response Duration Among ALK Fusion Variants in ALK -Positive Non–Small-Cell Lung Cancer, J. Clin. Oncol. 34 (2016) 3383–3389. doi:10.1200/JCO.2015.65.8732.

[51] J.J. Lin, V.W. Zhu, S. Yoda, B.Y. Yeap, A.B. Schrock, I. Dagogo-Jack, N.A. Jessop, G.Y. Jiang, L.P. Le, K. Gowen, P.J. Stephens, J.S. Ross, S.M. Ali, V.A. Miller, M.L. Johnson, C.M. Lovly, A.N. Hata, J.F. Gainor, A.J. Iafrate, A.T. Shaw, S.-H.I. Ou, Impact of EML4-ALK Variant on Resistance Mechanisms and Clinical Outcomes in ALK -Positive Lung Cancer, J. Clin. Oncol. 36 (2018) 1199–1206. doi:10.1200/JCO.2017.76.2294.

[52] C.G. Woo, S. Seo, S.W. Kim, S.J. Jang, K.S. Park, J.Y. Song, B. Lee, M.W. Richards, R. Bayliss, D.H. Lee, J. Choi, Differential protein stability and clinical responses of EML4-ALK fusion variants to various ALK inhibitors in advanced ALK -rearranged non–small cell lung cancer, Ann. Oncol. (2016) mdw693. doi:10.1093/annonc/mdw693.

[53] R.E. George, T. Sanda, M. Hanna, S. Fröhling, W. Luther, J. Zhang, Y. Ahn, W. Zhou, W.B. London, P. McGrady, L. Xue, S. Zozulya, V.E. Gregor, T.R. Webb, N.S. Gray, D.G. Gilliland, L. Diller, H. Greulich, S.W. Morris, M. Meyerson, A.T. Look, Activating mutations in ALK provide a therapeutic target in neuroblastoma., Nature. 455 (2008) 975–8. doi:10.1038/nature07397.

[54] Z. Chen, T. Sasaki, X. Tan, J. Carretero, T. Shimamura, D. Li, C. Xu, Y. Wang, G.O. Adelmant, M. Capelletti, H.J. Lee, S.J. Rodig, C. Borgman, S.-I. Park, H.R. Kim, R. Padera, J.A. Marto, N.S. Gray, A.L. Kung, G.I. Shapiro, P.A. Jänne, K.-K. Wong, Inhibition of ALK, PI3K/MEK, and HSP90 in murine lung adenocarcinoma induced by EML4-ALK fusion oncogene., Cancer Res. 70 (2010) 9827–36. doi:10.1158/0008-5472.CAN-10-1671.

[55] C. Schönherr, K. Ruuth, S. Kamaraj, C.-L. Wang, H.-L. Yang, V. Combaret, A. Djos, T. Martinsson, J.G. Christensen, R.H. Palmer, B. Hallberg, Anaplastic Lymphoma Kinase (ALK) regulates initiation of transcription of MYCN in neuroblastoma cells, Oncogene. 31 (2012) 5193–5200. doi:10.1038/onc.2012.12.

[56] D. Maddalo, E. Manchado, C.P. Concepcion, C. Bonetti, J. a. Vidigal, Y.-C. Han, P. Ogrodowski, A. Crippa, N. Rekhtman, E. de Stanchina, S.W. Lowe, A. Ventura, In vivo engineering of oncogenic chromosomal rearrangements with the CRISPR/Cas9 system, Nature. 516 (2014) 423–427. doi:10.1038/nature13902.

[57] J.M. Pacheco, D.R. Camidge, Searching for a chemoimmunotherapy signal in patients with non-small-cell lung cancer and EGFR mutations, Lancet Respir. Med. 7 (2019) 366–367. doi:10.1016/s2213-2600(19)30112-2.

[58] Dhillon, Hagan, Rath, Kolch, MAP kinase signalling pathways in cancer., Oncogene. 26 (2007) 3279–90. doi:10.1038/sj.onc.1210421.

[59] J. Tanizaki, I. Okamoto, K. Takezawa, K. Sakai, K. Azuma, K. Kuwata, H. Yamaguchi, E. Hatashita, K. Nishio, P. Janne, K. Nakagawa, Combined effect of ALK and MEK inhibitors in EML4–ALK-positive non-small-cell lung cancer cells, Br. J. Cancer. 106 (2012) 763–767. doi:10.1038/bjc.2011.586.

[60] G. Umapathy, J. Guan, D.E. Gustafsson, N. Javanmardi, D. Cervantes-Madrid, A. Djos, T. Martinsson, R.H. Palmer, B. Hallberg, MEK inhibitor trametinib does not prevent the growth of anaplastic lymphoma kinase (ALK)–addicted neuroblastomas, Sci. Signal. 10 (2017) eaam7550. doi:10.1126/scisignal.aam7550.

[61] A.F. Gadzar, Activating and resistance mutations of EGFR in non-small cell lung cancer: role in clinical response to EGFR tyrosine kinase inhibitors, Oncogene. 28 (2010) 1–14. doi:10.1038/onc.2009.198.Activating.

[62] A. Midha, S. Dearden, R. McCormack, EGFR mutation incidence in non-small-cell lung cancer of adenocarcinoma histology: a systematic review and global map by ethnicity (mutMapII)., Am. J. Cancer Res. 5 (2015) 2892–911. doi:10.5194/hess-11-1609-2007.

[63] M. Fukuoka, S. Yano, G. Giaccone, T. Tamura, K. Nakagawa, J.-Y. Douillard, Y. Nishiwaki, J. Vansteenkiste, S. Kudoh, D. Rischin, R. Eek, T. Horai, K. Noda, I. Takata, E. Smit, S. Averbuch, A. Macleod, A. Feyereislova, R.-P. Dong, J. Baselga, Multi-institutional randomized phase II trial of gefitinib for previously treated patients with advanced non-

small-cell lung cancer (The IDEAL 1 Trial) [corrected]., J. Clin. Oncol. 21 (2003) 2237–46. doi:10.1200/JCO.2003.10.038.

[64] J.G. Paez, EGFR Mutations in Lung Cancer: Correlation with Clinical Response to Gefitinib Therapy, Science (80-.). 304 (2004) 1497–1500. doi:10.1126/science.1099314.

[65] T.J. Lynch, D.W. Bell, R. Sordella, S. Gurubhagavatula, R.A. Okimoto, B.W. Brannigan, P.L. Harris, S.M. Haserlat, J.G. Supko, F.G. Haluska, D.N. Louis, D.C. Christiani, J. Settleman, D.A. Haber, Activating Mutations in the Epidermal Growth Factor Receptor Underlying Responsiveness of Non–Small-Cell Lung Cancer to Gefitinib, N. Engl. J. Med. 350 (2004) 2129–2139. doi:10.1056/NEJMoa040938.

[66] C. Zhou, Y.L. Wu, G. Chen, J. Feng, X.Q. Liu, C. Wang, S. Zhang, J. Wang, S. Zhou, S. Ren, S. Lu, L. Zhang, C. Hu, C. Hu, Y. Luo, L. Chen, M. Ye, J. Huang, X. Zhi, Y. Zhang, Q. Xiu, J. Ma, L. Zhang, C. You, Erlotinib versus chemotherapy as first-line treatment for patients with advanced EGFR mutation-positive non-small-cell lung cancer (OPTIMAL, CTONG-0802): a multicentre, open-label, randomised, phase 3 study, Lancet Oncol. 12 (2011) 735–742. doi:10.1016/S1470-2045(11)70184-X.

[67] Y.-L. Wu, C. Zhou, C.-P. Hu, J. Feng, S. Lu, Y. Huang, W. Li, M. Hou, J.H. Shi, K.Y. Lee, C.-R. Xu, D. Massey, M. Kim, Y. Shi, S.L. Geater, Afatinib versus cisplatin plus gemcitabine for first-line treatment of Asian patients with advanced non-small-cell lung cancer harbouring EGFR mutations (LUX-Lung 6): an open-label, randomised phase 3 trial, Lancet Oncol. 15 (2014) 213–222. doi:10.1016/S1470-2045(13)70604-1.

[68] J.C.H. Yang, M.J. Ahn, D.W. Kim, S.S. Ramalingam, L. V. Sequist, W.C. Su, S.W. Kim, J.H. Kim, D. Planchard, E. Felip, F. Blackhall, D. Haggstrom, K. Yoh, S. Novello, K. Gold, T. Hirashima, C.C. Lin, H. Mann, M. Cantarini, S. Ghiorghiu, P.A. Jänne, Osimertinib in pretreated T790M-positive advanced non-small-cell lung cancer: AURA study phase II extension component, J. Clin. Oncol. 35 (2017) 1288–1296. doi:10.1200/JCO.2016.70.3223.

[69] A. Tartarone, C. Lazzari, R. Lerose, V. Conteduca, G. Improta, A. Zupa, A. Bulotta, M. Aieta, V. Gregorc, Mechanisms of resistance to EGFR tyrosine kinase inhibitors gefitinib/erlotinib and to ALK inhibitor crizotinib, Lung Cancer. 81 (2013) 328–336. doi:10.1016/j.lungcan.2013.05.020.

[70] T.J. Gonda, R.G. Ramsay, Directly targeting transcriptional dysregulation in cancer, Nat. Rev. Cancer. 15 (2015) 686–694. doi:10.1038/nrc4018.

[71] M. Reck, T.S.K. Mok, M. Nishio, R.M. Jotte, F. Cappuzzo, F. Orlandi, D. Stroyakovskiy, N. Nogami, D. Rodríguez-Abreu, D. Moro-Sibilot, C.A. Thomas, F. Barlesi, G. Finley, A. Lee, S. Coleman, Y. Deng, M. Kowanetz, G. Shankar, W. Lin, M.A. Socinski, M. Reck, T.S. Mok, M. Nishio, R.M. Jotte, F. Cappuzzo, F. Orlandi, D. Stroyakovskiy, N. Nogami, D. Rodríguez-Abreu, D. Moro-Sibilot, C.A. Thomas, F. Barlesi, G. Finley, A. Lee, S. Coleman, Y. Deng, M.

Kowanetz, G. Shankar, W. Lin, M.A. Socinski, Atezolizumab plus bevacizumab and chemotherapy in non-small-cell lung cancer (IMpower150): key subgroup analyses of patients with EGFR mutations or baseline liver metastases in a randomised, open-label phase 3 trial, Lancet Respir. Med. (2019) 1–15. doi:10.1016/S2213-2600(19)30084-0.

[72] A. Ogino, H. Kitao, S. Hirano, A. Uchida, M. Ishiai, T. Kozuki, N. Takigawa, M. Takata, K. Kiura, M. Tanimoto, Emergence of epidermal growth factor receptor T790M mutation during chronic exposure to gefitinib in a non-small cell lung cancer cell line, Cancer Res. 67 (2007) 7807–7814. doi:10.1158/0008-5472.CAN-07-0681.

[73] A.C. Faber, R.B. Corcoran, H. Ebi, L. V. Sequist, B.A. Waltman, E. Chung, J. Incio, S.R. Digumarthy, S.F. Pollack, Y. Song, A. Muzikansky, E. Lifshits, S. Roberge, E.J. Coffman, C.H. Benes, H.L. Gomez, J. Baselga, C.L. Arteaga, M.N. Rivera, D. Dias-Santagata, R.K. Jain, J.A. Engelman, BIM Expression in Treatment-Naive Cancers Predicts Responsiveness to Kinase Inhibitors, Cancer Discov. 1 (2011) 352–365. doi:10.1158/2159-8290.CD-11-0106.

[74] J. Xia, H. Bai, B. Yan, R. Li, M. Shao, L. Xiong, B. Han, Mimicking the BIM BH3 domain overcomes resistance to EGFR tyrosine kinase inhibitors in EGFR-mutant non-small cell lung cancer, Oncotarget. 8 (2017) 1–12. doi:10.18632/oncotarget.19411.

[75] E. Ichihara, D. Westover, C.B. Meador, Y. Yan, J.A. Bauer, P. Lu, F. Ye, A. Kulick, E. de Stanchina, R. McEwen, M. Ladanyi, D. Cross, W. Pao, C.M. Lovly, SFK/FAK Signaling Attenuates Osimertinib Efficacy in Both Drug-Sensitive and Drug-Resistant Models of EGFR-Mutant Lung Cancer, Cancer Res. 77 (2017) 2990–3000. doi:10.1158/0008-5472.CAN-16-2300.

[76] K.N. Shah, R. Bhatt, J. Rotow, J. Rohrberg, V. Olivas, V.E. Wang, G. Hemmati, M.M. Martins, A. Maynard, J. Kuhn, J. Galeas, H.J. Donnella, S. Kaushik, A. Ku, S. Dumont, G. Krings, H.J. Haringsma, L. Robillard, A.D. Simmons, T.C. Harding, F. McCormick, A. Goga, C.M. Blakely, T.G. Bivona, S. Bandyopadhyay, Aurora kinase A drives the evolution of resistance to third-generation EGFR inhibitors in lung cancer, Nat. Med. (2018). doi:10.1038/s41591-018-0264-7.

[77] L. Marcar, K. Bardhan, L. Gheorghiu, P. Dinkelborg, H. Pfäffle, Q. Liu, M. Wang, Z. Piotrowska, L. V. Sequist, K. Borgmann, J.E. Settleman, J.A. Engelman, A.N. Hata, H. Willers, Acquired Resistance of EGFR-Mutated Lung Cancer to Tyrosine Kinase Inhibitor Treatment Promotes PARP Inhibitor Sensitivity, Cell Rep. 27 (2019) 3422-3432.e4. doi:10.1016/j.celrep.2019.05.058.

[78] C.M. Blakely, T.B.K. Watkins, W. Wu, B. Gini, J.J. Chabon, C.E. McCoach, N. McGranahan, G.A. Wilson, N.J. Birkbak, V.R. Olivas, J. Rotow, A. Maynard, V. Wang, M.A. Gubens, K.C. Banks, R.B. Lanman, A.F. Caulin, J. St John, A.R. Cordero, P. Giannikopoulos, A.D. Simmons, P.C. Mack, D.R. Gandara, H. Husain, R.C. Doebele, J.W. Riess, M. Diehn, C. Swanton, T.G. Bivona, Evolution and clinical impact of co-occurring genetic alterations in

advanced-stage EGFR-mutant lung cancers, Nat. Genet. 49 (2017) 1693–1704. doi:10.1038/ng.3990.

[79] Z. Yang, N. Yang, Q. Ou, Y. Xiang, T. Jiang, X. Wu, H. Bao, X. Tong, X. Wang, Y.W. Shao, Y. Liu, Y. Wang, C. Zhou, Investigating Novel Resistance Mechanisms to Third-Generation EGFR Tyrosine Kinase Inhibitor Osimertinib in Non–Small Cell Lung Cancer Patients, Clin. Cancer Res. (2018) clincanres.2310.2017. doi:10.1158/1078-0432.CCR-17-2310.

[80] D. Planchard, S. Popat, K. Kerr, S. Novello, E.F. Smit, C. Faivre-Finn, T.S. Mok, M. Reck, P.E. Van Schil, M.D. Hellmann, S. Peters, Metastatic non-small cell lung cancer: ESMO Clinical Practice Guidelines for diagnosis, treatment and follow-up†, Ann. Oncol. 29 (2018) iv192–iv237. doi:10.1093/annonc/mdy275.

[81] M.S. Tsao, F.R. Hirsch, Y. Yatabe, IASLC atlas of ALK and ROS1 testing in lung cancer, 2013.

[82] M.-S. Tsao, K.M. Kerr, S. Dacic, Y. Yatabe, F.R. Hirsch, IASLC atlas of ALK testing in lung cancer, 2017. https://www.iaslc.org/publications/iaslc-atlas-pd-l1-testing-lung-cancer.

[83] C.T. Hiley, J. Le Quesne, G. Santis, R. Sharpe, D.G. de Castro, G. Middleton, C. Swanton, Challenges in molecular testing in non-small-cell lung cancer patients with advanced disease, Lancet. 388 (2016) 1002–1011. doi:10.1016/S0140-6736(16)31340-X.

[84] B. Hallberg, R.H. Palmer, ALK and NSCLC: Targeted therapy with ALK inhibitors., F1000 Med. Rep. 3 (2011) 21. doi:10.3410/M3-21.

[85] D.R. Camidge, Y.-J. Bang, E.L. Kwak, a J. Iafrate, M. Varella-Garcia, S.B. Fox, G.J. Riely, B. Solomon, S.-H.I. Ou, D.-W. Kim, R. Salgia, P. Fidias, J. a Engelman, L. Gandhi, P. a Jänne, D.B. Costa, G.I. Shapiro, P. LoRusso, K. Ruffner, P. Stephenson, Y. Tang, K. Wilner, J.W. Clark, A.T. Shaw, Activity and safety of crizotinib in patients with ALK-positive non-small-cell lung cancer: updated results from a phase 1 study, Lancet Oncol. 13 (2012) 1011–1019. doi:10.1016/S1470-2045(12)70344-3.

[86] A.T. Shaw, D.-W. Kim, K. Nakagawa, T. Seto, L. Crinó, M.-J. Ahn, T. De Pas, B. Besse, B.J. Solomon, F. Blackhall, Y.-L. Wu, M. Thomas, K.J. O'Byrne, D. Moro-Sibilot, D.R. Camidge, T. Mok, V. Hirsh, G.J. Riely, S. Iyer, V. Tassell, A. Polli, K.D. Wilner, P.A. Jänne, Crizotinib versus Chemotherapy in Advanced ALK -Positive Lung Cancer, N. Engl. J. Med. 368 (2013) 2385–2394. doi:10.1056/NEJMoa1214886.

[87] M.M. Awad, A.T. Shaw, ALK inhibitors in non-small cell lung cancer: crizotinib and beyond., Clin. Adv. Hematol. Oncol. 12 (2014) 429–39. http://www.pubmedcentral.nih.gov/articlerender.fcgi?artid=4215402&tool=pmcentrez&rendertype=abstract.

[88] A.T. Shaw, T.M. Kim, L. Crinò, C. Gridelli, K. Kiura, G. Liu, S. Novello, A. Bearz, O. Gautschi,

T. Mok, M. Nishio, G. Scagliotti, D.R. Spigel, S. Deudon, C. Zheng, S. Pantano, P. Urban, C. Massacesi, K. Viraswami-Appanna, E. Felip, Ceritinib versus chemotherapy in patients with ALK -rearranged non-small-cell lung cancer previously given chemotherapy and crizotinib (ASCEND-5): a randomised, controlled, open-label, phase 3 trial, Lancet Oncol. 18 (2017) 874–886. doi:10.1016/S1470-2045(17)30339-X.

[89] D.R. Camidge, H.R. Kim, M.-J. Ahn, J.C.-H. Yang, J.-Y. Han, J.-S. Lee, M.J. Hochmair, J.Y.-C. Li, G.-C. Chang, K.H. Lee, C. Gridelli, A. Delmonte, R. Garcia Campelo, D.-W. Kim, A. Bearz, F. Griesinger, A. Morabito, E. Felip, R. Califano, S. Ghosh, A. Spira, S.N. Gettinger, M. Tiseo, N. Gupta, J. Haney, D. Kerstein, S. Popat, Brigatinib versus Crizotinib in ALK -Positive Non–Small-Cell Lung Cancer, N. Engl. J. Med. (2018) NEJMoa1810171. doi:10.1056/NEJMoa1810171.

[90] T. Hida, H. Nokihara, M. Kondo, Y.H. Kim, K. Azuma, T. Seto, Y. Takiguchi, M. Nishio, H. Yoshioka, F. Imamura, K. Hotta, S. Watanabe, K. Goto, M. Satouchi, T. Kozuki, T. Shukuya, K. Nakagawa, T. Mitsudomi, N. Yamamoto, T. Asakawa, R. Asabe, T. Tanaka, T. Tamura, Alectinib versus crizotinib in patients with ALK -positive non-small-cell lung cancer (J-ALEX): an open-label, randomised phase 3 trial, Lancet. 6736 (2017) 1–11. doi:10.1016/S0140-6736(17)30565-2.

[91] L. Horn, J.R. Infante, K.L. Reckamp, G.R. Blumenschein, T.A. Leal, S.N. Waqar, B.J. Gitlitz, R.E. Sanborn, J.G. Whisenant, L. Du, J.W. Neal, J.P. Gockerman, G. Dukart, K. Harrow, C. Liang, J.J. Gibbons, A. Holzhausen, C.M. Lovly, H.A. Wakelee, Ensartinib (X-396) in ALK-Positive Non–Small Cell Lung Cancer: Results from a First-in-Human Phase I/II, Multicenter Study, Clin. Cancer Res. 24 (2018) 2771–2779. doi:10.1158/1078-0432.CCR-17-2398.

[92] B.J. Solomon, B. Besse, T.M. Bauer, E. Felip, R.A. Soo, D.R. Camidge, R. Chiari, A. Bearz, C. Lin, S.M. Gadgeel, G.J. Riely, E.H. Tan, T. Seto, L.P. James, J.S. Clancy, A. Abbattista, J. Martini, J. Chen, G. Peltz, H. Thurm, S.-H.I. Ou, A.T. Shaw, Lorlatinib in patients with ALK-positive non-small-cell lung cancer: results from a global phase 2 study, Lancet Oncol. 19 (2018) 1654–1667. doi:10.1016/S1470-2045(18)30649-1.

[93] J.M. Pacheco, D. Gao, D. Smith, T. Purcell, M. Hancock, P. Bunn, T. Robin, A. Liu, S. Karam, L. Gaspar, B. Kavanagh, C. Rusthoven, D. Aisner, R. Doebele, D.R. Camidge, Natural History and Factors Associated with Overall Survival in Stage IV ALK-Rearranged Non–Small Cell Lung Cancer, J. Thorac. Oncol. 14 (2019) 691–700. doi:10.1016/j.jtho.2018.12.014.

[94] A. Guérin, M. Sasane, H. Wakelee, J. Zhang, K. Culver, K. Dea, R. Nitulescu, P. Galebach, A.R. Macalalad, Treatment, overall survival, and costs in patients with ALK -positive non-small-cell lung cancer after crizotinib monotherapy, Curr. Med. Res. Opin. 31 (2015) 1587–1597. doi:10.1185/03007995.2015.1057115.

[95] W. Wu, F. Haderk, T. Bivona, Non-Canonical Thinking for Targeting ALK-Fusion Onco-Proteins in Lung Cancer, Cancers (Basel). 9 (2017) 164. doi:10.3390/cancers9120164.

[96] T.C. Tsou, K. Gowen, S.M. Ali, V.A. Miller, A.B. Schrock, C.M. Lovly, K.L. Reckamp, Variable Response to ALK Inhibitors in NSCLC with a Novel MYT1L-ALK Fusion, J. Thorac. Oncol. 14 (2019) e29–e30. doi:S1556086418334580.

[97] J. Yin, Y. Zhang, Y. Zhang, F. Peng, Y. Lu, Reporting on Two Novel Fusions, DYSF-ALK and ITGAV-ALK, Coexisting in One Patient with Adenocarcinoma of Lung, Sensitive to Crizotinib, J. Thorac. Oncol. 13 (2018) e43–e45. doi:10.1016/j.jtho.2017.10.025.

[98] J. Guan, E.R. Tucker, H. Wan, D. Chand, L.S. Danielson, K. Ruuth, A. El Wakil, B. Witek, Y. Jamin, G. Umapathy, S.P. Robinson, T.W. Johnson, T. Smeal, T. Martinsson, L. Chesler, R.H. Palmer, B. Hallberg, The ALK inhibitor PF-06463922 is effective as a single agent in neuroblastoma driven by expression of ALK and MYCN, Dis. Model. Mech. 9 (2016) 941–952. doi:10.1242/dmm.024448.

[99] A.J.M. Ferreri, S. Govi, S.A. Pileri, K.J. Savage, Anaplastic large cell lymphoma, ALK-negative, Crit. Rev. Oncol. Hematol. 85 (2013) 206–215. doi:10.1016/j.critrevonc.2012.06.004.

[100] Y.P. Mossé, S.D. Voss, M.S. Lim, D. Rolland, C.G. Minard, E. Fox, P. Adamson, K. Wilner, S.M. Blaney, B.J. Weigel, Targeting ALK with crizotinib in pediatric anaplastic large cell lymphoma and inflammatory myofibroblastic tumor: A Children's Oncology Group study, J. Clin. Oncol. 35 (2017) 3215–3221. doi:10.1200/JCO.2017.73.4830.

[101] A.S. Mansfield, S.J. Murphy, F.R. Harris, S.I. Robinson, R.S. Marks, S.H. Johnson, J.B. Smadbeck, G.C. Halling, E.S. Yi, D. Wigle, G. Vasmatzis, J. Jen, Chromoplectic TPM3-ALK rearrangement in a patient with inflammatory myofibroblastic tumor who responded to ceritinib after progression on crizotinib, Ann. Oncol. 27 (2016) 2111–2117. doi:10.1093/annonc/mdw405.

[102] L. V Debelenko, S.C. Raimondi, N. Daw, B.R. Shivakumar, D. Huang, M. Nelson, J.A. Bridge, Renal cell carcinoma with novel VCL–ALK fusion: new representative of ALK-associated tumor spectrum, Mod. Pathol. 24 (2011) 430–442. doi:10.1038/modpathol.2010.213.

[103] A. Drilon, S. Siena, S.H.I. Ou, M. Patel, M.J. Ahn, J. Lee, T.M. Bauer, A.F. Farago, J.J. Wheler, S. V. Liu, R. Doebele, L. Giannetta, G. Cerea, G. Marrapese, M. Schirru, A. Amatu, K. Bencardino, L. Palmeri, A. Sartore-Bianchi, A. Vanzulli, S. Cresta, S. Damian, M. Duca, E. Ardini, G. Li, J. Christiansen, K. Kowalski, A.D. Johnson, R. Patel, D. Luo, E. Chow-Maneval, Z. Hornby, P.S. Multani, A.T. Shaw, F.G. De Braud, Safety and antitumor activity of the multitargeted pan-TRK, ROS1, and ALK inhibitor entrectinib: Combined results from two phase I trials (ALKA-372-001 and STARTRK-1), Cancer Discov. 7 (2017) 400–409. doi:10.1158/2159-8290.CD-16-1237.

[104] T. Wiesner, W. Lee, A.C. Obenauf, L. Ran, R. Murali, Q.F. Zhang, E.W.P. Wong, W. Hu, S.N. Scott, R.H. Shah, I. Landa, J. Button, N. Lailler, A. Sboner, D. Gao, D. a. Murphy, Z. Cao, S.

Shukla, T.J. Hollmann, L. Wang, L. Borsu, T. Merghoub, G.K. Schwartz, M. a. Postow, C.E. Ariyan, J. a. Fagin, D. Zheng, M. Ladanyi, K.J. Busam, M.F. Berger, Y. Chen, P. Chi, Alternative transcription initiation leads to expression of a novel ALK isoform in cancer, Nature. (2015). doi:10.1038/nature15258.

[105] K.L. Couts, J. Bemis, J.A. Turner, S.M. Bagby, D. Murphy, J. Christiansen, J.D. Hintzsche, A. Le, T.M. Pitts, K. Wells, A. Applegate, C. Amato, P. Multani, E. Chow-Maneval, J.J. Tentler, Y.G. Shellman, M.J. Rioth, A.-C. Tan, R. Gonzalez, T. Medina, R.C. Doebele, W.A. Robinson, ALK Inhibitor Response in Melanomas Expressing EML4-ALK Fusions and Alternate ALK Isoforms, Mol. Cancer Ther. 17 (2018) 222–231. doi:10.1158/1535-7163.MCT-17-0472.

[106] L. Horn, J.G. Whisenant, H. Wakelee, K.L. Reckamp, H. Qiao, T.A. Leal, L. Du, J. Hernandez, V. Huang, G.R. Blumenschein, S.N. Waqar, S.P. Patel, J. Nieva, G.R. Oxnard, R.E. Sanborn, T. Shaffer, K. Garg, A. Holzhausen, K. Harrow, C. Liang, L.P. Lim, M. Li, C.M. Lovly, Monitoring therapeutic response and resistance: analysis of circulating tumor DNA in patients with ALK+ lung cancer, J. Thorac. Oncol. 14 (2019) 1901–1911. doi:10.1016/j.jtho.2019.08.003.

[107] I. Dagogo-Jack, A.R. Brannon, L.A. Ferris, C.D. Campbell, J.J. Lin, K.R. Schultz, J. Ackil, S. Stevens, L. Dardaei, S. Yoda, H. Hubbeling, S.R. Digumarthy, M. Riester, A.N. Hata, L. V. Sequist, I.T. Lennes, A.J. Iafrate, R.S. Heist, C.G. Azzoli, A.F. Farago, J.A. Engelman, J.K. Lennerz, C.H. Benes, R.J. Leary, A.T. Shaw, J.F. Gainor, Tracking the Evolution of Resistance to ALK Tyrosine Kinase Inhibitors Through Longitudinal Analysis of Circulating Tumor DNA, JCO Precis. Oncol. (2018) 1–14. doi:10.1200/PO.17.00160.

[108] S. Yoda, J.J. Lin, M.S. Lawrence, B.J. Burke, L. Friboulet, A. Langenbucher, L. Dardaei, K. Prutisto-Chang, I. Dagogo-Jack, S. Timofeevski, H. Hubbeling, J.F. Gainor, L.A. Ferris, A.K. Riley, K.E. Kattermann, D. Timonina, R.S. Heist, A.J. Iafrate, C.H. Benes, J.K. Lennerz, M. Mino-Kenudson, J.A. Engelman, T.W. Johnson, A.N. Hata, A.T. Shaw, Sequential ALK Inhibitors Can Select for Lorlatinib-Resistant Compound ALK Mutations in ALK-Positive Lung Cancer, Cancer Discov. 8 (2018) 714–729. doi:10.1158/2159-8290.CD-17-1256.

[109] A.T. Shaw, L. Friboulet, I. Leshchiner, J.F. Gainor, S. Bergqvist, A. Brooun, B.J. Burke, Y.-L. Deng, W. Liu, L. Dardaei, R.L. Frias, K.R. Schultz, J. Logan, L.P. James, T. Smeal, S. Timofeevski, R. Katayama, A.J. Iafrate, L. Le, M. McTigue, G. Getz, T.W. Johnson, J.A. Engelman, Resensitization to Crizotinib by the Lorlatinib ALK Resistance Mutation L1198F., N. Engl. J. Med. 374 (2015) 54–61. doi:10.1056/NEJMoa1508887.

[110] M.J. Niederst, J. a Engelman, Bypass mechanisms of resistance to receptor tyrosine kinase inhibition in lung cancer., Sci. Signal. 6 (2013) re6. doi:10.1126/scisignal.2004652.

[111] J.P. Wong, J.R. Todd, M.A. Finetti, F. McCarthy, M. Broncel, S. Vyse, M.T. Luczynski, S. Crosier, K.A. Ryall, K. Holmes, L.S. Payne, F. Daley, P. Wai, A. Jenks, B. Tanos, A.C. Tan, R.C. Natrajan, D. Williamson, P.H. Huang, Dual Targeting of PDGFRα and FGFR1 Displays

Synergistic Efficacy in Malignant Rhabdoid Tumors, Cell Rep. 17 (2016) 1265–1275. doi:10.1016/j.celrep.2016.10.005.

[112] A.S. Crystal, A.T. Shaw, L. V Sequist, L. Friboulet, M.J. Niederst, E.L. Lockerman, R.L. Frias, J.F. Gainor, A. Amzallag, P. Greninger, D. Lee, A. Kalsy, M. Gomez-Caraballo, L. Elamine, E. Howe, W. Hur, E. Lifshits, H.E. Robinson, R. Katayama, A.C. Faber, M.M. Awad, S. Ramaswamy, M. Mino-Kenudson, a J. Iafrate, C.H. Benes, J. a Engelman, Patient-derived models of acquired resistance can identify effective drug combinations for cancer, Science (80-.). 346 (2014) 1480–1486. doi:10.1126/science.1254721.

[113] R. Katayama, A.T. Shaw, T.M. Khan, M. Mino-Kenudson, B.J. Solomon, B. Halmos, N.A. Jessop, J.C. Wain, A.T. Yeo, C. Benes, L. Drew, J.C. Saeh, K. Crosby, L. V Sequist, A.J. Iafrate, J.A. Engelman, Mechanisms of Acquired Crizotinib Resistance in ALK-Rearranged Lung Cancers, Sci. Transl. Med. 4 (2012) 120ra17-120ra17. doi:10.1126/scitranslmed.3003316.

[114] J. Tanizaki, I. Okamoto, T. Okabe, K. Sakai, K. Tanaka, H. Hayashi, H. Kaneda, K. Takezawa, K. Kuwata, H. Yamaguchi, E. Hatashita, K. Nishio, K. Nakagawa, Activation of HER family signaling as a mechanism of acquired resistance to ALK inhibitors in EML4-ALK-positive non-small cell lung cancer, Clin. Cancer Res. 18 (2012) 6219–6226. doi:10.1158/1078-0432.CCR-12-0392.

[115] D.R. Camidge, W. Pao, L. V Sequist, Acquired resistance to TKIs in solid tumours: learning from lung cancer., Nat. Rev. Clin. Oncol. 11 (2014) 473–81. doi:10.1038/nrclinonc.2014.104.

[116] S.K. Nelson-Taylor, A.T. Le, M. Yoo, L. Schubert, K.M. Mishall, A. Doak, M. Varella-Garcia, A.-C. Tan, R.C. Doebele, Resistance to RET-Inhibition in RET-Rearranged NSCLC Is Mediated By Reactivation of RAS/MAPK Signaling, Mol. Cancer Ther. 16 (2017) 1623–1633. doi:10.1158/1535-7163.MCT-17-0008.

[117] C.M. Blakely, E. Pazarentzos, V. Olivas, S. Asthana, J.J. Yan, I. Tan, G. Hrustanovic, E. Chan, L. Lin, D.S. Neel, W. Newton, K.L. Bobb, T.R. Fouts, J. Meshulam, M.A. Gubens, D.M. Jablons, J.R. Johnson, S. Bandyopadhyay, N.J. Krogan, T.G. Bivona, NF-κB-Activating Complex Engaged in Response to EGFR Oncogene Inhibition Drives Tumor Cell Survival and Residual Disease in Lung Cancer, Cell Rep. 11 (2015) 98–110. doi:10.1016/j.celrep.2015.03.012.

[118] a. L. Pritchard, N.K. Hayward, Molecular Pathways: Mitogen-Activated Protein Kinase Pathway Mutations and Drug Resistance, Clin. Cancer Res. 19 (2013) 2301–2309. doi:10.1158/1078-0432.CCR-12-0383.

[119] L. Dardaei, H.Q. Wang, M. Singh, P. Fordjour, K.X. Shaw, S. Yoda, G. Kerr, K. Yu, J. Liang, Y. Cao, Y. Chen, M.S. Lawrence, A. Langenbucher, J.F. Gainor, L. Friboulet, I. Dagogo-Jack,

D.T. Myers, E. Labrot, D. Ruddy, M. Parks, D. Lee, R.H. DiCecca, S. Moody, H. Hao, M. Mohseni, M. LaMarche, J. Williams, K. Hoffmaster, G. Caponigro, A.T. Shaw, A.N. Hata, C.H. Benes, F. Li, J.A. Engelman, SHP2 inhibition restores sensitivity in ALK-rearranged non-small-cell lung cancer resistant to ALK inhibitors, Nat. Med. 24 (2018) 512–517. doi:10.1038/nm.4497.

[120] A. Courtin, T. Smyth, K. Hearn, H.K. Saini, N.T. Thompson, J.F. Lyons, N.G. Wallis, Emergence of resistance to tyrosine kinase inhibitors in non-small-cell lung cancer can be delayed by an upfront combination with the HSP90 inhibitor onalespib, Br. J. Cancer. 115 (2016) 1069–1077. doi:10.1038/bjc.2016.294.

[121] M.A. Nieto, R.Y.-J. Huang, R.A. Jackson, J.P. Thiery, EMT: 2016, Cell. 166 (2016) 21–45. doi:10.1016/j.cell.2016.06.028.

[122] H.R. Kim, W.S. Kim, Y.J. Choi, C.M. Choi, J.K. Rho, J.C. Lee, Epithelial-mesenchymal transition leads to crizotinib resistance in H2228 lung cancer cells with EML4-ALK translocation, Mol. Oncol. 7 (2013) 1093–1102. doi:10.1016/j.molonc.2013.08.001.

[123] C. Voena, L.M. Varesio, L. Zhang, M. Menotti, T. Poggio, E. Panizza, Q. Wang, V.G. Minero, S. Fagoonee, M. Compagno, F. Altruda, S. Monti, R. Chiarle, Oncogenic ALK regulates EMT in non-small cell lung carcinoma through repression of the epithelial splicing regulatory protein 1, Oncotarget. (2016). doi:10.18632/oncotarget.8955.

[124] A. Gower, W.-H. Hsu, S.-T. Hsu, Y. Wang, G. Giaccone, EMT is associated with, but does not drive resistance to ALK inhibitors among EML4-ALK non-small cell lung cancer, Mol. Oncol. 10 (2016) 601–609. doi:10.1016/j.molonc.2015.11.007.

[125] K. Fukuda, S. Takeuchi, S. Arai, R. Katayama, S. Nanjo, A. Tanimoto, A. Nishiyama, T. Nakagawa, H. Taniguchi, T. Suzuki, T. Yamada, H. Nishihara, H. Ninomiya, Y. Ishikawa, S. Baba, K. Takeuchi, A. Horiike, N. Yanagitani, M. Nishio, S. Yano, Epithelial-to-Mesenchymal Transition Is a Mechanism of ALK Inhibitor Resistance in Lung Cancer Independent of ALK Mutation Status, Cancer Res. 79 (2019) 1658–1670. doi:10.1158/0008-5472.CAN-18-2052.

[126] S. V. Sharma, D.Y. Lee, B. Li, M.P. Quinlan, F. Takahashi, S. Maheswaran, U. McDermott, N. Azizian, L. Zou, M.A. Fischbach, K.K. Wong, K. Brandstetter, B. Wittner, S. Ramaswamy, M. Classon, J. Settleman, A Chromatin-Mediated Reversible Drug-Tolerant State in Cancer Cell Subpopulations, Cell. 141 (2010) 69–80. doi:10.1016/j.cell.2010.02.027.

[127] M. Greaves, C.C. Maley, Clonal evolution in cancer., Nature. 481 (2012) 306–13. doi:10.1038/nature10762.

[128] A. V. Kurtova, J. Xiao, Q. Mo, S. Pazhanisamy, R. Krasnow, S.P. Lerner, F. Chen, T.T. Roh, E. Lay, P.L. Ho, K.S. Chan, Blocking PGE2-induced tumour repopulation abrogates bladder cancer chemoresistance, Nature. 517 (2014) 209–213. doi:10.1038/nature14034.

[129] A. Singh, J. Settleman, EMT, cancer stem cells and drug resistance: an emerging axis of evil in the war on cancer, Oncogene. 29 (2010) 4741–4751. doi:10.1038/onc.2010.215.

[130] D. Raha, T.R. Wilson, J. Peng, D. Peterson, P. Yue, M. Evangelista, C. Wilson, M. Merchant, J. Settleman, The Cancer Stem Cell Marker Aldehyde Dehydrogenase Is Required to Maintain a Drug-Tolerant Tumor Cell Subpopulation, Cancer Res. 74 (2014) 3579–3590. doi:10.1158/0008-5472.CAN-13-3456.

[131] M. Vinogradova, V.S. Gehling, A. Gustafson, S. Arora, C.A. Tindell, C. Wilson, K.E. Williamson, G.D. Guler, P. Gangurde, W. Manieri, J. Busby, E.M. Flynn, F. Lan, H. Kim, S. Odate, A.G. Cochran, Y. Liu, M. Wongchenko, Y. Yang, T.K. Cheung, T.M. Maile, T. Lau, M. Costa, G. V Hegde, E. Jackson, R. Pitti, D. Arnott, C. Bailey, S. Bellon, R.T. Cummings, B.K. Albrecht, J.-C. Harmange, J.R. Kiefer, P. Trojer, M. Classon, An inhibitor of KDM5 demethylases reduces survival of drug-tolerant cancer cells, Nat. Chem. Biol. 12 (2016) 531–538. doi:10.1038/nchembio.2085.

[132] M. Ramirez, S. Rajaram, R.J. Steininger, D. Osipchuk, M.A. Roth, L.S. Morinishi, L. Evans, W. Ji, C.-H. Hsu, K. Thurley, S. Wei, A. Zhou, P.R. Koduru, B.A. Posner, L.F. Wu, S.J. Altschuler, Diverse drug-resistance mechanisms can emerge from drug-tolerant cancer persister cells, Nat. Commun. 7 (2016) 10690. doi:10.1038/ncomms10690.

[133] M.J. Hangauer, V.S. Viswanathan, M.J. Ryan, D. Bole, J.K. Eaton, A. Matov, J. Galeas, H.D. Dhruv, M.E. Berens, S.L. Schreiber, F. McCormick, M.T. McManus, Drug-tolerant persister cancer cells are vulnerable to GPX4 inhibition, Nature. (2017). doi:10.1038/nature24297.

[134] M. Jamal-Hanjani, G.A. Wilson, N. McGranahan, N.J. Birkbak, T.B.K. Watkins, S. Veeriah, S. Shafi, D.H. Johnson, R. Mitter, R. Rosenthal, M. Salm, S. Horswell, M. Escudero, N. Matthews, A. Rowan, T. Chambers, D.A. Moore, S. Turajlic, H. Xu, S.-M. Lee, M.D. Forster, T. Ahmad, C.T. Hiley, C. Abbosh, M. Falzon, E. Borg, T. Marafioti, D. Lawrence, M. Hayward, S. Kolvekar, N. Panagiotopoulos, S.M. Janes, R. Thakrar, A. Ahmed, F. Blackhall, Y. Summers, R. Shah, L. Joseph, A.M. Quinn, P.A. Crosbie, B. Naidu, G. Middleton, G. Langman, S. Trotter, M. Nicolson, H. Remmen, K. Kerr, M. Chetty, L. Gomersall, D.A. Fennell, A. Nakas, S. Rathinam, G. Anand, S. Khan, P. Russell, V. Ezhil, B. Ismail, M. Irvin-Sellers, V. Prakash, J.F. Lester, M. Kornaszewska, R. Attanoos, H. Adams, H. Davies, S. Dentro, P. Taniere, B. O'Sullivan, H.L. Lowe, J.A. Hartley, N. Iles, H. Bell, Y. Ngai, J.A. Shaw, J. Herrero, Z. Szallasi, R.F. Schwarz, A. Stewart, S.A. Quezada, J. Le Quesne, P. Van Loo, C. Dive, A. Hackshaw, C. Swanton, Tracking the Evolution of Non–Small-Cell Lung Cancer, N. Engl. J. Med. 376 (2017) 2109–2121. doi:10.1056/NEJMoa1616288.

[135] C. Grassberger, D.M. McClatchy, C. Geng, S.C. Kamran, F. Fintelmann, Y.E. Maruvka, Z. Piotrowska, H. Willers, L. V Sequist, A.N. Hata, H. Paganetti, Patient-specific tumor growth trajectories determine persistent and resistant cancer cell populations during treatment with targeted therapies, Cancer Res. (2019) canres.3652.2018. doi:10.1158/0008-5472.CAN-18-

3652.

[136] H. Terai, S. Kitajima, D.S. Potter, Y. Matsui, L.G. Quiceno, T. Chen, T. Kim, M. Rusan, T.C. Thai, F. Piccioni, K.A. Donovan, N. Kwiatkowski, K. Hinohara, G. Wei, N.S. Gray, E.S. Fischer, K.-K. Wong, T. Shimamura, A. Letai, P.S. Hammerman, D.A. Barbie, ER Stress Signaling Promotes the Survival of Cancer "Persister Cells" Tolerant to EGFR Tyrosine Kinase Inhibitors, Cancer Res. 78 (2018) 1044–1057. doi:10.1158/0008-5472.CAN-17-1904.

[137] R. Vander Velde, N. Yoon, V. Marusyk, A. Dhawan, O. Balynska, D. Peral, D. Myroshnychenko, J. Poleszczuk, L. Kenian, O. Mian, M. Abazeed, E. Haura, J.G. Scott, A. Marusyk, Resistance to ALK targeting therapies as a gradual Darwinian adaptation to inhibitor specific selective pressures, BioArxiv. (2019). doi:10.1101/504837.

[138] A. Kaznatcheev, J. Peacock, D. Basanta, A. Marusyk, J.G. Scott, Fibroblasts and alectinib switch the evolutionary games played by non-small cell lung cancer, Nat. Ecol. Evol. 3 (2019) 450–456. doi:10.1038/s41559-018-0768-z.

[139] D. Hanahan, R. a Weinberg, Hallmarks of cancer: the next generation., Cell. 144 (2011) 646–74. doi:10.1016/j.cell.2011.02.013.

[140] M. Malumbres, M. Barbacid, Mammalian cyclin-dependent kinases, Trends Biochem. Sci. 30 (2005) 630–641. doi:10.1016/j.tibs.2005.09.005.

[141] J. Cicenas, K. Kalyan, A. Sorokinas, A. Jatulyte, D. Valiunas, A. Kaupinis, M. Valius, Highlights of the Latest Advances in Research on CDK Inhibitors, Cancers (Basel). 6 (2014) 2224–2242. doi:10.3390/cancers6042224.

[142] K.E. Knudsen, J. Alan Diehl, C.A. Haiman, E.S. Knudsen, Cyclin D1: Polymorphism, aberrant splicing and cancer risk, Oncogene. 25 (2006) 1620–1628. doi:10.1038/sj.onc.1209371.

[143] F. Lu, A.B. Gladden, J.A. Diehl, An alternatively spliced cyclin D1 isoform, cyclin D1b, is a nuclear oncogene., Cancer Res. 63 (2003) 7056–61. doi:10.1158/0008-5472.CAN-06-1484.

[144] A.M. Karst, P.M. Jones, N. Vena, A.H. Ligon, J.F. Liu, M.S. Hirsch, D. Etemadmoghadam, D.D.L. Bowtell, R. Drapkin, Cyclin E1 deregulation occurs early in secretory cell transformation to promote formation of fallopian tube-derived high-grade serous ovarian cancers, Cancer Res. 74 (2014) 1141–1152. doi:10.1158/0008-5472.CAN-13-2247.

[145] U. Asghar, A.K. Witkiewicz, N.C. Turner, E.S. Knudsen, The history and future of targeting cyclin-dependent kinases in cancer therapy, Nat. Rev. Drug Discov. 14 (2015) 130–146. doi:10.1038/nrd4504.

[146] K. Aaltonen, R.M. Amini, P. Heikkilä, K. Aittomäki, A. Tamminen, H. Nevanlinna, C. Blomqvist, High cyclin B1 expression is associated with poor survival in breast cancer, Br. J. Cancer. 100 (2009) 1055–1060. doi:10.1038/sj.bjc.6604874.

[147] P.K. Gopalan, M.C. Pinder, A. Chiappori, A.M. Ivey, A. Gordillo Villegas, F.J. Kaye, A phase II clinical trial of the CDK 4/6 inhibitor palbociclib (PD 0332991) in previously treated, advanced non-small cell lung cancer (NSCLC) patients with inactivated CDKN2A., J. Clin. Oncol. 32 (2014) 8077. doi:10.1200/jco.2014.32.15_suppl.8077.

[148] A.M. Senderowicz, D. Headlee, S.F. Stinson, R.M. Lush, N. Kalil, L. Villalba, K. Hill, S.M. Steinberg, W.D. Figg, A. Tompkins, S.G. Arbuck, E.A. Sausville, Phase I trial of continuous infusion flavopiridol, a novel cyclin-dependent kinase inhibitor, in patients with refractory neoplasms., J. Clin. Oncol. 16 (1998) 2986–99. doi:10.1200/JCO.1998.16.9.2986.

[149] D. Parry, T. Guzi, F. Shanahan, N. Davis, D. Prabhavalkar, D. Wiswell, W. Seghezzi, K. Paruch, M.P. Dwyer, R. Doll, A. Nomeir, W. Windsor, T. Fischmann, Y. Wang, M. Oft, T. Chen, P. Kirschmeier, E.M. Lees, Dinaciclib (SCH 727965), a Novel and Potent Cyclin-Dependent Kinase Inhibitor, Mol. Cancer Ther. 9 (2010) 2344–2353. doi:10.1158/1535-7163.MCT-10-0324.

[150] N. Kwiatkowski, T. Zhang, P.B. Rahl, B.J. Abraham, J. Reddy, S.B. Ficarro, A. Dastur, A. Amzallag, S. Ramaswamy, B. Tesar, C.E. Jenkins, N.M. Hannett, D. McMillin, T. Sanda, T. Sim, N.D. Kim, T. Look, C.S. Mitsiades, A.P. Weng, J.R. Brown, C.H. Benes, J.A. Marto, R.A. Young, N.S. Gray, Targeting transcription regulation in cancer with a covalent CDK7 inhibitor, Nature. 511 (2014) 616–620. doi:10.1038/nature13393.

[151] D.W. Fry, P.J. Harvey, P.R. Keller, W.L. Elliott, M. Meade, E. Trachet, M. Albassam, X. Zheng, W.R. Leopold, N.K. Pryer, P.L. Toogood, Specific inhibition of cyclin-dependent kinase 4/6 by PD 0332991 and associated antitumor activity in human tumor xenografts., Mol. Cancer Ther. 3 (2004) 1427–38. doi:3/11/1427 [pii].

[152] A.C. Wood, K. Krytska, H.T. Ryles, N.R. Infarinato, R. Sano, T.D. Hansel, L.S. Hart, F.J. King, T.R. Smith, E. Ainscow, K.B. Grandinetti, T. Tuntland, S. Kim, G. Caponigro, Y.Q. He, S. Krupa, N. Li, J.L. Harris, Y.P. Mossé, Dual ALK and CDK4/6 Inhibition Demonstrates Synergy against Neuroblastoma, Clin. Cancer Res. 23 (2017) 2856–2868. doi:10.1158/1078-0432.CCR-16-1114.

[153] J.E. Bradner, D. Hnisz, R.A. Young, Transcriptional Addiction in Cancer, Cell. 168 (2017) 629–643. doi:10.1016/j.cell.2016.12.013.

[154] A. Valenciaga, M. Saji, L. Yu, X. Zhang, C. Bumrah, A.S. Yilmaz, C.M. Knippler, W. Miles, T.J. Giordano, G.J. Cote, M.D. Ringel, Transcriptional targeting of oncogene addiction in medullary thyroid cancer, JCI Insight. 3 (2018). doi:10.1172/jci.insight.122225.

[155] C.L. Christensen, N. Kwiatkowski, B.J. Abraham, J. Carretero, F. Al-Shahrour, T. Zhang, E. Chipumuro, G.S. Herter-Sprie, E.A. Akbay, A. Altabef, J. Zhang, T. Shimamura, M. Capelletti, J.B. Reibel, J.D. Cavanaugh, P. Gao, Y. Liu, S.R. Michaelsen, H.S. Poulsen, A.R. Aref, D.A. Barbie, J.E. Bradner, R.E. George, N.S. Gray, R.A. Young, K.-K. Wong, Targeting

Transcriptional Addictions in Small Cell Lung Cancer with a Covalent CDK7 Inhibitor, Cancer Cell. 27 (2015) 149. doi:10.1016/j.ccell.2014.12.007.

[156] M. Rusan, K. Li, Y. Li, C.L. Christensen, B.J. Abraham, N. Kwiatkowski, K.A. Buczkowski, B. Bockorny, T. Chen, S. Li, K. Rhee, H. Zhang, W. Chen, H. Terai, T. Tavares, A.L. Leggett, T. Li, Y. Wang, T. Zhang, T.-J. Kim, S.-H. Hong, N. Poudel-Neupane, M. Silkes, T. Mudianto, L. Tan, T. Shimamura, M. Meyerson, A.J. Bass, H. Watanabe, N.S. Gray, R.A. Young, K.-K. Wong, P.S. Hammerman, Suppression of Adaptive Responses to Targeted Cancer Therapy by Transcriptional Repression, Cancer Discov. 8 (2018) 59–73. doi:10.1158/2159-8290.CD-17-0461.

[157] P.K. Parua, G.T. Booth, M. Sansó, B. Benjamin, J.C. Tanny, J.T. Lis, R.P. Fisher, A Cdk9-PP1 switch regulates the elongation-termination transition of RNA polymerase II, Nature. 558 (2018) 460–464. doi:10.1038/s41586-018-0214-z.

[158] C.C. Ebmeier, B. Erickson, B.L. Allen, M.A. Allen, H. Kim, N. Fong, J.R. Jacobsen, K. Liang, A. Shilatifard, R.D. Dowell, W.M. Old, D.L. Bentley, D.J. Taatjes, Human TFIIH Kinase CDK7 Regulates Transcription-Associated Chromatin Modifications, Cell Rep. 20 (2017) 1173–1186. doi:10.1016/j.celrep.2017.07.021.

[159] K.M. Harlen, L.S. Churchman, The code and beyond: Transcription regulation by the RNA polymerase II carboxy-terminal domain, Nat. Rev. Mol. Cell Biol. 18 (2017) 263–273. doi:10.1038/nrm.2017.10.

[160] M.S. Akhtar, M. Heidemann, J.R. Tietjen, D.W. Zhang, R.D. Chapman, D. Eick, A.Z. Ansari, TFIIH Kinase Places Bivalent Marks on the Carboxy-Terminal Domain of RNA Polymerase II, Mol. Cell. 34 (2009) 387–393. doi:10.1016/j.molcel.2009.04.016.

[161] S. Larochelle, R. Amat, K. Glover-Cutter, M. Sansó, C. Zhang, J.J. Allen, K.M. Shokat, D.L. Bentley, R.P. Fisher, Cyclin-dependent kinase control of the initiation-to-elongation switch of RNA polymerase II, Nat. Struct. Mol. Biol. 19 (2012) 1108–1115. doi:10.1038/nsmb.2399.

[162] N. Czudnochowski, C.A. Bösken, M. Geyer, Serine-7 but not serine-5 phosphorylation primes RNA polymerase II CTD for P-TEFb recognition, Nat. Commun. 3 (2012). doi:10.1038/ncomms1846.

[163] C.M. Olson, Y. Liang, A. Leggett, W.D. Park, L. Li, C.E. Mills, S.Z. Elsarrag, S.B. Ficarro, T. Zhang, R. Düster, M. Geyer, T. Sim, J.A. Marto, P.K. Sorger, K.D. Westover, C.Y. Lin, N. Kwiatkowski, N.S. Gray, Development of a Selective CDK7 Covalent Inhibitor Reveals Predominant Cell-Cycle Phenotype, Cell Chem. Biol. (2019) 1–12. doi:10.1016/j.chembiol.2019.02.012.

[164] H. Zhang, S. Pandey, M. Travers, H. Sun, G. Morton, J. Madzo, W. Chung, J. Khowsathit, O. Perez-Leal, C.A. Barrero, C. Merali, Y. Okamoto, T. Sato, J. Pan, J. Garriga, N. V. Bhanu, J. Simithy, B. Patel, J. Huang, N.J.-M. Raynal, B.A. Garcia, M.A. Jacobson, C. Kadoch, S.

Merali, Y. Zhang, W. Childers, M. Abou-Gharbia, J. Karanicolas, S.B. Baylin, C.A. Zahnow, J. Jelinek, X. Graña, J.-P.J. Issa, Targeting CDK9 Reactivates Epigenetically Silenced Genes in Cancer, Cell. 175 (2018) 1244-1258.e26. doi:10.1016/j.cell.2018.09.051.

[165] L. Galluzzi, I. Vitale, S.A. Aaronson, J.M. Abrams, D. Adam, P. Agostinis, E.S. Alnemri, L. Altucci, I. Amelio, D.W. Andrews, M. Annicchiarico-Petruzzelli, A. V. Antonov, E. Arama, E.H. Baehrecke, N.A. Barlev, N.G. Bazan, F. Bernassola, M.J.M. Bertrand, K. Bianchi, M. V. Blagosklonny, K. Blomgren, C. Borner, P. Boya, C. Brenner, M. Campanella, E. Candi, D. Carmona-Gutierrez, F. Cecconi, F.K.M. Chan, N.S. Chandel, E.H. Cheng, J.E. Chipuk, J.A. Cidlowski, A. Ciechanover, G.M. Cohen, M. Conrad, J.R. Cubillos-Ruiz, P.E. Czabotar, V. D'Angiolella, T.M. Dawson, V.L. Dawson, V. De Laurenzi, R. De Maria, K.-M. Debatin, R.J. DeBerardinis, M. Deshmukh, N. Di Daniele, F. Di Virgilio, V.M. Dixit, S.J. Dixon, C.S. Duckett, B.D. Dynlacht, W.S. El-Deiry, J.W. Elrod, G.M. Fimia, S. Fulda, A.J. García-Sáez, A.D. Garg, C. Garrido, E. Gavathiotis, P. Golstein, E. Gottlieb, D.R. Green, L.A. Greene, H. Gronemeyer, A. Gross, G. Hajnoczky, J.M. Hardwick, I.S. Harris, M.O. Hengartner, C. Hetz, H. Ichijo, M. Jäättelä, B. Joseph, P.J. Jost, P.P. Juin, W.J. Kaiser, M. Karin, T. Kaufmann, O. Kepp, A. Kimchi, R.N. Kitsis, D.J. Klionsky, R.A. Knight, S. Kumar, S.W. Lee, J.J. Lemasters, B. Levine, A. Linkermann, S.A. Lipton, R.A. Lockshin, C. López-Otín, S.W. Lowe, T. Luedde, E. Lugli, M. MacFarlane, F. Madeo, M. Malewicz, W. Malorni, G. Manic, J.-C. Marine, S.J. Martin, J.-C. Martinou, J.P. Medema, P. Mehlen, P. Meier, S. Melino, E.A. Miao, J.D. Molkentin, U.M. Moll, C. Muñoz-Pinedo, S. Nagata, G. Nuñez, A. Oberst, M. Oren, M. Overholtzer, M. Pagano, T. Panaretakis, M. Pasparakis, J.M. Penninger, D.M. Pereira, S. Pervaiz, M.E. Peter, M. Piacentini, P. Pinton, J.H.M. Prehn, H. Puthalakath, G.A. Rabinovich, M. Rehm, R. Rizzuto, C.M.P. Rodrigues, D.C. Rubinsztein, T. Rudel, K.M. Ryan, E. Sayan, L. Scorrano, F. Shao, Y. Shi, J. Silke, H.-U. Simon, A. Sistigu, B.R. Stockwell, A. Strasser, G. Szabadkai, S.W.G. Tait, D. Tang, N. Tavernarakis, A. Thorburn, Y. Tsujimoto, B. Turk, T. Vanden Berghe, P. Vandenabeele, M.G. Vander Heiden, A. Villunger, H.W. Virgin, K.H. Vousden, D. Vucic, E.F. Wagner, H. Walczak, D. Wallach, Y. Wang, J.A. Wells, W. Wood, J. Yuan, Z. Zakeri, B. Zhivotovsky, L. Zitvogel, G. Melino, G. Kroemer, Molecular mechanisms of cell death: recommendations of the Nomenclature Committee on Cell Death 2018, Cell Death Differ. 25 (2018) 486–541. doi:10.1038/s41418-017-0012-4.

[166] G.R. Bean, Y.T. Ganesan, Y. Dong, S. Takeda, H. Liu, P.M. Chan, Y. Huang, L.A. Chodosh, G.P. Zambetti, J.J.-D. Hsieh, E.H.-Y. Cheng, PUMA and BIM Are Required for Oncogene Inactivation-Induced Apoptosis, Sci. Signal. 6 (2013) ra20–ra20. doi:10.1126/scisignal.2003483.

[167] A.N. Hata, J.A. Engelman, A.C. Faber, The BCL2 family: Key mediators of the apoptotic response to targeted anticancer therapeutics, Cancer Discov. 5 (2015) 475–487. doi:10.1158/2159-8290.CD-15-0011.

[168] C. Du, M. Fang, Y. Li, L. Li, X. Wang, Smac, a mitochondrial protein that promotes

cytochrome c-dependent caspase activation by eliminating IAP inhibition, Cell. 102 (2000) 33–42. doi:10.1016/S0092-8674(00)00008-8.

[169] P. Li, D. Nijhawan, I. Budihardjo, S.M. Srinivasula, M. Ahmad, E.S. Alnemri, X. Wang, Cytochrome c and dATP-Dependent Formation of Apaf-1/Caspase-9 Complex Initiates an Apoptotic Protease Cascade, Cell. 91 (1997) 479–489. doi:10.1016/S0092-8674(00)80434-1.

[170] O. Julien, J.A. Wells, Caspases and their substrates, Cell Death Differ. 24 (2017) 1380–1389. doi:10.1038/cdd.2017.44.

[171] B.P. Eckelman, G.S. Salvesen, F.L. Scott, Human inhibitor of apoptosis proteins: Why XIAP is the black sheep of the family, EMBO Rep. 7 (2006) 988–994. doi:10.1038/sj.embor.7400795.

[172] Y. Subburaj, K. Cosentino, M. Axmann, E. Pedrueza-Villalmanzo, E. Hermann, S. Bleicken, J. Spatz, A.J. García-Sáez, Bax monomers form dimer units in the membrane that further self-assemble into multiple oligomeric species, Nat. Commun. 6 (2015) 1–11. doi:10.1038/ncomms9042.

[173] A.R.D. Delbridge, S. Grabow, A. Strasser, D.L. Vaux, Thirty years of BCL-2: translating cell death discoveries into novel cancer therapies, Nat. Rev. Cancer. 16 (2016) 99–109. doi:10.1038/nrc.2015.17.

[174] M.C. Wei, W. Zong, E.H. Cheng, T. Lindsten, A.J. Ross, K.A. Roth, G.R. Macgregor, B. Craig, S.J. Korsmeyer, Proapoptotic Bax and Bak: A Requesite Gateway to Mitochondrial Dysfunction and Death, Science (80-.). 292 (2001) 727–730. doi:10.1126/science.1059108.Proapoptotic.

[175] L. Galluzzi, J.M. Bravo-San Pedro, G. Kroemer, Organelle-specific initiation of cell death, Nat. Cell Biol. 16 (2014) 728–736. doi:10.1038/ncb3005.

[176] P.E. Czabotar, G. Lessene, A. Strasser, J.M. Adams, Control of apoptosis by the BCL-2 protein family: implications for physiology and therapy, Nat. Rev. Mol. Cell Biol. 15 (2014) 49–63. doi:10.1038/nrm3722.

[177] F. Llambi, T. Moldoveanu, S.W.G. Tait, L. Bouchier-Hayes, J. Temirov, L.L. McCormick, C.P. Dillon, D.R. Green, A Unified Model of Mammalian BCL-2 Protein Family Interactions at the Mitochondria, Mol. Cell. 44 (2011) 517–531. doi:10.1016/j.molcel.2011.10.001.

[178] A.C. Faber, R.B. Corcoran, H. Ebi, L. V. Sequist, B.A. Waltman, E. Chung, J. Incio, S.R. Digumarthy, S.F. Pollack, Y. Song, A. Muzikansky, E. Lifshits, S. Roberge, E.J. Coffman, C.H. Benes, H.L. Gómez, J. Baselga, C.L. Arteaga, M.N. Rivera, D. Dias-Santagata, R.K. Jain, J.A. Engelman, BIM expression in treatment-naïve cancers predicts responsiveness to kinase inhibitors, Cancer Discov. 1 (2011) 352–365. doi:10.1158/2159-8290.CD-11-0106.

[179] K.-A. Song, Y. Hosono, C. Turner, S. Jacob, T.L. Lochmann, Y. Murakami, N.U. Patel, J. Ham, B. Hu, K.M. Powell, C.M. Coon, B.E. Windle, Y. Oya, J.E. Koblinski, H. Harada, J.D. Leverson, A.J. Souers, A.N. Hata, S. Boikos, Y. Yatabe, H. Ebi, A.C. Faber, Increased Synthesis of MCL-1 Protein Underlies Initial Survival of EGFR -Mutant Lung Cancer to EGFR Inhibitors and Provides a Novel Drug Target, Clin. Cancer Res. 24 (2018) 5658–5672. doi:10.1158/1078-0432.CCR-18-0304.

[180] T.H. Marsilje, W. Pei, B. Chen, W. Lu, T. Uno, Y. Jin, T. Jiang, S. Kim, N. Li, M. Warmuth, Y. Sarkisova, F. Sun, A. Steffy, A.C. Pferdekamper, A.G. Li, S.B. Joseph, Y. Kim, B. Liu, T. Tuntland, X. Cui, N.S. Gray, R. Steensma, Y. Wan, J. Jiang, G. Chopiuk, J. Li, W.P. Gordon, W. Richmond, K. Johnson, J. Chang, T. Groessl, Y.-Q. He, A. Phimister, A. Aycinena, C.C. Lee, B. Bursulaya, D.S. Karanewsky, H.M. Seidel, J.L. Harris, P.-Y. Michellys, Synthesis, Structure–Activity Relationships, and in Vivo Efficacy of the Novel Potent and Selective Anaplastic Lymphoma Kinase (ALK) Inhibitor 5-Chloro- N 2-(2-isopropoxy-5-methyl-4-(piperidin-4-yl)phenyl)- N 4-(2-(isopropylsulfonyl)phenyl)pyrimidine-2,4-, J. Med. Chem. 56 (2013) 5675–5690. doi:10.1021/jm400402q.

[181] T. Arao, H. Fukumoto, M. Takeda, T. Tamura, N. Saijo, K. Nishio, Small in-frame deletion in the epidermal growth factor receptor as a target for ZD6474., Cancer Res. 64 (2004) 9101–4. doi:10.1158/0008-5472.CAN-04-2360.

[182] W. Pao, V.A. Miller, K.A. Politi, G.J. Riely, R. Somwar, M.F. Zakowski, M.G. Kris, H. Varmus, Acquired resistance of lung adenocarcinomas to gefitinib or erlotinib is associated with a second mutation in the EGFR kinase domain, PLoS Med. 2 (2005) 0225–0235. doi:10.1371/journal.pmed.0020073.

[183] A.N. Hata, M.J. Niederst, H.L. Archibald, M. Gomez-Caraballo, F.M. Siddiqui, H.E. Mulvey, Y.E. Maruvka, F. Ji, H.-E.C. Bhang, V. Krishnamurthy Radhakrishna, G. Siravegna, H. Hu, S. Raoof, E. Lockerman, A. Kalsy, D. Lee, C.L. Keating, D.A. Ruddy, L.J. Damon, A.S. Crystal, C. Costa, Z. Piotrowska, A. Bardelli, A.J. Iafrate, R.I. Sadreyev, F. Stegmeier, G. Getz, L. V Sequist, A.C. Faber, J.A. Engelman, Tumor cells can follow distinct evolutionary paths to become resistant to epidermal growth factor receptor inhibition., Nat. Med. 22 (2016) 262–269. doi:10.1038/nm.4040.

[184] G. Piro, S. Giacopuzzi, M. Bencivenga, C. Carbone, G. Verlato, M. Frizziero, M. Zanotto, M.M. Mina, V. Merz, R. Santoro, A. Zanoni, G. De Manzoni, G. Tortora, D. Melisi, TAK1-regulated expression of BIRC3 predicts resistance to preoperative chemoradiotherapy in oesophageal adenocarcinoma patients, Br. J. Cancer. 113 (2015) 878–885. doi:10.1038/bjc.2015.283.

[185] S. Huang, M. Hölzel, T. Knijnenburg, A. Schlicker, P. Roepman, U. McDermott, M. Garnett, W. Grernrum, C. Sun, A. Prahallad, F.H. Groenendijk, L. Mittempergher, W. Nijkamp, J. Neefjes, R. Salazar, P. ten Dijke, H. Uramoto, F. Tanaka, R.L. Beijersbergen, L.F.A. Wessels,

R. Bernards, MED12 Controls the Response to Multiple Cancer Drugs through Regulation of TGF-β Receptor Signaling, Cell. 151 (2012) 937–950. doi:10.1016/j.cell.2012.10.035.

[186] C. Perks, H. Zielinska, J. Holly, A. Bahl, Epithelial-to-mesenchymal transition in breast cancer: a role for insulin-like growth factor I and insulin-like growth factor–binding protein 3?, Breast Cancer Targets Ther. 7 (2015) 9. doi:10.2147/BCTT.S43932.

[187] S. Nakamichi, M. Seike, A. Miyanaga, M. Chiba, F. Zou, A. Takahashi, A. Ishikawa, S. Kunugi, R. Noro, K. Kubota, A. Gemma, Overcoming drug-tolerant cancer cell subpopulations showing AXL activation and epithelial-mesenchymal transition is critical in conquering ALK-positive lung cancer, Oncotarget. 9 (2018) 27242–27255. doi:10.18632/oncotarget.25531.

[188] S.J. Holland, A. Pan, C. Franci, Y. Hu, B. Chang, W. Li, M. Duan, A. Torneros, J. Yu, T.J. Heckrodt, J. Zhang, P. Ding, A. Apatira, J. Chua, R. Brandt, P. Pine, D. Goff, R. Singh, D.G. Payan, Y. Hitoshi, R428, a Selective Small Molecule Inhibitor of Axl Kinase, Blocks Tumor Spread and Prolongs Survival in Models of Metastatic Breast Cancer, Cancer Res. 70 (2010) 1544–1554. doi:10.1158/0008-5472.CAN-09-2997.

[189] J.A. Beaver, L. Amiri-Kordestani, R. Charlab, W. Chen, T. Palmby, A. Tilley, J.F. Zirkelbach, J. Yu, Q. Liu, L. Zhao, J. Crich, X.H. Chen, M. Hughes, E. Bloomquist, S. Tang, R. Sridhara, P.G. Kluetz, G. Kim, A. Ibrahim, R. Pazdur, P. Cortazar, FDA Approval: Palbociclib for the Treatment of Postmenopausal Patients with Estrogen Receptor-Positive, HER2-Negative Metastatic Breast Cancer, Clin. Cancer Res. 21 (2015) 4760–4766. doi:10.1158/1078-0432.CCR-15-1185.

[190] Y. Wang, A. Cornett, F.J. King, Y. Mao, F. Nigsch, C.G. Paris, G. McAllister, J.L. Jenkins, Evidence-Based and Quantitative Prioritization of Tool Compounds in Phenotypic Drug Discovery, Cell Chem. Biol. 23 (2016) 862–874. doi:10.1016/j.chembiol.2016.05.016.

[191] J.C. Byrd, C. Shinn, J.K. Waselenko, E.J. Fuchs, T.A. Lehman, P.L. Nguyen, I.W. Flinn, L.F. Diehl, E. Sausville, M.R. Grever, Flavopiridol induces apoptosis in chronic lymphocytic leukemia cells via activation of caspase-3 without evidence of bcl-2 modulation or dependence on functional p53., Blood. 92 (1998) 3804–16. doi:10.1182/blood.V100.1.194.

[192] A. Russell-Swetek, A.N. West, J.E. Mintern, J. Jenkins, C. Rodriguez-Galindo, R. Ribeiro, G.P. Zambetti, Identification of a novel TP53 germline mutation E285V in a rare case of paediatric adrenocortical carcinoma and choroid plexus carcinoma, J. Med. Genet. 45 (2008) 603–606. doi:10.1136/jmg.2008.059568.

[193] Y. Ma, W.D. Cress, E.B. Haura, Flavopiridol-induced apoptosis is mediated through up-regulation of E2F1 and repression of Mcl-1., Mol. Cancer Ther. 2 (2003) 73–81. http://www.ncbi.nlm.nih.gov/pubmed/12533675.

[194] N.R. Wall, D.S. O'Connor, J. Plescia, Y. Pommier, D.C. Altieri, Suppression of survivin phosphorylation on Thr^{34} by flavopiridol enhances tumor cell apoptosis, Cancer Res. 63 (2003) 230–235.

[195] M. V. Blagosklonny, Flavopiridol, An Inhibitor of Transcription: Implications, Problems and Solutions, Cell Cycle. 3 (2004) 1537–1542. doi:10.4161/cc.3.12.1278.

[196] R. Katayama, T. Sakashita, N. Yanagitani, H. Ninomiya, A. Horiike, L. Friboulet, J.F. Gainor, N. Motoi, A. Dobashi, S. Sakata, Y. Tambo, S. Kitazono, S. Sato, S. Koike, A. John Iafrate, M. Mino-Kenudson, Y. Ishikawa, A.T. Shaw, J.A. Engelman, K. Takeuchi, M. Nishio, N. Fujita, P-glycoprotein Mediates Ceritinib Resistance in Anaplastic Lymphoma Kinase-rearranged Non-small Cell Lung Cancer, EBioMedicine. 3 (2015) 54–66. doi:10.1016/j.ebiom.2015.12.009.

[197] M.R. Yun, H.M. Choi, Y.W. Lee, H.S. Joo, C.W. Park, J.W. Choi, D.H. Kim, H.N. Kang, K.-H. Pyo, E.J. Shin, H.S. Shim, R.A. Soo, J.C.-H. Yang, S.S. Lee, H. Chang, M.H. Kim, M.H. Hong, H.R. Kim, B.C. Cho, Targeting <scp>YAP</scp> to overcome acquired resistance to <scp>ALK</scp> inhibitors in *<scp>ALK</scp>* -rearranged lung cancer, EMBO Mol. Med. (2019) e10581. doi:10.15252/emmm.201910581.

[198] M.R. Yun, S.M. Lim, S.-K. Kim, H.M. Choi, K.H. Pyo, S.K. Kim, J.M. Lee, Y.W. Lee, J.W. Choi, H.R. Kim, M.H. Hong, K. Haam, N. Huh, J.H. Kim, Y.S. Kim, H.S. Shim, R.A. Soo, J.-Y. Shih, J.C.-H. Yang, M. Kim, B.C. Cho, Enhancer remodeling and microRNA alterations are associated with acquired resistance to ALK inhibitors, Cancer Res. (2018) canres.3146.2017. doi:10.1158/0008-5472.CAN-17-3146.

[199] K. Jacobsen, J. Bertran-Alamillo, M.A. Molina, C. Teixidó, N. Karachaliou, M.H. Pedersen, J. Castellví, M. Garzón, C. Codony-Servat, J. Codony-Servat, A. Giménez-Capitán, A. Drozdowskyj, S. Viteri, M.R. Larsen, U. Lassen, E. Felip, T.G. Bivona, H.J. Ditzel, R. Rosell, Convergent Akt activation drives acquired EGFR inhibitor resistance in lung cancer, Nat. Commun. 8 (2017). doi:10.1038/s41467-017-00450-6.

[200] J. Zhang, J.D. Webster, D.L. Dugger, T. Goncharov, M. Roose-Girma, J. Hung, Y.C. Kwon, D. Vucic, K. Newton, V.M. Dixit, Ubiquitin Ligases cIAP1 and cIAP2 Limit Cell Death to Prevent Inflammation, Cell Rep. 27 (2019) 2679-2689.e3. doi:10.1016/j.celrep.2019.04.111.

[201] K. Okamoto, I. Okamoto, E. Hatashita, K. Kuwata, H. Yamaguchi, A. Kita, K. Yamanaka, M. Ono, K. Nakagawa, Overcoming Erlotinib Resistance in EGFR Mutation-Positive Non-Small Cell Lung Cancer Cells by Targeting Survivin, Mol. Cancer Ther. 11 (2012) 204–213. doi:10.1158/1535-7163.MCT-11-0638.

[202] D.D. Shao, W. Xue, E.B. Krall, A. Bhutkar, F. Piccioni, X. Wang, A.C. Schinzel, S. Sood, J. Rosenbluh, J.W. Kim, Y. Zwang, T.M. Roberts, D.E. Root, T. Jacks, W.C. Hahn, KRAS and

YAP1 converge to regulate EMT and tumor survival, Cell. 158 (2014) 171–184. doi:10.1016/j.cell.2014.06.004.

[203] J. Boshuizen, L.A. Koopman, O. Krijgsman, A. Shahrabi, E.G. van den Heuvel, M.A. Ligtenberg, D.W. Vredevoogd, K. Kemper, T. Kuilman, J.-Y. Song, N. Pencheva, J.T. Mortensen, M.G. Foppen, E.A. Rozeman, C.U. Blank, M.L. Janmaat, D. Satijn, E.C.W. Breij, D.S. Peeper, P.W.H.I. Parren, Cooperative targeting of melanoma heterogeneity with an AXL antibody-drug conjugate and BRAF/MEK inhibitors, Nat. Med. 24 (2018) 203–212. doi:10.1038/nm.4472.

[204] I. Zhang, N.G. Zaorsky, J.D. Palmer, R. Mehra, B. Lu, Targeting brain metastases in ALK-rearranged non-small-cell lung cancer, Lancet Oncol. 16 (2015) e510–e521. doi:10.1016/S1470-2045(15)00013-3.

[205] C. Hsu, L.-I. Lin, Y.-C. Cheng, Z.-R. Feng, Y.-Y. Shao, A.-L. Cheng, D.-L. Ou, Cyclin E1 Inhibition can Overcome Sorafenib Resistance in Hepatocellular Carcinoma Cells Through Mcl-1 Suppression, Clin. Cancer Res. 22 (2016) 2555–2564. doi:10.1158/1078-0432.CCR-15-0499.

[206] T. Oelgeschläger, Regulation of RNA polymerase II activity by CTD phosphorylation and cell cycle control, J. Cell. Physiol. 190 (2002) 160–169. doi:10.1002/jcp.10058.

[207] S. Sampathi, P. Acharya, Y. Zhao, J. Wang, K.R. Stengel, Q. Liu, M.R. Savona, S.W. Hiebert, The CDK7 inhibitor THZ1 alters RNA polymerase dynamics at the 5′ and 3′ ends of genes, Nucleic Acids Res. (2019) 1–16. doi:10.1093/nar/gkz127.

[208] I. Jonkers, H. Kwak, J.T. Lis, Genome-wide dynamics of Pol II elongation and its interplay with promoter proximal pausing, chromatin, and exons, Elife. 2014 (2014). doi:10.7554/eLife.02407.

[209] C. Thangavel, E. Boopathi, Y. Liu, C. McNair, A. Haber, M. Perepelyuk, A. Bhardwaj, S. Addya, A. Ertel, S. Shoyele, R. Birbe, J.M. Salvino, A.P. Dicker, K.E. Knudsen, R.B. Den, Therapeutic Challenge With a CDK 4/6 Inhibitor Induces an RB-dependent SMAC Mediated Apoptotic Response in Non-Small Cell Lung Cancer, Clin. Cancer Res. (2018) clincanres.2074.2017. doi:10.1158/1078-0432.CCR-17-2074.

[210] B.M. Kuenzi, L.L. Remsing Rix, P.A. Stewart, B. Fang, F. Kinose, A.T. Bryant, T.A. Boyle, J.M. Koomen, E.B. Haura, U. Rix, Polypharmacology-based ceritinib repurposing using integrated functional proteomics, Nat. Chem. Biol. 13 (2017) 1222–1231. doi:10.1038/nchembio.2489.

[211] G.I. Shapiro, J.G. Supko, A. Patterson, C. Lynch, J. Lucca, P.F. Zacarola, A. Muzikansky, J.J. Wright, T.J. Lynch, B.J. Rollins, A phase II trial of the cyclin-dependent kinase inhibitor flavopiridol in patients with previously untreated stage IV non-small cell lung cancer., Clin. Cancer Res. 7 (2001) 1590–9. papers://5aecfcca-9729-4def-92fe-

c46e5cd7cc81/Paper/p80067%5Cnhttp://www.ncbi.nlm.nih.gov/pubmed/11410495.

[212] J.C. Byrd, T.S. Lin, J.T. Dalton, D. Wu, M.A. Phelps, B. Fischer, M. Moran, K.A. Blum, B. Rovin, M. Brooker-McEldowney, S. Broering, L.J. Schaaf, A.J. Johnson, D.M. Lucas, N.A. Heerema, G. Lozanski, D.C. Young, J.R. Suarez, A.D. Colevas, M.R. Grever, Flavopiridol administered using a pharmacologically derived schedule is associated with marked clinical efficacy in refractory, genetically high-risk chronic lymphocytic leukemia, Blood. 109 (2007) 399–404. doi:10.1182/blood-2006-05-020735.

[213] J.J. Stephenson, J. Nemunaitis, A.A. Joy, J.C. Martin, Y.-M.M. Jou, D. Zhang, P. Statkevich, S.-L.L. Yao, Y. Zhu, H. Zhou, K. Small, R. Bannerji, M.J. Edelman, Randomized phase 2 study of the cyclin-dependent kinase inhibitor dinaciclib (MK-7965) versus erlotinib in patients with non-small cell lung cancer, Lung Cancer. 83 (2014) 219–223. doi:10.1016/j.lungcan.2013.11.020.

[214] A. Kotschy, Z. Szlavik, J. Murray, J. Davidson, A.L. Maragno, G. Le Toumelin-Braizat, M. Chanrion, G.L. Kelly, J.N. Gong, D.M. Moujalled, A. Bruno, M. Csekei, A. Paczal, Z.B. Szabo, S. Sipos, G. Radics, A. Proszenyak, B. Balint, L. Ondi, G. Blasko, A. Robertson, A. Surgenor, P. Dokurno, I. Chen, N. Matassova, J. Smith, C. Pedder, C. Graham, A. Studeny, G. Lysiak-Auvity, A.M. Girard, F. Gravï¿½, D. Segal, C.D. Riffkin, G. Pomilio, L.C.A. Galbraith, B.J. Aubrey, M.S. Brennan, M.J. Herold, C. Chang, G. Guasconi, N. Cauquil, F. Melchiore, N. Guigal-Stephan, B. Lockhart, F. Colland, J.A. Hickman, A.W. Roberts, D.C.S. Huang, A.H. Wei, A. Strasser, G. Lessene, O. Geneste, The MCL1 inhibitor S63845 is tolerable and effective in diverse cancer models, Nature. 538 (2016) 477–482. doi:10.1038/nature19830.

[215] B. Carlson, T. Lahusen, S. Singh, A. Loaiza-Perez, P.J. Worland, R. Pestell, C. Albanese, E.A. Sausville, A.M. Senderowicz, Down-regulation of cyclin D1 by transcriptional repression in MCF-7 human breast carcinoma cells induced by flavopiridol, Cancer Res. 59 (1999) 4634–4641.

[216] J. Bogenberger, C. Whatcott, N. Hansen, D. Delman, C.-X. Shi, W. Kim, H. Haws, K. Soh, Y.S. Lee, P. Peterson, A. Siddiqui-Jain, S. Weitman, K. Stewart, D. Bearss, R. Mesa, S. Warner, R. Tibes, Combined venetoclax and alvocidib in acute myeloid leukemia, Oncotarget. 8 (2017) 107206–107222. doi:10.18632/oncotarget.22284.

[217] S.A. Moharram, K. Shah, F. Khanum, A. Marhäll, M. Gazi, J.U. Kazi, Efficacy of the CDK inhibitor dinaciclib in vitro and in vivo in T-cell acute lymphoblastic leukemia, Cancer Lett. 405 (2017) 73–78. doi:10.1016/j.canlet.2017.07.019.

[218] Z. Chen, Z. Wang, J.C. Pang, Y. Yu, S. Bieerkehazhi, J. Lu, T. Hu, Y. Zhao, X. Xu, H. Zhang, J.S. Yi, S. Liu, J. Yang, Multiple CDK inhibitor dinaciclib suppresses neuroblastoma growth via inhibiting CDK2 and CDK9 activity, Sci. Rep. 6 (2016) 1–12. doi:10.1038/srep29090.

[219] C. Hu, T. Dadon, V. Chenna, S. Yabuuchi, R. Bannerji, R. Booher, P. Strack, N. Azad, B.D.

Nelkin, A. Maitra, Combined Inhibition of Cyclin-Dependent Kinases (Dinaciclib) and AKT (MK-2206) Blocks Pancreatic Tumor Growth and Metastases in Patient-Derived Xenograft Models, Mol. Cancer Ther. 14 (2015) 1532–1539. doi:10.1158/1535-7163.MCT-15-0028.

[220] P. Zhang, H. Kawakami, W. Liu, X. Zeng, K. Strebhardt, K. Tao, S. Huang, F.A. Sinicrope, Targeting CDK1 and MEK/ERK Overcomes Apoptotic Resistance in BRAF-Mutant Human Colorectal Cancer, Mol. Cancer Res. 16 (2018) 378–389. doi:10.1158/1541-7786.MCR-17-0404.

[221] D. Santamaría, C. Barrière, A. Cerqueira, S. Hunt, C. Tardy, K. Newton, J.F. Cáceres, P. Dubus, M. Malumbres, M. Barbacid, Cdk1 is sufficient to drive the mammalian cell cycle, Nature. 448 (2007) 811–815. doi:10.1038/nature06046.

[222] S. Djebali, C. a Davis, A. Merkel, A. Dobin, T. Lassmann, A. Mortazavi, A. Tanzer, J. Lagarde, W. Lin, F. Schlesinger, C. Xue, G.K. Marinov, J. Khatun, B. a Williams, C. Zaleski, J. Rozowsky, M. Röder, F. Kokocinski, R.F. Abdelhamid, T. Alioto, I. Antoshechkin, M.T. Baer, N.S. Bar, P. Batut, K. Bell, I. Bell, S. Chakrabortty, X. Chen, J. Chrast, J. Curado, T. Derrien, J. Drenkow, E. Dumais, J. Dumais, R. Duttagupta, E. Falconnet, M. Fastuca, K. Fejes-Toth, P. Ferreira, S. Foissac, M.J. Fullwood, H. Gao, D. Gonzalez, A. Gordon, H. Gunawardena, C. Howald, S. Jha, R. Johnson, P. Kapranov, B. King, C. Kingswood, O.J. Luo, E. Park, K. Persaud, J.B. Preall, P. Ribeca, B. Risk, D. Robyr, M. Sammeth, L. Schaffer, L.-H. See, A. Shahab, J. Skancke, A.M. Suzuki, H. Takahashi, H. Tilgner, D. Trout, N. Walters, H. Wang, J. Wrobel, Y. Yu, X. Ruan, Y. Hayashizaki, J. Harrow, M. Gerstein, T. Hubbard, A. Reymond, S.E. Antonarakis, G. Hannon, M.C. Giddings, Y. Ruan, B. Wold, P. Carninci, R. Guigó, T.R. Gingeras, Landscape of transcription in human cells., Nature. 489 (2012) 101–8. doi:10.1038/nature11233.

[223] K. V. Morris, J.S. Mattick, The rise of regulatory RNA, Nat. Rev. Genet. 15 (2014) 423–437. doi:10.1038/nrg3722.

[224] F. Calore, F. Lovat, M. Garofalo, Non-coding RNAs and cancer., Int. J. Mol. Sci. 14 (2013) 17085–110. doi:10.3390/ijms140817085.

[225] A. Fatica, I. Bozzoni, Long non-coding RNAs: new players in cell differentiation and development., Nat. Rev. Genet. 15 (2014) 7–21. doi:10.1038/nrg3606.

[226] R.C. Lee, R.L. Feinbaum, V. Ambros, The C. elegans heterochronic gene lin-4 encodes small RNAs with antisense complementarity to lin-14, Cell. 75 (1993) 843–854. doi:10.1016/0092-8674(93)90529-Y.

[227] S.L. Ameres, P.D. Zamore, Diversifying microRNA sequence and function., Nat. Rev. Mol. Cell Biol. 14 (2013) 475–88. doi:10.1038/nrm3611.

[228] J.R. Lytle, T. a Yario, J. a Steitz, Target mRNAs are repressed as efficiently by microRNA-binding sites in the 5′ UTR as in the 3′ UTR., Proc. Natl. Acad. Sci. U. S. A. 104 (2007)

9667–9672. doi:10.1073/pnas.0703820104.

[229] Y. Tay, J. Zhang, A.M. Thomson, B. Lim, I. Rigoutsos, MicroRNAs to Nanog, Oct4 and Sox2 coding regions modulate embryonic stem cell differentiation., Nature. 455 (2008) 1124–8. doi:10.1038/nature07299.

[230] A. Helwak, G. Kudla, T. Dudnakova, D. Tollervey, Mapping the Human miRNA Interactome by CLASH Reveals Frequent Noncanonical Binding, Cell. 153 (2013) 654–665. doi:10.1016/j.cell.2013.03.043.

[231] H. Guo, N.T. Ingolia, J.S. Weissman, D.P. Bartel, Mammalian microRNAs predominantly act to decrease target mRNA levels, Nature. 466 (2010) 835–840. doi:10.1038/nature09267.

[232] J. Béthune, C.G. Artus-Revel, W. Filipowicz, Kinetic analysis reveals successive steps leading to miRNA-mediated silencing in mammalian cells., EMBO Rep. 13 (2012) 716–23. doi:10.1038/embor.2012.82.

[233] P. Ramalingam, J.K. Palanichamy, A. Singh, P. Das, M. Bhagat, M.A. Kassab, S. Sinha, P. Chattopadhyay, Biogenesis of intronic miRNAs located in clusters by independent transcription and alternative splicing, RNA. 20 (2014) 76–87. doi:10.1261/rna.041814.113.

[234] Y. Lee, M. Kim, J. Han, K.H. Yeom, S. Lee, S.H. Baek, V.N. Kim, MicroRNA genes are transcribed by RNA polymerase II, EMBO J. 23 (2004) 4051–4060. doi:10.1038/sj.emboj.7600385\n7600385 [pii].

[235] J. Han, Y. Lee, K.-H. Yeom, Y.-K. Kim, H. Jin, V.N. Kim, The Drosha-DGCR8 complex in primary microRNA processing., Genes Dev. 18 (2004) 3016–27. doi:10.1101/gad.1262504.

[236] T. Kawamata, Y. Tomari, Making RISC, Trends Biochem. Sci. 35 (2010) 368–376. doi:10.1016/j.tibs.2010.03.009.

[237] S. Jonas, E. Izaurralde, Towards a molecular understanding of microRNA-mediated gene silencing., Nat. Rev. Genet. 16 (2015) 421–433. doi:10.1038/nrg3965.

[238] G.A. Calin, C.D. Dumitru, M. Shimizu, R. Bichi, S. Zupo, E. Noch, H. Aldler, S. Rattan, M. Keating, K. Rai, L. Rassenti, T. Kipps, M. Negrini, F. Bullrich, C.M. Croce, Frequent deletions and down-regulation of micro- RNA genes miR15 and miR16 at 13q14 in chronic lymphocytic leukemia., Proc. Natl. Acad. Sci. U. S. A. 99 (2002) 15524–9. doi:10.1073/pnas.242606799.

[239] F. Lovat, M. Fassan, D. Sacchi, P. Ranganathan, A. Palamarchuk, M. Bill, M. Karunasiri, P. Gasparini, G. Nigita, R. Distefano, D. Veneziano, A.M. Dorrance, R. Garzon, C.M. Croce, Knockout of both miR-15/16 loci induces acute myeloid leukemia, Proc. Natl. Acad. Sci. 115 (2018) 13069–13074. doi:10.1073/pnas.1814980115.

[240] J. Lu, G. Getz, E. a. Miska, E. Alvarez-Saavedra, J. Lamb, D. Peck, A. Sweet-Cordero, B.L.

Ebert, R.H. Mak, A. a. Ferrando, J.R. Downing, T. Jacks, H.R. Horvitz, T.R. Golub, MicroRNA expression profiles classify human cancers, Nature. 435 (2005) 834–838. doi:10.1038/nature03702.

[241] G.A. Calin, C. Sevignani, C.D. Dumitru, T. Hyslop, E. Noch, S. Yendamuri, M. Shimizu, S. Rattan, F. Bullrich, M. Negrini, C.M. Croce, Human microRNA genes are frequently located at fragile sites and genomic regions involved in cancers, Proc. Natl. Acad. Sci. 101 (2004) 2999–3004. doi:10.1073/pnas.0307323101.

[242] M.S. Kumar, J. Lu, K.L. Mercer, T.R. Golub, T. Jacks, Impaired microRNA processing enhances cellular transformation and tumorigenesis, Nat. Genet. 39 (2007) 673–677. doi:10.1038/ng2003.

[243] C. Mayr, D.P. Bartel, Widespread Shortening of 3'UTRs by Alternative Cleavage and Polyadenylation Activates Oncogenes in Cancer Cells, Cell. 138 (2009) 673–684. doi:10.1016/j.cell.2009.06.016.

[244] P.P. Medina, M. Nolde, F.J. Slack, OncomiR addiction in an in vivo model of microRNA-21-induced pre-B-cell lymphoma, Nature. 467 (2010) 86–90. doi:10.1038/nature09284.

[245] O. Barca-Mayo, Q. Richard Lu, Fine-tuning oligodendrocyte development by micrornas, Front. Neurosci. 6 (2012) 13. doi:10.3389/fnins.2012.00013.

[246] P. Joshi, J. Middleton, Y.-J. Jeon, M. Garofalo, MicroRNAs in lung cancer., World J. Methodol. 4 (2014) 59–72. doi:10.5662/wjm.v4.i2.59.

[247] a L. Kasinski, K. Kelnar, C. Stahlhut, E. Orellana, J. Zhao, E. Shimer, S. Dysart, X. Chen, a G. Bader, F.J. Slack, A combinatorial microRNA therapeutics approach to suppressing non-small cell lung cancer, Oncogene. 34 (2015) 3547–3555. doi:10.1038/onc.2014.282.

[248] Y. Hayashita, A Polycistronic MicroRNA Cluster, miR-17-92, Is Overexpressed in Human Lung Cancers and Enhances Cell Proliferation, Cancer Res. 65 (2005) 9628–9632. doi:10.1158/0008-5472.CAN-05-2352.

[249] K. a O'Donnell, E.A. Wentzel, K.I. Zeller, C. V Dang, J.T. Mendell, c-Myc-regulated microRNAs modulate E2F1 expression., Nature. 435 (2005) 839–43. doi:10.1038/nature03677.

[250] J.T. Mendell, miRiad Roles for the miR-17-92 Cluster in Development and Disease, Cell. 133 (2008) 217–222. doi:10.1016/j.cell.2008.04.001.

[251] A. Bonauer, G. Carmona, M. Iwasaki, M. Mione, M. Koyanagi, A. Fischer, J. Burchfield, H. Fox, C. Doebele, K. Ohtani, E. Chavakis, M. Potente, M. Tjwa, C. Urbich, A.M. Zeiher, S. Dimmeler, MicroRNA-92a Controls Angiogenesis and Functional Recovery of Ischemic Tissues in Mice, Science (80-.). 324 (2009) 1710–1713. doi:10.1126/science.1174381.

[252] S.G. Chaulk, Z. Xu, M.J.N. Glover, R.P. Fahlman, MicroRNA miR-92a-1 biogenesis and mRNA targeting is modulated by a tertiary contact within the miR-17~92 microRNA cluster, Nucleic Acids Res. 42 (2014) 5234–5244. doi:10.1093/nar/gku133.

[253] R. Borkowski, L. Du, Z. Zhao, E. McMillan, a. Kosti, C.-R. Yang, M. Suraokar, I.I. Wistuba, a. F. Gazdar, J.D. Minna, M. a. White, a. Pertsemlidis, Genetic Mutation of p53 and Suppression of the miR-17 92 Cluster Are Synthetic Lethal in Non-Small Cell Lung Cancer due to Upregulation of Vitamin D Signaling, Cancer Res. 75 (2015) 666–675. doi:10.1158/0008-5472.CAN-14-1329.

[254] V. Olive, I. Jiang, L. He, mir-17-92, a cluster of miRNAs in the midst of the cancer network., Int. J. Biochem. Cell Biol. 42 (2010) 1348–54. doi:10.1016/j.biocel.2010.03.004.

[255] Y.-C. Han, J. a Vidigal, P. Mu, E. Yao, I. Singh, A.J. González, C.P. Concepcion, C. Bonetti, P. Ogrodowski, B. Carver, L. Selleri, D. Betel, C. Leslie, A. Ventura, An allelic series of miR-17~92–mutant mice uncovers functional specialization and cooperation among members of a microRNA polycistron, Nat. Genet. 47 (2015) 766–775. doi:10.1038/ng.3321.

[256] a Holleman, I. Chung, R.R. Olsen, B. Kwak, a Mizokami, N. Saijo, a Parissenti, Z. Duan, E.E. Voest, B.R. Zetter, miR-135a contributes to paclitaxel resistance in tumor cells both in vitro and in vivo., Oncogene. 30 (2011) 4386–98. doi:10.1038/onc.2011.148.

[257] Z. Dong, Z. Zhong, L. Yang, S. Wang, Z. Gong, MicroRNA-31 inhibits cisplatin-induced apoptosis in non-small cell lung cancer cells by regulating the drug transporter ABCB9, Cancer Lett. 343 (2014) 249–257. doi:10.1016/j.canlet.2013.09.034.

[258] M. Garofalo, G. Romano, G. Di Leva, G. Nuovo, Y.-J. Jeon, A. Ngankeu, J. Sun, F. Lovat, H. Alder, G. Condorelli, J. a Engelman, M. Ono, J.K. Rho, L. Cascione, S. Volinia, K.P. Nephew, C.M. Croce, EGFR and MET receptor tyrosine kinase-altered microRNA expression induces tumorigenesis and gefitinib resistance in lung cancers., Nat. Med. 18 (2011) 74–82. doi:10.1038/nm.2577.

[259] Y.-J. Jeon, J. Middleton, T. Kim, A. Laganà, C. Piovan, P. Secchiero, G.J. Nuovo, R. Cui, P. Joshi, G. Romano, G. Di Leva, B.-K. Lee, H.-L. Sun, Y. Kim, P. Fadda, H. Alder, M. Garofalo, C.M. Croce, A set of NF-κB–regulated microRNAs induces acquired TRAIL resistance in Lung cancer, Proc. Natl. Acad. Sci. 112 (2015) 3355–3364. doi:10.1073/pnas.1504630112.

[260] S. Naidu, M. Garofalo, microRNAs: An Emerging Paradigm in Lung Cancer Chemoresistance, Front. Med. 2 (2015) 1–8. doi:10.3389/fmed.2015.00077.

[261] L. Du, A. Pertsemlidis, microRNA regulation of cell viability and drug sensitivity in lung cancer, Expert Opin. Biol. Ther. 12 (2015) 1221–1239. doi:10.1517/14712598.2012.697149.

[262] M. Li, W. Chen, H. Zhang, Y. Zhang, F. Ke, X. Wu, Y. Zhang, M. Weng, Y. Liu, W. Gong, M. Li, W. Chen, H. Zhang, Y. Zhang, F. Ke, X. Wu, Y. Zhang, M. Weng, Y. Liu, W. Gong, MiR-

31 regulates the cisplatin resistance by targeting Src in gallbladder cancer, Oncotarget. 7 (2016) 83060–83070. doi:10.18632/oncotarget.13067.

[263] M.A. Cortez, C. Bueso-Ramos, J. Ferdin, G. Lopez-Berestein, A.K. Sood, G.A. Calin, MicroRNAs in body fluids-the mix of hormones and biomarkers, Nat. Rev. Clin. Oncol. 8 (2011) 467–477. doi:10.1038/nrclinonc.2011.76.

[264] Q. Leng, Y. Lin, F. Jiang, C.-J. Lee, M. Zhan, H. Fang, Y. Wang, F. Jiang, A plasma miRNA signature for lung cancer early detection, Oncotarget. 8 (2017) 111902–111911. doi:10.18632/oncotarget.22950.

[265] E. Nadal, A. Truini, A. Nakata, J. Lin, R.M. Reddy, A.C. Chang, N. Ramnath, N. Gotoh, D.G. Beer, G. Chen, A Novel Serum 4-microRNA Signature for Lung Cancer Detection., Sci. Rep. 5 (2015) 12464. doi:10.1038/srep12464.

[266] Y. Xie, N.W. Todd, Z. Liu, M. Zhan, H. Fang, H. Peng, M. Alattar, J. Deepak, S.A. Stass, F. Jiang, Altered miRNA expression in sputum for diagnosis of non-small cell lung cancer, Lung Cancer. 67 (2010) 170–176. doi:10.1016/j.lungcan.2009.04.004.

[267] P. Gasparini, L. Cascione, L. Landi, S. Carasi, F. Lovat, C. Tibaldi, G. Alì, A. D'Incecco, G. Minuti, A. Chella, G. Fontanini, M. Fassan, F. Cappuzzo, C.M. Croce, microRNA classifiers are powerful diagnostic/prognostic tools in ALK- , EGFR- , and KRAS -driven lung cancers, Proc. Natl. Acad. Sci. 112 (2015) 14924–14929. doi:10.1073/pnas.1520329112.

[268] J. Shang, S. Wang, Y. Jiang, Y. Duan, G. Cheng, D. Liu, J. Xiao, Z. Zhao, Identification of key lncRNAs contributing to diabetic nephropathy by gene co-expression network analysis, Sci. Rep. 9 (2019) 3328. doi:10.1038/s41598-019-39298-9.

[269] V.N. Kadali, S. Chandran, S. Murthy, Long Non-Coding RNAs and their "Orchestration" in Cancers, J. Appl. Biol. Biotechnol. 6 (2018) 57–60. doi:10.7324/JABB.2018.60509.

[270] X.D. Xiong, X. Ren, M.Y. Cai, J.W. Yang, X. Liu, J.M. Yang, Long non-coding RNAs: An emerging powerhouse in the battle between life and death of tumor cells, Drug Resist. Updat. 26 (2016) 28–42. doi:10.1016/j.drup.2016.04.001.

[271] Y.-Y. Tseng, B.S. Moriarity, W. Gong, R. Akiyama, A. Tiwari, H. Kawakami, P. Ronning, B. Reuland, K. Guenther, T.C. Beadnell, J. Essig, G.M. Otto, M.G. O'Sullivan, D.A. Largaespada, K.L. Schwertfeger, Y. Marahrens, Y. Kawakami, A. Bagchi, PVT1 dependence in cancer with MYC copy-number increase, Nature. 512 (2014) 82–86. doi:10.1038/nature13311.

[272] W. Zhou, Y. Yang, F. Liu, S. Wang, Q. Tao, G. Yang, Y. Wang, W. Pan, J. Ma, T. Wang, S. Sun, Y. Guo, C. Zhou, F. Yang, J. Yuan, N. Yang, F. Wang, A Long Noncoding RNA Activated by TGF-β Promotes the Invasion-Metastasis Cascade in Hepatocellular Carcinoma, Cancer Cell. 25 (2014) 666–681. doi:10.1016/j.ccr.2014.03.010.

[273] J. Seiler, M. Breinig, M. Caudron-Herger, M. Polycarpou-Schwarz, M. Boutros, S. Diederichs,

The lncRNA VELUCT strongly regulates viability of lung cancer cells despite its extremely low abundance, Nucleic Acids Res. (2017) 1–12. doi:10.1093/nar/gkx076.

[274] J. Zheng, X. Huang, W. Tan, D. Yu, Z. Du, J. Chang, L. Wei, Y. Han, C. Wang, X. Che, Y. Zhou, X. Miao, G. Jiang, X. Yu, X. Yang, G. Cao, C. Zuo, Z. Li, C. Wang, S.T. Cheung, Y. Jia, X. Zheng, H. Shen, C. Wu, D. Lin, Pancreatic cancer risk variant in LINC00673 creates a miR-1231 binding site and interferes with PTPN11 degradation, Nat. Genet. (2016). doi:10.1038/ng.3568.

[275] A. Bhan, S.S. Mandal, LncRNA HOTAIR: A master regulator of chromatin dynamics and cancer, Biochim. Biophys. Acta - Rev. Cancer. 1856 (2015) 151–164. doi:10.1016/j.bbcan.2015.07.001.

[276] E. Leucci, R. Vendramin, M. Spinazzi, P. Laurette, M. Fiers, J. Wouters, E. Radaelli, S. Eyckerman, C. Leonelli, K. Vanderheyden, A. Rogiers, E. Hermans, P. Baatsen, S. Aerts, F. Amant, S. Van Aelst, J. van den Oord, B. de Strooper, I. Davidson, D.L.J. Lafontaine, K. Gevaert, J. Vandesompele, P. Mestdagh, J.-C. Marine, Melanoma addiction to the long non-coding RNA SAMMSON, Nature. 531 (2016) 518–522. doi:10.1038/nature17161.

[277] Y. Zhang, Q. He, Z. Hu, Y. Feng, L. Fan, Z. Tang, J. Yuan, W. Shan, C. Li, X. Hu, J.L. Tanyi, Y. Fan, Q. Huang, K. Montone, C. V Dang, L. Zhang, Long noncoding RNA LINP1 regulates repair of DNA double-strand breaks in triple-negative breast cancer, Nat. Struct. Mol. Biol. 23 (2016) 522–530. doi:10.1038/nsmb.3211.

[278] D.S.W. Tan, F.T. Chong, H.S. Leong, S.Y. Toh, D.P. Lau, X.L. Kwang, X. Zhang, G.M. Sundaram, G.S. Tan, M.M. Chang, B.T. Chua, W.T. Lim, E.H. Tan, M.K. Ang, T.K.H. Lim, P. Sampath, B. Chowbay, A.J. Skanderup, R. DasGupta, N.G. Iyer, Long noncoding RNA EGFR-AS1 mediates epidermal growth factor receptor addiction and modulates treatment response in squamous cell carcinoma, Nat. Med. 23 (2017) 1167–1175. doi:10.1038/nm.4401.

[279] Y. Lu, X. Zhao, Q. Liu, C. Li, R. Graves-Deal, Z. Cao, B. Singh, J.L. Franklin, J. Wang, H. Hu, T. Wei, M. Yang, T.J. Yeatman, E. Lee, K. Saito-Diaz, S. Hinger, J.G. Patton, C.H. Chung, S. Emmrich, J.-H. Klusmann, D. Fan, R.J. Coffey, lncRNA MIR100HG-derived miR-100 and miR-125b mediate cetuximab resistance via Wnt/β-catenin signaling, Nat. Med. 23 (2017) 1331–1341. doi:10.1038/nm.4424.

[280] L. Qu, J. Ding, C. Chen, Z.-J. Wu, B. Liu, Y. Gao, W. Chen, F. Liu, W. Sun, X.-F. Li, X. Wang, Y. Wang, Z.-Y. Xu, L. Gao, Q. Yang, B. Xu, Y.-M. Li, Z.-Y. Fang, Z.-P. Xu, Y. Bao, D.-S. Wu, X. Miao, H.-Y. Sun, Y. Sun, H.-Y. Wang, L. Wang, Exosome-Transmitted lncARSR Promotes Sunitinib Resistance in Renal Cancer by Acting as a Competing Endogenous RNA, Cancer Cell. 29 (2016) 653–668. doi:10.1016/j.ccell.2016.03.004.

[281] C. le Sage, R. Nagel, D. a Egan, M. Schrier, E. Mesman, A. Mangiola, C. Anile, G. Maira, N.

Mercatelli, S.A. Ciafrè, M.G. Farace, R. Agami, Regulation of the p27(Kip1) tumor suppressor by miR-221 and miR-222 promotes cancer cell proliferation., EMBO J. 26 (2007) 3699–708. doi:10.1038/sj.emboj.7601790.

[282] P. Mestdagh, N. Hartmann, L. Baeriswyl, D. Andreasen, N. Bernard, C. Chen, D. Cheo, P. D'Andrade, M. DeMayo, L. Dennis, S. Derveaux, Y. Feng, S. Fulmer-Smentek, B. Gerstmayer, J. Gouffon, C. Grimley, E. Lader, K.Y. Lee, S. Luo, P. Mouritzen, A. Narayanan, S. Patel, S. Peiffer, S. Rüberg, G. Schroth, D. Schuster, J.M. Shaffer, E.J. Shelton, S. Silveria, U. Ulmanella, V. Veeramachaneni, F. Staedtler, T. Peters, T. Guettouche, L. Wong, J. Vandesompele, Evaluation of quantitative miRNA expression platforms in the microRNA quality control (miRQC) study., Nat. Methods. 11 (2014) 809–815. doi:10.1038/nmeth.3014.

[283] J.-J. Zhao, Z.-B. Chu, Y. Hu, J. Lin, Z. Wang, M. Jiang, M. Chen, X. Wang, Y. Kang, Y. Zhou, T.N. Chonghaile, M.E. Johncilla, Y.-T. Tai, J.Q. Cheng, A. Letai, N.C. Munshi, K.C. Anderson, R.D. Carrasco, Targeting the miR-221-222/PUMA/BAK/BAX Pathway Abrogates Dexamethasone Resistance in Multiple Myeloma, Cancer Res. 75 (2015) 4384–4397. doi:10.1158/0008-5472.CAN-15-0457.

[284] X. Zheng, K. He, L. Zhang, J. Yu, Crizotinib induces PUMA-dependent apoptosis in colon cancer cells., Mol. Cancer Ther. 12 (2013) 777–86. doi:10.1158/1535-7163.MCT-12-1146.

[285] K.J. Mavrakis, J. Van Der Meulen, A.L. Wolfe, X. Liu, E. Mets, T. Taghon, A.A. Khan, M. Setty, P. Rondou, P. Vandenberghe, E. Delabesse, Y. Benoit, N.B. Socci, C.S. Leslie, P. Van Vlierberghe, F. Speleman, H.-G. Wendel, A cooperative microRNA-tumor suppressor gene network in acute T-cell lymphoblastic leukemia (T-ALL), Nat. Genet. 43 (2011) 673–678. doi:10.1038/ng.858.

[286] E. Spaccarotella, E. Pellegrino, M. Ferracin, C. Ferreri, G. Cuccuru, C. Liu, J. Iqbal, D. Cantarella, R. Taulli, P. Provero, F. Di Cunto, E. Medico, M. Negrini, W.C. Chan, G. Inghirami, R. Piva, STAT3-mediated activation of microRNA cluster 17 92 promotes proliferation and survival of ALK-positive anaplastic large cell lymphoma, Haematologica. 99 (2014) 116–124. doi:10.3324/haematol.2013.088286.

[287] Z. Yagil, H. Nechushtan, G. Kay, C.M. Yang, D.M. Kemeny, E. Razin, The enigma of the role of Protein inhibitor of Activated STAT3 (PIAS3) in the immune response, Trends Immunol. 31 (2010) 199–204. doi:10.1016/j.it.2010.01.005.

[288] S. Naidu, L. Shi, P. Magee, J.D. Middleton, A. Laganá, S. Sahoo, H.S. Leong, M. Galvin, K. Frese, C. Dive, V. Guzzardo, M. Fassan, M. Garofalo, PDGFR-modulated miR-23b cluster and miR-125a-5p suppress lung tumorigenesis by targeting multiple components of KRAS and NF-kB pathways, Sci. Rep. 7 (2017) 15441. doi:10.1038/s41598-017-14843-6.

[289] A. Khan, O. Fornes, A. Stigliani, M. Gheorghe, J.A. Castro-Mondragon, R. Van Der Lee, A.

Bessy, J. Chèneby, S.R. Kulkarni, G. Tan, D. Baranasic, D.J. Arenillas, A. Sandelin, K. Vandepoele, B. Lenhard, B. Ballester, W.W. Wasserman, F. Parcy, A. Mathelier, JASPAR 2018: Update of the open-access database of transcription factor binding profiles and its web framework, Nucleic Acids Res. (2018). doi:10.1093/nar/gkx1126.

[290] K.M. Tracy, C.E. Tye, P.N. Ghule, H.L.H. Malaby, J. Stumpff, J.L. Stein, G.S. Stein, J.B. Lian, Mitotically-Associated lncRNA (MANCR) Affects Genomic Stability and Cell Division in Aggressive Breast Cancer, Mol. Cancer Res. (2018) molcanres.0548.2017. doi:10.1158/1541-7786.MCR-17-0548.

[291] C.A. Stein, J.B. Hansen, J. Lai, S. Wu, A. Voskresenskiy, A. H∅g, J. Worm, M. Hedtjärn, N. Souleimanian, P. Miller, H.S. Soifer, D. Castanotto, L. Benimetskaya, H. Ørum, T. Koch, Efficient gene silencing by delivery of locked nucleic acid antisense oligonucleotides, unassisted by transfection reagents, Nucleic Acids Res. 38 (2010) e3–e3. doi:10.1093/nar/gkp841.

[292] A.R. Paliouras, T. Monteverde, M. Garofalo, Oncogene-induced regulation of microRNA expression: Implications for cancer initiation, progression and therapy, Cancer Lett. 421 (2018) 152–160. doi:10.1016/j.canlet.2018.02.029.

[293] G.C. Chang, S.L. Hsu, J.R. Tsai, F.P. Liang, S.Y. Lin, G.T. Sheu, C.Y. Chen, Molecular mechanisms of ZD1839-induced G1-cell cycle arrest and apoptosis in human lung adenocarcinoma A549 cells, Biochem. Pharmacol. 68 (2004) 1453–1464. doi:10.1016/j.bcp.2004.06.006.

[294] J.P. Koivunen, C. Mermel, K. Zejnullahu, C. Murphy, E. Lifshits, A.J. Holmes, H.G. Choi, J. Kim, D. Chiang, R. Thomas, J. Lee, W.G. Richards, D.J. Sugarbaker, C. Ducko, N. Lindeman, J.P. Marcoux, J. a. Engelman, N.S. Gray, C. Lee, M. Meyerson, P. a. Jänne, EML4-ALK fusion gene and efficacy of an ALK kinase inhibitor in lung cancer, Clin. Cancer Res. 14 (2008) 4275–4283. doi:10.1158/1078-0432.CCR-08-0168.

[295] G. Zhang, H. Scarborough, J. Kim, A.I. Rozhok, Y.A. Chen, X. Zhang, L. Song, Y. Bai, B. Fang, R.Z. Liu, J. Koomen, A.C. Tan, J. Degregori, E.B. Haura, Coupling an EML4-ALK-centric interactome with RNA interference identifies sensitizers to ALK inhibitors, Sci. Signal. 9 (2016) rs12–rs12. doi:10.1126/scisignal.aaf5011.

[296] C.S. Tellez, D.E. Juri, K. Do, A.M. Bernauer, C.L. Thomas, L.A. Damiani, M. Tessema, S. Leng, S.A. Belinsky, EMT and Stem Cell-Like Properties Associated with miR-205 and miR-200 Epigenetic Silencing Are Early Manifestations during Carcinogen-Induced Transformation of Human Lung Epithelial Cells, Cancer Res. 71 (2011) 3087–3097. doi:10.1158/0008-5472.CAN-10-3035.

[297] T. Kan, F. Sato, T. Ito, N. Matsumura, S. David, Y. Cheng, R. Agarwal, B.C. Paun, Z. Jin, A. V. Olaru, F.M. Selaru, J.P. Hamilton, J. Yang, J.M. Abraham, Y. Mori, S.J. Meltzer, The miR-

106b-25 Polycistron, Activated by Genomic Amplification, Functions as an Oncogene by Suppressing p21 and Bim, Gastroenterology. 136 (2009) 1689–1700. doi:10.1053/j.gastro.2009.02.002.

[298] L. Poliseno, L. Salmena, L. Riccardi, A. Fornari, M.S. Song, R.M. Hobbs, P. Sportoletti, S. Varmeh, A. Egia, G. Fedele, L. Rameh, M. Loda, P.P. Pandolfi, Identification of the miR-106b 25 MicroRNA Cluster as a Proto-Oncogenic PTEN-Targeting Intron That Cooperates with Its Host Gene MCM7 in Transformation, Sci. Signal. 3 (2010) ra29–ra29. doi:10.1126/scisignal.2000594.

[299] Y. Zhou, Y. Hu, M. Yang, P. Jat, K. Li, Y. Lombardo, D. Xiong, R.C. Coombes, S. Raguz, E. Yagüe, The miR-106b~25 cluster promotes bypass of doxorubicin-induced senescence and increase in motility and invasion by targeting the E-cadherin transcriptional activator EP300, Cell Death Differ. 21 (2014) 462–474. doi:10.1038/cdd.2013.167.

[300] Y. Wang, X. Zheng, Z. Zhang, J. Zhou, G. Zhao, J. Yang, L. Xia, R. Wang, X. Cai, H. Hu, C. Zhu, Y. Nie, K. Wu, D. Zhang, D. Fan, MicroRNA-149 Inhibits Proliferation and Cell Cycle Progression through the Targeting of ZBTB2 in Human Gastric Cancer, PLoS One. 7 (2012) e41693. doi:10.1371/journal.pone.0041693.

[301] S.-H. Chan, W.-C. Huang, J.-W. Chang, K.-J. Chang, W.-H. Kuo, M.-Y. Wang, K.-Y. Lin, Y.-H. Uen, M.-F. Hou, C.-M. Lin, T.-H. Jang, C.-W. Tu, Y.-R. Lee, Y.-H. Lee, M.-T. Tien, L.-H. Wang, MicroRNA-149 targets GIT1 to suppress integrin signaling and breast cancer metastasis, Oncogene. 33 (2014) 4496–4507. doi:10.1038/onc.2014.10.

[302] D.-X. He, X.-T. Gu, Y.-R. Li, L. Jiang, J. Jin, X. Ma, Methylation-regulated miR-149 modulates chemoresistance by targeting GlcNAc N -deacetylase/ N -sulfotransferase-1 in human breast cancer, FEBS J. 281 (2014) 4718–4730. doi:10.1111/febs.13012.

[303] G. Martello, A. Rosato, F. Ferrari, A. Manfrin, M. Cordenonsi, S. Dupont, E. Enzo, V. Guzzardo, M. Rondina, T. Spruce, A.R. Parenti, M.G. Daidone, S. Bicciato, S. Piccolo, A MicroRNA Targeting Dicer for Metastasis Control, Cell. 141 (2010) 1195–1207. doi:10.1016/j.cell.2010.05.017.

[304] P. Hydbring, Y. Wang, A. Fassl, D.G. Anderson, C. Li, P. Sicinski, P. Hydbring, Y. Wang, A. Fassl, X. Li, V. Matia, T. Otto, Y.J. Choi, Cell-Cycle-Targeting MicroRNAs as Therapeutic Tools against Refractory Cancers, Cancer Cell. 31 (2017) 576-590.e8. doi:10.1016/j.ccell.2017.03.004.

[305] A. Wittrup, J. Lieberman, Knocking down disease: a progress report on siRNA therapeutics, Nat. Rev. Genet. 16 (2015) 543–552. doi:10.1038/nrg3978.

[306] L. Fattore, R. Mancini, M. Acunzo, G. Romano, A. Laganà, M.E. Pisanu, D. Malpicci, G. Madonna, D. Mallardo, M. Capone, F. Fulciniti, L. Mazzucchelli, G. Botti, C.M. Croce, P.A. Ascierto, G. Ciliberto, miR-579-3p controls melanoma progression and resistance to target

therapy, Proc. Natl. Acad. Sci. (2016) 201607753. doi:10.1073/pnas.1607753113.

[307] I.A. Zaporozhchenko, E.S. Morozkin, A.A. Ponomaryova, E.Y. Rykova, N. V. Cherdyntseva, A.A. Zheravin, O.A. Pashkovskaya, E.A. Pokushalov, V. V. Vlassov, P.P. Laktionov, Profiling of 179 miRNA Expression in Blood Plasma of Lung Cancer Patients and Cancer-Free Individuals, Sci. Rep. 8 (2018) 1–13. doi:10.1038/s41598-018-24769-2.

[308] Y. Ma, X. Pan, P. Xu, Y. Mi, W. Wang, X. Wu, Q. He, X. Liu, W. Tang, H.-X. An, Plasma microRNA alterations between EGFR-activating mutational NSCLC patients with and without primary resistance to TKI., Oncotarget. 8 (2017) 88529–88536. doi:10.18632/oncotarget.19874.

[309] V. El-Khoury, S. Pierson, T. Kaoma, F. Bernardin, G. Berchem, Assessing cellular and circulating miRNA recovery: The impact of the RNA isolation method and the quantity of input material, Sci. Rep. 6 (2016) 1–14. doi:10.1038/srep19529.

[310] B.J. Solomon, D.W. Kim, Y.L. Wu, K. Nakagawa, T. Mekhail, E. Felip, F. Cappuzzo, J. Paolini, T. Usari, Y. Tang, K.D. Wilner, F. Blackhall, T.S. Mok, Final overall survival analysis from a study comparing first-line crizotinib versus chemotherapy in alk-mutation-positive non–small-cell lung cancer, J. Clin. Oncol. 36 (2018) 2251–2258. doi:10.1200/JCO.2017.77.4794.

[311] D.R. Camidge, S. Peters, T. Mok, S.M. Gadgeel, P.K. Cheema, N. Pavlakis, F. De Marinis, D.L. Stroyakovskiy, B.C. Cho, L. Zhang, D. Moro-Sibilot, A.H. Zeaiter, E. Mitry, B. Balas, B. Müller, A. Shaw, Updated efficacy and safety data from the global phase III ALEX study of alectinib (ALC) vs crizotinib (CZ) in untreated advanced ALK+ NSCLC., J. Clin. Oncol. 36 (2018) 9043–9043. doi:10.1200/JCO.2018.36.15_suppl.9043.

[312] L. Li, Y. Wang, T. Peng, K. Zhang, C. Lin, R. Han, C. Lu, Y. He, Y.H. Li Li, Yubo Wang, Tao Peng, Kejun Zhang, Caiyu Lin, Rui Han, Conghua Lu, Metformin restores crizotinib sensitivity in crizotinib-resistant human lung cancer cells through inhibition of IGF1-R signaling pathway, Oncotarget. 5 (2016) 1–11. doi:10.18632/oncotarget.9120.

[313] O. Arrieta, F. Barrón, M.-Á.S. Padilla, A. Avilés-Salas, L.A. Ramírez-Tirado, M.J. Arguelles Jiménez, E. Vergara, Z.L. Zatarain-Barrón, N. Hernández-Pedro, A.F. Cardona, G. Cruz-Rico, P. Barrios-Bernal, M. Yamamoto Ramos, R. Rosell, Effect of Metformin Plus Tyrosine Kinase Inhibitors Compared With Tyrosine Kinase Inhibitors Alone in Patients With Epidermal Growth Factor Receptor–Mutated Lung Adenocarcinoma, JAMA Oncol. (2019) e192553. doi:10.1001/jamaoncol.2019.2553.

[314] D.R. Camidge, R.C. Doebele, K.M. Kerr, Comparing and contrasting predictive biomarkers for immunotherapy and targeted therapy of NSCLC, Nat. Rev. Clin. Oncol. 3 (2019). doi:10.1038/s41571-019-0173-9.

[315] X. Kong, T. Kuilman, A. Shahrabi, J. Boshuizen, K. Kemper, J.-Y. Song, H.W.M. Niessen, E.A. Rozeman, M.H. Geukes Foppen, C.U. Blank, D.S. Peeper, Cancer drug addiction is

relayed by an ERK2-dependent phenotype switch, Nature. (2017). doi:10.1038/nature24037.